DOT/FAA/TC-17/40

Federal Aviation Administration
William J. Hughes Technical Center
Aviation Research Division
Atlantic City International Airport
New Jersey 08405

Further Airframe Usage and Operational Loads Monitoring of ASM/Lead Aircraft

November 2017

Final Report

U.S. Department of Transportation
Federal Aviation Administration

NOTICE

Technical Report Documentation Page

1. Report No.	2. Government Accession No.	3. Recipient's Catalog No.
DOT/FAA/TC-17/40		

4. Title and Subtitle	5. Report Date
FURTHER AIRFRAME USAGE AND OPERATIONAL LOADS MONITORING OF ASM/LEAD AIRCRAFT	November 2017
	6. Performing Organization Code

7. Author(s)	8. Performing Organization Report No.
Linda K. Kliment, Kamran Rokhsaz, and Alok N. Menon	

9. Performing Organization Name and Address	10. Work Unit No. (TRAIS)
Wichita State University 1845 Fairmount Wichita, KS 67260-0044	
	11. Contract or Grant No. Grant No. 15-G-002

12. Sponsoring Agency Name and Address	13. Type of Report and Period Covered
U.S. Department of Transportation Federal Aviation Administration Los Angeles ACO 3960 Paramount Blvd Lakewood, CA 90712	Final Report
	14. Sponsoring Agency Code ANM-210L

15. Supplementary Notes

The FAA William J. Hughes Technical Center Aviation Research Division COR was Sohrob Mottaghi.

16. Abstract

The FAA and the United States Forest Service (USFS) supported Wichita State University in examining the factors that affect the structural integrity of aircraft flying in firefighting missions. This program was aimed at conducting operational loads analysis of the Beechcraft King Air fleet flown in support of various operations to evaluate typical operational in-service data and compare the results with the data used in the design and qualification of such aircraft. The ultimate goal was to provide a basis to improve the structural criteria and methods of operation and maintenance of these airplanes by providing processed data in statistical formats, which would enable the FAA, the USFS, and the operators to better understand and control the factors that influence their structural integrity.

Data were collected from a fleet of C90A, C90GT, and E90 airframes in actual operation during several fire seasons. A total of 3,829 distinct ground-air-ground (GAG) flights, consisting of approximately 7,100 flight hours, were identified. Only the data from the 2014 season contained information on flap deflection. Four basic missions were identified and, in firefighting cases, each mission was divided into various phases.

GAG (i.e. overall) airframe usage included examination of altitude and airspeed, and their comparisons with the published limits, as well as pitch and roll angles and overall load factors versus airspeed. In a number of cases, the V_{MO} of 226 Knots Indicated Airspeed was exceeded, but by no more than 10% above the limit. Over-speeding was shown to be as likely during ferry flights as it was during other missions. With flaps retracted, load factors remained within the prescribed limits, except in one case in a C90A. However, in many firefighting operations, the maximum allowable load factor was exceeded when the flaps were deployed.

Exceedance spectra were developed for gust and maneuver loads and derived gust velocities for the overall flights and for specific flight phases. The results correlated much better with above ground level (AGL) altitude bands. The frequency of occurrence of incremental gust load factors for firefighting missions was higher than those of ferry missions. Maneuver load factors occurred in two orders of magnitude more frequently during firefighting cases than they did during ferry missions. Their frequency also increased with decreasing AGL altitude.

The report concludes with some recommendations for improved data acquisition for future similar efforts.

17. Key Words	18. Distribution Statement
Flight profiles, Flight loads spectrum, Statistical loads data	This document is available to the U.S. public through the National Technical Information Service (NTIS), Springfield, Virginia 22161. This document is also available from the Federal Aviation Administration William J. Hughes Technical Center at actlibrary.tc.faa.gov.

19. Security Classif. (of this report)	20. Security Classif. (of this page)	21. No. of Pages	22. Price
Unclassified	Unclassified	174	

ACKNOWLEDGEMENTS

The work reported in this document was performed by the Flight Loads Group within the Department of Aerospace Engineering of the College of Engineering at Wichita State University (WSU). This effort was funded by the FAA under grant 08-G-015. At WSU, the principal investigators were Dr. Kamran Rokhsaz and Dr. Linda K. Kliment of the Department of Aerospace Engineering. Mr. Alok N. Menon developed the data-reduction algorithms and software and established the data-reduction criteria. The format used for presentation of the statistical data was adopted from the work previously performed by the principal investigators and the University of Dayton Research Institute. The Program Managers for the FAA were Drs. Sohrob Mottaghi and Edward Weinstein of the FAA William J. Hughes Technical Center. Technical guidance was provided by Mr. David Rathfelder of the FAA Los Angeles Aircraft Certification Office.

TABLE OF CONTENTS

LIST OF FIGURES

LIST OF TABLES

LIST OF SYMBOLS

A_r	aspect ratio b^2/S
a	speed of sound (ft/sec)
b	wing span (ft)
$\overline{C}$	aircraft discrete gust response factor
$\bar{c}$	wing mean geometric chord (ft)
C_{l_α}	wing lift curve slope (per radian)
C_{L_α}	airplane lift curve slope (per radian)
D	distance
g	gravity constant, 32.17 ft/sec^2
K_g	discrete gust alleviation factor, $0.88\,\mu/(5.3 + \mu)$
l_t'	horizontal tail moment arm (ft)
M	Mach number
n_z	normal load factor (g)
Δn_z	incremental normal load factor (g)
P	pressure (lb/ft^2)
$\overline{R}$	specific gas constant, 1716 ft-lb/slug-°R
S	wing area (ft^2)
S_t	horizontal tail area (ft^2)
T	temperature (°R)
t	time (sec)
U_{de}	derived gust velocity (ft/sec)
V_C	calibrated or design cruise speed
V_e	equivalent airspeed
V_i	indicated airspeed
V_{MO}	maximum operating speed
V_T	true airspeed
W	weight (lb)

Greek Symbols

α	angle of attack (rad)
β	$\sqrt{1-M^2}$, compressibility effect
γ	ratio of specific heat constants, 1.4 for air
ε	downwash angle (rad)
Λ	wing quarter-chord sweep angle (rad)
μ	reduced mass
ρ	air density at altitude, slugs/ft^3
ρ_0	standard sea level air density 0.0023769 slugs/ft^3

LIST OF ACRONYMS

AGL	Above ground level
ASM	Aerial Supervision Module
ATGS	Air Tactical Group Supervisor
ATSM	Air Tactical Supervision Module
CSV	Comma separated variables
DFDR	Digital flight data recorder
GAG	Ground-air-ground
GPS	Global Positioning System
KIAS	Knots indicated airspeed
MSL	Mean sea level
NED	National Elevation Dataset
NTSB	National Transportation Safety Board
OEM	Original Equipment Manufacturer
OLM	Operational loads monitoring
UDRI	University of Dayton Research Institute
USFS	United States Forest Service
USGS	United States Geological Survey
WSU	Wichita State University

EXECUTIVE SUMMARY

Wichita State University (WSU) investigated usage, flight loads, and discrete gust velocities from a fleet of Beechcraft King Airs for comparison with their civil aviation use. The United States Forest Service (USFS) funded this investigation through the FAA as an element of its Operational Loads Monitoring program.

Digital flight data recorders were installed on a fleet of aircraft operated by USFS. The recorded data from these aircraft were collected by USFS and were stored in a central repository. These data were made available to WSU for further analysis.

The fleet consisted of various models of King Air: three of C90A, three of C90GT, and one of E90. These aircraft were used primarily as Aerial Supervision Modules leading air tankers into and out of the fire traffic area (ASM/Lead) and as Air Tactical Supervision Modules or Air Tactical Group Supervisor coordinating larger firefighting activities.

Usage data extracted and presented in statistical format consisted of basic flight parameters, such as airspeed, altitude, flight duration, and bank and pitch angles. The formats used for presentation of the results were kept consistent with past practices. Flights were divided into various phases, and results were developed for all, in addition to the results from the entire mission.

For each phase and for the entire flight, normal load factors were categorized into those caused by gusts and those caused by maneuvering. The results were used to develop loads spectra for each. The gust loads were also used for extracting information on discrete gust velocities for various phases. These results also led to the development of exceedance charts for various phases and altitudes. These data were shown to correlate better with above ground level (AGL) altitude than with absolute mean sea level altitude.

The statistical formats used in this study are those developed previously by the principal investigators and by the University of Dayton Research Institute. The data presented in this form allow easy comparison of the design criteria with actual usage data. As such, they provide the aircraft operators with a better understanding of those factors that influence the structural integrity of these aircraft. These data could also be used by the original equipment manufacturer for better understanding of the actual airframe usage and loads. Finally, this information can be used to refine the regulations concerning the design of these aircraft.

1. INTRODUCTION

Following two catastrophic in-flight failures of heavy air tankers in 2002, the National Transportation Safety Board issued Recommendation A-04-29 stating that the United States Forest Service (USFS) should "develop maintenance and inspection programs for aircraft that are used in firefighting operations that take into account and are based on the magnitude of maneuver loading and the level of turbulence in the firefighting environment and the effect of these factors on remaining operational life" [1]. In response, the USFS started developing maintenance and inspection programs driven by the operational loads experienced by its fleet [2]. One aspect of this effort has been methodically collecting operational loads via digital flight data recorders (DFDRs) and storing them in a central repository. This database currently contains information from thousands of flights for a variety of aircraft, collected over a number of years.

The first phase of this plan was focused on instrumentation of heavy air tankers, the results of which were published in Bramlette [3] and FAA report AR-11/7 [4]. The second phase of the plan was to perform the same type of analysis for light twin-engine aircraft flying in support of firefighting operations.

Currently, the majority of these aircraft are Beechcraft King Airs, mostly of the 90 series. These aircraft support the USFS aerial firefighting missions in several roles, while operating in environments vastly different from their intended design. In 2009, Beechcraft performed a preliminary analysis of a limited amount of data collected on one airframe [5]. The results are shown in figure 1 and clearly demonstrate the severity of the loads while flying these missions, compared with the typical commercial usage. As the result, Beechcraft recommended a revised inspection program for these aircraft.

Since 2006, the USFS has collected a large amount of data from a fleet of nine King Air aircraft. These data consist of all recorded information from 2006 through 2014. However, starting in 2009, USFS switched to DFDRs made and supported by the Appareo Systems, recording data at a constant 8 Hz. The focus of the present report is on analyzing the data from 2009 through 2014.

The scope of the present effort covered the following items:

- By agreement with the USFS, all the recorded flight data would be made available to Wichita State University (WSU) for post processing.
- Usage and loads information would be extracted and analyzed statistically for the airborne segments of the flights.
- The analysis would be performed on data from 2009 through 2014 fire seasons.
- The analysis would be limited to recorded data from the Beechcraft King Air fleet.
- Processing would be limited to the data acquired by the data acquisition systems manufactured by Appareo Systems.

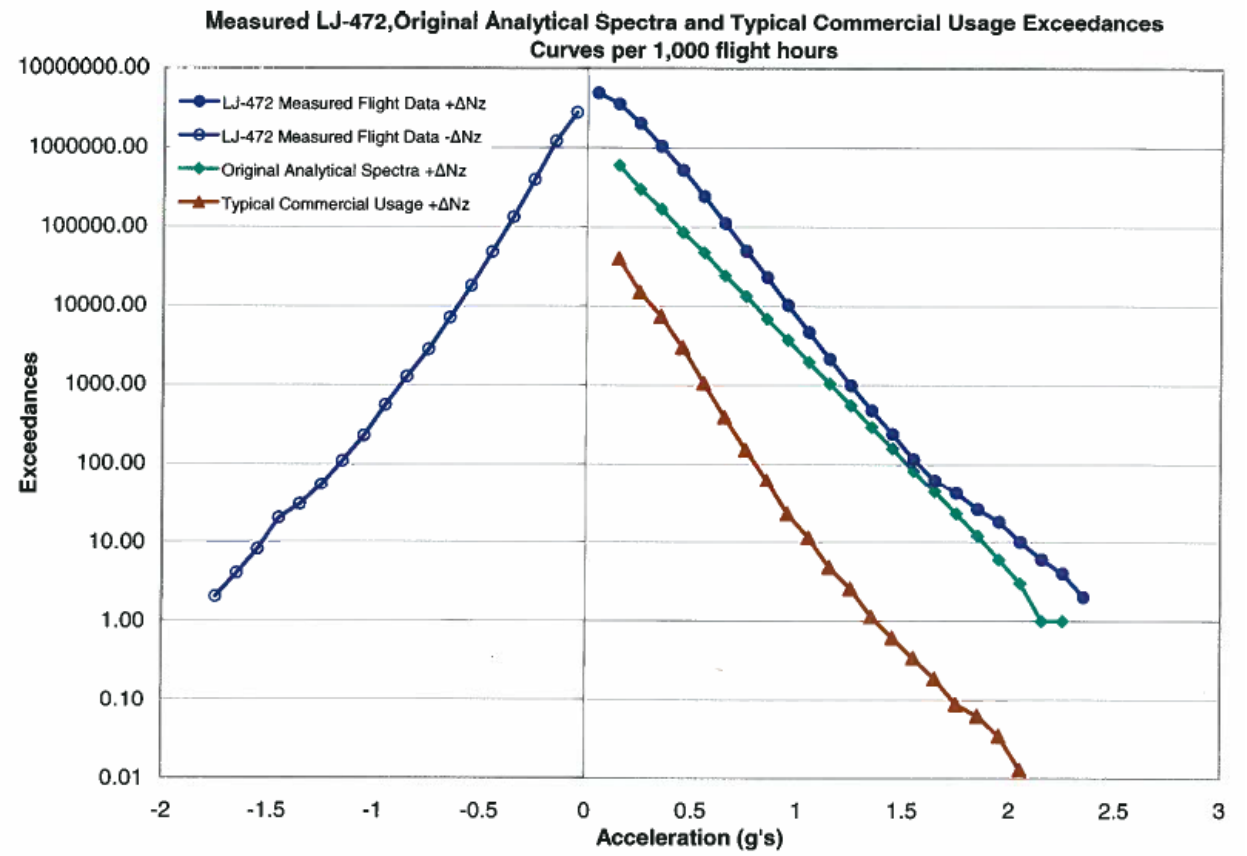

Figure 1. Loads spectra, from [5]

Mission definition, phase profiles, and gust and maneuver load separation would be performed in the course of this investigation. The deliverables were to include the:

- Examination of the recorded data thoroughly for completeness and making recommendations concerning future improvements of the recorded information.
- Separation of the available data into groups according to mission type.
- Definition of various flight phases within each mission type and dividing the data accordingly.
- Determination of the statistical usage information within each flight phase and for the entire flight for each mission type.
- Comparison of the usage data with the limitations outlined by the manufacturer.
- Separation of the normal load factors due to gusts and maneuvers within each flight phase and for the entire flight for each mission type and showing the results in the form of exceedance spectra.
- Presentation of the results at appropriate venues.
- Submission of a final report containing the method of analysis and the associated results.

The statistical formats used for presenting the results are those developed and used earlier by University of Dayton Research Institute (UDRI) and the authors. The data presented in this form

should allow an objective examination of these parameters, affording the operators a better understanding and control of those factors that influence the structural integrity of these aircraft.

2. AIRCRAFT DESCRIPTION

The majority of the Aerial Supervision Modules (ASM) aircraft currently are Beechcraft King Airs, mostly of the 90 series. These aircraft, which were originally certified under Civil Air Regulations Part 3, support the USFS aerial firefighting missions in several roles, while operating in environments vastly different from their intended design. Some of the characteristics of the King Air 90 models equipped with DFDR are shown in table 1, with some of the limitations shown in table 2.

Table 1. King Air 90 aircraft characteristics per pilot operating handbooks

Parameter*	C90A	C90GT	E90
Aspect ratio	8.57	8.60	8.57
Maximum range at 21,000 ft and maximum TO weight (nm)	1,317	1,321	1,624
Maximum rate of climb (fpm)	2,155	2,200	1,870
Maximum cruise speed (KIAS)	226	226	226
Stall speed at max. weight with flaps up (KIAS)	88	88	88
Certified maximum altitude (ft)	31,500	30,000	31,000
Fuel capacity (gallons)	384	384	474
Typical empty weight (lbs)	6,045	6,950	5,876
Maximum takeoff weight (lbs)	9,650	10,100	10,100

* [6–7]
KIAS = Knots indicated airspeed

Table 2. Operational limitations per pilot operating handbooks

Aircraft Model	V_{MO} (KIAS) Flaps Up	V_{FE} (KIAS) Flaps Extended Approach/Full	Max n_z (g) Flaps Up	Max n_z (g) Flaps Extended	Min n_z (g) Flaps Up	Min n_z (g) Flaps Extended
C90A	226	184/148	3.29	2.00	-1.33	0.00
C90GT	226	184/148	3.29	2.00	-1.33	0.00
E90	226	174/130	3.70	---	-1.68	---

These aircraft are used in a variety of missions in firefighting operations. These missions are outlined below.

- ASM/lead missions: In the lead role, the aircraft is used to lead air tankers into and out of the retardant drop site. One air tanker is led in each pass, with each mission consisting of multiple passes. The air tanker's type and performance are taken into account, and each pass can be made between 60 and 200 ft above the terrain. In the ASM role, the aircraft has an Air Tactical Group Supervisor (ATGS) on board. The aircraft can be used as a lead plane or an ATGS platform during the mission.
- Air-Tac/ATGS missions: The aircraft is flown with two crew members and is used in loiter mode above the fire site. The purpose is to coordinate all air traffic in and out of the fire traffic area, and coordinate aviation operations in conjunction with the ground resources. These missions are usually flown at altitudes higher than the ASM/Lead missions, typically 2000–2500 ft above ground level (AGL). In addition, they are flown at relatively low loiter airspeeds.
- Ferry/passenger missions: The aircraft is simply transported from one base to another with little maneuvering. A typical mission consists of one takeoff, one cruise, and one landing. Cruise altitudes and airspeeds can reach 25,000 ft and 250 KIAS, respectively.
- Unusual attitude flights: In these flights, the aircraft may or may not be used in firefighting operations. In some short flights, the pilot simply departs an airport, flies a pattern, and lands at the same airport. Some longer flights resemble a ferry/passenger mission but include some in-flight maneuvers that do not resemble those done in ASM/lead or Air-Tac missions, but entail large attitude excursions.

In many instances, combinations of missions are flown. For example, an aircraft can be flown in a lead mission, but act as air traffic control while waiting for the tankers to return after refilling.

3. DATA COLLECTION AND EDITING

3.1 FLIGHT DATA

Operational data were collected from DFDR developed by Appareo Systems. Seven aircraft were instrumented, and data collection began in 2009. The USFS placed the data in a library managed by the company HBM nCode. WSU downloaded these files from the library and translated them from the company's proprietary .s3t format into .csv format. Codes were written for processing and analyzing the data.

The data presented in this report were collected from 2009–2014. A summary of the type of data and number of flight files for each aircraft is shown in table 3. In this table, the identification has been omitted, and the aircraft have been simply numbered. A total of 4844 flight files was available for analysis (see table 3). However, examination of these files for data integrity resulted in dismissing close to 1000 files. In addition, some files contained data from multiple flights. These factors resulted in 3829 flights representing 7076 hours of airborne operations, covering 1,290,516 nautical miles.

Table 3. Summary of available flight files

Year	Aircraft							
	1	2	3	4	5	6	7	Total
2009	160	195	152	240	250	205	8	1210
2010	150	122	148	177	133	0	107	837
2011	161	20	150	197	115	0	72	715
2012	161	71	137	153	187	0	0	709
2013	149	51	152	114	144	3	0	613
2014	173	49	190	120	124	104	0	760
Total	954	508	929	1001	953	312	187	4844

3.2 RECORDED DATA

Data recorded by the DFDR are shown in table 4. The data were recorded at a fixed rate of 8 Hz. Appareo Systems records data that allow simulation of the flights. Therefore, the information that was collected was related to guidance and navigation. However, the data also contained airframe accelerations along all three axes and all three rotation rates. The system did not record propulsion information or angular accelerations. In addition, the squat switch was not always reliable. Flap-deflection information was added after the 2013 season. Therefore, only the data from the 2014 season contained this information. A binary channel was used for flap deflection, which indicated whether the flaps were down or up.

Table 4. Parameters recorded by the DFDR

Channel	Parameter	Units
1	Line number	---
2	Elapsed time	Seconds
3	Bay door[2]	Binary
4	Discretes[2]	Binary
5	GPS latitude	Degrees
6	Elevation	Feet
7	GPS longitude	Degrees
8	Pitch	Degrees
9	Roll	Degrees
10	GPS speed	Knots
11	Vertical speed[1]	Feet per minute
12	Heading	Degrees
13	Pitch rate	Degrees per second
14	Roll rate	Degrees per second
15	Yaw rate	Degrees per second
16	Longitudinal acceleration	G
17	Lateral acceleration	G
18	Normal acceleration	G
19	True airspeed[1]	Knots
20	Equivalent airspeed[1]	Knots
21	Indicated airspeed	Knots
22	Course direction	Degrees
23	Pitot pressure	Inches of mercury
24	Static pressure	Inches of mercury
25	Outside air temperature	Degrees Celsius
26	Horizontal accuracy[2]	Millimeter
27	Vertical accuracy[2]	Millimeter
28	Weight on Wheels[3]	Binary
29	Discrete1[3]	Binary
30	Discrete2[2]	Binary
31	Discrete3[4]	Binary
32	Discrete4[2]	Binary

GPS = Global Positioning System
[1] Quantities calculated in post processing
[2] Did not contain any useful information, or data were a duplicate of another channel
[3] Squat switch data could be in either, both, or neither of these channels
[4] Showed flap deflection in the 2014 data, otherwise did not contain useful information

The system did exhibit some anomalies. These include:

- The squat switch information was sometimes in the "Weight on Wheels" channel, and other times it was in the "Discrete1" channel. Certain files had the information in both of those columns. However, some files did not contain squat switch information in either the "Weight on Wheels" or the "Discrete1" channel.
- The squat switch information was sometimes unreliable. The instant when the discrete signal changed could differ from the actual takeoff or landing point by several seconds.
- The data in the nCode library were in a few different formats. The basic format is shown in table 4. At a certain date, the data began to have an additional column titled "Time Offset," which mirrored the "Elapsed Time" information. At another date, the "Weight on Wheels" column was eliminated, although the "Discrete1" column still had squat switch information.

4. WSU DATA PROCESSING

4.1 FILTERING

The noise in the recorded data prevented clear identification of various altitudes. Therefore, the recorded altitude was filtered using a 2-second running average.

4.2 DERIVED AND EXTRACTED PARAMETERS

Some information could be extracted or derived from the time history of other parameters. In those cases when aircraft parameters had to be derived, the values used were those that best represented the fleet of aircraft. Issues pertaining to specific calculations and the derivations of the required parameters are described in the following subsection.

4.2.1 Identification of Liftoff and Touchdown

For the analysis, the liftoff and touchdown point had to be determined. The squat switch information was available for a majority of the files. However, sometimes the squat switch indicated takeoff or landing points that were erroneous. Therefore, the squat switch alone could not be used to find liftoff and touchdown points. Instead, the points were found using a combination of three different variables: the squat switch, the AGL altitude, and the indicated airspeed.

To find the liftoff point, the instant that the discrete signal changed was examined. If the indicated airspeed at that instant was between 95 knots and 120 knots, that was called the liftoff point. If the squat switch changed when the indicated airspeed was less than 95 knots, then the discrete signal was ignored, and the liftoff point was defined as the instant when the airplane was traveling at 95 KIAS. If the airspeed was greater than 120 KIAS when the squat switch changed, the discrete signal was also ignored, and liftoff was defined as when the indicated airspeed was 95 knots. If the squat switch information was not available for the file, then the liftoff point was defined as the instant when the indicated airspeed was 95 knots. If the file began with an indicated airspeed greater than 120 knots, it was considered an incomplete flight because the aircraft must already be off the ground.

The landing point was also found by examining the instant that the squat switch signal changed. If the indicated airspeed was between 70 knots and 80 knots at the instant the squat switch changed, it was considered the touchdown. If the airspeed was greater than 80 KIAS or less than 70 KIAS when the squat switch changed, the discrete channel was ignored. In those cases, the landing was found by determining the instant when the indicated airspeed was between 70 knots and 80 knots, the AGL altitude was less than 100 ft, and the average AGL altitude for the next 5 seconds was less than 100 ft. If the file ended shortly after touchdown, and the average AGL altitude could not be found for a full 5 seconds, the average was found for as much time was remaining. If the last line of the file had an indicated airspeed between 70 knots and 80 knots, it was taken to be the landing point, even if the AGL criteria were not met. If the last line of the file had an indicated airspeed greater than 100 knots, it was probable that the aircraft had not landed, and it was considered an incomplete flight.

The squat switch signal was used to define both the liftoff and touchdown points or was used for neither. This criterion was because of the notion that the squat switch signal was reliable or it was not.

4.2.2 Flight Distance

Flight distance was found by integration of the true airspeed and by calculation of the great-circle distance based on Global Positioning System (GPS) coordinates of the departure and arrival points. However, the latter was used only for separation of ferry flights from other missions.

$$D = \sum_{t_{liftoff}}^{t_{touchdown}} V_T \left(\Delta t \right) \tag{1}$$

where:

D	=	distance
V_T	=	true airspeed
Δt	=	time increment

In the absence of additional information, the indicated airspeed was assumed to be the same as calibrated airspeed. Because the airspeeds were not large enough to require inclusion of compressibility effects, true airspeed was derived from the indicated airspeed using the ratio of air densities; that is:

$$V_T = V_C \sqrt{\frac{\rho_0}{\rho}} \approx V_i \sqrt{\frac{\rho_0}{\rho}} \tag{2}$$

where:

V_C	=	calibrated airspeed
V_i	=	indicated airspeed
ρ_0	=	sea level air density
ρ	=	local air density

The outside air temperature and pressure were among the recorded parameters. Therefore, the corresponding air density could be calculated from

$$\rho = \frac{P}{\overline{R}T} \tag{3}$$

Where:

P = Local absolute pressure (lbf/ft^2)
$\overline{R}$ = 1716 ft-lbf/slug-°R, specific gas constant for air
T = Local absolute temperature (°R)

The true airspeed calculated using this method closely matched the true airspeed provided in the data files. Consequently, the true airspeed in the data files was used for analysis.

4.2.2.1 Great-Circle Distance

GPS locations were recorded in the form of degrees given to five decimal places. This resolution of the angles corresponded to a 60 ft resolution in position. The method outlined in appendix B of FAA Report AR-04/44 [8] was used to convert the GPS data into distances. The GPS coordinates of the aircraft before takeoff and after landing were used to find the direct distance between the two airports.

4.2.3 Flight Duration

The flight duration was defined as the time from aircraft liftoff to touchdown.

4.2.4 AGL Altitude

Mean sea level (MSL) altitude was available in the recorded parameters. However, for definition of takeoff and landing points and lead runs, the AGL altitude was more useful. AGL altitude could also help in better understanding of the nature of the mission. One example is shown in figure 2, in which the crew makes multiple passes very close to the side of a hill whereas the MSL altitude remains above 1500 ft. Prior to any analysis, the GPS coordinates were used to determine the local terrain elevation to within 30 ft. from the National Elevation Dataset, maintained by the US Geological Survey.

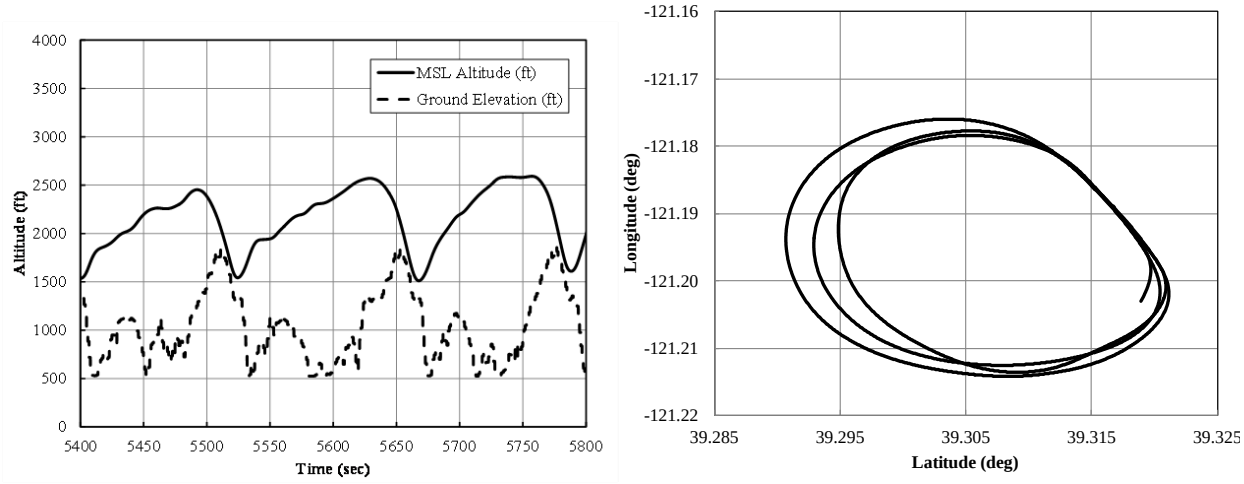

(a) Elevation

(b) Top view of the flight path

Figure 2. Example of comparison of MSL altitude and ground elevation: (a) elevation and (b) top view of the flight path

The GPS latitude and longitude were available in the recorded parameters. Knowing the latitude and longitude, the ground elevation could be found by querying a reliable database. The first option was the Google™ Earth elevation database. The second option was the National Elevation Dataset (NED), which is produced and maintained by the United States Geological Survey (USGS).

The elevation data obtained from Google Earth were compared with the NED for accuracy purposes. Twenty-four flight files were chosen at random. A single instant was also chosen at random within each flight file. Using the recorded latitude and longitude at each instant, the ground elevation was found using Google Earth and NED. The ground elevations are shown in table 5, along with the difference between the Google Earth and NED. The difference between the two elevations never exceeded 20 ft. The average difference between the two elevations was less than 1 ft, and the standard deviation was approximately 5.5 ft.

Based on the data shown in table 5, Google Earth and NED were both deemed acceptable for obtaining ground elevation. However, Google Earth had a daily query limit; thus, NED was chosen to obtain ground elevations for all of the flights.

Given the quantity of flight data that had to be processed, it was decided to find the ground elevation of every eighth entry in the files. Because the data were recorded at 8 Hz, this would result in finding the ground elevation every second during the flight. At a cruise speed of 200 KIAS, this resulted in one ground elevation for every 340 ft traveled. This increased the file-processing speed considerably. The ground elevations for the other lines of data were found by interpolation, assuming a linear variation between points.

Table 5. Elevations found using Google Earth and the USGS NED

Google Earth Ground Elevation (ft)	USGS NED Ground Elevation (ft)	Difference (ft)
5369.88	5370.49	-0.60
7771.69	7767.87	3.82
7479.59	7476.80	2.79
7815.38	7826.38	-11.00
7748.69	7745.30	3.39
7640.71	7643.13	-2.42
7465.08	7458.07	7.01
7646.26	7642.75	3.51
7649.62	7645.76	3.86
7761.47	7762.57	-1.09
7013.12	7031.74	-18.62
7730.32	7730.12	0.20
7328.53	7328.03	0.50
7764.19	7770.58	-6.39
7738.75	7740.88	-2.13
7464.00	7455.52	8.48
6805.86	6801.39	4.47
6864.84	6864.67	0.16
7742.02	7741.16	0.87
7806.11	7805.75	0.36
7245.29	7239.32	5.96
6930.66	6931.56	-0.90
5684.45	5684.15	0.30
5304.63	5304.85	-0.23
Average Difference		0.10

4.2.5 Derived Gust Velocities

Derived gust velocities were calculated from measured normal accelerations, but only for vertical gusts. For these calculations, air density was estimated from equation 3. Equivalent airspeed was determined from:

$$V_e = V_T \sqrt{\frac{\rho}{\rho_0}} \tag{4}$$

where:

V_e = equivalent airspeed (ft/s)

With this information, derived gust velocity was computed from the values of incremental normal gust acceleration as:

$$U_{de} = \frac{\Delta n_z}{\overline{C}} \tag{5}$$

where:

U_{de} = derived gust velocity (ft/s)

Δn_z = incremental vertical load factor (g)

The aircraft response factor, $\overline{C}$, was calculated from:

$$\overline{C} = \frac{\rho_0 V_e C_{L_\alpha} S}{2W} K_g \tag{6}$$

ρ_0 = 0.002377 slug/ft^3, standard sea level air density

V_e = equivalent airspeed (ft/s)

C_{L_α} = aircraft lift-curve slope (per radian)

S = wing reference area (ft^2)

W = 7640 lb, typical operating weight

K_g = $\frac{0.88\mu}{5.3+\mu}$, gust alleviation factor

μ = $\frac{2W}{\rho g \bar{c} C_{L_\alpha} S}$, reduced mass

ρ = air density at altitude from equation 3

g = 32.17 ft/s^2, acceleration of gravity

$\bar{c}$ = wing mean geometric chord (ft)

Average weight, W, was calculated assuming 60% fuel and two crew onboard. Following the procedure used in Etkin [9], aircraft lift-curve slope, C_{L_α}, was determined from:

$$C_{L_\alpha} = C_{l_{\alpha,wb}} \left[1 + \frac{C_{l_{\alpha,t}}}{C_{l_{\alpha,wb}}} \frac{S_t}{S} \left(1 - \frac{\partial \varepsilon}{\partial \alpha} \right) \right] \tag{7}$$

where:

$C_{l_{\alpha,wb}}$ = wing lift-curve slope (1/rad)

$C_{l_{\alpha,t}}$ = horizontal tail lift-curve slope (1/rad)

S_t = horizontal tail area (ft^2)
S = wing area (ft^2)
$\frac{\partial \varepsilon}{\partial \alpha}$ = rate of change of downwash at the tail due to the wing, given by [10]

$$\frac{\partial \varepsilon}{\partial \alpha} \approx \frac{0.349 C_{l_{\alpha,wb}}}{\lambda^{0.3} A_r^{0.725}} \left(\frac{3\overline{c}}{l_t'} \right)^{0.25} \tag{8}$$

where:

λ = wing taper ratio
A_r = wing aspect ratio
$\overline{c}$ = wing mean geometric chord (ft)
l_t' = distance between the wing and the horizontal tail aerodynamic centers (ft)

In all of the above expressions, from Roskam [11], assuming thin airfoils with lift-curve slopes of 2π per radian, the wing and the tail lift-curve slopes were found from:

$$\left(C_{l_\alpha} \right)_{\text{Wing or tail}} = \frac{2\pi A_r}{\sqrt{2 + \left[4 + A_r^2 \beta^2 \left(1 + \frac{\tan^2 \Lambda}{\beta^2} \right) \right]}} \tag{9}$$

where:

A_r = b^2 / S, aspect ratio
b = span (ft)
β = $\sqrt{1 - M^2}$, compressibility effect
M = V_T / a, flight Mach number
Λ = wing quarter-chord sweep angle
a = $\sqrt{\gamma \bar{R} T}$, local speed of sound (ft/s)

4.3 DATA MANAGEMENT

All downloaded data were initially screened for observable anomalies, such as missing or incomplete data fields and cases in which readings did not appear to be correct. These files were separated from those used for analysis. In all, a total of 4844 data files were available. However, close to 1000 data files were determined to have erroneous information and were not used. These were placed in the "BAD DATA" folder. The files with useable information were placed in the "GOOD DATA" folder and totaled 3829 flights.

Flight files were identified as "BAD DATA" for any of the following reasons:

- They contained only ground operations, which were not analyzed for this study.
- They were incomplete (i.e., the file began or ended when the airplane was in the air).
- The data consisted of repeated blocks of lines. This would result in multiple lines of data that were identical although they appeared to have been recorded ⅛ second apart.

- They had erroneous indicated airspeeds. In those files, the airspeed would fluctuate 20–30 knots between two lines of data that were recorded ⅛ second apart.
- The data exhibited error in the vertical acceleration. In those files, the vertical acceleration would be greater than 3.0 g for one data entry, whereas data on either side of that entry were close to 1.0 g. It was deemed improbable that the airplane experienced that magnitude of vertical acceleration for ⅛ second.

Because of the above issues, not all flight data files were used in assembling the statistical information. In general, the percentage of the files that were eliminated from analysis was small and decreased over time. In 2009, the useful files consisted of only 48% of the data. This percentage increased rapidly to 94% in 2010 and remained in that vicinity.

4.4 DATA REDUCTION CRITERIA

4.4.1 Phases of Flight

First, the ferry/passenger flights were identified. This was done by finding the direct distance between the takeoff and landing GPS coordinates and dividing them by the flight duration. If the resulting speed was greater than 150 knots, the flights were categorized as ferry/passenger. These flights should most resemble those for which the airplane was designed, typically containing one each of climb, cruise, and descent. Therefore, these flights were used as baselines for comparison.

Many of the remaining flights contained a combination of missions. Therefore, the individual missions could not be recognized and separated consistently. Therefore, the remaining flights were divided into specific airborne phases, as shown schematically in figure 3.

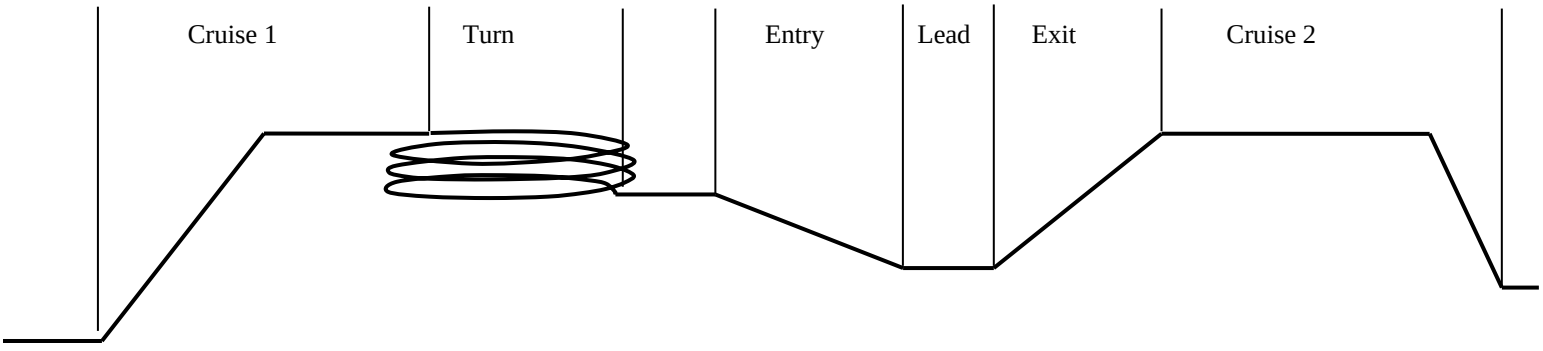

Figure 3. Airborne phases of firefighting missions

Because not all files contained ground operation data, only airborne phases were considered for this report. These airborne phases consisted of:

- Cruise 1
- Entry into a lead
- Lead
- Exit from a lead
- Turn
- Cruise 2

The lead phase was determined from the portions of the flight in which the airplane had an AGL altitude of less than 300 ft and an absolute rate of climb of less than 250 fpm for a minimum of 2 seconds. This logic would miss the lead phases if they were flown up or down a slope requiring more than ±250 fpm rate of climb. The entry into and the exit from the lead phase were based on duration alone. Entry was defined as the portion of flight 60 seconds before the lead phase began. Exit was the 60 seconds after the lead phase ended. If several leads happened in succession, these three phases would begin to overlap. Therefore, if lead phases occurred within 2 minutes of each other, the phases were combined to form one long lead phase with a single entry and exit.

During a turn, the aircraft circled with no straight flight portions. To be categorized as a turn, the aircraft had to have a continuous change in heading, with the total change greater than 360º. The end of the turn was when the heading remained constant or changed in the opposite direction for more than 2 seconds.

Cruise 1 started at the takeoff point and ended at either the first entry or the first turn. The start time for Cruise 2 was the end time of the last exit or the last turn in the flight. Cruise 2 ended at the landing. Cruise 1 and Cruise 2 contained climbs and descents as well as any maneuvers not categorized as an entry, lead, exit, or turn.

Each phase could occur several times per flight, each time that the criterion was met. Therefore, many flights had numerous entry, lead, exit, and turn phases.

4.4.2 Computer Programs

All analysis was performed using FORTRAN codes developed in-house at WSU. Overall usage information was determined for takeoff to landing. This information was deemed most pertinent to determining the number of ground-air-ground (GAG) cycles. However, usage information was also extracted per flight phase to pinpoint the specific characteristics of each phase.

4.4.3 Sign Convention

Acceleration data were recorded in three directions: normal (z), longitudinal (x), and lateral (y). As shown in figure 4, the positive z direction is up, and the positive x direction is forward.

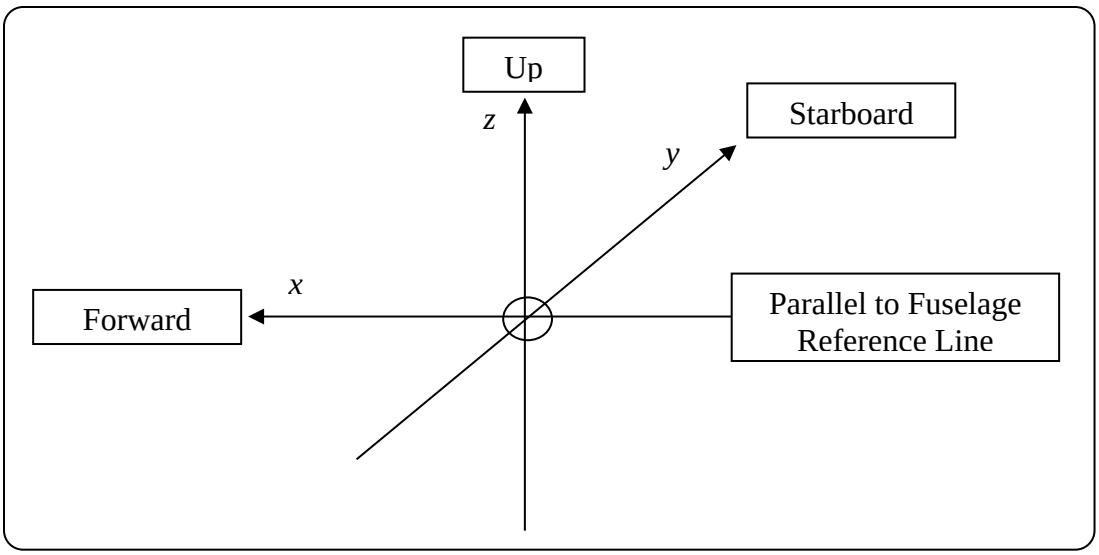

Figure 4. Sign convention for airplane accelerations

4.4.4 Peak and Valley Selection

The peak-between-means method of FAA report CT-94/57 [12] was used to select the peaks and valleys in the acceleration and derived gust velocity data. This method is consistent with past practices and pertains to all accelerations, whether due to gusts or maneuvers. In this method, only one peak or valley is counted between two successive crossings of the mean. A threshold zone (dead band) is used in the data reduction to ignore irrelevant load variations around the mean. This is shown schematically in figure 5. The same dead band values were used for gusts and maneuvers. The dead bands associated with the loads and the derived gust velocities are shown in table 6.

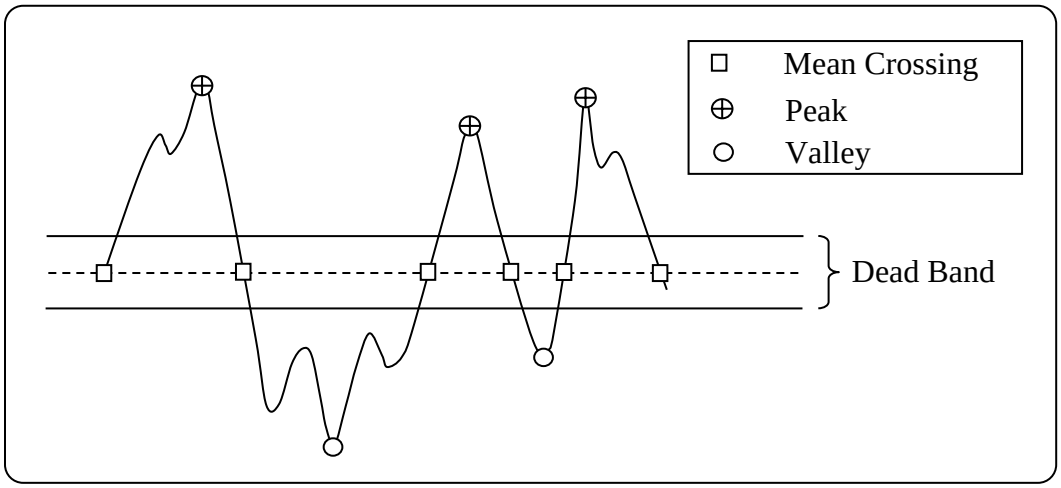

Figure 5. Peak-between-means classification of loads

Table 6. Peak-valley dead band limits

Parameter (Units)	Dead Band Width
Incremental vertical acceleration (g)	±0.050
Derived vertical gust velocity (ft/s)	±2.00

4.4.5 Separation of Maneuver and Gust Load Factors

The incremental acceleration measured at the center of gravity (c.g.) of the aircraft may be the result of either maneuvers or gusts. To derive gust and maneuver statistics, the maneuver-induced accelerations and gust-response accelerations had to be separated from the total acceleration history. FAA report AR-99/14 [13] published the results of a UDRI study to evaluate methods of separating maneuver and gust load factors from measured acceleration time histories. As a result of this study, it was recommended and accepted by the FAA that a cycle duration rule be used to separate gusts and maneuvers. A cycle duration of 2 seconds was recommended for use with B-737 and MD-82/83 aircraft. Review of the King Air 90 response characteristics has shown that this cycle duration can also be used for the data presented in the study. To avoid the inclusion of peaks and valleys associated with very small load variations that are insignificant to the aircraft structure, a dead band zone of $\Delta n_z = \pm 0.05$ g was established. An algorithm was then developed to extract the acceleration peaks and valleys.

For the airborne phases, the cumulative occurrences of incremental load factors were determined as cumulative counts per nautical mile and cumulative counts per 1000 hours using the peak-between-means counting method of FAA report CT-94/57 [12], as explained in the previous section.

4.4.6 Altitude Bands

Data were plotted in altitude bands. For the results shown in this document, the focus was on the AGL altitude because the airplane could have quite a large pressure altitude while flying very close to the ground. The data were plotted in AGL or MSL altitudes, as shown in table 7. Pressure altitude was used for usage data, whereas AGL and MSL altitudes were used for presentation of flight loads. The derived gust velocities correlated best with AGL altitudes.

Table 7. MSL and AGL altitude bands

Bands	Altitude (ft)
1	< 500
2	501–1,500
3	1,501–4,500
4	4,501–9,500
5	9,501–14,500
6	14,501–19,500
7	19,501–24,500
8	> 24,501

5. USAGE DATA PRESENTATION

This section focuses on the discussion of the results associated with aircraft usage. Overall usage is presented first, followed by the discussion of the individual airborne phases. The list of figures pertaining to this section is given in table 8, with the associated figures presented in appendix A.

Table 8. Statistical formats—usage data

Aircraft Usage Data	Figure
OVERALL FLIGHT	
Summary of durations and distances, overall flight	A-1
Summary of durations and distances, ferry flights	A-2
Percentage of flights based on flight duration, overall flight	A-3
Flight duration and coincident flight distance, overall flight	A-4
Flight duration and coincident flight distance by model, overall flight	A-5
Maximum altitude and coincident flight distance, overall flight	A-6
Maximum altitude and coincident indicated airspeed, overall flight	A-7
Maximum altitude and coincident indicated airspeed by model, overall flight	A-8
Maximum indicated airspeed and coincident altitude, overall flight	A-9
Maximum indicated airspeed and coincident altitude by model, overall flight	A-10
Cumulative probability of pitch angle, overall flight	A-11
Average and standard deviation of maximum and minimum pitch angle, entire flight	A-12
Maximum and minimum pitch angle, overall flight	A-13
Cumulative probability of roll angle, overall flight	A-14
Average and standard deviation of maximum and minimum roll angle, entire flight	A-15
Maximum and minimum roll angle, overall flight	A-16
Cumulative probability of rate of climb, overall flight	A-17
Average and standard deviation of maximum and minimum rate of climb, entire flight	A-18
Maximum and minimum rate of climb, overall flight	A-19
Summary of durations and distances, overall flight without flap information	A-20
V-n diagram, overall flight without flap information	A-21
V-n diagram by model, overall flight without flap information	A-22
Summary of durations and distances, overall flight with flap information	A-23
V-n diagram, overall flight with flaps retracted	A-24
V-n diagram by model, overall flight with flaps retracted	A-25
V-n diagram, overall flight with flaps deflected	A-26

Table 8. Statistical formats—usage data (continued)

Aircraft Usage Data	Figure
V-n diagram by model, overall flight with flaps deflected	A-27
Summary of the number of flights containing unusual attitudes	A-28
Summary of durations and distances for unusual attitude flights	A-29
Summary of durations and distances for unusual attitude flights by model	A-30
Maximum and minimum pitch angle for unusual attitude flights	A-31
Maximum and minimum roll angle for unusual attitude flights	A-32
Maximum and minimum rate of climb for unusual attitude flights	A-33
V-n diagram for unusual attitude flights without flap information	A-34
CRUISE 1 PHASE	
Summary of durations and distances, Cruise 1 phase	A-35
Percentage of phases based on duration, Cruise 1 phase	A-36
Flight duration and coincident flight distance, Cruise 1 phase	A-37
Maximum altitude and coincident flight distance, Cruise 1 phase	A-38
Maximum altitude and coincident indicated airspeed, Cruise 1 phase	A-39
Maximum indicated airspeed and coincident altitude, Cruise 1 phase	A-40
Cumulative probability of pitch angle, Cruise 1 phase	A-41
Cumulative probability of roll angle, Cruise 1 phase	A-42
Cumulative probability of rate of climb, Cruise 1 phase	A-43
V-n diagram, Cruise 1 phase	A-44
CRUISE 2 PHASE	
Summary of durations and distances, Cruise 2 phase	A-45
Percentage of phases based on duration, Cruise 2 phase	A-46
Flight duration and coincident flight distance, Cruise 2 phase	A-47
Maximum altitude and coincident flight distance, Cruise 2 phase	A-48
Maximum altitude and coincident indicated airspeed, Cruise 2 phase	A-49
Maximum indicated airspeed and coincident altitude, Cruise 2 phase	A-50
Cumulative probability of pitch angle, Cruise 2 phase	A-51
Cumulative probability of roll angle, Cruise 2 phase	A-52
Cumulative probability of rate of climb, Cruise 2 phase	A-53
V-n diagram, Cruise 2 phase	A-54

Table 8. Statistical formats and usage data (continued)

Aircraft Usage Data	Figure
ENTRY PHASE	
Summary of durations and distances, entry phase	A-55
Maximum altitude and coincident flight distance, entry phase	A-56
Maximum altitude and coincident indicated airspeed, entry phase	A-57
Maximum indicated airspeed and coincident altitude, entry phase	A-58
Cumulative probability of pitch angle, entry phase	A-59
Cumulative probability of roll angle, entry phase	A-60
Cumulative probability of rate of climb, entry phase	A-61
V-n diagram, entry phase	A-62
LEAD PHASE	
Summary of durations and distances, lead phase	A-63
Percentage of phases based on duration, lead phase	A-64
Flight duration and coincident flight distance, lead phase	A-65
Maximum altitude and coincident flight distance, lead phase	A-66
Maximum altitude and coincident indicated airspeed, lead phase	A-67
Maximum indicated airspeed and coincident altitude, lead phase	A-68
Cumulative probability of pitch angle, lead phase	A-69
Cumulative probability of roll angle, lead phase	A-70
Cumulative probability of rate of climb, lead phase	A-71
V-n diagram, lead phase	A-72
EXIT PHASE	
Summary of durations and distances, exit phase	A-73
Maximum altitude and coincident flight distance, exit phase	A-74
Maximum altitude and coincident indicated airspeed, exit phase	A-75
Maximum indicated airspeed and coincident altitude, exit phase	A-76
Cumulative probability of pitch angle, exit phase	A-77
Cumulative probability of roll angle, exit phase	A-78
Cumulative probability of rate of climb, exit phase	A-79
V-n diagram, exit phase	A-80

Table 8. Statistical formats and usage data (concluded)

Aircraft Usage Data	Figure
TURN PHASE	
Summary of durations and distances, Turn phase	A-81
Percentage of phases based on duration, Turn phase	A-82
Flight duration and coincident flight distance, Turn phase	A-83
Maximum altitude and coincident flight distance, Turn phase	A-84
Maximum altitude and coincident indicated airspeed, Turn phase	A-85
Maximum indicated airspeed and coincident altitude, Turn phase	A-86
Cumulative probability of pitch angle, Turn phase	A-87
Cumulative probability of roll angle, Turn phase	A-88
Cumulative probability of rate of climb, Turn phase	A-89
V-n diagram, Turn phase	A-90
FLAP USAGE	
Number of flap deployments per mission type	A-91
Flap deployment per flight as a percentage of flights	A-92
Number of flap deployments per mission type	A-93
Flap deployment per flight as a percentage of flights	A-94

The percentage of the useful flight files increased rapidly as the program matured. On average, approximately 80% of the flight files contained complete flights with correct recorded data.

5.1 OVERALL FLIGHT

Total number of flights with their duration and distance are summarized in figure A-1 of appendix A. This figure shows only the information pertaining to the flights that were complete and had useful information. There were very few flight files from aircraft 7, whereas the largest number of flights was from the C90GT model. Not all flight data were from firefighting missions. Figure A-2 of appendix A shows that 1564 missions, or roughly 40% of the flights, were used to ferry the aircraft or carry passengers. For this reason, ferry flights were analyzed separately, and the results were used as a baseline for comparison whenever possible.

Flights were sorted by duration, and the results are shown in figure A-3. It is evident from this figure that the majority of the ferry flights lasted less than 2 hours, whereas it was not unusual for other missions to last more than 4 hours. In this and subsequent figures, “Other” refers to all non-ferry flights.

The correlation between distance and duration is presented in figures A-4 and A-5. In figure A-4, the results are presented for all flights, in addition to lines corresponding to average

maximum and minimum indicated airspeeds. The dashed line shows a minimum average indicated airspeed of approximately 136 KTAS, which was mostly driven by firefighting missions. The solid line shows a higher maximum average velocity that was biased by ferry missions. This can be seen more clearly when examining the data for individual models, as shown in different parts of figure A-5. Parts (a), (b), and (c) of this figure clearly show how the data from the ferry flights exhibited a much tighter correlation between distance and duration. This is evident even for the E90 model, shown in part (c), despite the scarcity of the data for this aircraft.

Figure A-6 shows maximum MSL altitude versus flight distance. For transport missions, this figure would consist of a linear part from sea level to maximum cruise altitude, joined with a flat line at the latter. In the present case, no direct correlation existed between the two parameters. This behavior was expected in light of the diversity of missions flown in these aircraft.

Maximum MSL altitudes and coincident indicated airspeeds are shown in figures A-7 and A-8. Figure A-7 shows the data from all flights in all three aircraft types. This figure indicates that in no case did the maximum altitude exceed 30,000 ft. Various parts of figure A-8 show the same data for individual aircraft types. In these parts, the results from ferry flights are separated from those of other missions. It is clear from these results that the highest altitudes reached were associated with the C90GT model. These figures also show that, with the exception of a handful of cases, maximum MSL altitudes for non-ferry missions were less than 20,000 ft.

Maximum indicated airspeeds and coincident MSL altitudes are presented in figures A-9 and A-10. Figure A-9 shows the results for all missions and all aircraft types, whereas the different parts of figure A-10 pertain to the results for individual models, with ferry missions separated from the others. It is clear from these figures that in a noticeable number of cases, the V_{MO} of 226 KIAS was exceeded. However, the maximum indicated airspeed never reached more than 10% above the limit. These figures also show that over-speeding was as likely during ferry flights as it was during other missions. However, in firefighting missions, significant numbers of flights were flown at maximum airspeeds well below 200 KIAS.

Cumulative probabilities of maximum and minimum pitch angles are shown in figure A-11 with the corresponding averages and standard deviations presented in figure A-12. Although the average values seemed reasonable, in some cases, unusual values in excess of ±30° were recorded. This behavior can be seen more clearly in figure A-13, in which each pair of points pertains to one flight. Similar trends were also present in the roll angles whose cumulative probabilities, averages of maximum and minimum, and standard deviations are shown in figures A-14 and A-15. A scatter plot of the roll angle is given in figure A-16, which shows values exceeding ±90°. The large excursions in pitch and roll angles necessitated further separation of the flights into “Normal” and “Unusual Attitudes,” which will be discussed further.

Figures A-17 and A-18 show the cumulative probabilities of maximum and minimum climb rate, which were consistent with the above results. Maximum climb rates exceeding +6000 ft/min and less than -9000 ft/min were present in the data (see figure A-19). However, the noise inherent in determining the climb rate made the very extreme values questionable.

Data collected prior to 2014 did not include any information about flap deployment. Therefore, when examining the vertical load factors and associated indicated airspeeds, it was not possible to

determine whether or not the maximum loads with flaps deployed were exceeded. Consequently, the results are presented here in two groups, depending on availability of flap information.

The distribution of the data from various airframes without flap information is summarized in figure A-20. These data were collected entirely prior to the 2014 fire season. The corresponding incremental vertical load factor versus indicated airspeed for all aircraft is presented in figure A-21. This figure shows that in one case, the maximum vertical load factor for a C90A exceeded the positive limit of +3.29 g (i.e., +2.29 g incremental). This is shown more clearly in figure A-22, which shows the *V-n* diagram for the three airframes separately. The three stall lines shown in each part of this figure correspond to gross weight (7640 lbs) and empty weight. This was necessary because the aircraft weight was not a recorded parameter. With the exception of one case in a C90A, the maximum vertical load factors remained within the limits of +3.29 g and -1.33 g.

Durations and distances flown during the 2014 season, when the flap information was available, are summarized in figure A-23. As indicated in this figure, no more data were collected from the E90 model. The following results are also divided based on whether the flaps were deployed or not. The flap signal was recorded in a binary channel and did not indicate the degree of flap deflection.

Figure A-24 shows maximum and minimum incremental vertical load factors versus indicated airspeed for C90A and C90GT models with retracted flaps. Unlike in the previous case, the maximum and minimum allowable load factors were never exceeded. The corresponding *V-n* diagrams are presented in figure A-25, which corroborate the above statement. However, examination of the results with the flaps deflected (i.e., 2014 data) (see figures A-26 and A-27) revealed many cases when the limit load factors were exceeded. The majority of these cases occurred at indicated airspeeds of 120 KIAS–170 KIAS, typical of those associated with lead missions, when the flaps are typically placed in the first detent. The Pilot Operating Handbook did not specify different load factor limits per flap detent, but it did show different values for maximum indicated airspeed for the first and the last detents. These are shown as different maximum airspeed limits in figure A-27.

Reproduction of some of the flights with unusual attitudes in a simulator revealed what appeared to be training flights or flights during check rides. In light of detection of unusual attitudes, overall flights were re-examined for such large excursion. Figure A-28 shows the number of cases in which the pitch angle or the roll angle exceeded predefined limits. Based on these results, flights exhibiting pitch angles greater than ±30° or roll angles exceeding 80° in either direction were placed in the “Unusual Attitude” category. As show in figure A-29, 147 flights fell in this category, with only 9 exceeding both limits simultaneously. The distribution of the “Unusual Attitude” flight by aircraft type is shown in figure A-30. This figure also shows that there were approximately three times as many such flights in C90GT as there were in C90A models. This is in contrast with the fact that the total number of flights in the C90GT model was twice as high as in the C90A model.

No clear correlation could be made between flight distance (or duration) and the category of flight, as indicated in figures A-31 and A-32. Flights with unusual attitude could be as long or as short as other flights. The maximum and minimum values of the rate of climb and the load factors,

presented in figures A-33 and A-34, also proved to be as likely during flights with unusual attitude as they were in normal flights.

5.2 PHASE-SPECIFIC RESULTS

The phase-specific information that is discussed here did not include ferry flights.

5.2.1 Cruise 1 Phase

The number of Cruise 1 phases, along with their total distances and durations, are shown in figure A-35. The average duration of 27 minutes for Cruise 1 is somewhat misleading in that almost 70% of these phases lasted 30 minutes or less (see figure A-36). This is consistent with the results obtained from heavy air tankers, as reported in reference 4.

Correlation between distance and duration for this phase is shown in figure A-37. Since this phase is very similar to the ferry mission, the close correlation between these two parameters was expected, as can be seen in this figure. However, no correlation could be seen between maximum MSL altitude and the distance traveled for Cruise 1, as evident from figure A-38. What is clear in this figure is that the majority of these phases were flown at relatively low altitudes.

Maximum MSL altitude and coincident indicated airspeed are shown in figure A-39. Again, no clear correlation between the two parameters could be observed, but it is clear that the majority of the flights took place at MSL altitudes lower than 12,000 ft. Conversely, maximum indicated airspeed and coincident MSL altitude are presented in figure A-40. It is clear from this figure that in a noticeable number of cases, the maximum indicated airspeed of 226 KIAS was slightly exceeded.

Cumulative probabilities of maximum and minimum pitch angle, roll angle, and rate of climb, shown in figures A-41 through A-43 did not reveal anything unusual. Incremental vertical load factors remained below +2.0 g (i.e., +3.0 g total), as shown in figure A-44, and left turns seemed to be slightly more probable than right turns.

5.2.2 Cruise 2 Phase

Both the Cruise 1 and Cruise 2 phases involve relatively simple flying, except that Cruise 1 takes place at a slightly lower wing loading. Cruise 2 phases lasted slightly less than Cruise 1 and at lower average airspeeds (see figures A-45 and A-46). However, approximately 75% of the cases lasted 30 minutes or less.

Much like Cruise 1, a relatively tight correlation was observed between distance and duration (see figure A-47), but none between maximum altitude and flight distance (see figure A-48).

No correlation could be observed between maximum MSL altitude and coincident indicated airspeed (see figure A-49). However, maximum indicated airspeed versus coincident MSL altitude (see figure A-50) showed a noticeable number of cases in which the limit airspeed of 226 KIAS was exceeded slightly. This trend was in contrast to the lower average airspeed of this phase compared with Cruise 1. The majority of these cases occurred in the C90GT.

Cumulative probabilities of the maximum and minimum pitch angle, roll angle, and the rate of climb are shown in figures A-51 through A-53. The trends in these parameters were comparable with those of the Cruise 1 phase, with slightly higher values of maximum pitch angle in the latter case. In the case of Cruise 2, the maximum bank angles were equally likely in either direction. The *V-n* diagram for this phase (see figure A-54) showed a single case of C90GT flight with a minimum incremental vertical load factor near -2.0 g and an indicated airspeed of nearly 75 KIAS. This point belonged to a flight prior to the 2014 season that had no flap indication. Therefore, further examination of this case in comparison with the airframe limitations was not quite possible.

5.2.3 Entry Phase

Distance and duration for the entry phase is summarized in figure A-55. This phase was assumed to span 1 minute immediately before the start of the lead phase. Consequently, flight distances shown in figure A-56 are closely packed. Figure A-56 shows the range of MSL altitudes at which the entry phases took place. Considering that the air tankers release their retardants at approximately 150 ft AGL, the higher altitudes shown in figure A-56 can only be attributed to the high ground elevation in the fire traffic area. The maximum altitudes associated with the entry also typically occur near the beginning of the phase.

Figures A-57 and A-58 show the correlation of MSL altitude and indicated airspeed during this phase. It is clear from these figures that the airspeeds were closely packed in the range of 100 KIAS–175 KIAS, with very few cases exceeding the upper limit.

Contrary to public perception, entry phases are flown relatively flat, with minimal maneuvering, in consideration of the heavily loaded air tanker that follows. This is quite evident in the cumulative probabilities of the maximum and minimum pitch angle, roll angle, and rate of climb given in figures A-59 through A-61. Compared with Cruise 1 and Cruise 2, the entry phases were flown with much smaller pitch and roll angles and rates of descent/climb. Left turns were slightly more likely, and the associated load factors (see figure A-62) were much smaller than those of other phases.

5.2.4 Lead Phase

Figure A-63 shows the number of the lead phases detected in the dataset and the total distance and duration flown in each aircraft. The average airspeed for the lead missions was 145 KIAS, consistent with the best drop speed for the heavier air tankers. The number of flights based on duration is depicted in figure A-64, which shows that the lead phases were less than 1 minute in more than 90% of the cases.

The lead phases were generally the most precisely flown phases, as indicated by the close correlation between distance and duration (see figure A-65). Such correlation could not be detected between maximum MSL altitude and coincident airspeed (see figure A-66), only due to the large variations in the terrain elevations. Airspeeds were very closely grouped in the range of 100 KIAS–170 KIAS, which is the optimum for retardant release (see figures A-67 and A-68).

The lead phase was also flown with the least amount of maneuvering, as demonstrated by the cumulative probabilities of the pitch angle, the roll angle, and the rate of climb (see figures A-69

through A-71). Little variations were present in these quantities. Figure A-71 clearly shows that this phase consists of almost level flight with little variation in the normal load factor (see figure A-72).

5.2.5 Exit Phase

Much like the entry phase, the exit phase was assumed to span one minute immediately following the lead phase. Consequently, all exit phases would have the same duration and almost the same distance (see figure A-73).

Similar to the previous two phases, the variations in the maximum MSL altitude during this phase (see figure A-74) was driven by the terrain elevation and the altitude at the end of the exit. Airspeeds and altitudes were very similar to those of the previous two cases (see figures A-75 and A-76).

In general, the exit phase entailed the most aggressive maneuvering so as to clear the path for the following air tanker to exit the area. In many instances, the lead pilot executes a sharp turn to assess the effectiveness of the drop. This can be seen in the larger positive pitch angles, left turns, and predominantly positive climb rates (see figures A-77 through A-79). The associated load factors were not excessive, mostly due to the lower airspeeds (see figure A-80). However, in a few cases, the normal load factor did approach +3.0 g (i.e., 2.0 g incremental).

5.2.6 Turn Phase

These phases were mostly associated with ATGS missions and entailed complete turns. A total of 20,375 turn phases averaging 3.2 minutes each were detected in the dataset (see figure A-81). Distribution of the turn phases by duration is shown in figure A-82. Clear correlation between distance and duration could be seen in this case (see figure A-83). However, maximum MSL altitude, indicated airspeed, and flight distance did not correlate (see figures A-84 through A-86).

Typically, ATGS missions are flown with a crew of two, and the person in the right seat handles communications and the traffic flow management. Therefore, the turn phases associated with the ATGS missions involve many climbs and descents and right turns. The maximum and minimum pitch angle, the roll angle, and the rate of climb shown in figures A-87 through A-89 are consistent with this type of flight. However, the results shown in figure A-88 indicated the prevalence of left turns in the data, which was counter to the authors' expectations.

Finally, the maximum and minimum incremental vertical load factors and their coincident airspeeds are presented in figure A-90. It is clear from this figure that the vertical load factor covered a broader range of values during the turn missions. The one case in which the vertical load factor exceeded the maximum value for the clean aircraft is also evident in this figure.

5.3 FLAP USAGE

Flap usage is summarized in figures A-91 through A-94. Figure A-91 shows the average number of flap deployments per 100 GAG cycles and per 100 flight hours for ferry and firefighting missions. Ferry flights are compared with firefighting mission in that the former resembles the commercial usage of these airframes. The same information is depicted graphically in

figure A-93. Ferry flights lasted an average of 1.28 hours and almost invariably included two flap deployments. As a result, the number of flap utilizations per 100 cycles and per 100 hours was nearly the same. However, firefighting missions, which included flights with unusual attitude, averaged approximately 2.24 hours each and entailed many flap extensions and retractions. Therefore, in their cases, the number of flap deflections and retractions per flight hour was almost half as much as that per GAG cycle.

Figure A-92 shows the percentage of flights in which flaps were deflected by the number of deployments. The same information is shown graphically in figure A-94. It is clear from this figure that flap deflection more than once per flight was a rare event in the case of ferry flights. However, firefighting missions entailed as many flap deployments per mission, with nearly 13% of the flights showing more than 15 events.

With this information, re-examination of flap maintenance schedules and procedures is highly recommended in firefighting environments.

6. FLIGHT LOADS BY MSL ALTITUDE

This section is devoted to the presentation of the vertical loads spectra, categorized by MSL altitude. The list of figures associated with this section is given in table 9, whereas the figures are presented in appendix B. These results are limited to the airborne phases and are void of ground loads. Phase-specific outcomes are examined first before presenting the results for the overall (i.e., GAG) flights.

Table 9. Statistical formats—flight loads data by MSL altitude

Flight Loads Data	Figure
Summary of durations and distances for all flight phases	B-1
CRUISE 1 PHASE	
Summary of durations and distances for Cruise 1 phases	B-2
Cumulative occurrences of incremental vertical gust load factor, Cruise 1 phases	B-3
Cumulative occurrences of incremental vertical maneuver load factor, Cruise 1 phases	B-4
CRUISE 2 PHASE	
Summary of durations and distances for Cruise 2 phases	B-5
Cumulative occurrences of incremental vertical gust load factor, Cruise 2 phases	B-6
Cumulative occurrences of incremental vertical maneuver load factor, Cruise 2 phases	B-7
ENTRY PHASE	
Summary of durations and distances for entry phases	B-8
Cumulative occurrences of incremental vertical gust load factor, entry phases	B-9
Cumulative occurrences of incremental vertical maneuver load factor, entry phases	B-10
LEAD PHASE	
Summary of durations and distances for lead phases	B-11
Cumulative occurrences of incremental vertical gust load factor, lead phases	B-12
Cumulative occurrences of incremental vertical maneuver load factor, lead phases	B-13
EXIT PHASE	
Summary of durations and distances for exit phases	B-14
Cumulative occurrences of incremental vertical gust load factor, exit phases	B-15
Cumulative occurrences of incremental vertical maneuver load factor, exit phases	B-16
TURN PHASE	
Summary of durations and distances for turn phases	B-17
Cumulative occurrences of incremental vertical gust load factor, turn phases	B-18
Cumulative occurrences of incremental vertical maneuver load factor, turn phases	B-19
OVERALL FLIGHT	
Summary of durations and distances for the overall flight	B-20
Cumulative occurrences of incremental vertical gust load factor, overall flight	B-21
Cumulative occurrences of incremental vertical maneuver load factor, overall flight	B-22
Cumulative occurrences of incremental vertical load factor for different types of flights	B-23

6.1 PHASE-SPECIFIC RESULTS

The number of occurrences of each phase, along with total time and distance, is summarized in figure B-1. In this figure, the sum of the numbers in each column does not equal the same parameter for the overall flight because short parts of the flight were omitted to ensure that ferry flights would be included and that the phases would not overlap. It is apparent that the majority of the data pertained to cruise phases and turns, characteristic of ATGS flights. The shortest total duration was associated with the lead phases, which typically lasted a few seconds each.

6.1.1 Cruise 1 Phase

Figure B-2 shows the distribution of the duration and distances flown within this phase per MSL altitude band. It is clear that most Cruise 1 phases were flown between MSL altitudes of 4,500 ft and 19,500 ft. Approximately 2% of the flights took place above 24,500 ft, but these were still below the maximum certified ceiling. The associated AGL altitudes corresponding to these flights are discussed in the next section.

Cumulative occurrences of incremental vertical gust load factors, per 1000 hours and per nautical mile, are shown in figure B-3. In broad terms, the effect of altitude on the frequency of the load factor can be observed in these figures. However, a clear correlation between the two is not evident in this figure. Also, because of scarcity of flight data above 19,500 ft, considerable scatter in the results can be seen in this altitude range. Cumulative occurrences of incremental maneuver load factor, presented in figure B-4, also showed similar behavior.

6.1.2 Cruise 2 Phase

The results from Cruise 2 phases are discussed here first because of their similarity with the Cruise 1 phases. Figure B-5 shows the distribution of the duration and distances flown within this phase per MSL altitude band. Whereas most of the Cruise 1 phases were flown below 19,500, the majority of Cruise 2 phases took place below 14,500 ft. Cruise 2 phases were also flown at a slightly lower average airspeed than that of Cruise 1 phases (183.8 KTAS versus 198.3 KTAS).

Figure B-6 shows the cumulative occurrence of incremental vertical gust load factors, per 1,000 hours and per nautical mile. The magnitudes and the frequencies were very similar to those of the Cruise 1 phase, as expected. Similar to the previous case, broad dependence of the frequency of the loads on altitude can be observed in this figure, without clear correlation between the two. In fact, close examination of this figure shows the vertical load factors were slightly more frequent for the altitude band of 4500–9500 ft than they were for lower bands. This is counterintuitive and can be attributed only to the fact that gust loads would correlate better with AGL altitudes. Similar trends are also evident in figure B-7, which shows the cumulative occurrence of incremental vertical maneuver load factors.

6.1.3 Entry Phase

The entry and the exit phases were based on a fixed duration and, therefore, had the exact same total duration. Total durations and distances flown in this phase, per altitude band, are shown in figure B-8. Because of the nature of this phase, the majority of the flights took place at very low altitudes. However, most of the altitudes above 4500 ft can only be attributed to higher terrain

elevations in those cases. Nevertheless, there were not enough data from altitudes above 9500 ft AGL to develop meaningful loads spectra in that range.

The cumulative occurrence of incremental gust vertical load factor (see figure B-9) indicated no altitude dependence. The results from all altitude bands, when available, nearly coincided and were slightly less frequent than those of the Cruise 1 and Cruise 2 phases. However, positive incremental maneuver load factors (see figure B-10) were more frequent than those of the other two phases.

6.1.4 Lead Phase

The total duration and distance associated with the lead phases, per altitude band, are summarized in figure B-11. Of the 16.8 hours of total time, close to 75% were flown at MSL altitudes above 4500 ft. Considering the fact that the lead phase mimics closely the drop phase of the following air tanker, this high of an altitude could only be credited to the terrain elevation.

Figures B-12 and B-13 show the cumulative occurrences of incremental vertical gust and maneuver load factors per 1000 hours and per nautical mile. Neither could be clearly correlated with the altitude, and both closely resembled those of the entry phases.

6.1.5 Exit Phase

The results from the exit phases are summarized in figures B-14 through B-16. Exit phases were separated based on duration, so the cumulative flight time in this phase was exactly the same as that of the entry phase, and the flights were distributed among the altitude bands in almost the same manner. However, the cumulative distance flown in this phase was slightly longer than that of the entry phase.

The cumulative occurrences of the incremental gust and maneuver vertical load factors per 1000 miles and per nautical mile are shown in figures B-15 and B-16. These results are also comparable with those of the previous phases. However, the cumulative occurrences of maneuver vertical load factors, per 1000 hours and per nautical mile, differed the most from the previous cases. At the same altitude, the same maneuver load factors occurred at three to four times higher frequencies. Also, several incremental load factors exceeding +1.5 g were detected in this case that were not present in the previous cases. Altogether, this outcome was expected in that during ASM/lead missions, the most aggressive maneuvering is usually associated with this phase to clear the path for the air tankers.

6.1.6 Turn Phase

This phase was assumed to be a characteristic of the ATGS missions, which are performed at altitudes higher than those of ASM/lead. However, some of the turns included in these results stemmed from exit phases in which the pilot performed a tight turn to assess the effectiveness of the drop. It is evident from figure B-17 that close to 70% of the cumulative time in this phase was spent between 4500 and 9500 ft MSL. This is in contrast with a typical ATGS altitude of 2500 ft AGL.

For incremental vertical load factors, the cumulative occurrences per 1000 hours and per nautical mile are shown in figures B-18 and B-19. Having data from a large number of turns and from close

to 1000 hours of flight time allowed relatively good definition of the exceedance spectra. However, with the exception of the turns in the lowest band, the effect of altitude on the load factors could not been seen clearly.

The distinctive difference of this phase from others was the behavior of the maneuver load factors. Figure B-19 shows the cumulative occurrences of incremental maneuver load factors. Comparing these results with those of the previous cases shows much higher frequencies and magnitudes associated with turn phases. The reader is cautioned that because of the method of separating the turn phases, some of the results from entry, lead, and exit phases may have been included here, especially at the lowest altitude.

6.2 OVERALL FLIGHT RESULTS

In this section, overall flight refers to the total airborne phase between takeoff and landing. As explained earlier, total duration and distance associated with the overall flights are not the same as the sums of the individual phases for three reasons: 1) when analyzing individual phases, certain gaps were introduced between consecutive phases to avoid overlaps; 2) in some flights, there were certain parts that could not be identified as any of the above phases; and 3) these results included those of ferry flights.

The total of durations and distances per altitude band for overall flights are summarized in figure B-20. The highest altitudes flown were below the maximum of 25,000 ft MSL, with the longest times spent between 4,500 and 14,500 ft.

Cumulative occurrences of incremental gust load factors per 1000 hours and per nautical mile are shown in figure B-21, whereas the associated maneuver load factors are given in figure B-22. In figure B-21, the effect of altitude can be seen in that the frequency of occurrence decreases with increasing altitude. This effect is more pronounced for the higher altitude bands because they are less influenced by ground proximity. Consequently, the results from the lowest five altitude bands are nearly indistinguishable. The same trends were present in the frequency of occurrence of incremental maneuver load factors shown in figure B-22. In this case, the positive load factors from the lowest five altitude bands seemed to be grouped together and apart from the results for the higher bands. At the time of writing, the source of this behavior and the reason for dependence of the maneuver loads on altitude cannot be explained.

6.2.1 Effect of Mission Type

The effect of mission type on overall loads was investigated next. Approximately 40% of the flights were used for ferry missions, but that corresponded to only 30% of the flight times. Conversely, 54% of the flights were recognized as ASM/lead or ATGS, which corresponded to 65% of the flight time. A small number of flights were placed in the unusual attitude category, based on the criteria described earlier.

Figure B-23 shows the cumulative occurrences of incremental gust and maneuver load factors, per 1000 hours and per nautical mile, for the overall flights according to mission type. The frequency of occurrence of incremental gust load factors was almost the same for normal missions and for those with unusual attitude, with much lower frequencies for the ferry missions. This behavior was

expected in that ferry missions were flown at higher altitudes than the other two and that the gust loads should be independent of the type of flying.

The effect of mission type could be seen clearly in incremental maneuver loads, which occurred at two orders of magnitude more frequently during normal and unusual attitudes than they did during ferry missions. One may argue that comparison of the maneuver loads with that of ferry missions may not be fair, but ferry missions resemble how the aircraft is used in general aviation. In either event, it is clear from these figures that flights with unusual attitudes subjected the airframe to higher load factors at higher frequencies per 1000 hours and per nautical mile. The limit of the incremental load factor in all these figures was ±2.5 g. Therefore, the one case in which a load factor of +3.7 g (see figure A-22(a)) was observed earlier is absent here.

7. FLIGHT LOADS BY AGL ALTITUDE

As with section 6, this section is devoted to the discussion of the flight loads categorized in terms of AGL altitudes. The results are presented in appendix C, and the list of associated figures is shown in table 10. These results pertain strictly to airborne phases, with the emphasis placed on missions and flight phases instead of aircraft type.

Table 10. Statistical formats—flight loads data by AGL altitude

Flight Loads Data	Figure
Summary of durations and distances for all flight phases	C-1
CRUISE 1 PHASE	
Summary of durations and distances for Cruise 1 phases	C-2
Cumulative occurrences of incremental vertical gust load factor, Cruise 1 phases	C-3
Cumulative occurrences of incremental vertical maneuver load factor, Cruise 1 phases	C-4
CRUISE 2 PHASE	
Summary of durations and distances for Cruise 2 phases	C-5
Cumulative occurrences of incremental vertical gust load factor, Cruise 2 phases	C-6
Cumulative occurrences of incremental vertical maneuver load factor, Cruise 2 phases	C-7
ENTRY PHASE	
Summary of durations and distances for entry phases	C-8
Cumulative occurrences of incremental vertical gust load factor, entry phases	C-9
Cumulative occurrences of incremental vertical maneuver load factor, entry phases	C-10
LEAD PHASE	
Summary of durations and distances for lead phases	C-11
Cumulative occurrences of incremental vertical gust load factor, lead phases	C-12
Cumulative occurrences of incremental vertical maneuver load factor, lead phases	C-13
EXIT PHASE	
Summary of durations and distances for exit phases	C-14
Cumulative occurrences of incremental vertical gust load factor, exit phases	C-15
Cumulative occurrences of incremental vertical maneuver load factor, exit phases	C-16
TURN PHASE	
Summary of durations and distances for turn phases	C-17
Cumulative occurrences of incremental vertical gust load factor, turn phases	C-18
Cumulative occurrences of incremental vertical maneuver load factor, turn phases	C-19
OVERALL FLIGHT	
Summary of durations and distances for the overall flight	C-20
Cumulative occurrences of incremental vertical gust load factor, overall flight	C-21
Cumulative occurrences of incremental vertical maneuver load factor, overall flight	C-22

7.1 PHASE-SPECIFIC LOADS

Total duration and distance flown in individual phases of firefighting missions is shown in figure C-1. Note that the totals shown in this figure pertain only to the flight phases and do not add up to the total number of hours flown. The differences stem from the fact that certain periods of flight in between phases had to be skipped to ensure that they would not overlap and that the ferry flights were excluded. The entry, the lead, and the exit phases were the shortest, whereas the turn phases required the most time.

7.1.1 Cruise 1 Phase

The durations and the distances associated with this phase, sorted by AGL altitude, are summarized in figure C-2. It is quite evident from these results that the majority of these phases (i.e., 87% of flight time) were flown at altitudes below 9500 ft.

The cumulative occurrences of incremental vertical gust load factor, per 1000 hours and per nautical mile, are shown in figure C-3. This figure shows a clear correlation between AGL altitude and the frequency of occurrence of these load factors. The absence of sufficient data at altitudes above 9500 ft resulted in significant scatter in the results and prevented establishing well-defined exceedance curves for these altitude bands.

More striking altitude dependence was observed in the cumulative occurrences of incremental maneuver load factors, presented in figure C-4, especially for positive load factors. The results in this figure seem to imply that ground proximity resulted in more aggressive maneuvering, as indicated by higher load factors at lower altitudes. In any event, the availability of a large volume of data resulted in clearly defined exceedance spectra at lower altitudes.

7.1.2 Cruise 2 Phase

The Cruise 2 phase is examined next for its similarity to the Cruise 1. Durations and distances flown in this phase for individual altitude bands are shown in figure C-5. A significant fraction of the Cruise 2 missions (i.e., 94% of flight time) was flown at altitudes below 9500 ft. Average flight speed for this phase was 183.8 KTAS, compared with 198.3 KTAS for the Cruise 1 phase.

Figure C-6 shows the cumulative occurrences of the incremental vertical gust load factors for this phase per 1000 hours and per nautical mile. These results appear identical to those from Cruise 1 (see figure C-3). The cumulative occurrences of the incremental vertical maneuver load factors (see figures C-4 and C-7) showed similar trends for the two phases.

7.1.3 Entry Phase

As a reminder, entry and exit phases were assumed to last 1 minute each. Therefore, the total durations of these phases were identical. Total duration and distance flown in this phase are summarized in figure C-8. Because of the nature of this mission, close to 95% of these phases were at altitudes of 1500 ft and lower. The average airspeed was 145 KTAS, matching most air tankers in this phase.

No significant altitude dependence was observed in the cumulative occurrences of the incremental vertical load factors from gusts or maneuvers (see figures C-9 and C-10). The entry phases were flown at a lower altitude compared with the cruise phases, and the frequency of occurrence of the maneuver load factors was slightly higher for this phase. However, cumulative occurrences of the incremental gust load factors were comparable for all three phases. This can be attributed to the lower airspeeds in the entry phase.

7.1.4 Lead Phase

Generally, each lead phase did not last longer than a few seconds and was flown very precisely, with little maneuvering. As a result, the total duration and distance associated with this phase were the least of all phases (see figure C-11).

More than 75% of these phases were flown at altitudes below 500 ft. Reliable cumulative occurrences of incremental load factors, for gusts and maneuvers, could be derived only for the lowest two of the altitude bands (see figures C-12 and C-13). The highest frequencies of occurrence of incremental load factors below +0.5 g were observed in this phase. However, the cumulative occurrences of the gust load factors were similar to those of other phases.

7.1.5 Exit Phase

As the exit phase was assumed to last 1 minute, the total duration of flight in this phase was identical to that of the entry phase (see figure C-14). More than 90% of these phases were flown at altitudes below 1500 ft.

Cumulative occurrences of the incremental gust load factors for exit phase appeared very similar to that of the previous phases (see figure C-15). However, exit phase often included turning sharply to clear the path for the following air tanker or for assessing the effectiveness of the drop. Consequently, the cumulative occurrences of the incremental maneuver load factors were slightly higher for this phase (see figure C-16). The availability of the data limited the extraction of the curves to the very lowest of the altitude bands.

7.1.6 Turn Phase

Turn phase was assumed to be a characteristic of the ATGS missions, which are performed at altitudes higher than those of ASM/lead. It is evident from figure C-17 that more than 98% of the cumulative time in this phase was spent below 4500 ft AGL, but less than 5% was flown below 500 ft AGL. It is also noteworthy that if a lead phase culminated with a complete turn to assess the effectiveness of the drop, it would be counted as a turn phase. This explains the 5% of the turns that took place in the lowest altitude band.

Figure C-18 shows the cumulative occurrences of the incremental vertical gust load factors, per 1000 hours and per nautical mile. Availability of data through the third altitude band resulted in well-defined curves in that range. Comparing these results with those of the previous cases showed that they were very similar in magnitude and frequency. However, the incremental maneuver load factors associated with this phase were higher in magnitude and frequency than any of the other phases. This can be seen clearly in figure C-19, which also shows the altitude dependence of the maneuver load factors. This figure also shows that at incremental vertical load factors greater than

+0.5 g, the frequency of occurrence in the lowest altitude band was one to two orders of magnitude higher than that in the fourth altitude band.

7.2 OVERALL LOADS

The overall GAG flight duration and distance are summarized in figure C-20. Unlike the previous cases, which were limited to firefighting missions, the data in this figure includes all flights, including the ferry missions.

Cumulative occurrences of the incremental gust load factor, per 1000 hours and per nautical mile, are shown in figure C-21. This figure clearly shows the altitude dependence of the gust load factors when the results are categorized by AGL altitudes. The influence of altitude on the frequency of occurrence of the load factors can be clearly observed down to the lowest AGL altitude. However, the scarcity of the data results in some scatter in the results for altitudes exceeding 19,500 ft.

When considering overall flight loads, maneuver loads were clearly grouped into two distinct classes above and below 14,500 ft MSL. When the results were categorized by AGL altitude, the frequency of occurrence was almost equally divided among all altitude bands (see figure C-22). The effect of ground proximity on maneuver loads was surprising.

The loads correlated better with AGL altitudes, as expected. The results are presented for both MSL and AGL altitude bands in the remainder of this document.

7.3 CONCLUDING OBSERVATIONS

The fact that gust load factors obtained from various phases were similar was not surprising. After all, these loads are due to atmospheric disturbances that should depend only on altitude and on AGL altitude. However, the dependence of the maneuver load factors on AGL altitude was surprising.

In every case, the previously presented results showed the frequency of the maneuver load factors to increase with decreasing AGL altitude. The dependence of the maneuver load factors on altitude almost implies that the flight crew fly differently based on ground proximity. However, at the time of writing, drawing a definitive conclusion is impossible, especially in light of the available information in the recorded data. Additionally, the methods used to identify various phases and to separate gust loads from maneuver loads can stand further scrutiny.

8. COMPARISONS WITH OTHER SOURCES

The results presented here were also compared with those from a number of other sources. The figures associated with this section are presented in appendix D and are listed in table 11.

Table 11. Statistical formats—comparison of loads with other sources

Load Comparisons	Figure
Cumulative occurrences of incremental vertical load factor compared with MIL 8866 maneuver loads for overall flight	D-1
Cumulative occurrences of incremental vertical load factor compared with AC 23-13A for overall flight	D-2
Cumulative occurrences of incremental vertical load factor per 1000 hours, overall flight	D-3
Summary of durations and distances for different types of flights	D-4
Cumulative occurrences of incremental vertical gust load factor for different types of flights compared with AC 23-13A	D-5
Cumulative occurrences of incremental vertical maneuver load factor for different types of flights compared with AC 23-13A	D-6
Cumulative occurrences of incremental vertical maneuver load factor for different types of flights compared with MIL 8866	D-7
Cumulative occurrences of incremental vertical load factor for different types of flights	D-8

The first were the results presented in Bernstorf [5] that were developed from a limited amount of flight data and were shown in figure 1. In this document, the loads were not divided into gust and maneuver loads, removing any uncertainty associated with the implementation of the 2-second rule. The second source was MIL 8866 in MIL-1-8866C(AS) [14]. Although this information was limited to maneuver loads of larger aircraft, it was deemed appropriate to be used here for illustrative purposes. The third source of data was AC 23-13A in FAA report AC 23-13A [15] because these aircraft were originally certified in this class. The fourth source for comparison was FAA report AR-05/35 [16], in which the flight loads from a variety of aircraft in firefighting operations were presented. Among the aircraft considered in this reference are some light twins used for ASM/lead and ATGS missions. However, the report does not explicitly state the aircraft type, but they did not include any King Air models.

Figure D-1 shows the results from the present effort compared with those of MIL 8866. Although the latter is only for maneuver loads, the gust and maneuver loads from the USFS fleet are presented separately in figure D-1. It is evident from this figure that for incremental load factors less than +1.5 g, the USFS fleet was subjected to a higher frequency of maneuver loads. Load factors above this level occurred less frequently than those set by MIL 8866.

In figure D-2, cumulative occurrences of incremental vertical load factors are compared with the guidelines from FAA report AC 23-13A [15]. As shown in the figure, maneuver loads matched AC 23-13A in the negative range, whereas the gust loads occurred with a lower frequency. The same was also true for positive gust loads. However, maneuver load factors occurred approximately two orders of magnitude more frequently than AC 23-13A guidelines. This was consistent with the results shown in figure 1 from Bernstorf [5].

Cumulative occurrences of combined gust and maneuver loads are compared with those of three other sets of results in figure D-3. In this figure, typical commercial usage is that of Bernstorf [5]. The curve for original analytical spectra is also from this reference, based on the analysis of a limited amount of data from ASM/lead and ATGS missions. The latter loads were more frequent, as expected (see figure 1). It is clear that for positive load factors, there was very good agreement between the present results and those of the previous analysis by Beechcraft. However, this figure also shows the data presented in FAA report AR-05/35 [16], which do not agree with the magnitude or trends of any of the other results. The same disagreement was also noted in the results from heavy air tankers, presented in FAA report AR-11/7 [4], and those from single-engine air tankers presented in Rokhsaz and Kliment [17]. At the time of this writing, the source of this discrepancy is not known.

Comparison of AC 23-13A with the overall gust and maneuver loads from all missions combined was presented in figure D-2. However, the results from individual missions were not clear. Figure D-4 shows the percentage of time and distance flown for each mission type. It is clear that approximately one-third of the flights consisted of ferry missions and that only a very small percentage of the flights belong in the unusual attitude category. The results for the gust loads are shown in figure D-5, in which the influence of each mission type is examined. In all cases, the gust loads were well below those of AC 23-13A in magnitude and in frequency. Cumulative occurrences of incremental vertical maneuver load factors for these missions are compared with those of AC 23-13A in figure D-6. It is clear from this figure that although the results from the ferry missions compared well with those of this document, the frequency of occurrence was roughly two orders of magnitude higher for the other missions.

In figure D-1, cumulative occurrences of maneuver loads from all missions were compared with MIL 8866. However, this figure did not show the relative contribution of various missions to the overall maneuver loads spectrum. Figure D-7 shows a comparison of the maneuver loads from various missions with MIL 8866. It is clear that the maneuver load factor associated with flights in unusual attitude exceeded those of MIL 8866 by approximately one order of magnitude in frequency.

Finally, in figure D-8, cumulative occurrences of combined maneuver and gust loads are compared with of three other references. It is clear from this figure that the only disagreement was between the results from FAA report AR-05/35 [16] and all the other results.

Three conclusions were drawn from these comparisons. The first was that firefighting missions in general subject the airframes to maneuver load factors larger than those outlined in AC 23-13A. This was an expected outcome and was consistent with the earlier estimates from Beechcraft. Second, the largest load factors appeared to be associated with flights in unusual attitude. Although the percentage of these flights was small, their resulting load factors were noticeably larger than those of other missions. Finally, although the present results are consistent with those of several other sources, the disagreement between them and those presented in FAA report AR-05/35 [16] cannot be explained at the time of this writing.

9. DERIVED GUST VELOCITIES BY MSL ALTITUDE

As the flight loads were presented by MSL and AGL altitudes separately, the derived gust velocities are also discussed consistently. This section is devoted to the presentation of the derived gust velocities categorized by MSL altitude. The associated figures are presented in appendix E, whereas the list of figures can be found in table 12. Phase-specific outcomes are presented first, followed by the results from the overall flights.

Table 12. Statistical formats—derived gust velocities by MSL altitude

Derived Gust Velocities	Figure
Cumulative occurrences of derived gust velocity, Cruise 1 phase	E-1
Cumulative occurrences of derived gust velocity, Cruise 2 phase	E-2
Cumulative occurrences of derived gust velocity, entry phase	E-3
Cumulative occurrences of derived gust velocity, lead phase	E-4
Cumulative occurrences of derived gust velocity, exit phase	E-5
Cumulative occurrences of derived gust velocity, turn phase	E-6
Cumulative occurrences of derived gust velocity, overall flight with all phases	E-7

Figure E-1 shows the cumulative occurrences of derived gust velocities for Cruise 1 phases per 1000 hours and per nautical mile. Although sufficient data were available for MSL altitudes up to 19,500 ft, only a broad dependence of the derived gust velocities on altitude can be observed in this figure. This behavior is consistent with those of incremental gust load factors that were discussed earlier. The altitude dependence is somewhat clearer for the Cruise 2 phases (see figure E-2). This figure also shows that the derived gust velocities at the lowest altitude band were more frequent than those of Cruise 1 phases. This was in contrast with the incremental vertical gust load factors that were discussed earlier. In all likelihood, this was caused by the differences in the aircraft weight between the two flight phases and the average airspeeds. As discussed earlier, Cruise 1 phases were flown at approximately 15 KTAS slower average speeds.

Cumulative occurrences of derived gust velocities for the entry phases are shown in figure E-3. Because of the nature of this phase, few data were available for higher altitude bands. The results from the remaining altitude bands were also practically indistinguishable.

The same trends were also visible in the results from the lead and exit phases (see in figures E-4 and E-5). However, the cumulative occurrences of the derived gust velocities for lead phases were slightly more frequent.

Cumulative occurrences of the derived gust velocities from the turn phases (see figure E-6) showed some resemblance to those of Cruise 2. However, the results from the turn phase extended to higher maximum values and were more frequent than those of the Cruise 2 phase.

The cumulative occurrences of the derived gust velocities per 1000 hours and per nautical mile are given in figure E-7. Availability of data allowed establishing well-defined spectra for all but the

highest altitude band. Correlation between altitude and magnitude of the derived gust velocities can be seen only in broad terms in figure E-7. Furthermore, these results appear to be divided into two categories, above and below 14,500 ft MSL. The cause of this division is not clearly understood, but it could be because terrain elevation has a stronger influence on the results from the lower altitude bands.

10. DERIVED GUST VELOCITIES BY AGL ALTITUDE

This section is devoted to the presentation of the derived gust velocities. In every case, the results are presented per 1000 hours and per nautical mile. As discussed earlier, cumulative occurrences of the incremental gust load factors correlated best with AGL altitude. Therefore, derived gust velocities were expected to behave similarly and were categorized into AGL altitude bands. The figures associated with this section are shown in appendix F and are listed in table 13.

Table 13. Statistical formats—derived gust velocities by AGL altitude

Derived Gust Velocities	Figure
Cumulative occurrences of derived gust velocity, Cruise 1 phase	F-1
Cumulative occurrences of derived gust velocity, Cruise 2 phase	F-2
Cumulative occurrences of derived gust velocity, entry phase	F-3
Cumulative occurrences of derived gust velocity, lead phase	F-4
Cumulative occurrences of derived gust velocity, exit phase	F-5
Cumulative occurrences of derived gust velocity, turn phase	F-6
Cumulative occurrences of derived gust velocity, overall flight with all phases	F-7

Figure F-1 shows the cumulative occurrences of derived gust velocities for Cruise 1 phases per 1000 hours and per nautical mile. In this case, sufficient data were available for AGL altitudes reaching 14,500 ft. Therefore, well-defined spectra could be established for the first five altitude bands, with little scatter. This was not true for flights above 14,500 ft, and although some results are shown for the higher altitude bands, the scatter in the results prevented establishing clearly defined spectra.

Cumulative occurrences of derived gust velocities for Cruise 2 phases per 1000 hours and per nautical mile are shown in figure F-2. The results from this phase are presented here to allow for side-by-side comparison with those of Cruise 1. Similar to Cruise 1, these phases were flown over a wide range of altitudes, yielding clearly defined results for the first five altitude bands or up to 14,500 ft AGL. The magnitudes and the frequencies of occurrence of these two flight phases were quite comparable.

The results for entry phases are shown in figure F-3. These phases consisted of 1 minute of flight time immediately preceding the lead phases. Therefore, they all occurred at AGL altitudes comparable with those of the lead phases. This is clear from figure F-3 in that these results were all limited to the three lowest altitude bands. Close examination of this figure also showed that the most amounts of data were associated with the first two altitude bands, resulting in spectra that

were better defined than that for the third. This material contained enough data to include derived gust velocities approaching 40 ft per second. However, the magnitudes were very comparable with those of the cruise phases in general.

Figure F-4 shows the derived gust velocity spectra for the lead phases. Because of the nature of the lead phases, the majority of these cases were flown at altitudes well below 1500 ft AGL. Consequently, results were free of scatter only for the lowest two altitude bands. Figure F-4 also shows some results from the third altitude band. It can be safely assumed that these results were either from incorrect phase recognition or flights in which the local terrain elevation changed very rapidly under the aircraft. In general, the frequency of occurrence of derived gust velocities for this phase was slightly higher than that of the preceding flight phases.

The exit phases and entry phases both lasted for 1 minute immediately following the lead phases. Therefore, they occurred at altitudes comparable with lead and entry phases. Cumulative occurrences of the derived gust velocity for the exit phases are shown in figure F-5. These results show that data were available only for the lowest three altitude bands, but even then, only 10% of the flight time was spent in the third band.

Comparison of the entry, lead, and exit phases showed close similarity among the three. All three phases were flown at comparable AGL altitudes and were therefore subjected to the same level of atmospheric turbulence. The similarity among these three phases was also evident when comparing their cumulative occurrences of gust load factors, but it did not extend into maneuver load factors that proved to be somewhat different.

The turn phases had equal probability of occurring at any of the lower altitudes. These phases were primarily connected with ATGS missions that were flown at altitudes higher than those of ASM/lead missions. Cumulative occurrences of the derived gust velocities (see figure F-6) support this fact. Sufficient data were available up to 9500 ft AGL to yield well-defined spectra. However, some of the results shown here for altitudes below 500 ft AGL were possibly the turns associated with ASM/lead missions. The highest derived gust velocity of nearly 40 ft per second was detected during one of the turn phases below 500 ft AGL.

Cumulative occurrences of derived gust velocities for overall flights per 1000 hours and per nautical mile are presented in figure F-7. The word “overall” in this context means GAG without separation of various flight phases. When considering the overall flights, sufficient data were available to arrive at well-defined results in all altitude bands, except for the highest two (i.e., above 19,500 ft AGL). It was shown in section 6 that although 5% of the overall flight time was spent at altitudes above 24,500 ft MSL, the percentage dropped to less than 1% in terms of AGL altitude.

It is clear from this figure that the results indeed correlated well with AGL altitude. As expected, the frequency of occurrence of the gust velocities decreased with increasing altitude. Derived gust velocities in excess of 25 ft per second were also associated only with altitudes below 4500 ft AGL. These results were all as expected in terms of magnitudes and frequencies, as well as correlation with AGL altitude.

11. SUMMARY

In-service recorded flight data were analyzed from a fleet of Beechcraft King Air models flown in support of the firefighting missions of United State Forest Service. The fleet consisted of three C90A, three C90GT, and one E90 models. These aircraft were flown primarily in three different roles: 1) ASM/lead; 2) Air-Tac/ATGS; and 3) ferry missions. However, a small number of flights involving unusual attitudes could not be associated with any of these missions and were therefore placed in a standalone category.

Of 4844 flight files examined, 3829 distinct GAG flights were identified, resulting in data from close to 7100 hours of flight time. Approximately 40% of the flights were used to ferry the aircraft or carry passengers. These flights were closer in nature to the general aviation mission of the aircraft and were therefore separated for comparison with the firefighting missions. The firefighting missions, which excluded ferry flights, were further divided into six distinct phases for a more refined analysis of the loads.

GAG (i.e., overall) airframe usage was studied in detail for the entire fleet and for individual models. These included examination of altitude and airspeed and their comparisons with the published limits, as well as pitch and roll angles and overall load factors versus airspeed. In a noticeable number of cases, the V_{MO} of 226 KIAS was exceeded but by no more than 10% above the limit. Over-speeding was shown to be as likely during ferry flights as it was during other missions. Nonetheless, in firefighting missions, a significant number of flights were flown at maximum airspeeds well below 200 KIAS.

The maximum vertical load factors and coincident indicated airspeeds were extracted and shown in the form of *V-n* diagrams, as were the limitations for each model. One case showed that the limit load factor of +3.29 g was exceeded in a C90A, but the negative load factors always remained within the prescribed limits. The absence of information about flap deployment in the data prior to 2014 prevented a more detailed examination of the limits in this case.

Data from the 2014 season included binary information on flap deflection and were analyzed separately. This analysis showed that, in many cases, the maximum allowable load factor was exceeded when the flaps were deployed. Most of these cases occurred in the indicated airspeed range of 120 KIAS–170 KIAS, typical of those associated with lead missions when the flaps are placed in the first detent.

There were 147 flights placed in the unusual attitude category, in which the pitch attitude reached greater than ±30° or roll angles exceeded 80° in either direction. There were approximately three times as many such flights in C90GT as there were in C90A models. The total number of flights in the former model was twice as many as those in the latter model. The percentage of flights in unusual attitude was slightly lower for the 2014 data.

Investigation of phase-specific airframe usage was limited to firefighting missions and excluded ferry flights. Cruise 1 and Cruise 2 cases showed the expected similarity with each other and with ferry missions. Clear correlation between distance and duration was quite evident in these cases, but no clear relationship between maximum MSL altitude and airspeed could be detected. In both

phases, the maximum indicated airspeed of 226 KIAS was exceeded in a noticeable number of cases but by no more than 10%.

In the absence of any other indicators, entry and exit cases were assumed to last 1 minute each, immediately before and after the lead phase. In these phases, indicated airspeeds were closely grouped in the range of 100 KIAS–175 KIAS. During the entry phases, the aircraft were flown with much smaller variations in pitch and roll angles, and the incremental vertical load factors were closely grouped in the range of ±1.0 g (i.e., 0.0 to +2.0 g total). However, the exit phase showed the most aggressive maneuvering, with incremental load factors approaching +2.0 g (i.e., +3.0 g total). The results clearly showed that during the entry, the aircraft were flown mindfully of the performance of the following air tankers, whereas the exit phases were flown so as to clear the path for the following air tankers to exit the area.

The lead phases were the most precisely flown, with little variation in pitch and roll angles or the vertical load factors. Conversely, the turn phases showed large variations in these parameters. There were 20,375 turn phases detected in the dataset.

The nature of the missions flown in these aircraft dictated a large volume of low-level flights. To identify these correctly, GPS coordinates were used to determine the local terrain elevation and therefore the altitude AGL.

Vertical load factors were divided into gust and maneuver loads using the 2-second rule. The method of peaks between means was used to count the cycles of gust of maneuver load factors and the derived gust velocities. From these, exceedance spectra were developed for the overall flights and for specific flight phases. Results were divided into various MSL and AGL altitude bands. Both sets of results were presented and discussed, but better correlation with AGL altitude bands became apparent.

Cumulative occurrences of incremental load factors per 1000 hours and per nautical mile were examined for different missions. The frequency of occurrence of incremental gust load factors was almost the same for firefighting missions and for those with unusual attitude, but was higher than those of ferry missions. However, maneuver loads occurred two orders of magnitudes more frequently during firefighting and unusual attitude cases than they did during ferry missions. Furthermore, the occurrence of much higher maneuver load factors during unusual attitude flight became evident.

For firefighting missions, different flight phases did not affect the frequency of occurrence of gust load factors. However, differences among the phases became more pronounced when considering the cumulative occurrence of incremental maneuver load factors. The maneuver loads from the two cruise phases had the lowest frequency of occurrence, whereas those of the turns had the highest. Leads, entries, and exits fell in between the others.

In every case, the results presented above showed the frequency of the maneuver load factors to increase with decreasing AGL altitude. The dependence of the maneuver load factors on altitude almost implied that the flight crew flew differently based on ground proximity.

The cumulative occurrence of gust and maneuver load factors were also compared with those from other references. It was shown that for incremental load factors less than +1.5 g, the aircraft were

subjected to a higher frequency of maneuver loads than those from MIL 8866. Gust load factors were comparable in frequency of occurrence to those indicated in AC 23-13A, but the maneuver load factors were up to two orders of magnitude more frequent than those of this document. Combined gust and maneuver loads were shown to be two orders of magnitude more frequent than those of typical commercial usage.

Spectra were also developed for derived gust velocities, for individual phases and for the overall flights. Consistent with the case of gust loads, very good correlation with AGL altitude could be seen in the results. The results from Cruise 1 and Cruise 2 phases yielded well-defined curves for AGL altitudes up to 14,500 ft. However, the results from the other phases were limited to the low AGL altitudes.

12. CONCLUSIONS AND RECOMMENDATIONS

More than 85% of the flight files collected in the course of this project were complete and contained useful information. Overall data quality was very good, although it had been collected during actual operations and in an uncontrolled environment. Collectively, sufficient data were also available from C90A and C90GT models to arrive at statistically reliable information in most cases.

The statistical data formats used in this study allowed thorough examination of various parameters related to the life cycle of the Aerial Supervision Modules (ASM)/lead aircraft. These results will be useful to the United States Forest Service and the manufacturer in better understanding and controlling the issues that impact the airworthiness of these aircraft.

The airframe usage results matched the expected outcomes, except for the following cases:

- A small percentage of flights contained relatively large pitch and roll angles that were atypical of ASM/lead or Air Tactical Supervision Modules (ATGS) missions. These flights could not be identified with any specific type of mission and, therefore, were placed in the "unusual-attitude" category. The percentage of these flights was slightly lower in the 2014 data.
- In a noticeable number of cases, the maximum indicated airspeeds were exceeded but remained within 10% of the prescribed value. These were as likely to occur during ferry flights as in firefighting missions.
- Vertical load factors did not exceed the published limitations in routine operations, with the exception of one case in a C90A. However, with the flap deflected, in a large number of flights the maximum load factor was in excess of the published limits. Almost exclusively, these occurred during firefighting flights, with the airspeeds suggesting that they were associated with ASM/lead missions. The binary nature of the information about flap deflection prevented examination of the limit airspeeds and further refinement of the loads by flap detent.

Examination of the cumulative occurrence of gust and maneuver load factors and derived gust velocities led to the following conclusions:

- The frequency of occurrence of incremental gust load factors was almost the same for firefighting missions and for those with unusual attitude, but was higher than those of ferry missions. This was a reflection of the environment in which they took place.
- Maneuver load factors occurred two orders of magnitude more frequently during firefighting and unusual attitude cases than they did during ferry missions. Furthermore, the occurrence of much higher maneuver load factors during unusual attitude flight was evident.
- The frequency of occurrence of the maneuver load factors increased with decreasing above ground level (AGL) altitude. The dependence of the maneuver load factors on altitude almost implied that the flight crew flew differently based on ground proximity.
- The cumulative occurrences of the load factors correlated more clearly with AGL altitude than with MSL altitude. Consequently, the same correlation could be seen in the altitude dependence of the derived gust velocities.

These trends deserve closer examination from the operational perspective and call for the following recommendations:

1. Standard operating procedures call for flap deployment during the entry, the lead, and the exit phases of flight. These phases are also more susceptible to overloading the structure or over-speeding due to pilot workload and the nature of the necessary maneuvers dictated by the terrain. In most cases, the associated airspeeds are large enough to bring into question the necessity of flap deflection for these maneuvers. Therefore, it is highly recommended that operating procedures be re-examined.
2. In many cases, such as leading single-engine air tankers, the slower flight speeds necessitate deploying the flaps. Therefore, the standard inspection intervals and procedures need to be modified to account for incidents of overloading the structure.
3. The degree of load factor exceedance might not be as critical for small flap deflections, typical of those used in ASM/lead missions. If that is the case, this calls for additional analysis or testing to establish various load factor limits for different flap settings.
4. At present, it is unclear whether the airspeed limits were exceeded while the flaps were deployed. Recording of the flap deflection by detent will allow for such an investigation. This will also aid in a more refined examination of the loads if various load factor limits are established for different flap settings.
5. It was clearly shown that the exceedance spectra for gust loads and derived gust velocities correlated best by AGL altitude bands. Therefore, the practice of expressing this information by MSL altitude may have to be revisited.
6. To ensure the integrity of the data, the authors recommend periodic calibration of the sensors. Throughout this report, the underlying assumption was that the recorded values were correct. Although there was strong evidence to believe that this was the case, instruments do drift, especially under daily field operation.
7. It is worth re-examining the method of analysis used in FAA report AR-05/35 [16] in light of persistent disagreements with the results it presented. It may be that the method of peaks-between-means, presented in *Beechcraft King Air E90, Pilot's Operating Manual* [7] and ASTM E 1049-85 [18] and described in this document, was not employed there.

13. REFERENCES

1. National Transportation Safety Board. (2004). *Safety Recommendations,* A-04-29 through -33.

2. US Forest Service Fire and Aviation Management. (2009). *Special Mission Airworthiness Assurance plan for Aerial Firefighting for FY 2010-2015*.

3. Bramlette, R. B., (2008). *Exploratory Flight Loads Investigation of P-2V Aircraft in Aerial Firefighting Operations,* M.S. Thesis in Aerospace Engineering, Wichita State University.

4. FAA Report. (2011). Usage and Maneuver Loads Monitoring of Heavy Airtankers (DOT/FAA/AR-11/7).

5. Bernstorf, D., "Wing Damage Tolerance Evaluation for the United States Forest Service (USFS)," Hawker Beechcraft Corp. to USFS, July 30, 2009.

6. Raytheon Aircraft Company. (2005). *Beechcraft King Air C90B (Model C90A), Pilot's Operating Handbook and Approved Airplane Flight Manual, P/N 90-590024-69B3*.

7. Beech Aircraft Corporation. (1997). *Beechcraft King Air E90, Pilot's Operating Manual, P/N 90-590012-5A5*. Wichita, Kansas.

8. FAA Report. (2005). Statistical Data for the Boeing-747-400 Aircraft in Commercial Operations. (DOT/FAA/AR-04/44).

9. Etkin, B. (1982). *Dynamics of Flight, Stability and Control* (2nd ed.). New York, NY: John Wiley & Sons.

10. Dommasch, D. O., Sherby, S. S., and Connolly, T. F. (1967). *Airplane Aerodynamics* (4th Ed.).,New York, NY: Pitman Publishing Corporation.

11. Roskam, J. (2001). *Airplane Flight Dynamics and Automatic Flight Controls – Part I, Third Printing*. Lawrence, KS: DARcorporation.

12. FAA Report. (1994).Reduction of Incremental Load Factor Acceleration Data to Gust Statistics (DOT/FAA/CT-94/57).

13. FAA Report. (1999). An Evaluation of Methods to Separate Maneuver and Gust Load Factors from Measured Acceleration Time Histories (DOT/FAA/AR-99/14).

14. Airplane Strength and Rigidity Reliability Requirements, Repeated Loads, Fatigue, and Damage Tolerance, MIL-1-8866C(AS), 20 May 1987.

15. FAA Report. (2005). Fatigue, Fail-Safe, and Damage Tolerance Evaluation of Metallic Structure for Normal, Utility, Acrobatic, and Commuter Category Airplanes (FAA AC 23-13A).

16. FAA Report. (2005). Consolidation and Analysis of Loading Data in Firefighting Operations: Analysis of Existing Data and Definition of Preliminary Airtanker and Lead Aircraft Spectra (DOT/FAA/AR-05/35).

17. Rokhsaz, K. and Kliment, L. K. (2015). *Preliminary investigation of flight loads of single-engine airtankers*, AIAA-2215-2062, Proceedings from the 56th AIAA/ASME/ASCE/AHS/ASC Structures, Structural Dynamics, and Materials Conference, Kissimee, FL.

18. ASTM E 1049-85 (Reapproved 2005) "Standard Practices for Cycle Counting in Fatigue Analysis," ASTM International, West Conshohocken, PA, 2003. doi: 10.1520/E1049-85R05

APPENDIX A—USAGE DATA PRESENTATION

Model	Airplane Number	Number of Good Flights	Duration (min)	Duration (hr)	Distance (nm)
C90A	1	815	86,584	1,443	273,638
	2	310	43,557	726	133,912
	3	253	22,326	372	68,818
C90GT	4	711	68,348	1,139	214,157
	5	794	87,445	1,457	254,199
	6	796	96,925	1,615	289,715
E90	7	150	19,352	323	56,077
Total	---	3,829	424,538	7,076	1,290,516

Figure A-1. Summary of durations and distances, overall flight

Model	Airplane Number	Number of Good Flights	Duration (min)	Duration (hr)	Distance (nm)
C90A	1	342	28,672	478	109,830
	2	88	8,202	137	30,324
	3	121	7,530	126	28,094
C90GT	4	362	26,588	443	100,360
	5	258	19,868	331	73,478
	6	315	23,465	391	91,267
E90	7	78	6,140	102	21,198
Total	---	1,564	120,464	2,008	454,551

Figure A-2. Summary of durations and distances, ferry flights

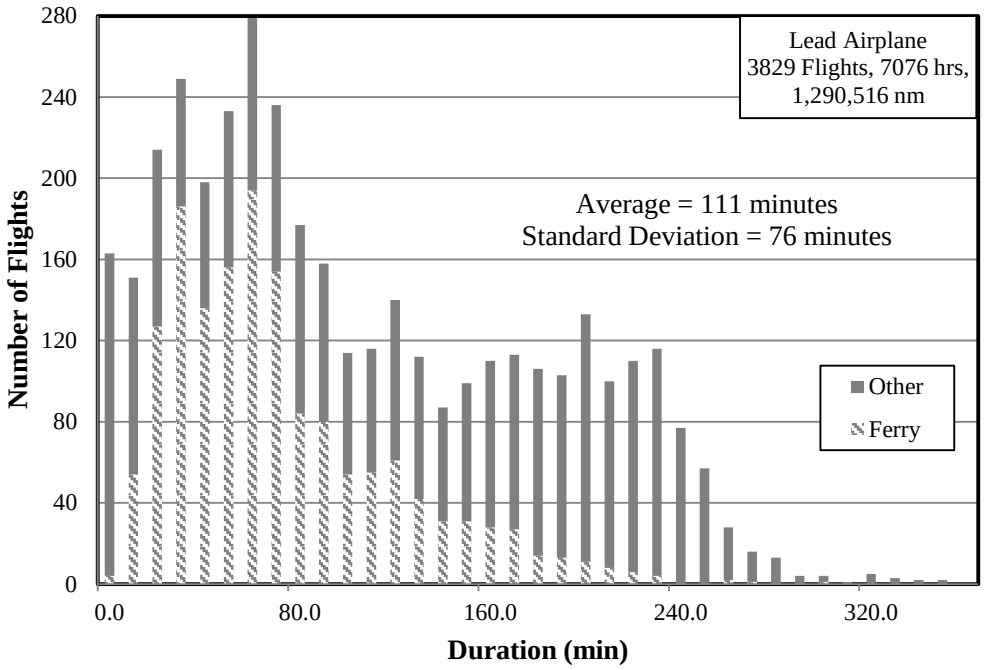

Figure A-3. Percentage of flights based on flight duration, overall flight

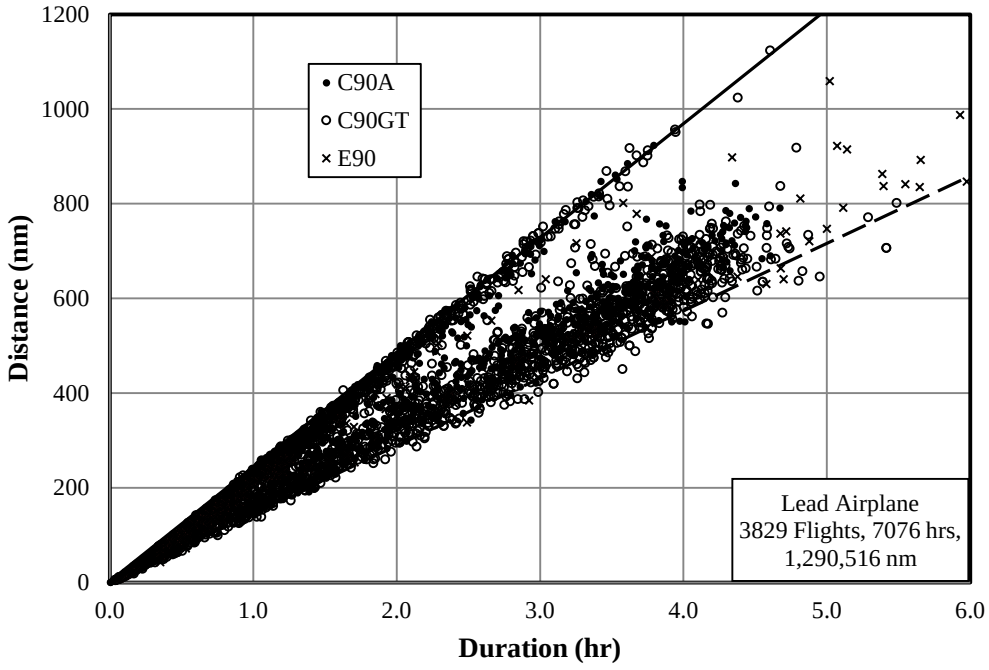

Figure A-4. Flight duration and coincident flight distance, overall flight

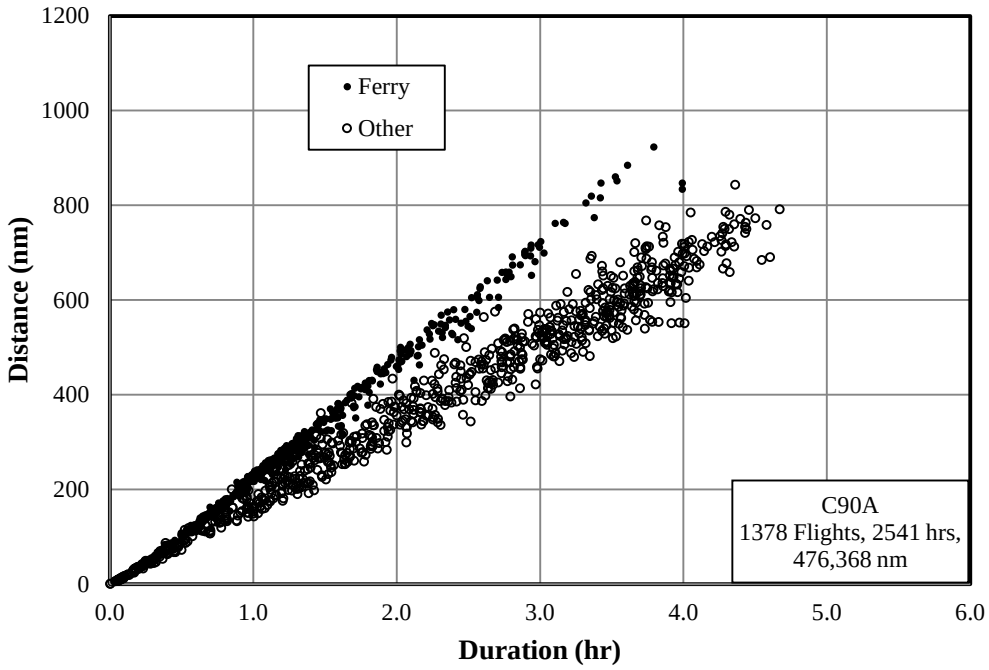

(a) C90A

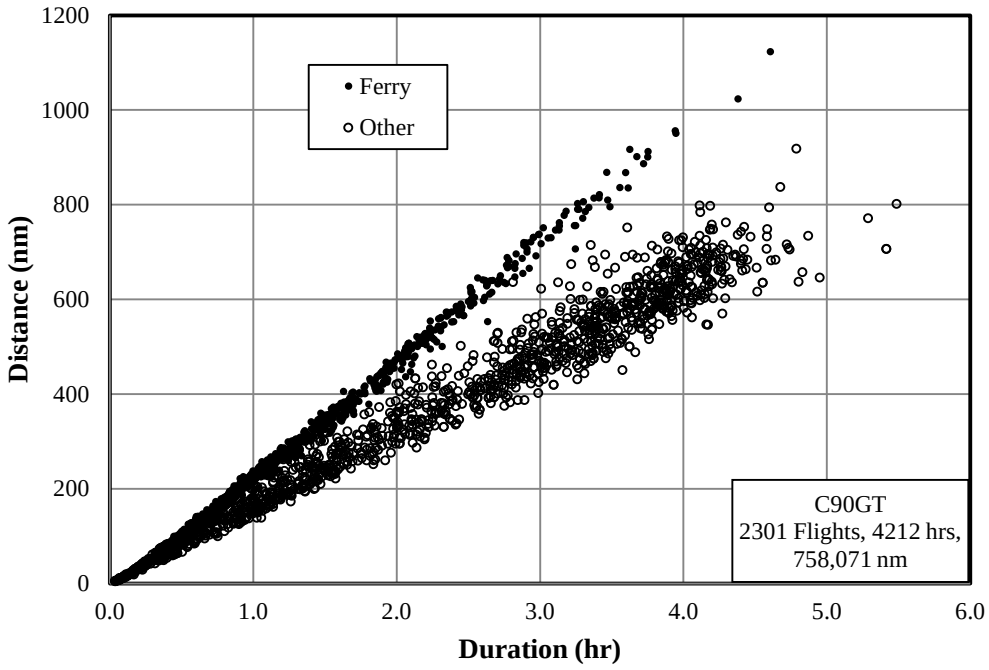

(b) C90GT

Figure A-5. Flight duration and coincident flight distance by model, overall flight, (a) C90A, (b) C90GT, and (c) E90

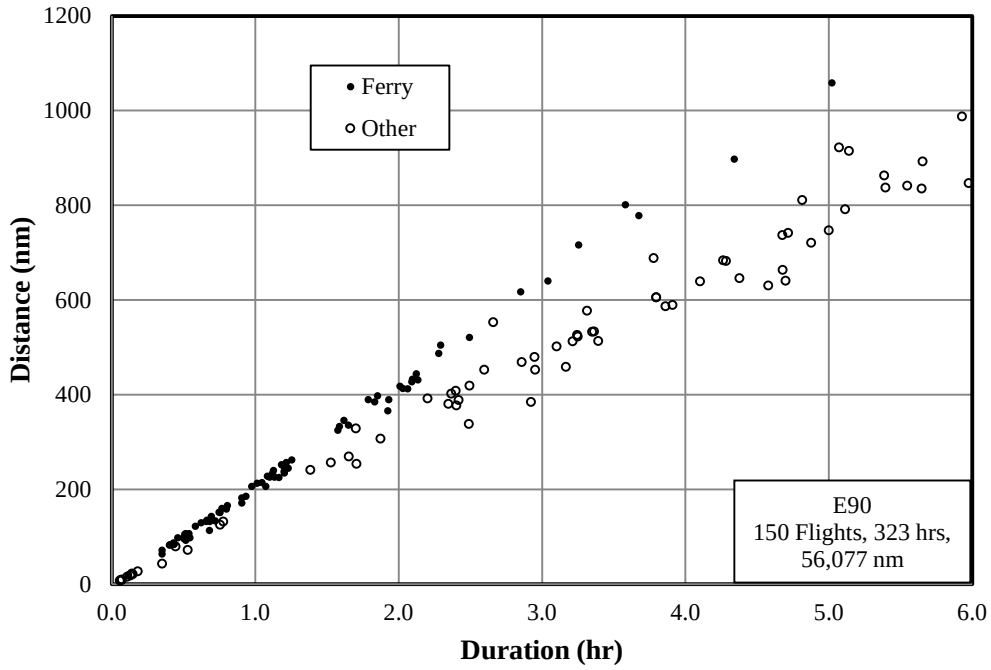

(c) E90

Figure A-5. Flight duration and coincident flight distance by model, overall flight, (a) C90A, (b) C90GT, and (c) E90 (continued)

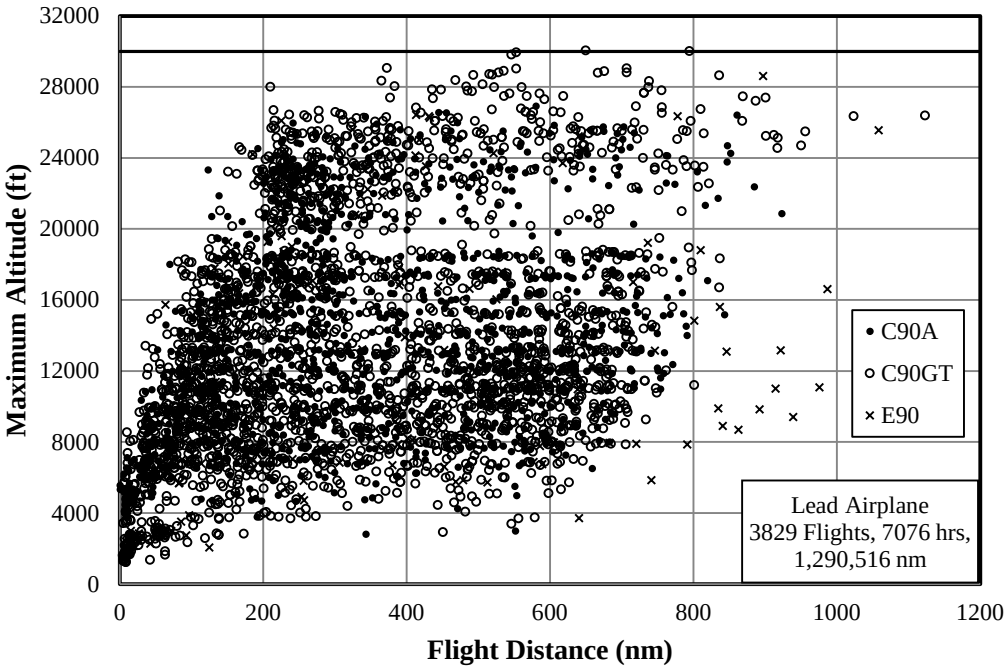

Figure A-6. Maximum altitude and coincident flight distance, overall flight

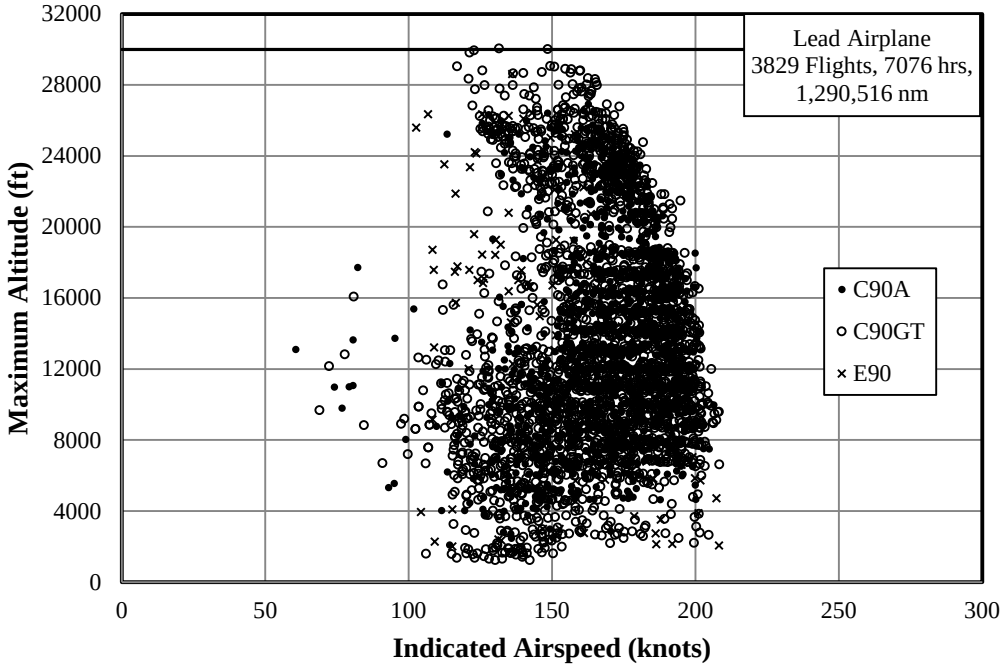

Figure A-7. Maximum altitude and coincident indicated airspeed, overall flight

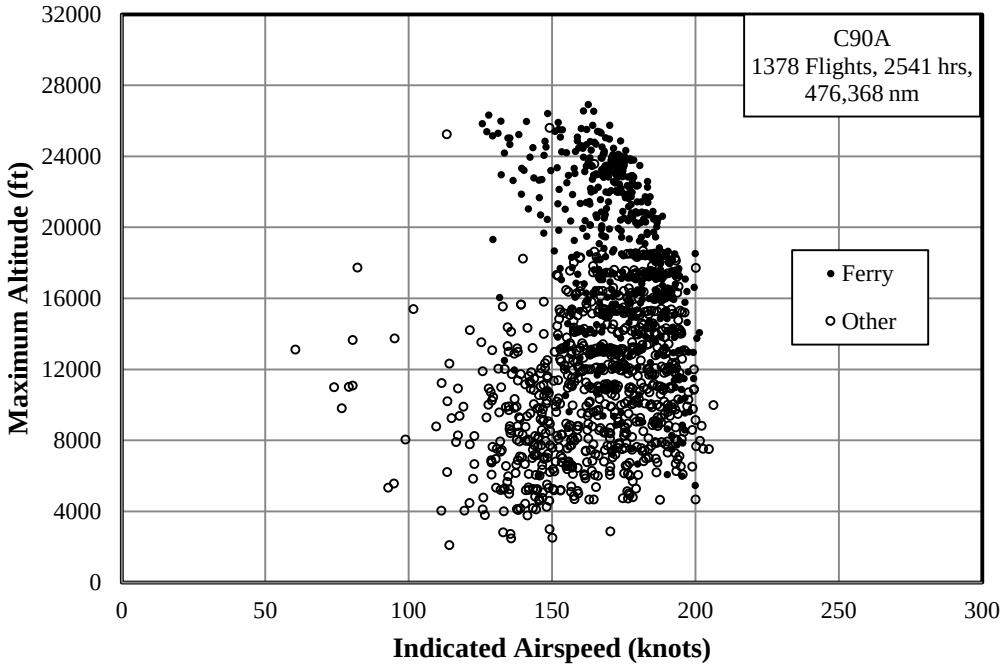

(a) C90A

Figure A-8. Maximum altitude and coincident indicated airspeed by model, overall flight: (a) C90A, (b) C90GT, and (c) E90

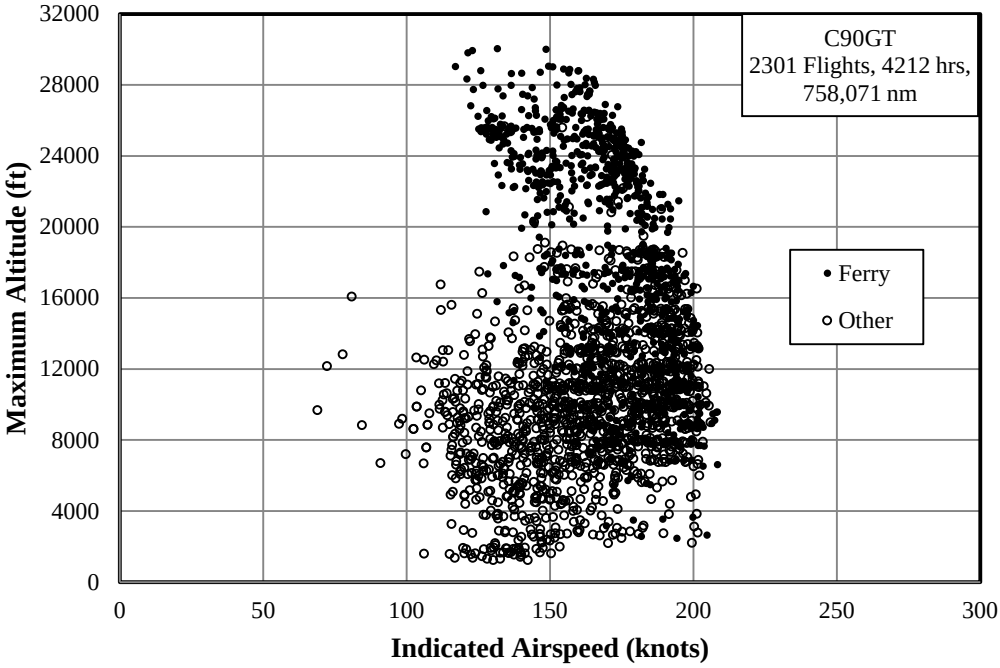

(b) C90GT

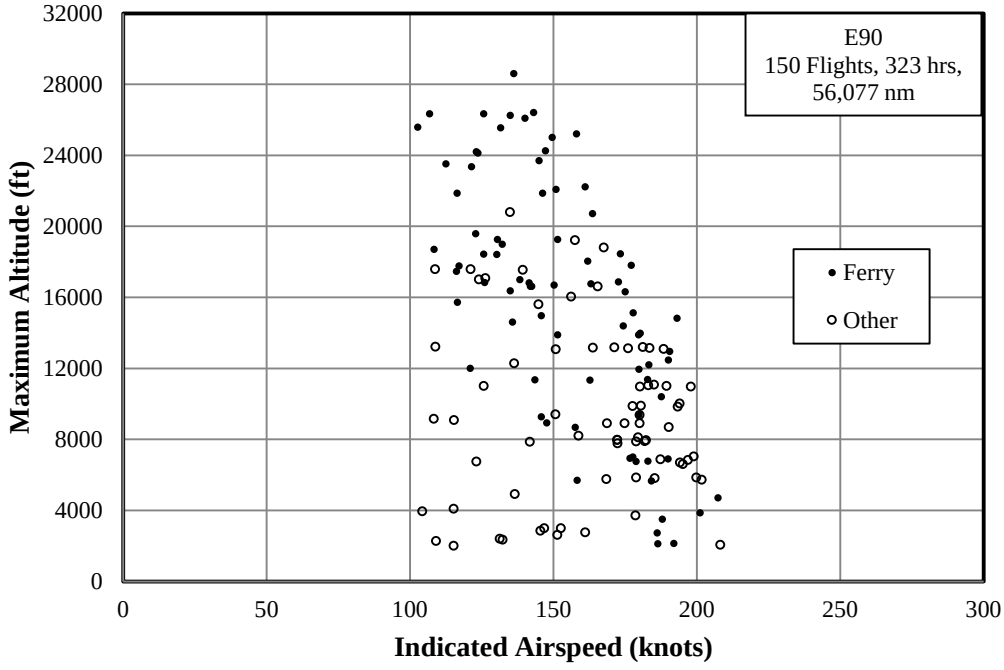

(c) E90

Figure A-8. Maximum altitude and coincident indicated airspeed by model, overall flight: (a) C90A, (b) C90GT, and (c) E90 (continued)

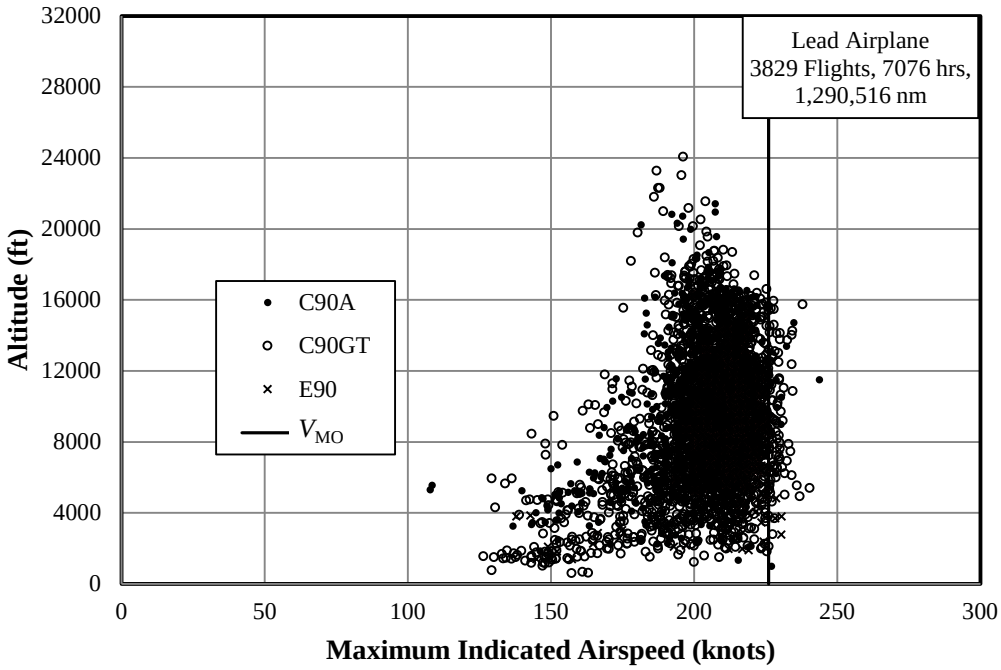

Figure A-9. Maximum indicated airspeed and coincident altitude, overall flight

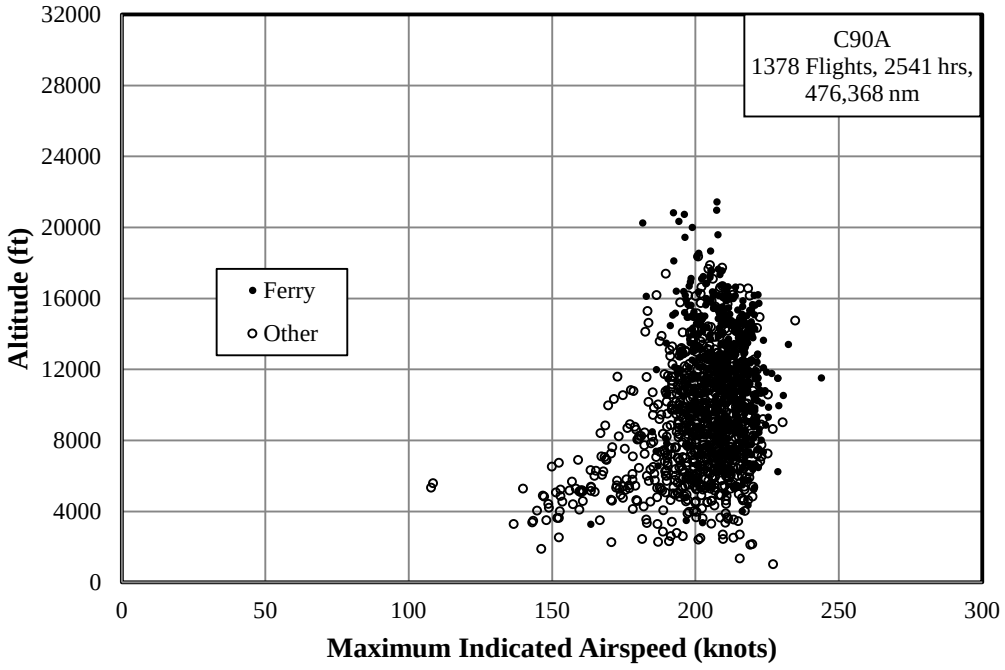

(a) C90A

Figure A-10. Maximum indicated airspeed and coincident altitude by model, overall flight: (a) C90A, (b) C90GT, and (c) E90

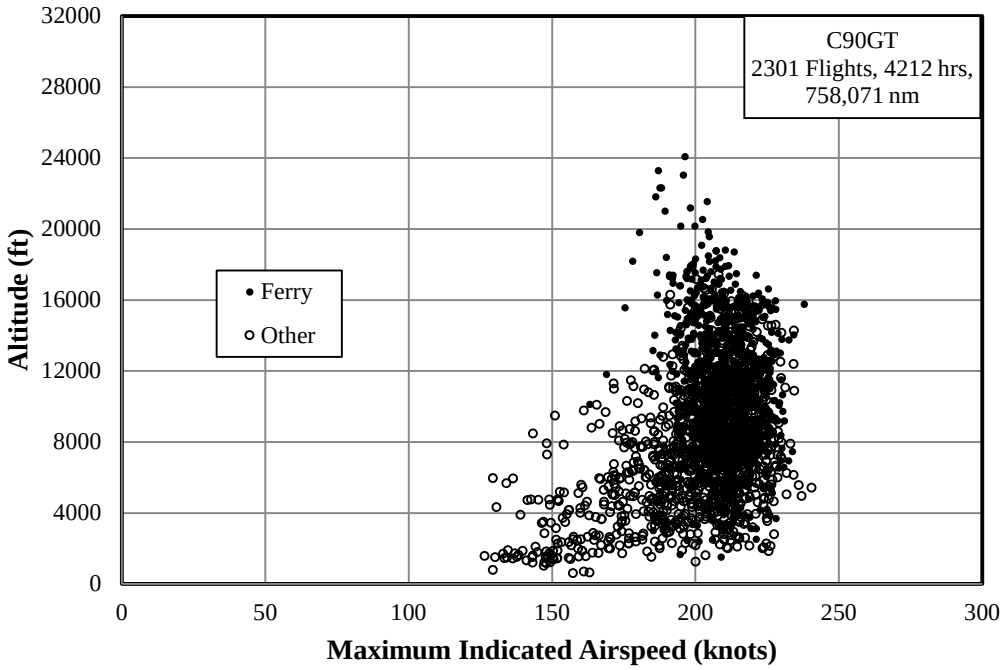

(b) C90GT

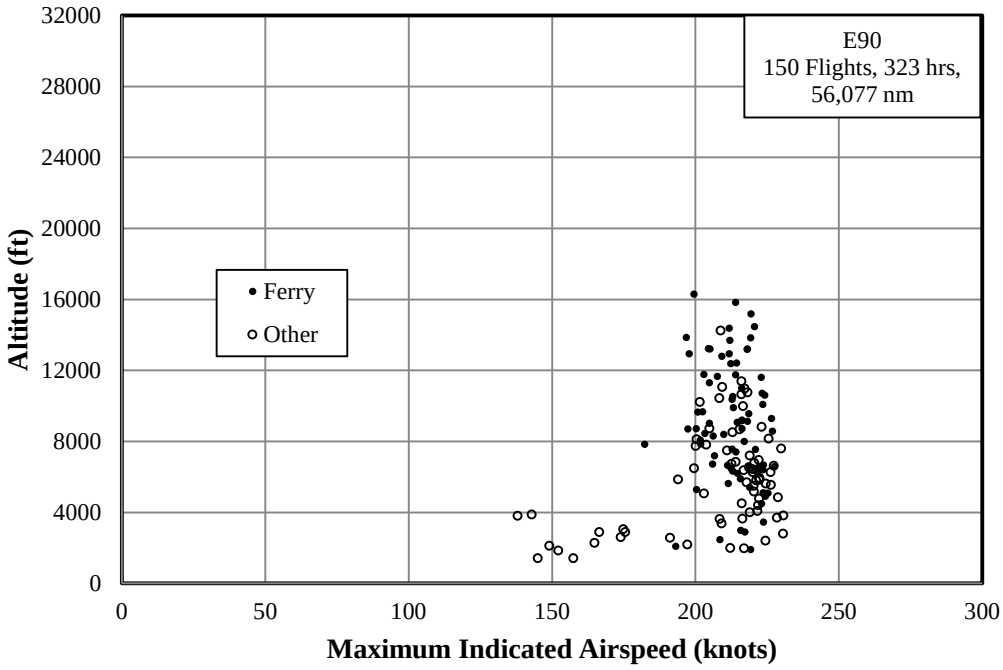

(c) E90

Figure A-10. Maximum indicated airspeed and coincident altitude by model, overall flight: (a) C90A, (b) C90GT, and (c) E90 (continued)

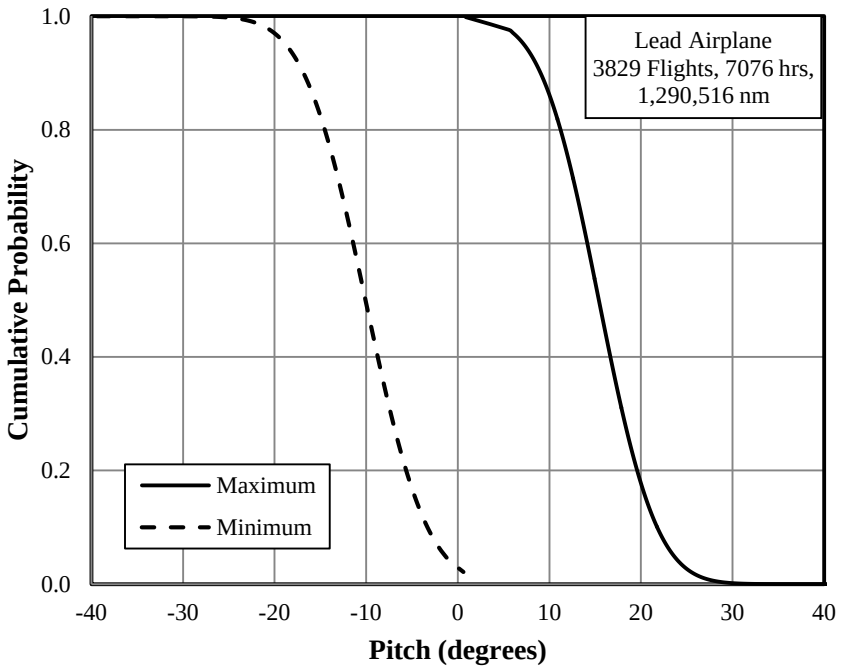

Figure A-11. Cumulative probability of pitch angle, overall flight

Model	Maximum Pitch Angle (degree)		Minimum Pitch Angle (degree)	
	Average	Standard Deviation	Average	Standard Deviation
C90A	14.16	4.86	-9.65	4.50
C90GT	16.11	4.84	-10.32	5.70
E90	16.03	5.71	-9.99	5.17

Figure A-12. Average and standard deviation of maximum and minimum pitch angle, entire flight

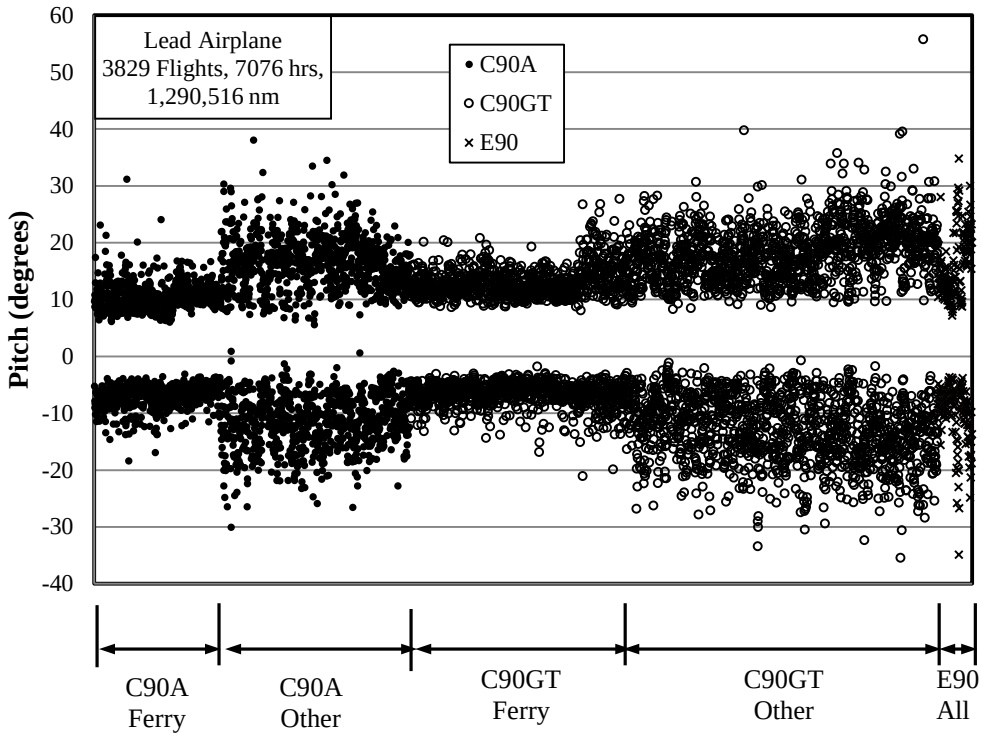

Figure A-13. Maximum and minimum pitch angle, overall flight

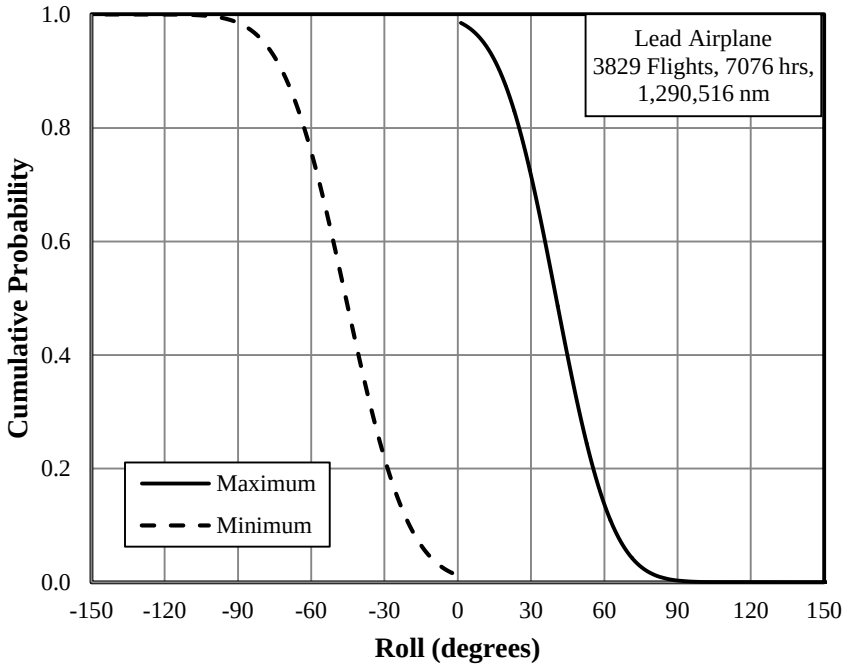

Figure A-14. Cumulative probability of roll angle, overall flight

Model	Maximum Roll Angle (degree)		Minimum Roll Angle (degree)	
	Average	Standard Deviation	Average	Standard Deviation
C90A	40.50	16.59	-46.09	18.94
C90GT	40.27	18.84	-45.74	20.97
E90	39.15	18.32	-44.51	21.98

Figure A-15. Average and standard deviation of maximum and minimum roll angle, entire flight

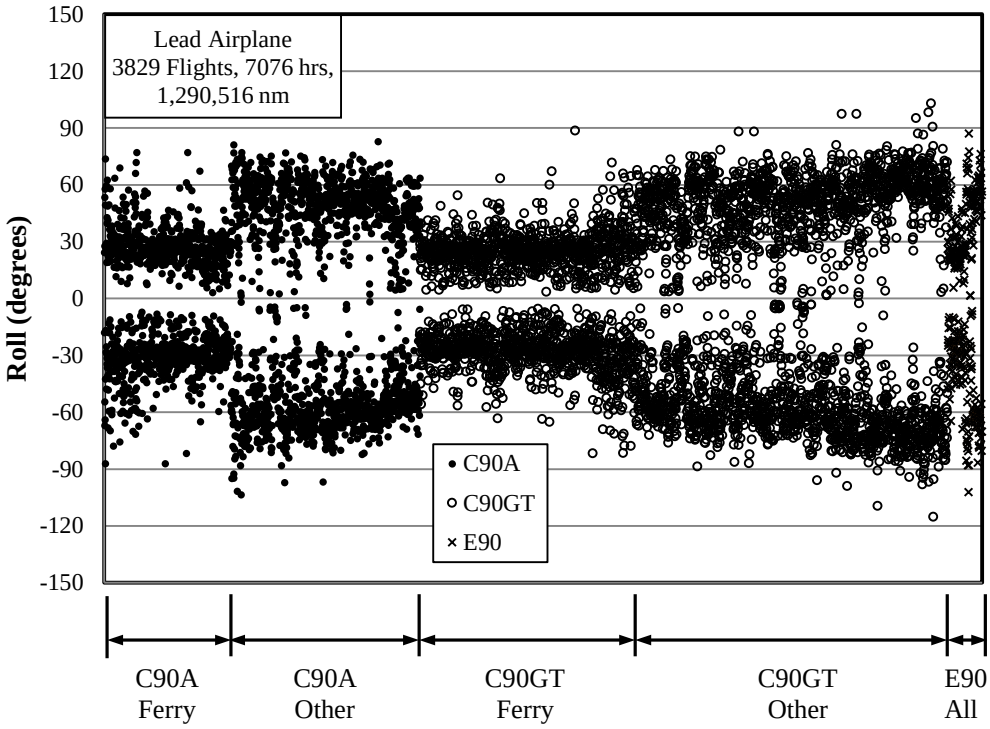

Figure A-16. Maximum and minimum roll angle, overall flight

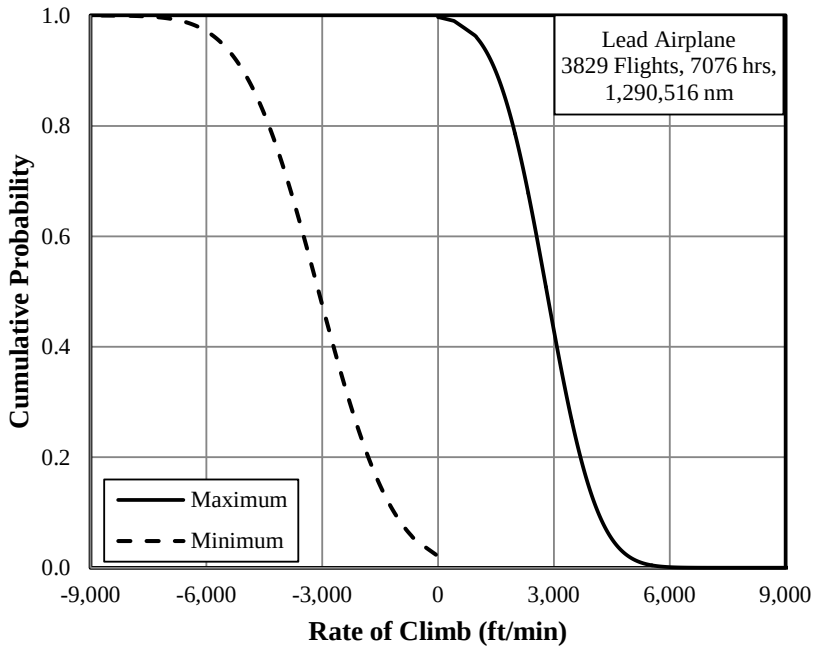

Figure A-17. Cumulative probability of rate of climb, overall flight

Model	Maximum Rate of Climb (ft/min)		Minimum Rate of Climb (ft/min)	
	Average	Standard Deviation	Average	Standard Deviation
C90A	2658.06	954.22	-2966.59	1372.29
C90GT	2913.99	1073.62	-3166.52	1606.12
E90	2797.49	1039.50	-3034.45	1606.63

Figure A-18. Average and standard deviation of maximum and minimum rate of climb, entire flight

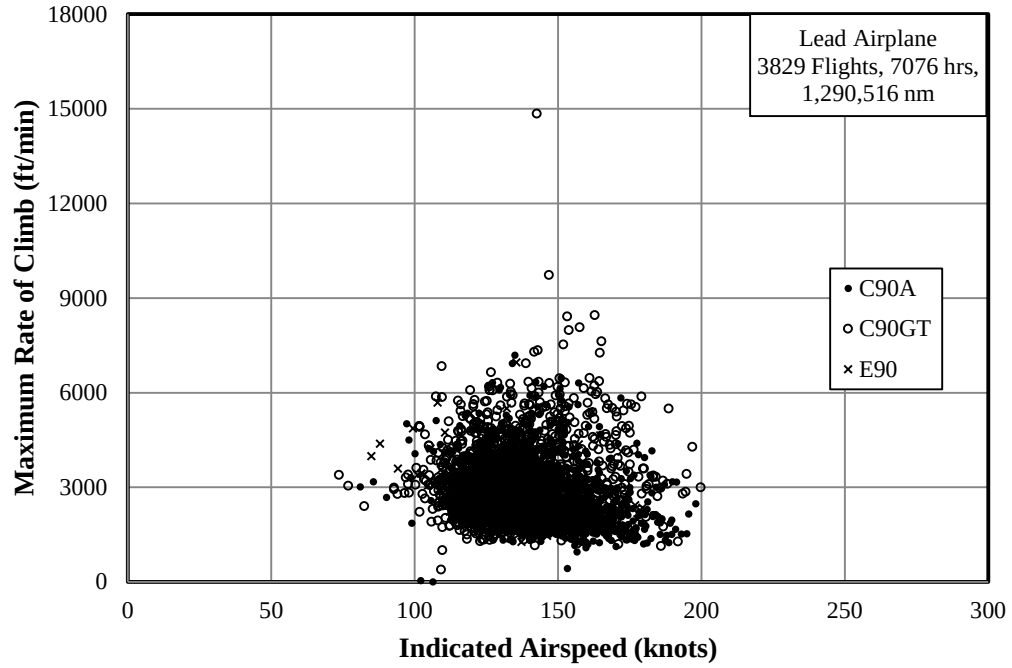

(a) Maximum

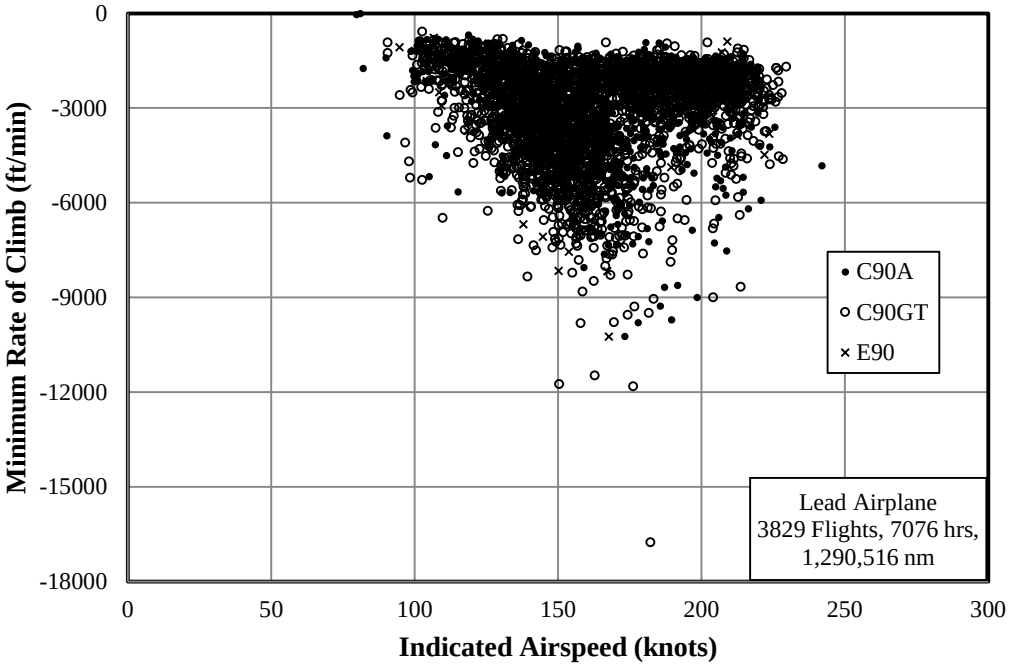

(b) Minimum

Figure A-19. Maximum and minimum rate of climb, overall flight: (a) maximum and (b) minimum

Model	Airplane Number	Number of Good Flights	Duration (min)	Duration (hr)	Distance (nm)
C90A	1	644	66,943	1,116	212,562
	2	264	37,051	618	114,287
	3	71	4,845	81	15,764
C90GT	4	586	58,351	973	185,075
	5	677	74,253	1,238	217,425
	6	698	85,274	1,421	254,122
E90	7	150	19,352	323	56,077
Total	---	3,090	346,070	5,768	1,055,313

Figure A-20. Summary of durations and distances, overall flight without flap information

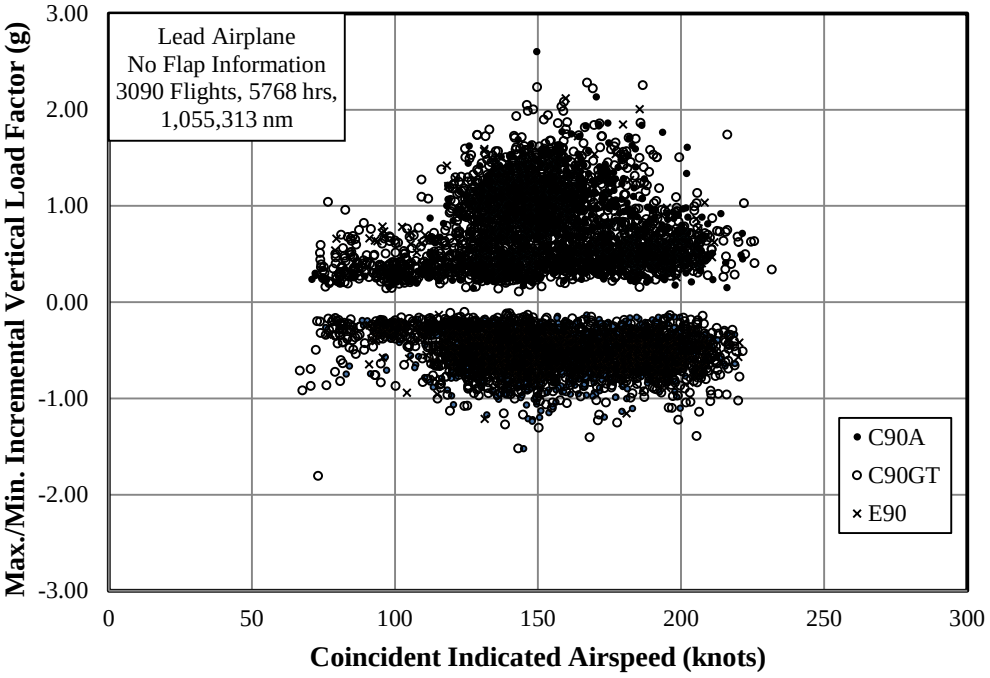

Figure A-21. *V-n* diagram, overall flight without flap information

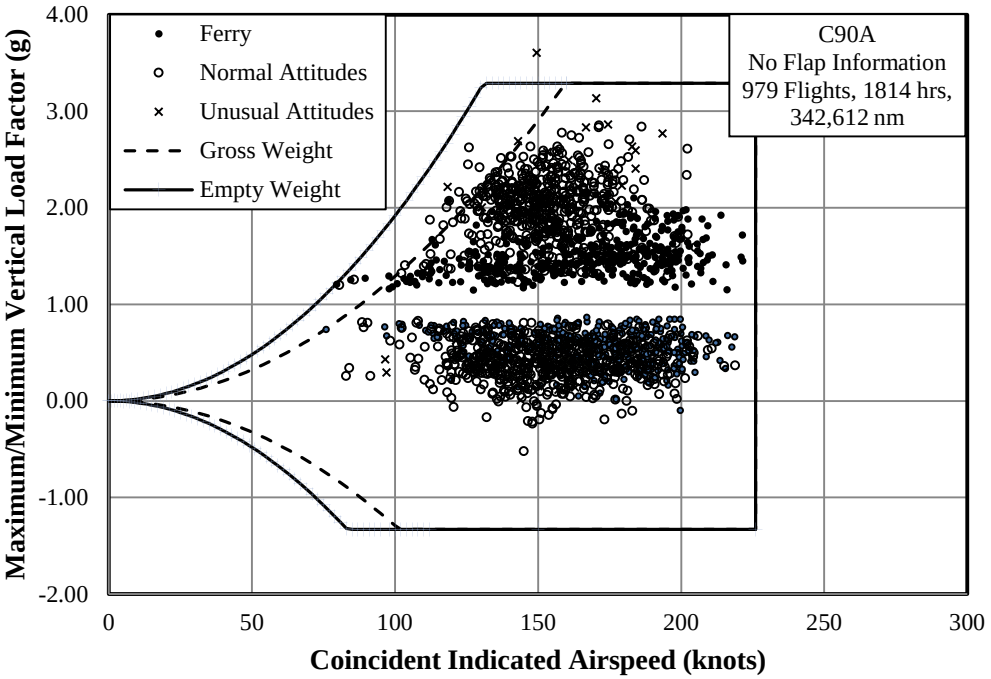

(a) C90A

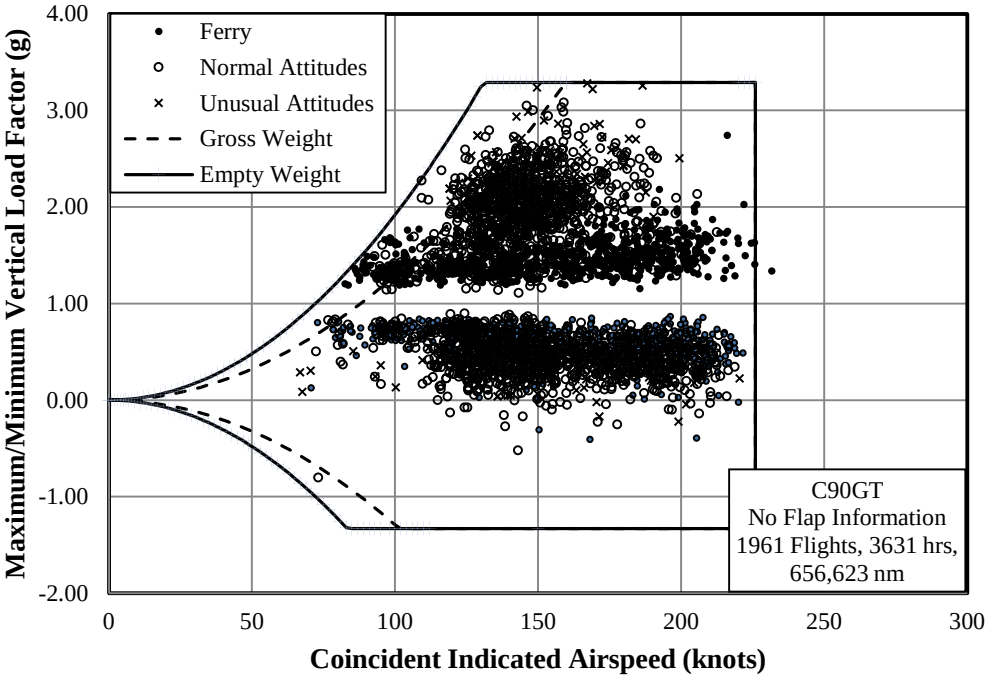

(b) C90GT

Figure A-22. *V-n* diagram by model, overall flight without flap information: (a) C90A, (b) C90GT, and (c) E90

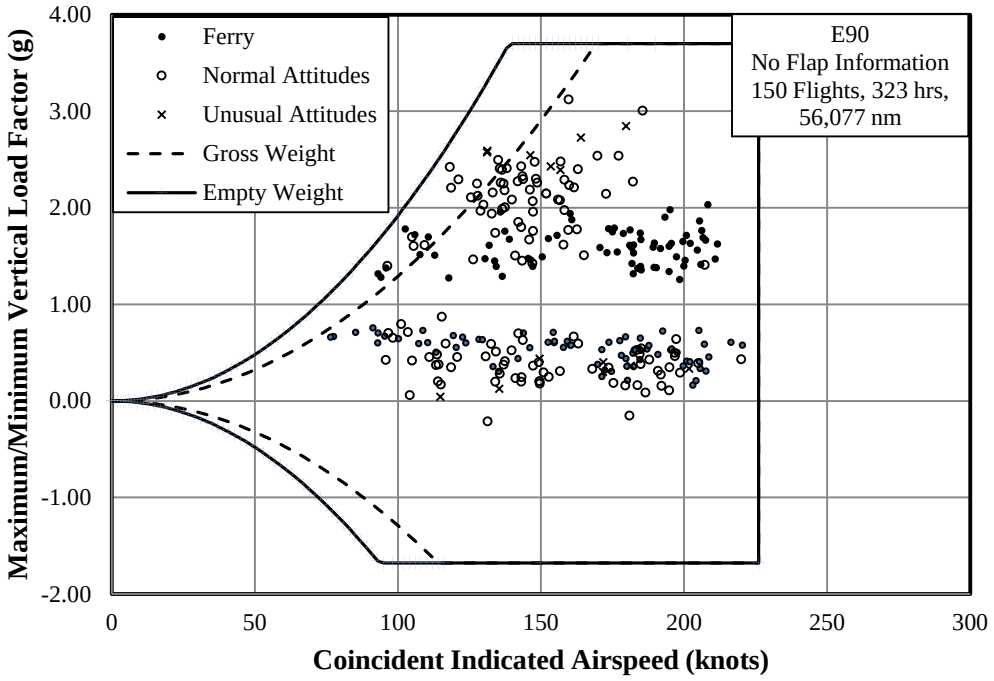

(c) E90

Figure A-22. *V-n* diagram by model, overall flight without flap information: (a) C90A, (b) C90GT, and (c) E90 (continued)

Model	Airplane Number	Number of Good Flights	Duration (min)	Duration (hr)	Distance (nm)
C90A	1	171	19,641	327	61,076
	2	46	6,507	108	19,626
	3	182	17,481	291	53,054
C90GT	4	125	9,997	167	29,081
	5	117	13,192	220	36,773
	6	98	11,650	194	35,593
E90	7	0	0	0	0
Total	---	739	78,468	1,308	235,203

Figure A-23. Summary of durations and distances, overall flight with flap information

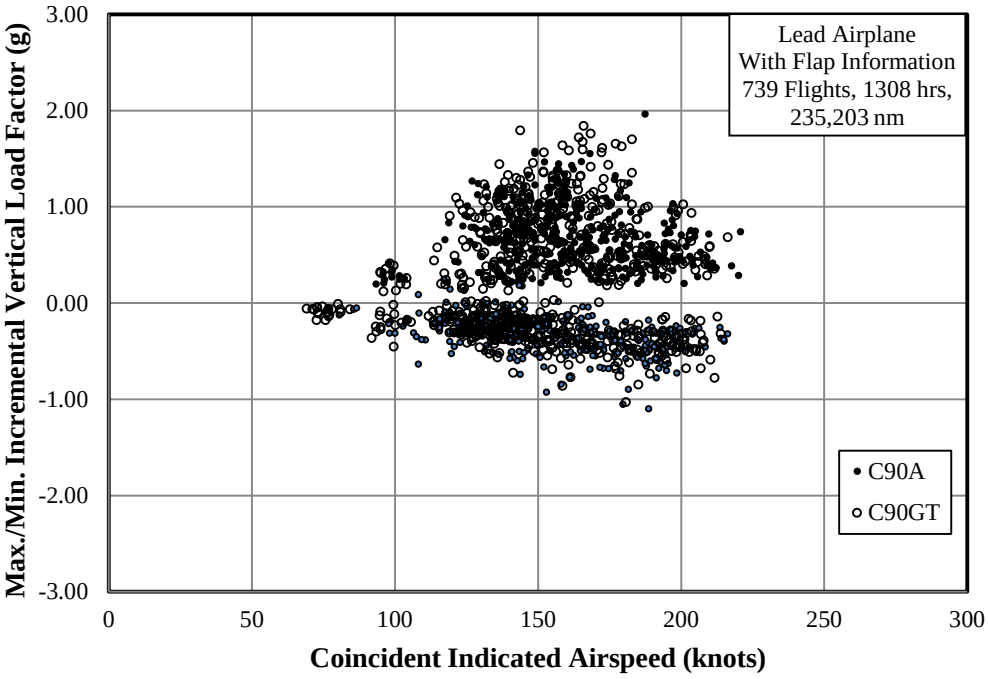

Figure A-24. *V-n* diagram, overall flight with flaps retracted

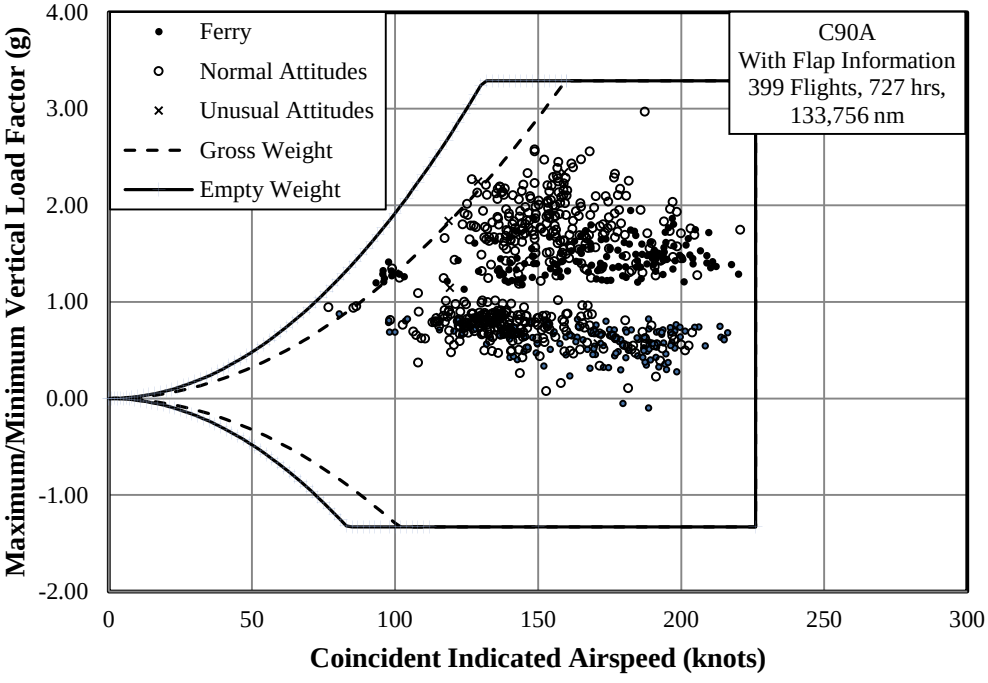

(a) C90A

Figure A-25. *V-n* diagram by model, overall flight with flaps retracted, (a) C90A and (b) C90GT

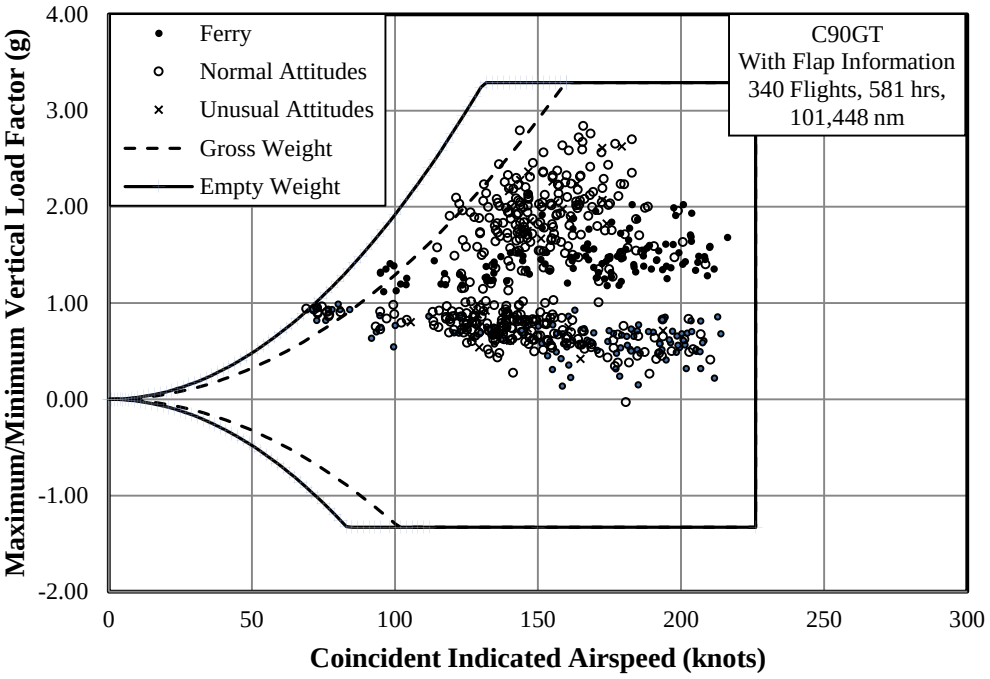

(b) C90GT

Figure A-25. *V-n* diagram by model, overall flight with flaps retracted, (a) C90A and (b) C90GT (continued)

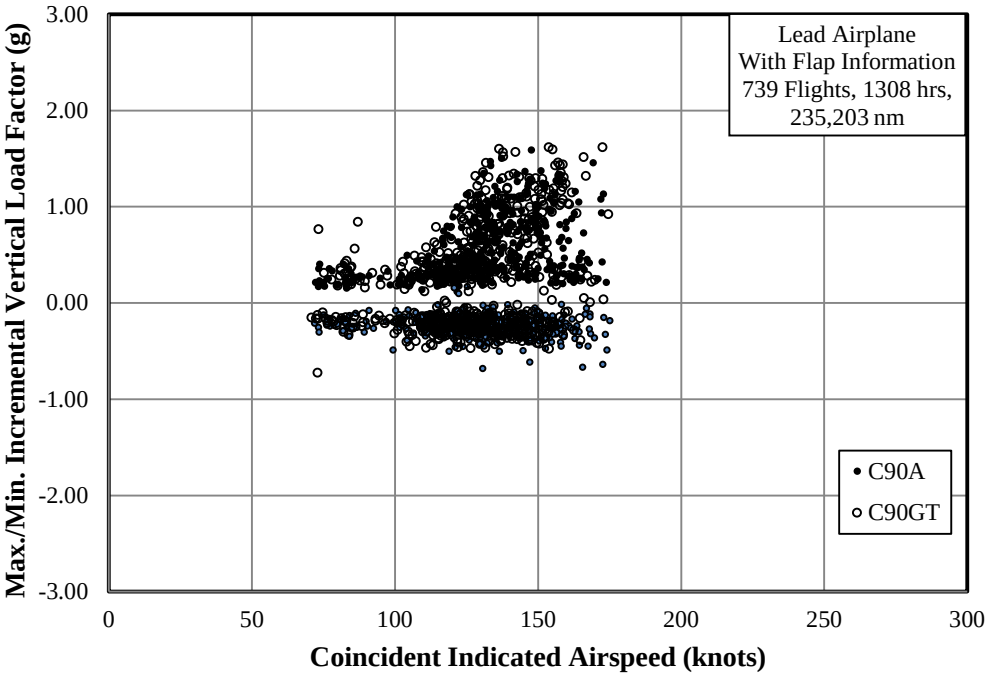

Figure A-26. *V-n* diagram, overall flight with flaps deflected

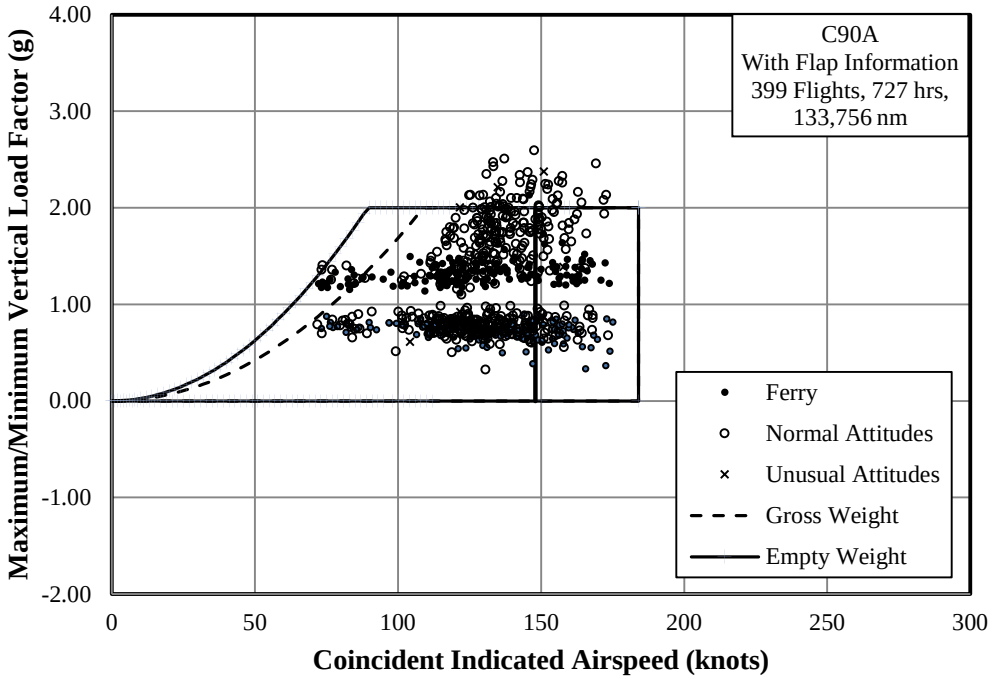

(a) C90A

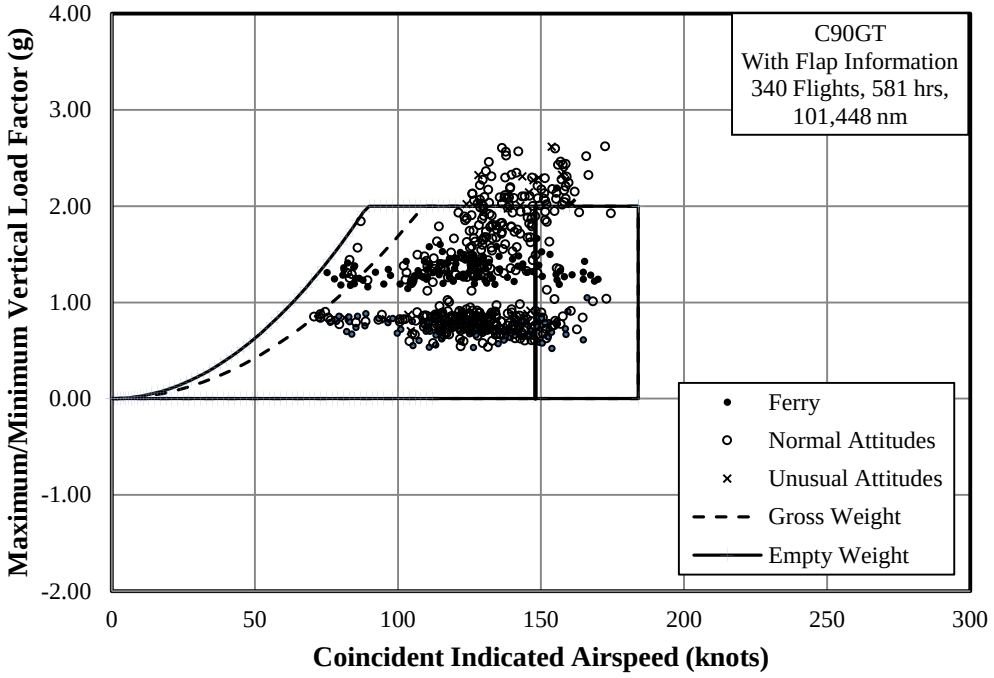

(b) C90GT

Figure A-27. *V-n* diagram by model, overall flight with flaps deflected, (a) C90A and (b) C90GT

Event		Number of Flights	Event		Number of Flights
Pitch Angle Exceeding	20°	720	Roll Angle Exceeding	60°	633
	25°	147		70°	152
	30°	28		80°	18
	-20°	201		-60°	1167
	-25°	44		-70°	480
	-30°	9		-80°	111

Figure A-28. Summary of the number of flights containing unusual attitudes

Event	Number of Flights	Duration (min)	Duration (hr)	Distance (nm)
Normal flights	3,682	399,043	6,650.7	1,221,258.7
Roll angle exceeding ±80°	113	20,237	337.3	55,101.3
Pitch angle exceeding ±30°	25	3,575	59.6	9,885.3
Both roll angle higher than ±80° and pitch angle higher than ±30°	9	1,683	28.0	4,270.3
Total	3829	424,538	7,075.6	1,290,515.6

Figure A-29. Summary of durations and distances for unusual attitude flights

Aircraft Model	Number of Flights	Duration (min)	Duration (hr)	Distance (nm)
Normal flights	3,682	399,043	6,650.7	1,221,258.7
C90A with unusual attitudes	31	4,728	78.8	13,995.4
C90GT with unusual attitudes	109	19,176	319.6	51,302.2
E90 with unusual attitudes	7	1,591	26.5	3,959.3
Total flights	3,829	424,538	7,075.6	1,290,515.6

Figure A-30. Summary of durations and distances for unusual attitude flights by model

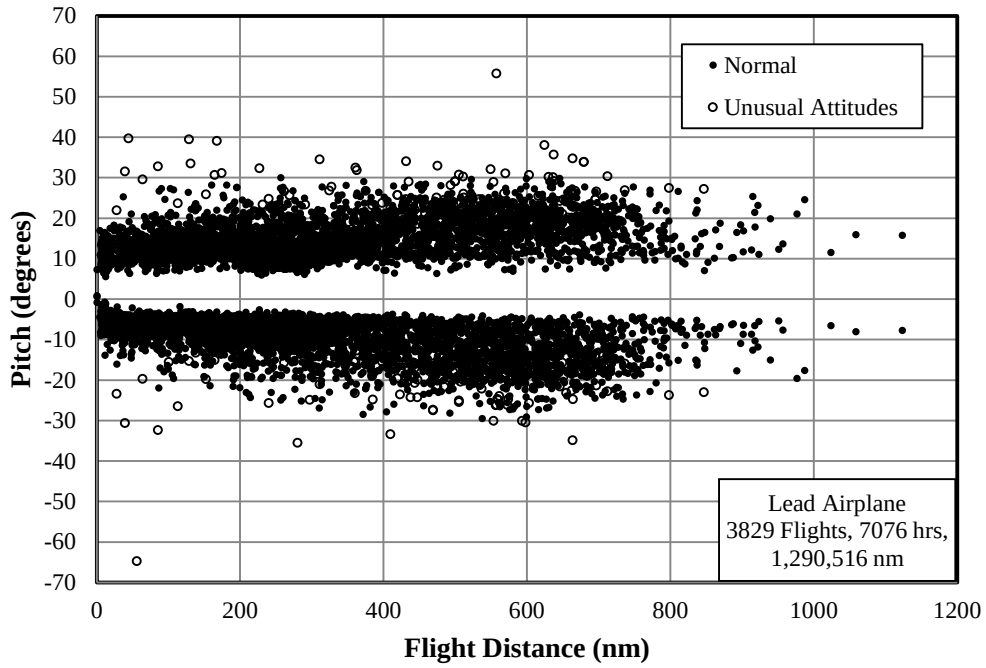

Figure A-31. Maximum and minimum pitch angle for unusual attitude flights

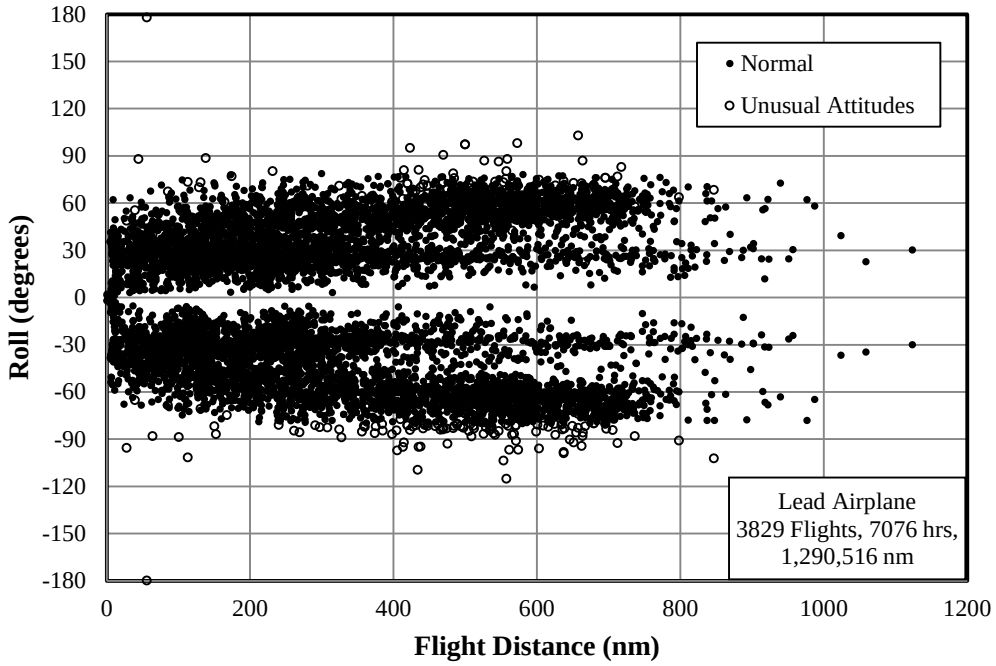

Figure A-32. Maximum and minimum roll angle for unusual attitude flights

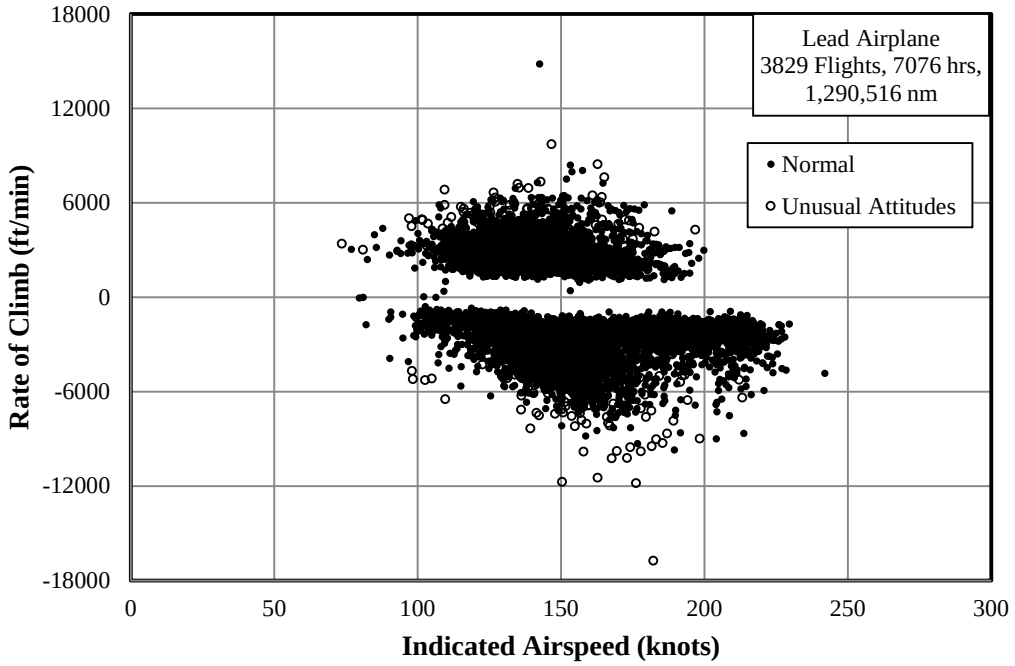

Figure A-33. Maximum and minimum rate of climb for unusual attitude flights

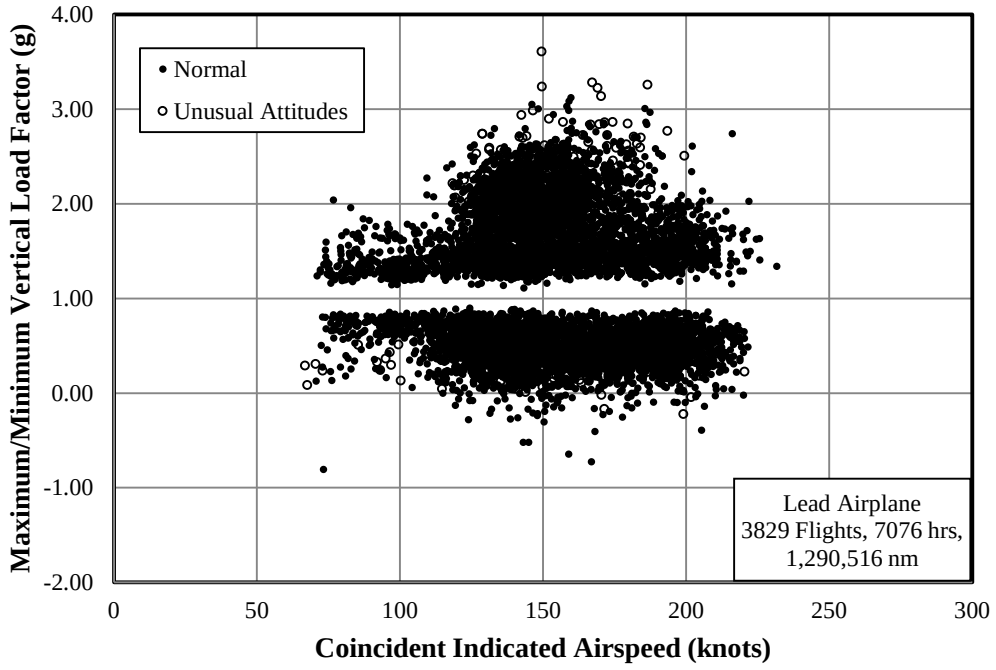

Figure A-34. *V-n* diagram for unusual attitude flights without flap information

Model	Airplane Number	Number of Cruise 1 Phases	Duration (min)	Duration (hr)	Distance (nm)
C90A	1	360	10,800	180	35,696
	2	202	6,204	103	20,761
	3	99	3,153	53	10,068
C90GT	4	261	6,627	110	21,437
	5	436	10,378	173	33,864
	6	439	11,319	189	38,279
E90	7	61	1,955	33	6,615
Total	---	1,858	50,437	841	166,720

Figure A-35. Summary of durations and distances, Cruise 1 phase

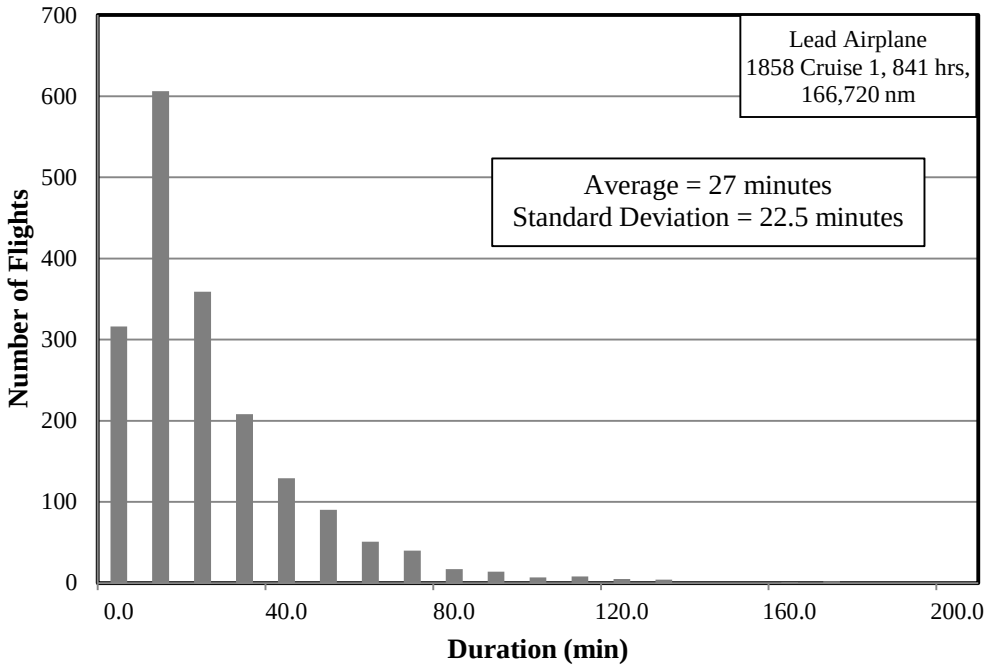

Figure A-36. Percentage of phases based on duration, Cruise 1 phase

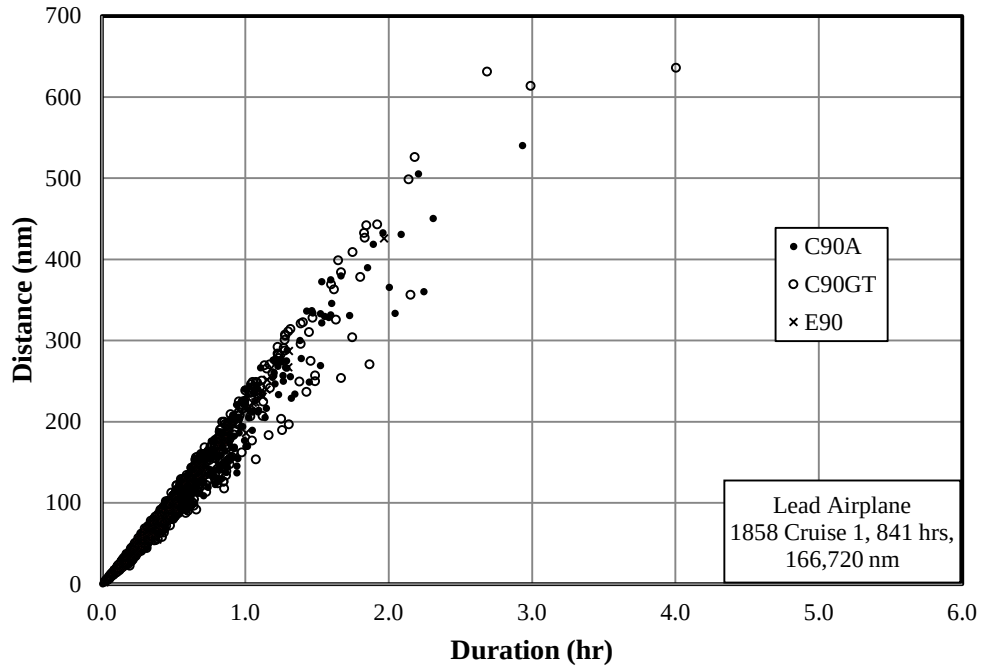

Figure A-37. Flight duration and coincident flight distance, Cruise 1 phase

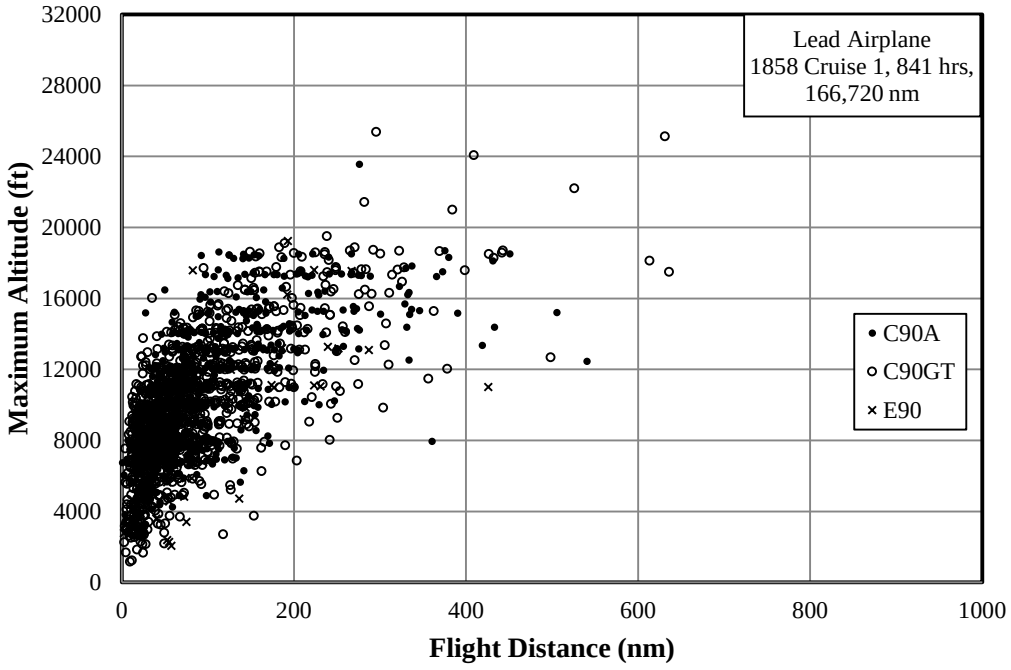

Figure A-38. Maximum altitude and coincident flight distance, Cruise 1 phase

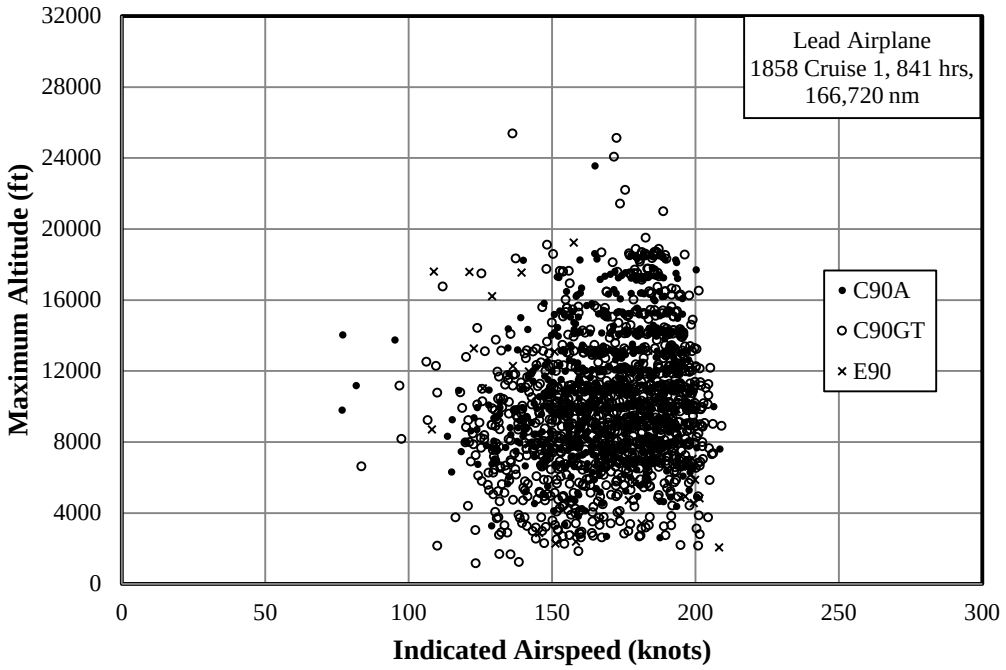

Figure A-39. Maximum altitude and coincident indicated airspeed, Cruise 1 phase

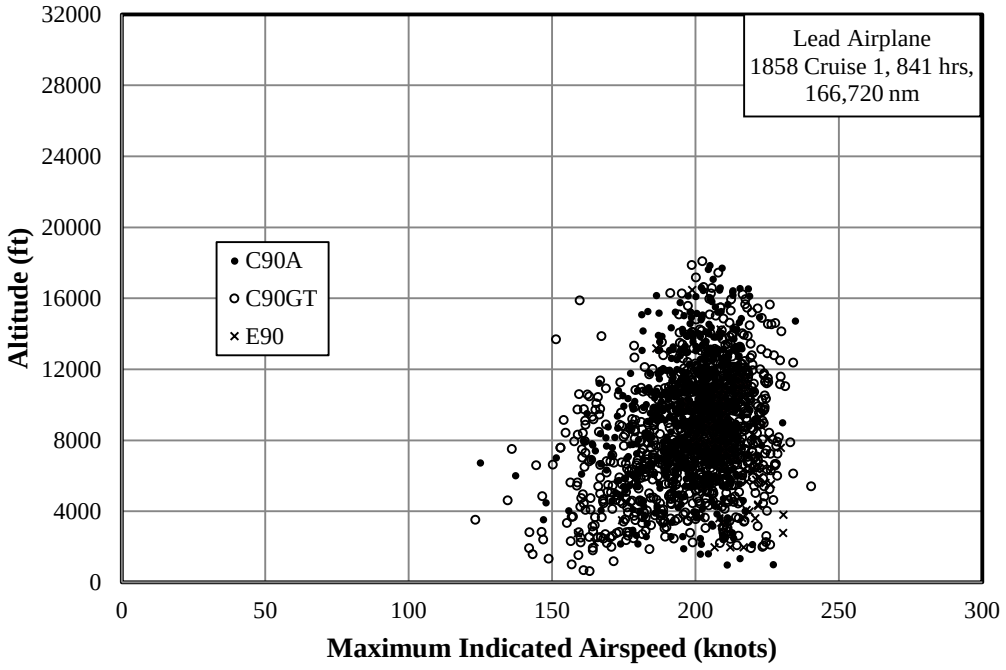

Figure A-40. Maximum indicated airspeed and coincident altitude, Cruise 1 phase

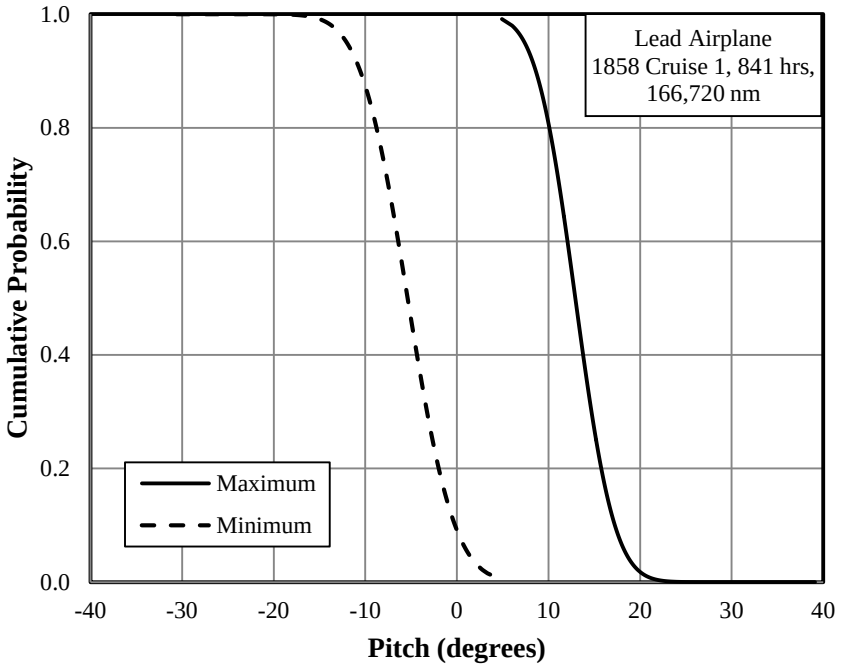

Figure A-41. Cumulative probability of pitch angle, Cruise 1 phase

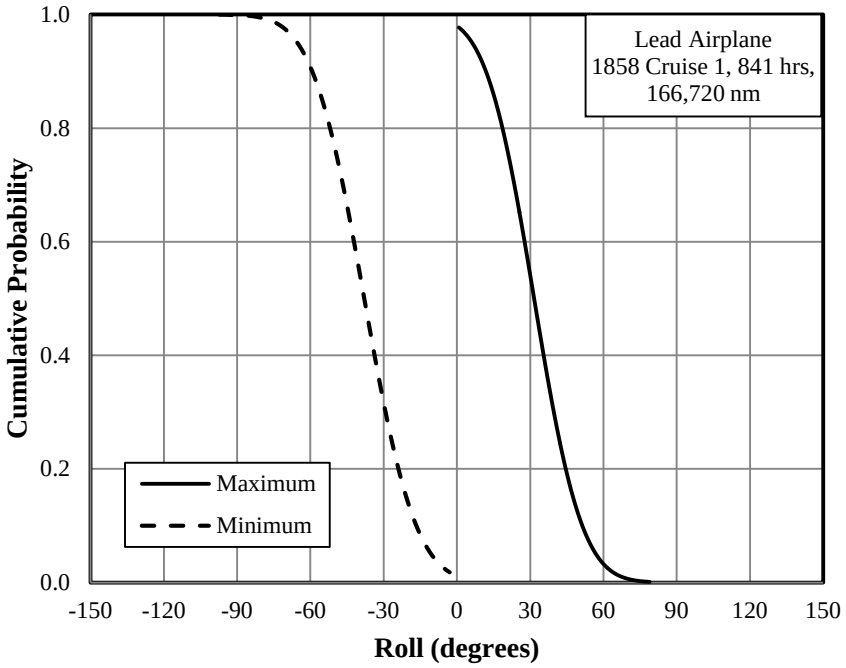

Figure A-42. Cumulative probability of roll angle, Cruise 1 phase

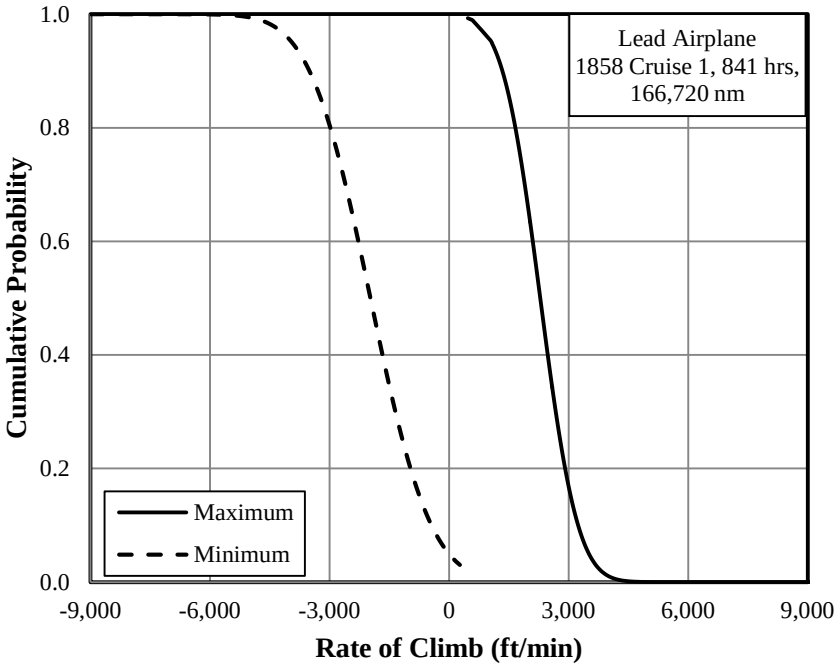

Figure A-43. Cumulative probability of rate of climb, Cruise 1 phase

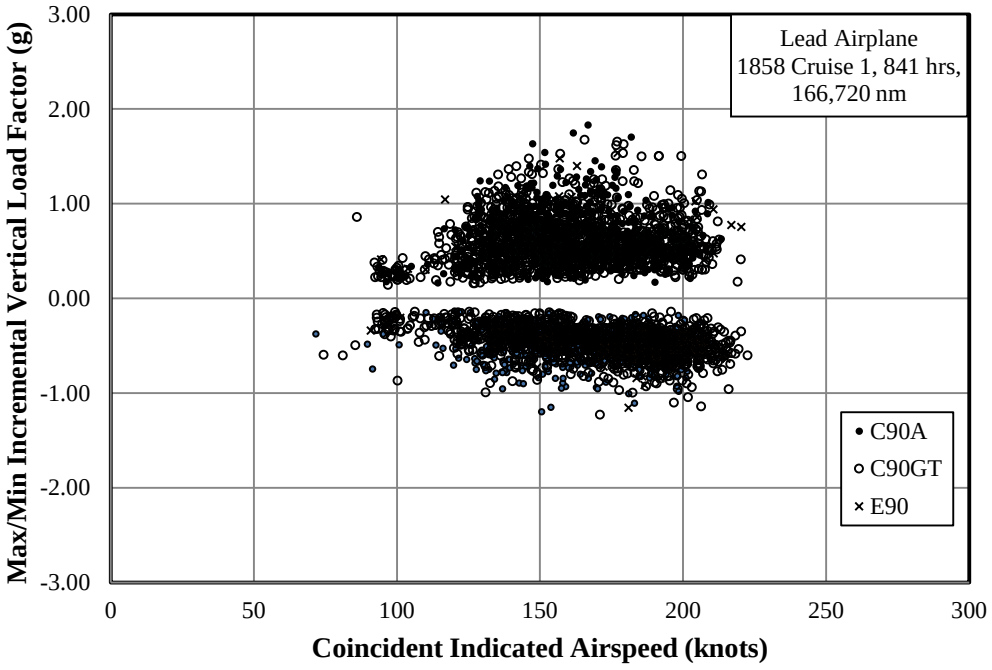

Figure A-44. *V-n* diagram, Cruise 1 phase

Model	Airplane Number	Number of Cruise 2 Phases	Duration (min)	Duration (hr)	Distance (nm)
C90A	1	360	10,175	170	30,789
	2	202	5,429	90	17,139
	3	99	2,667	44	7,984
C90GT	4	261	6,442	107	19,048
	5	436	9,292	155	27,972
	6	439	10,458	174	33,102
E90	7	61	1,607	27	5,092
Total	---	1,858	46,070	768	141,127

Figure A-45. Summary of durations and distances, Cruise 2 phase

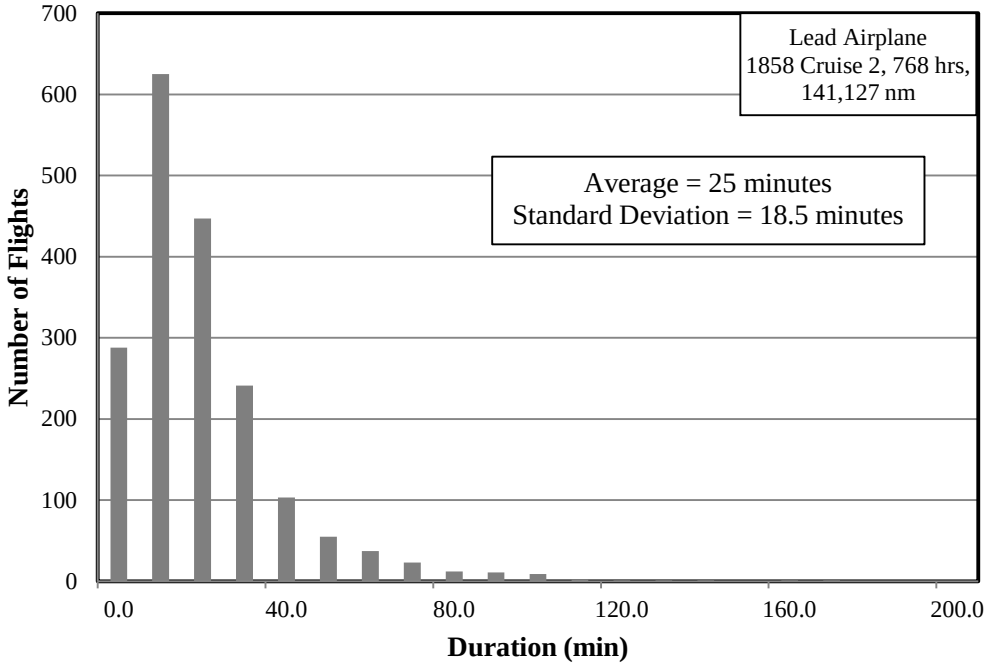

Figure A-46. Percentage of phases based on duration, Cruise 2 phase

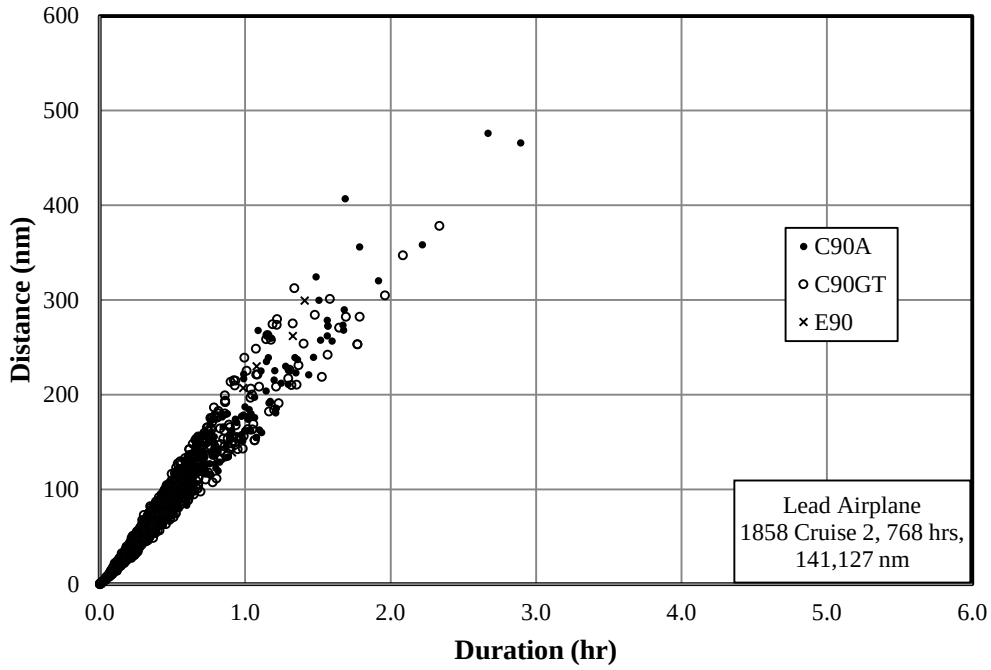

Figure A-47. Flight duration and coincident flight distance, Cruise 2 phase

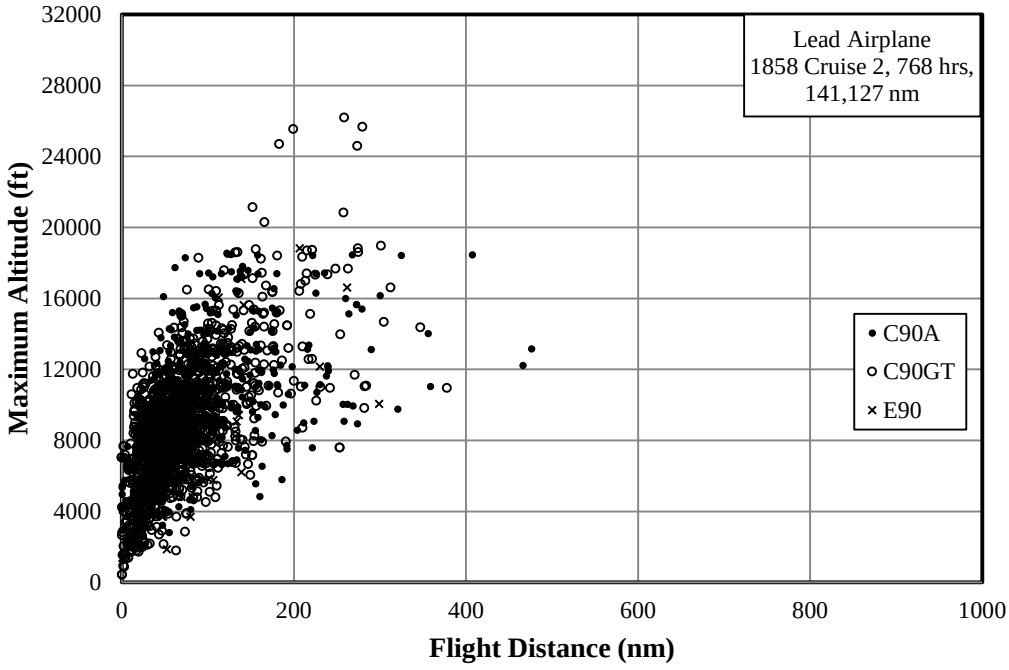

Figure A-48. Maximum altitude and coincident flight distance, Cruise 2 phase

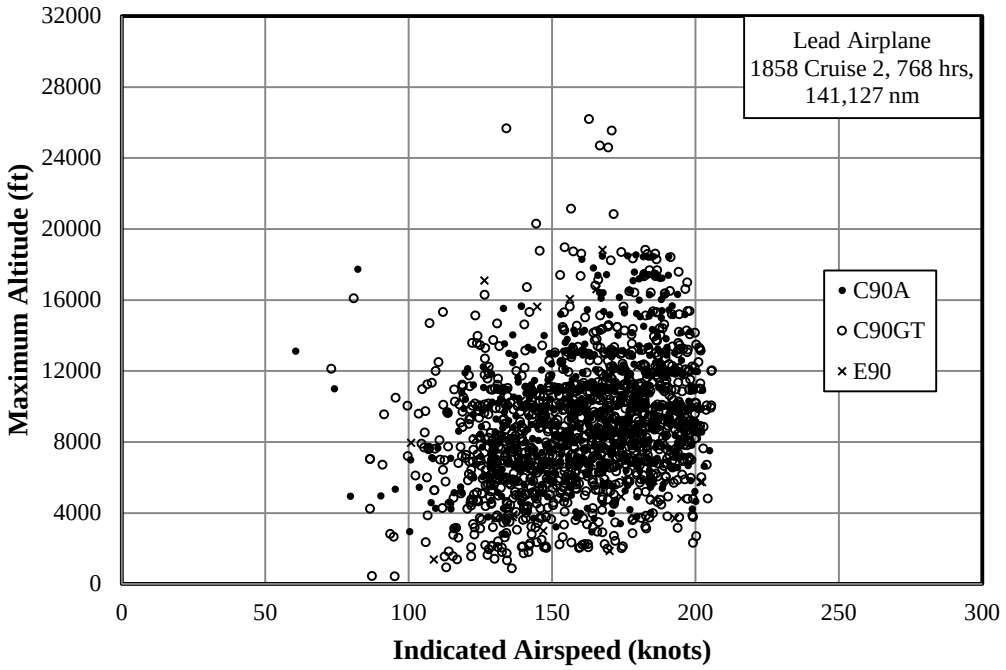

Figure A-49. Maximum altitude and coincident indicated airspeed, Cruise 2 phase

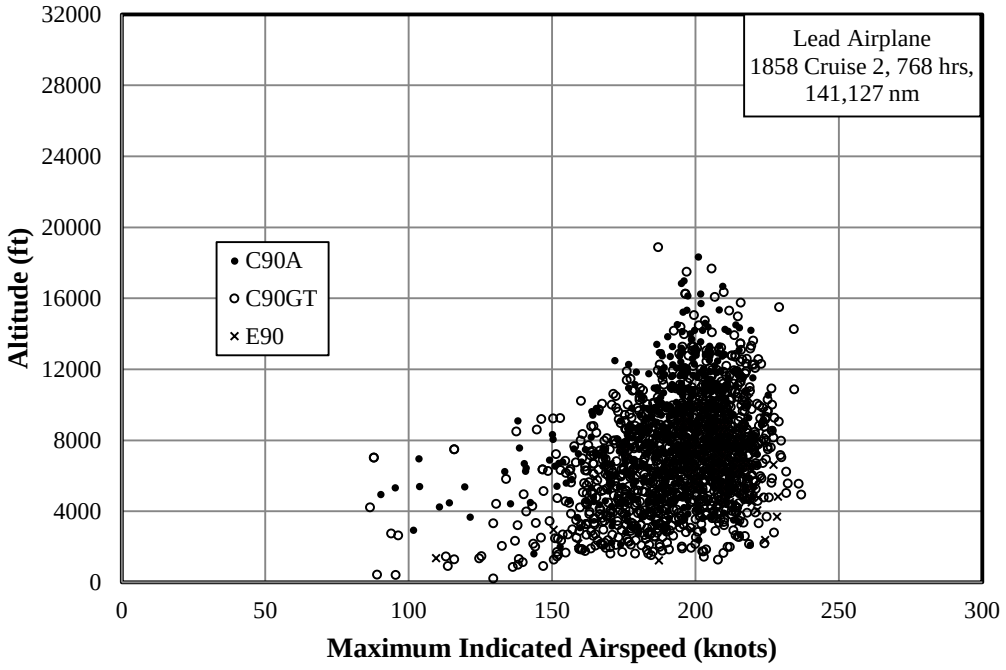

Figure A-50. Maximum indicated airspeed and coincident altitude, Cruise 2 phase

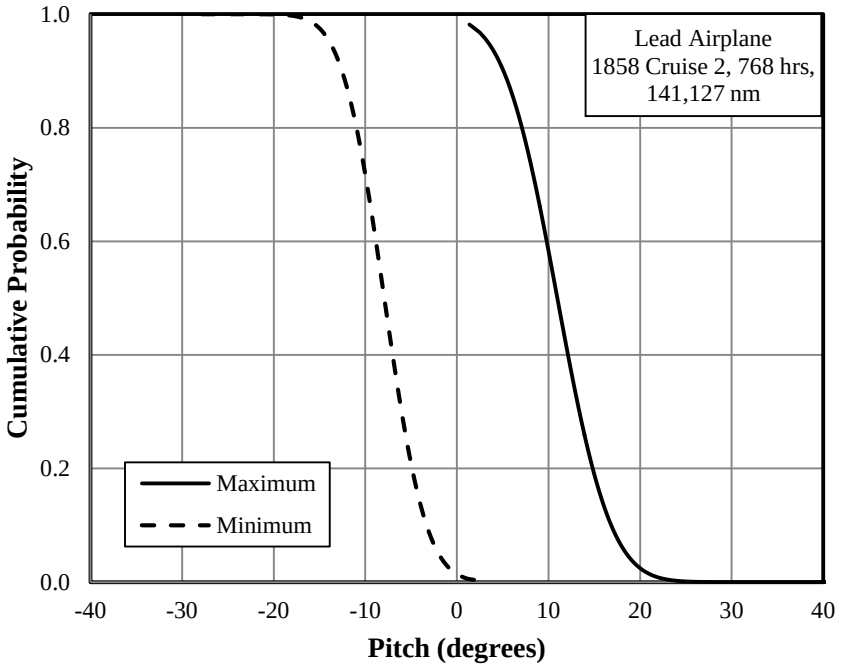

Figure A-51. Cumulative probability of pitch angle, Cruise 2 phase

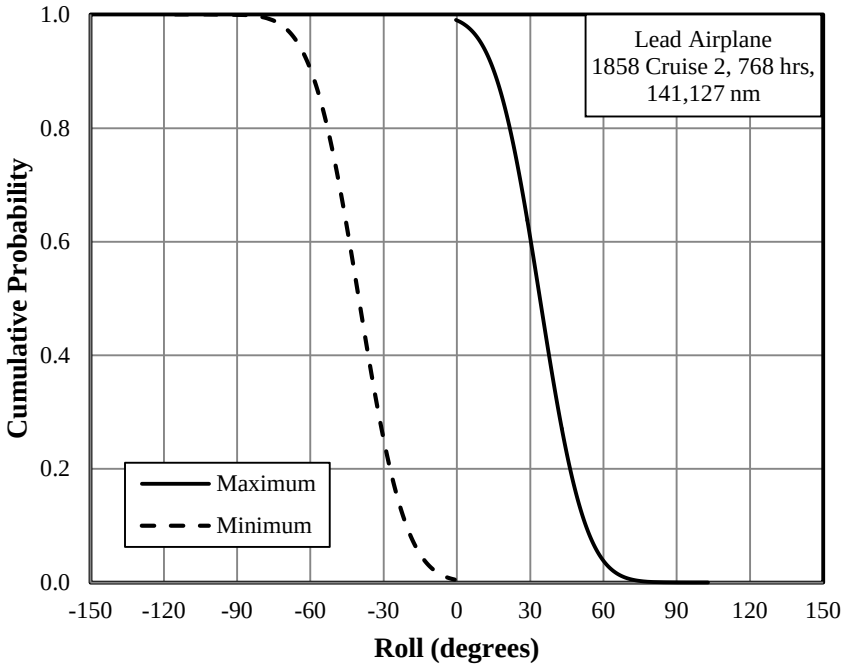

Figure A-52. Cumulative probability of roll angle, Cruise 2 phase

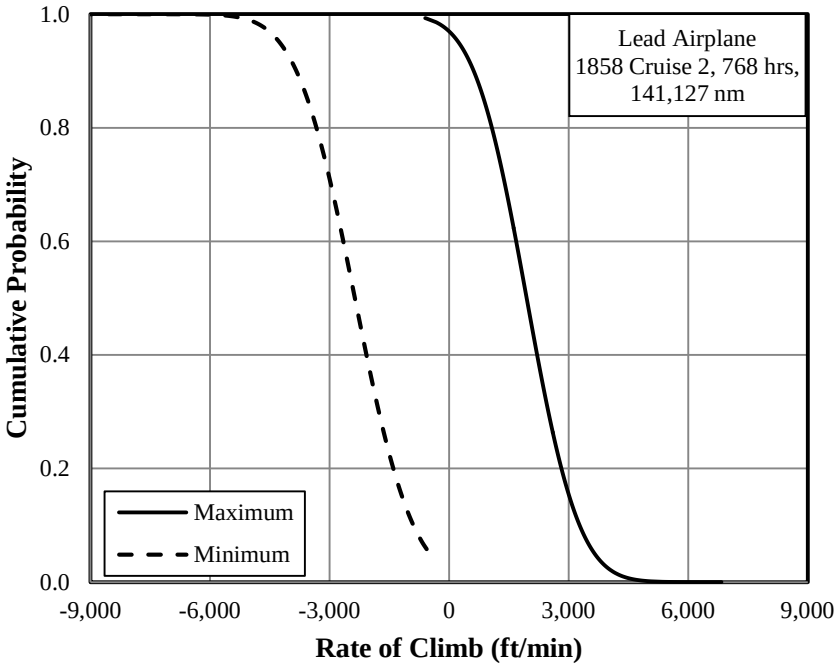

Figure A-53. Cumulative probability of rate of climb, Cruise 2 phase

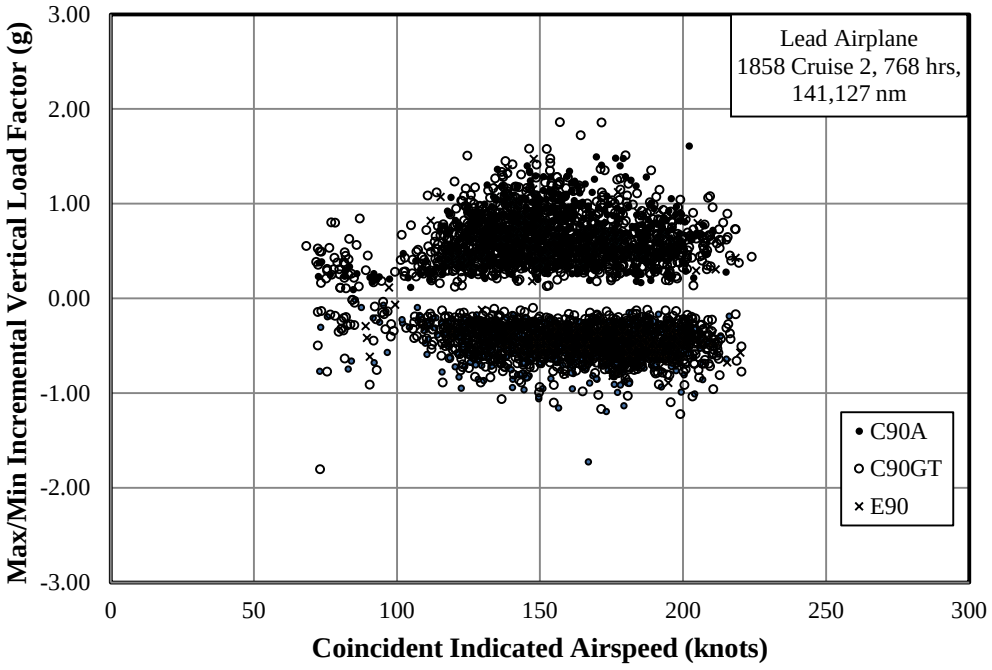

Figure A-54. *V-n* diagram, Cruise 2 phase

Model	Airplane Number	Number of Entry Phases	Duration (min)	Duration (hr)	Distance (nm)
C90A	1	932	932	16	2,292
	2	588	588	10	1,551
	3	185	185	3	435
C90GT	4	538	538	9	1,285
	5	1,039	1,039	17	2,436
	6	1,095	1,095	18	2,628
E90	7	386	386	6	901
Total	---	4,763	4,763	79	11,528

Figure A-55. Summary of durations and distances, entry phase

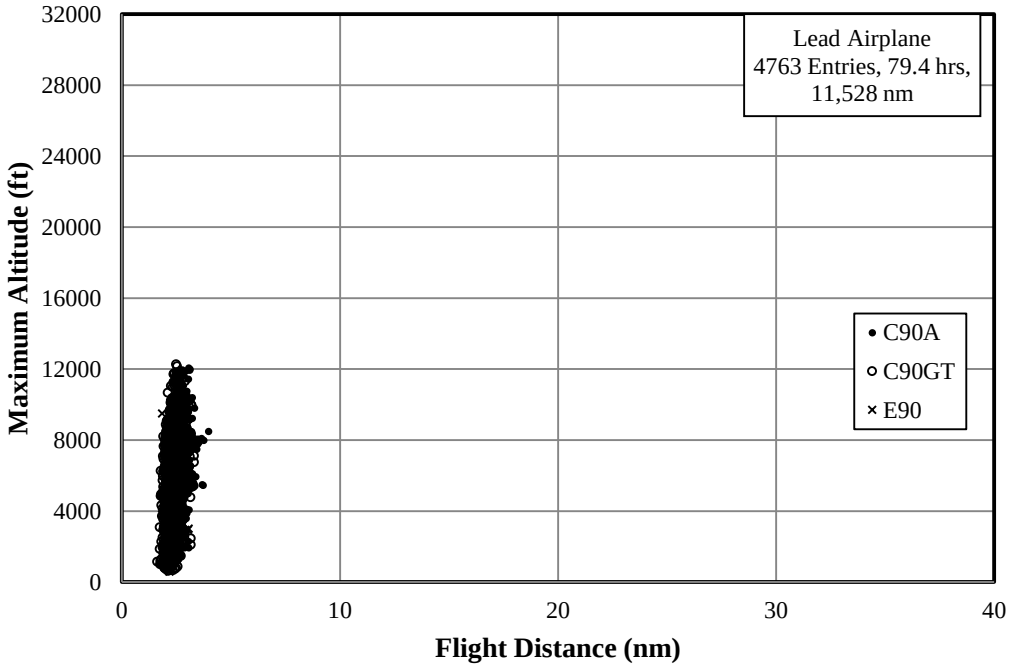

Figure A-56. Maximum altitude and coincident flight distance, entry phase

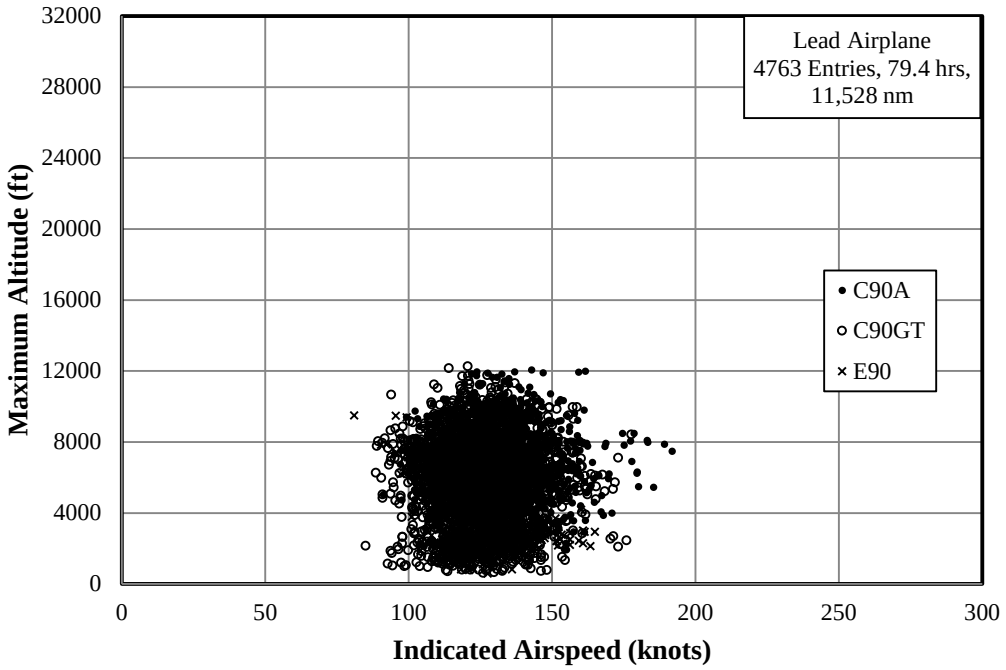

Figure A-57. Maximum altitude and coincident indicated airspeed, entry phase

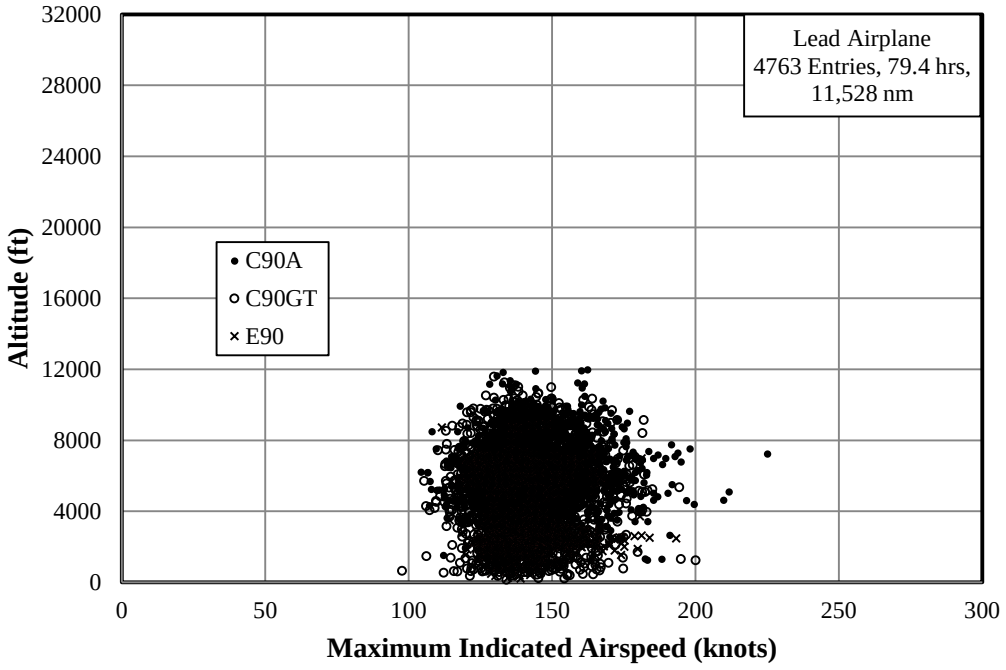

Figure A-58. Maximum indicated airspeed and coincident altitude, entry phase

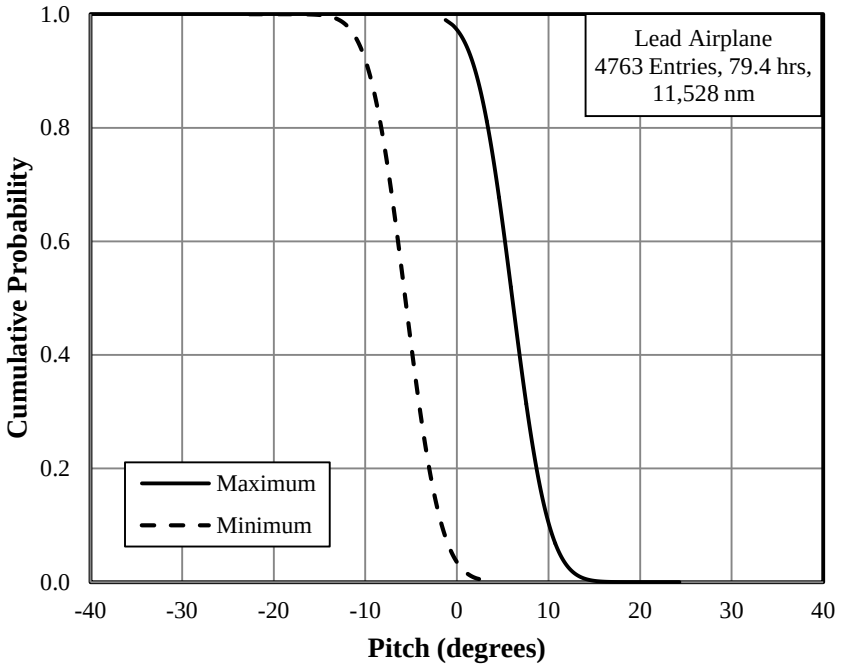

Figure A-59. Cumulative probability of pitch angle, entry phase

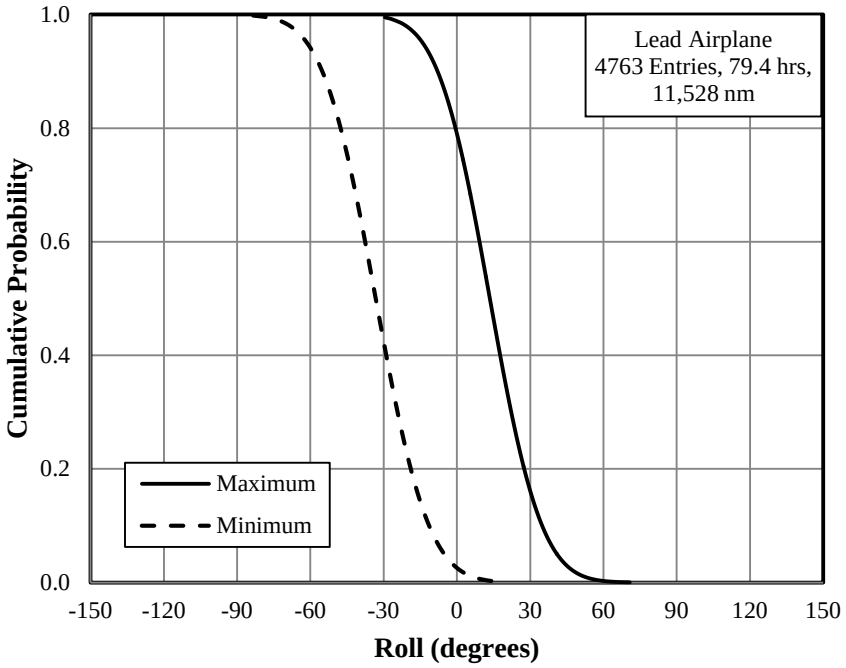

Figure A-60. Cumulative probability of roll angle, entry phase

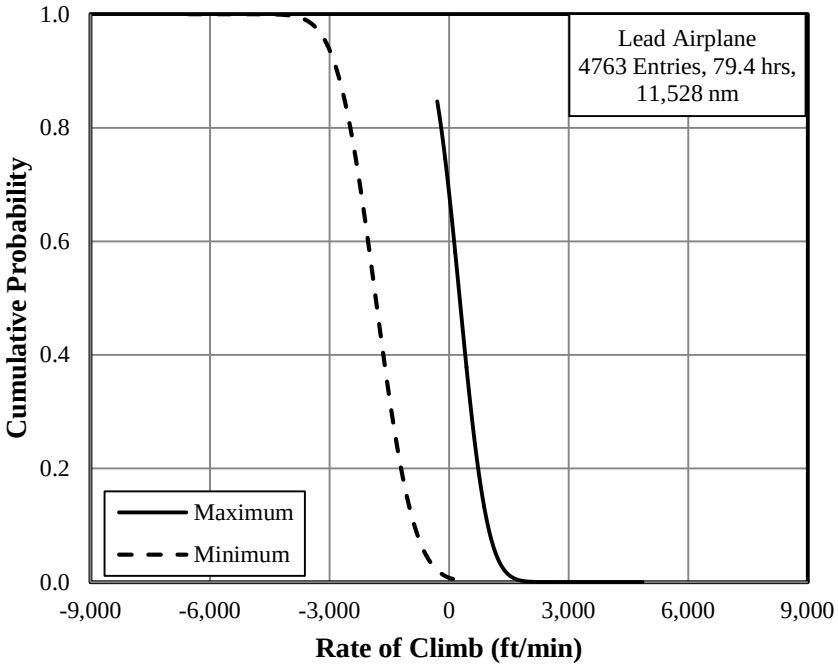

Figure A-61. Cumulative probability of rate of climb, entry phase

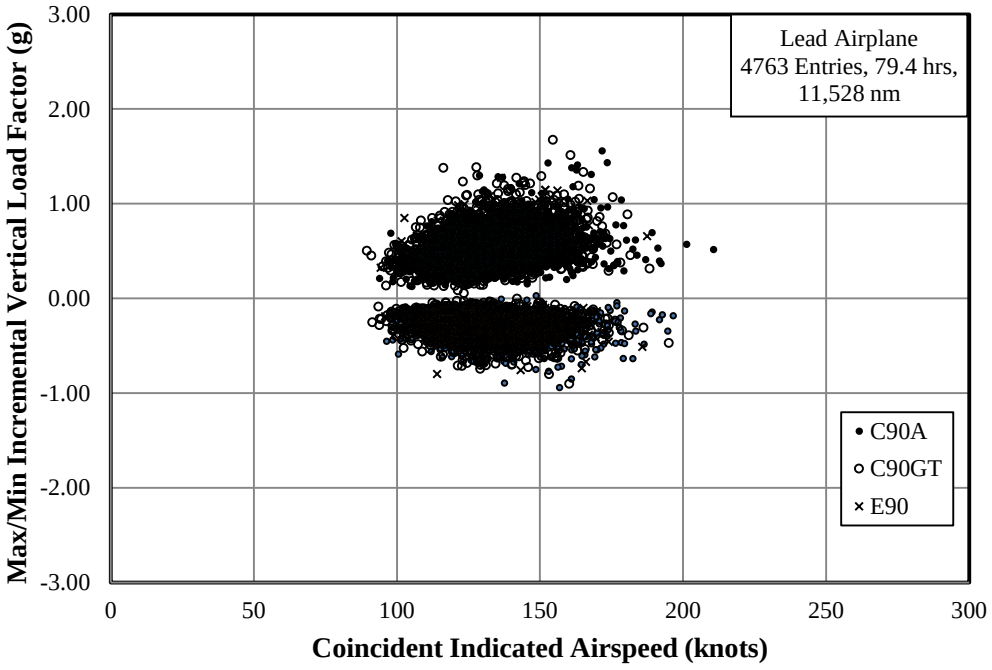

Figure A-62. *V-n* diagram, entry phase

Model	Airplane Number	Number of Lead Phases	Duration (min)	Duration (hr)	Distance (nm)
C90A	1	932	202	3	521
	2	588	141	2	386
	3	185	28	0	65
C90GT	4	538	65	1	160
	5	1039	252	4	592
	6	1095	214	4	520
E90	7	386	98	2	230
Total	---	4763	1001	17	2473

Figure A-63. Summary of durations and distances, lead phase

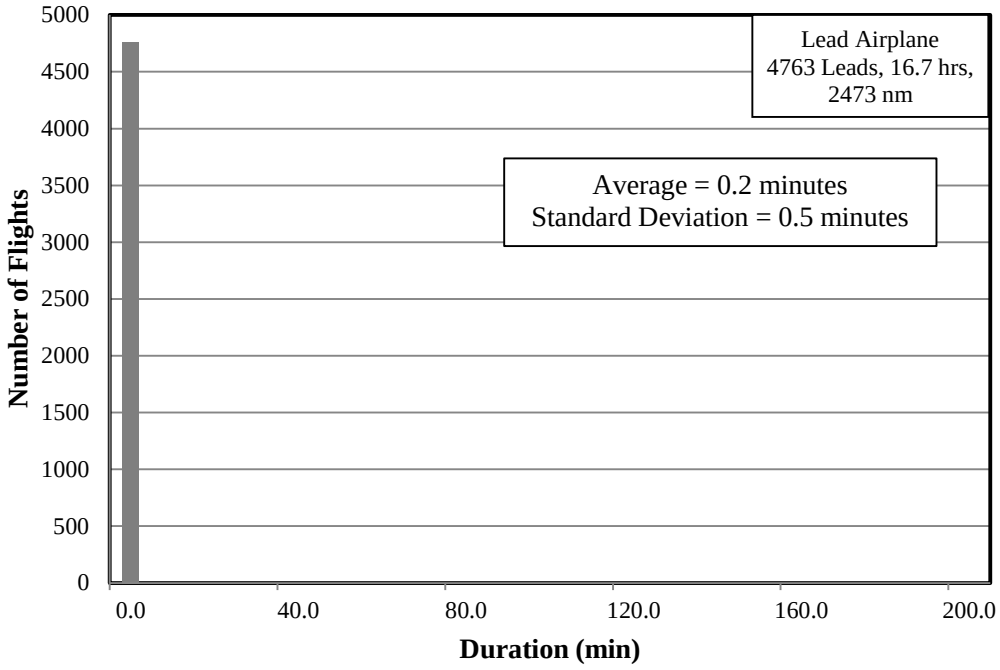

Figure A-64. Percentage of phases based on duration, lead phase

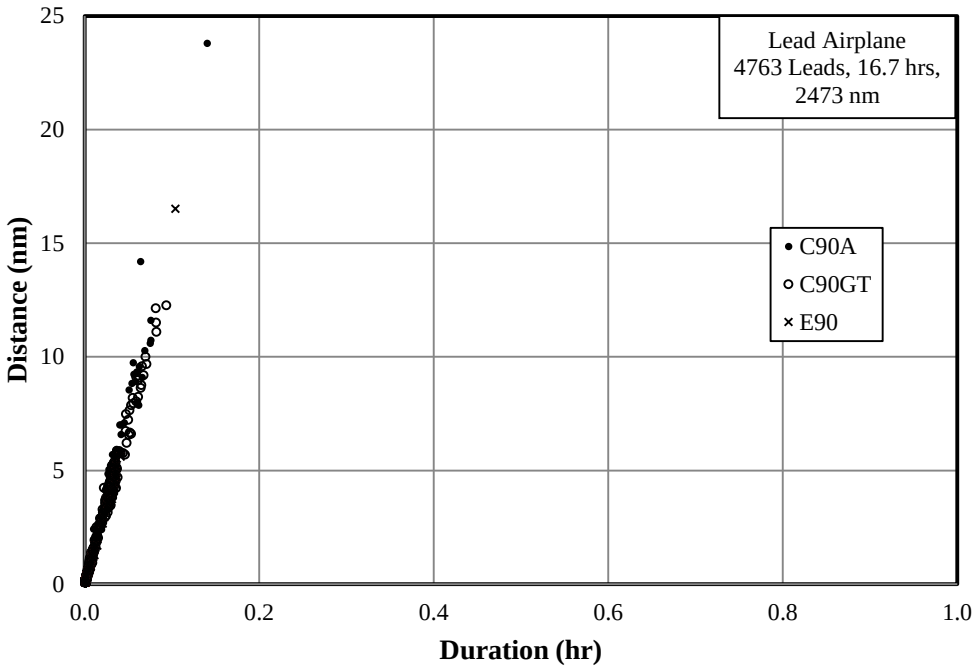

Figure A-65. Flight duration and coincident flight distance, lead phase

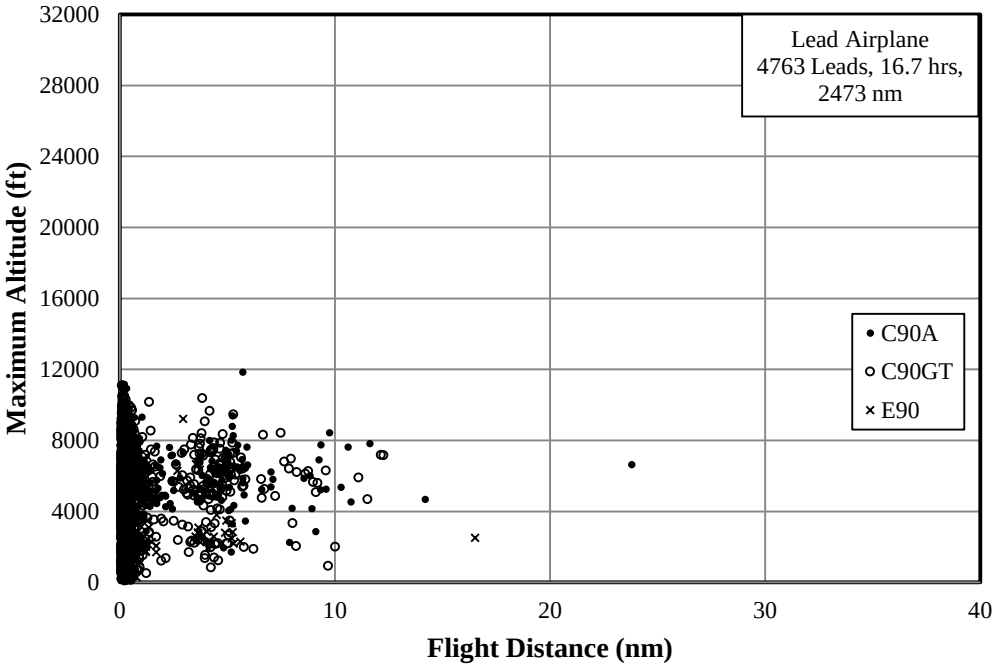

Figure A-66. Maximum altitude and coincident flight distance, lead phase

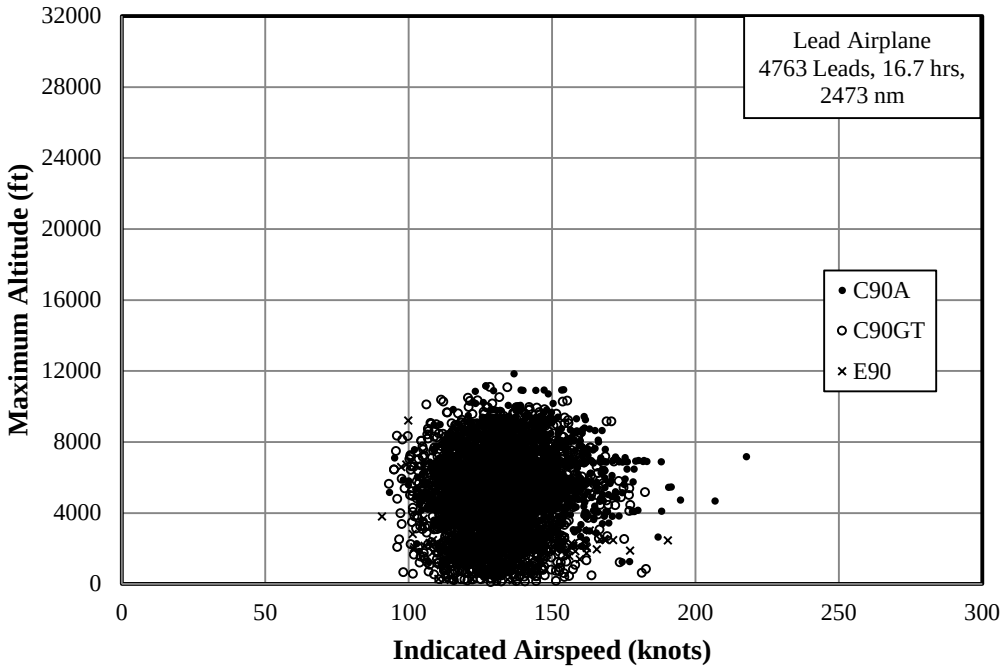

Figure A-67. Maximum altitude and coincident indicated airspeed, lead phase

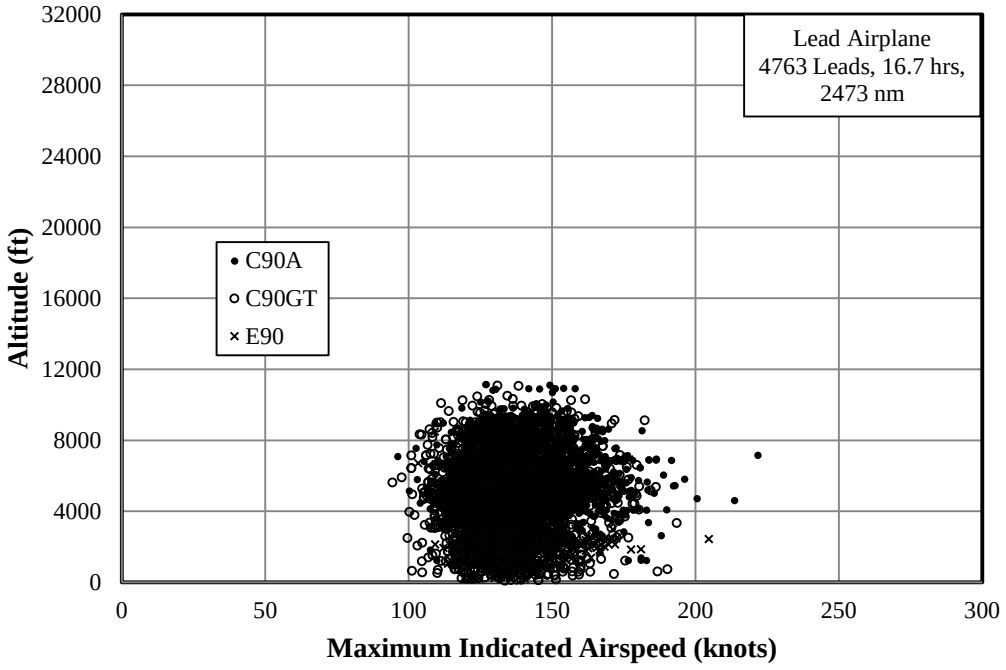

Figure A-68. Maximum indicated airspeed and coincident altitude, lead phase

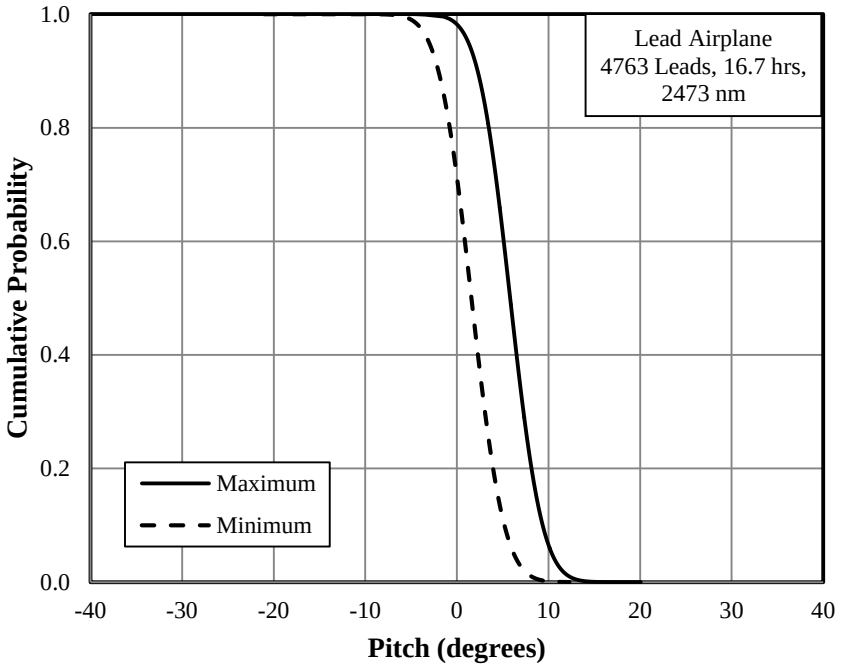

Figure A-69. Cumulative probability of pitch angle, lead phase

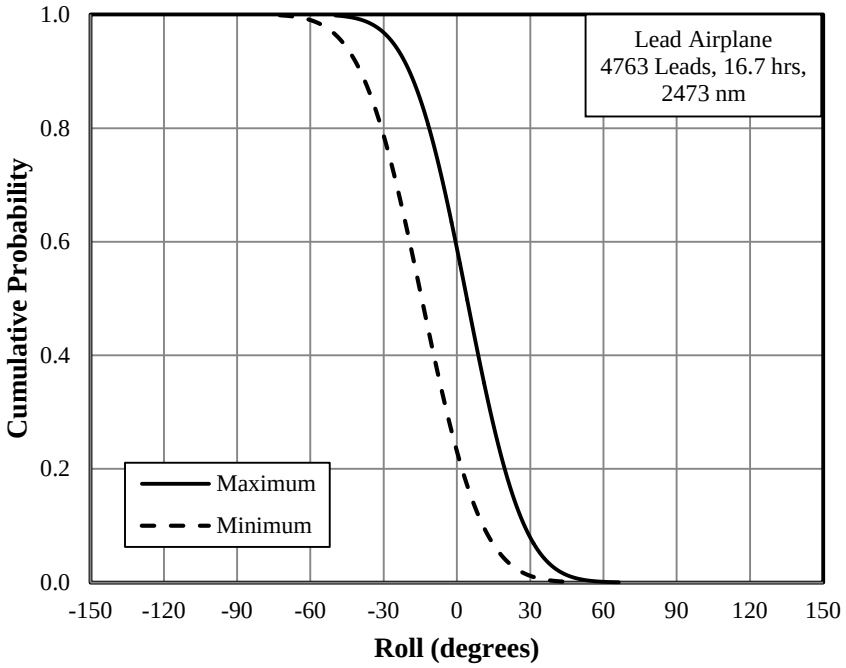

Figure A-70. Cumulative probability of roll angle, lead phase

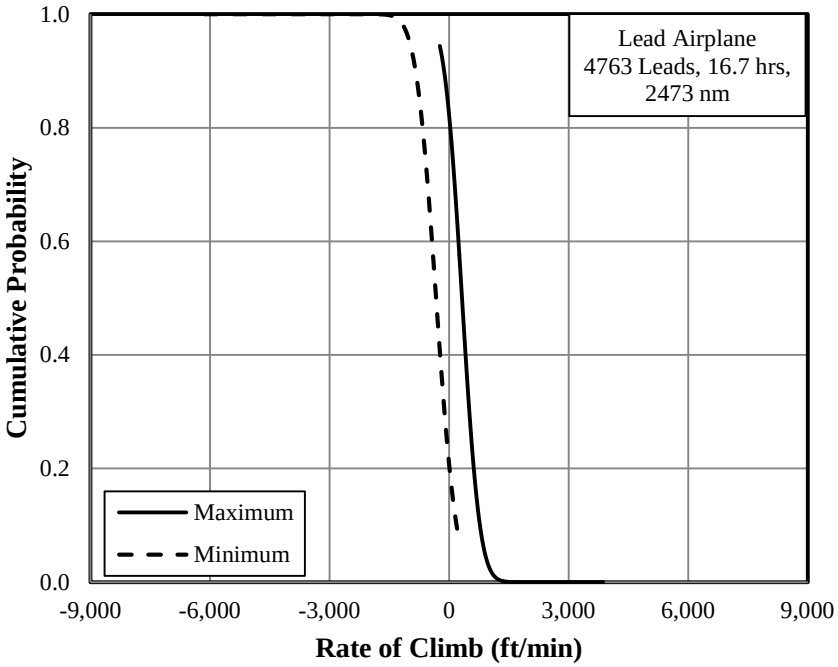

Figure A-71. Cumulative probability of rate of climb, lead phase

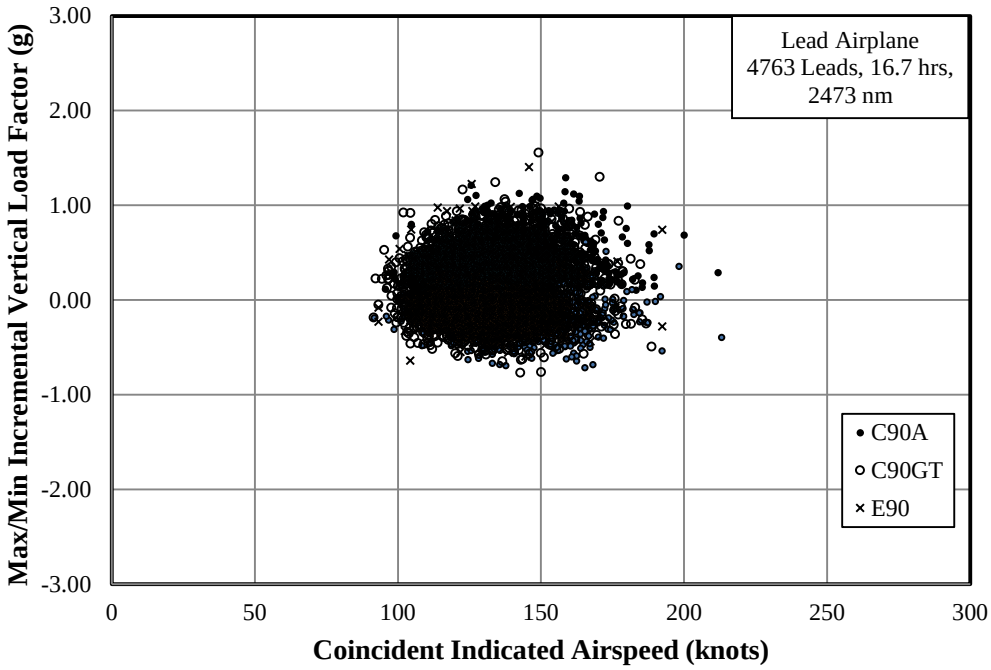

Figure A-72. *V-n* diagram, lead phase

Model	Airplane Number	Number of Exit Phases	Duration (min)	Duration (hr)	Distance (nm)
C90A	1	932	932	16	2,347
	2	588	588	10	1,553
	3	185	185	3	441
C90GT	4	538	538	9	1,308
	5	1,039	1,039	17	2,476
	6	1,095	1,095	18	2,638
E90	7	386	386	6	898
Total	---	4,763	4,763	79	11,660

Figure A-73. Summary of durations and distances, exit phase

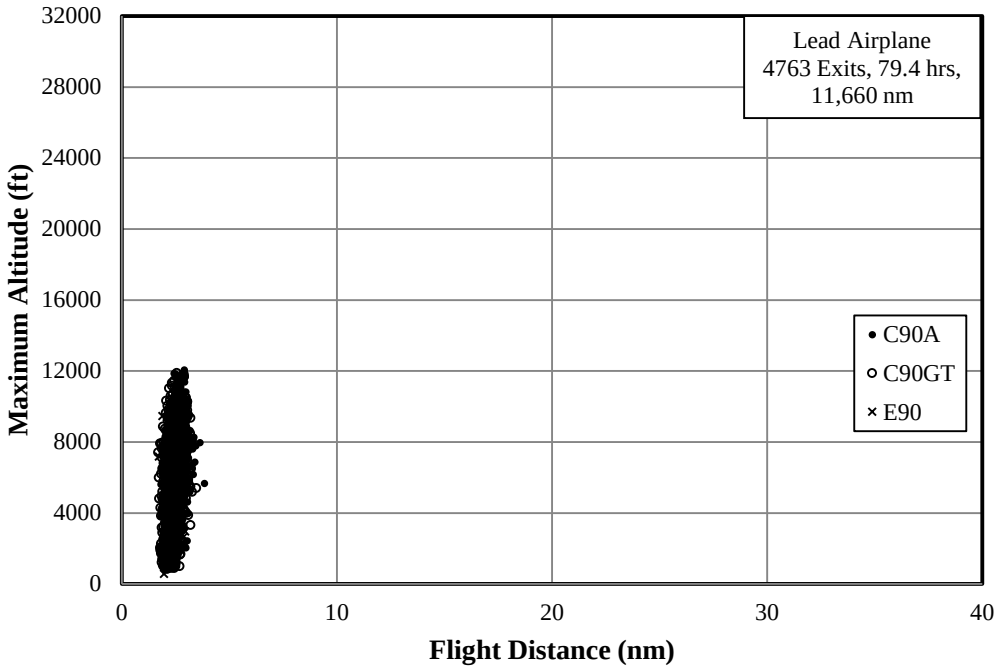

Figure A-74. Maximum altitude and coincident flight distance, exit phase

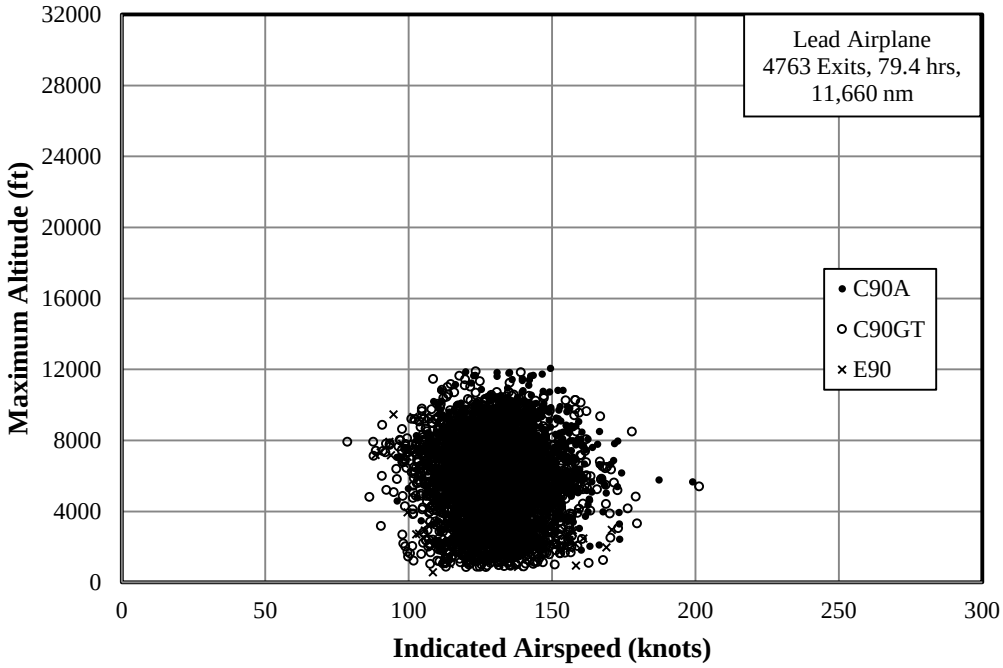

Figure A-75. Maximum altitude and coincident indicated airspeed, exit phase

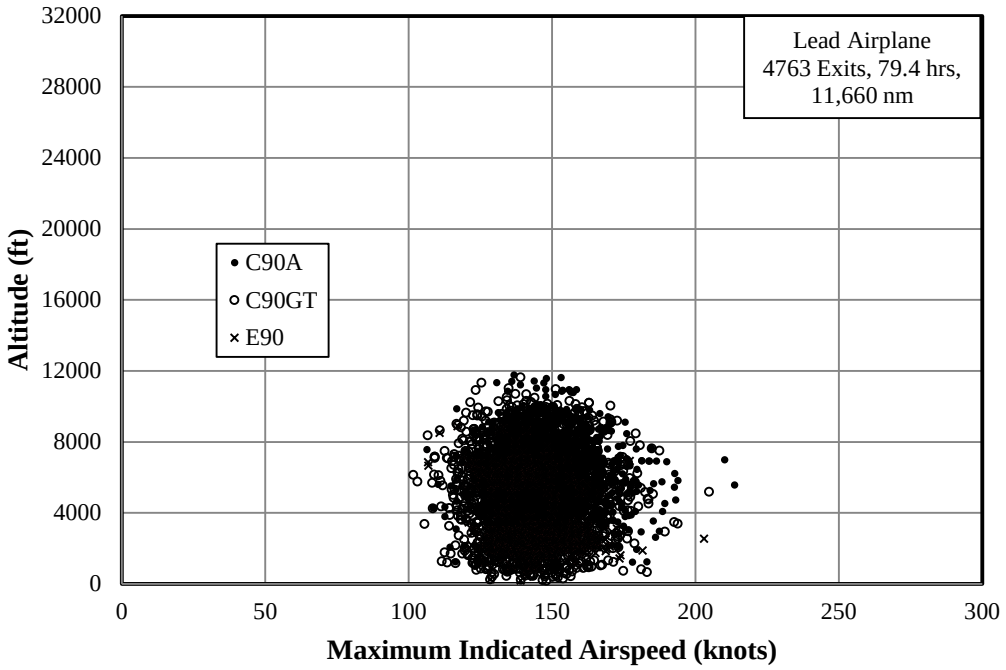

Figure A-76. Maximum indicated airspeed and coincident altitude, exit phase

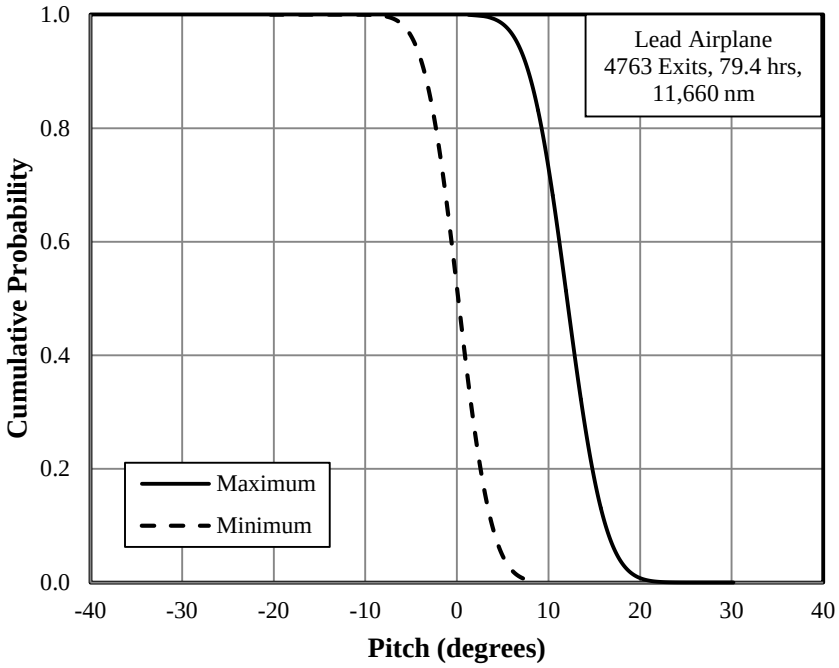

Figure A-77. Cumulative probability of pitch angle, exit phase

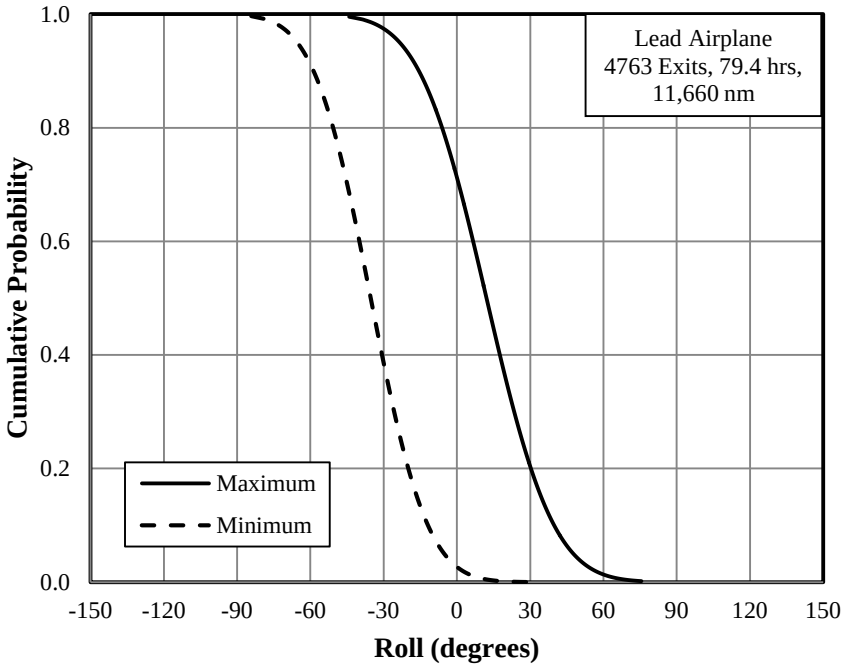

Figure A-78. Cumulative probability of roll angle, exit phase

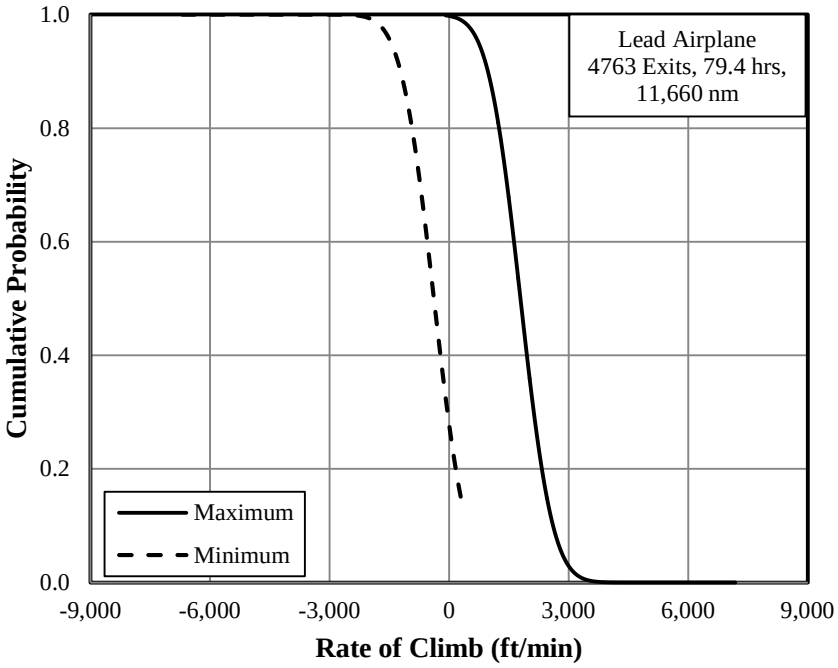

Figure A-79. Cumulative probability of rate of climb, exit phase

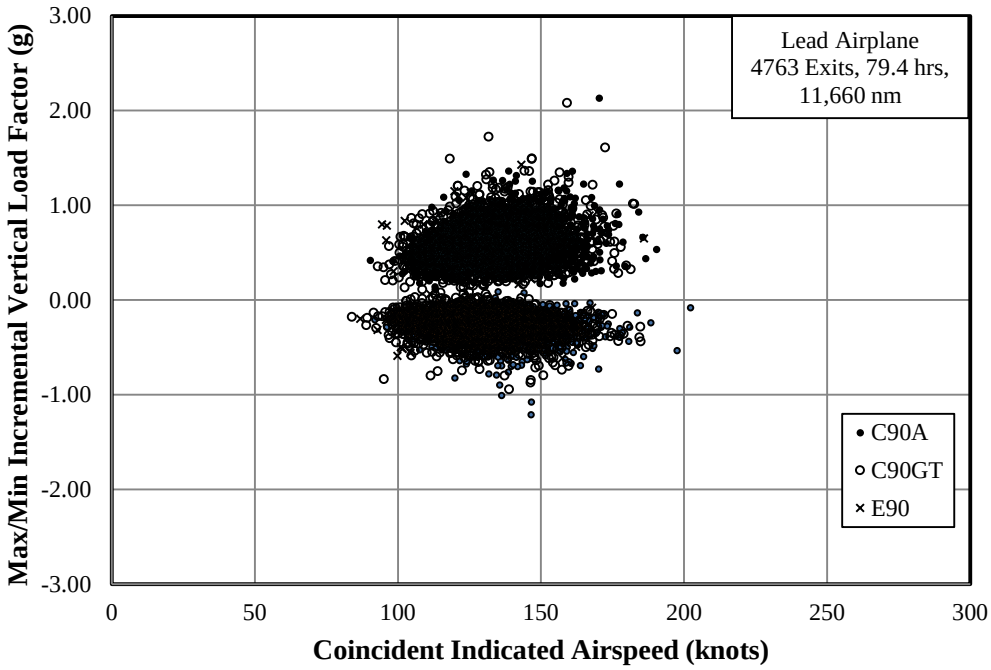

Figure A-80. *V-n* diagram, exit phase

Model	Airplane Number	Number of Turn Phases	Duration (min)	Duration (hr)	Distance (nm)
C90A	1	2,852	7,722	129	19,661
	2	2,163	7,658	128	21,021
	3	695	2,403	40	5,946
C90GT	4	2,542	8,126	135	20,240
	5	5,202	18,467	308	45,066
	6	5,770	17,690	295	41,535
E90	7	1,151	3,733	62	8,774
Total	---	20,375	65,799	1,097	162,244

Figure A-81. Summary of durations and distances, turn phase

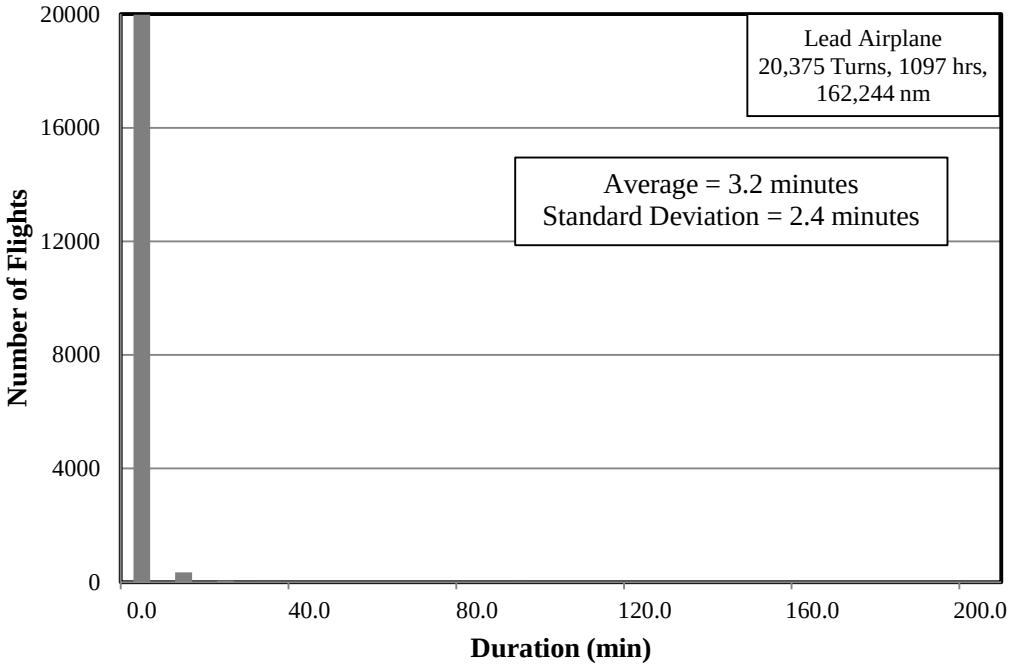

Figure A-82. Percentage of phases based on duration, turn phase

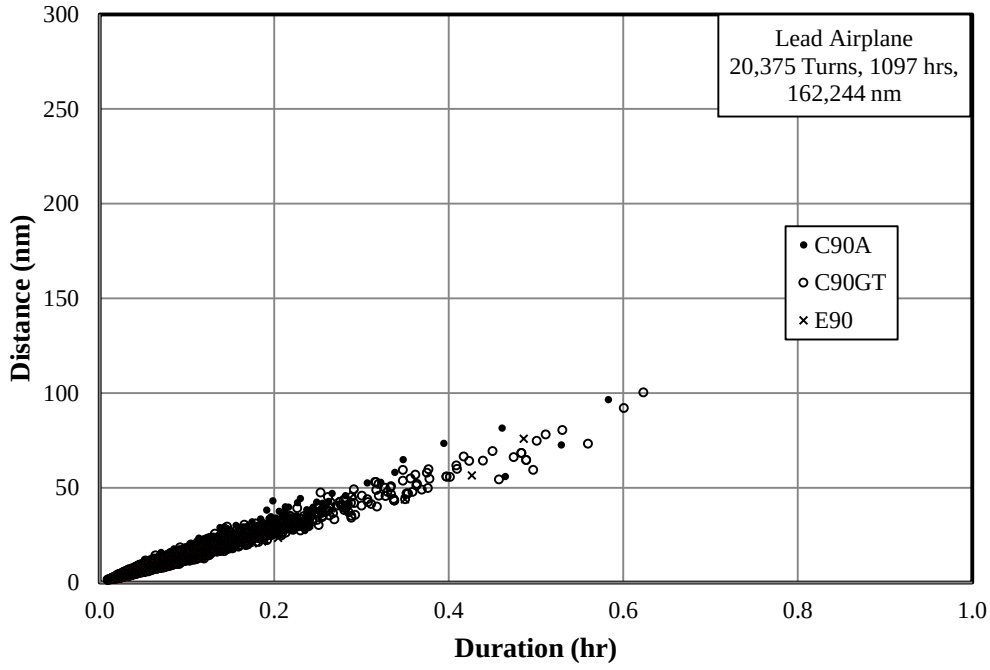

Figure A-83. Flight duration and coincident flight distance, turn phase

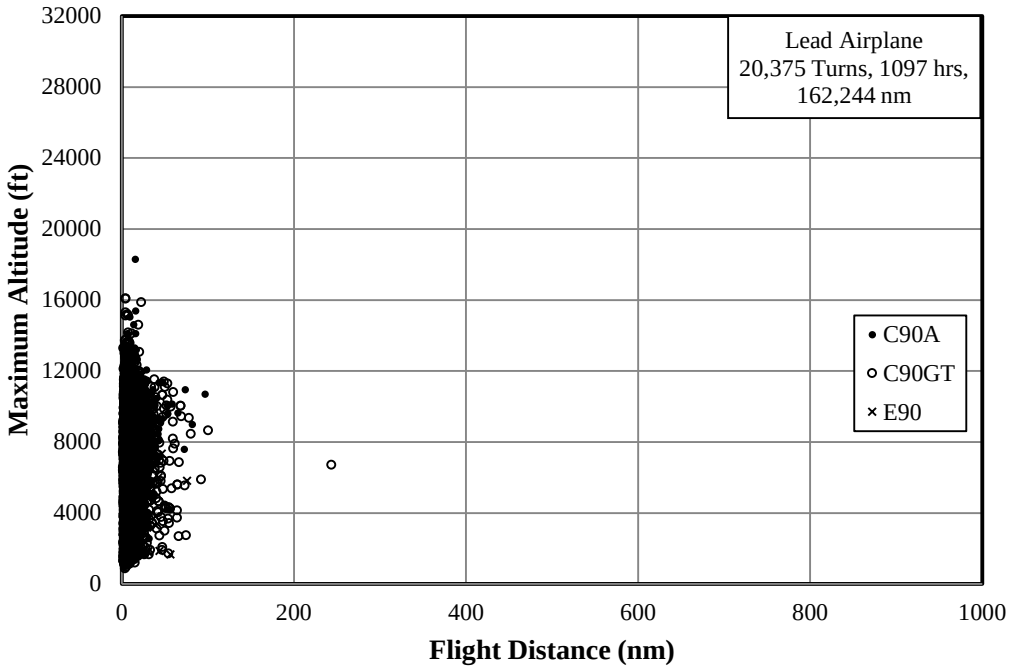

Figure A-84. Maximum altitude and coincident flight distance, turn phase

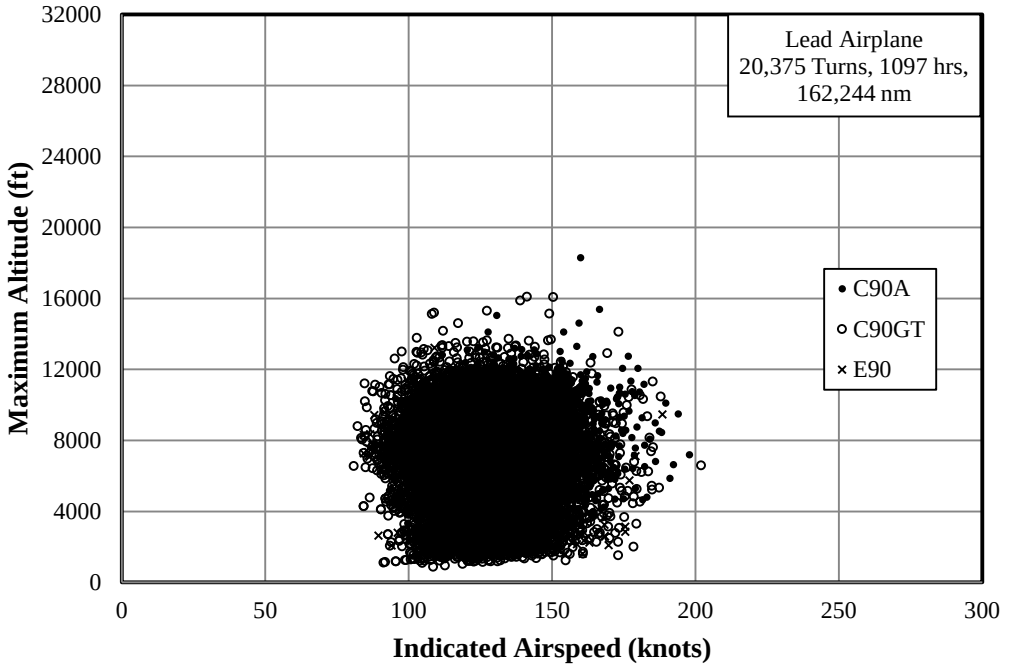

Figure A-85. Maximum altitude and coincident indicated airspeed, turn phase

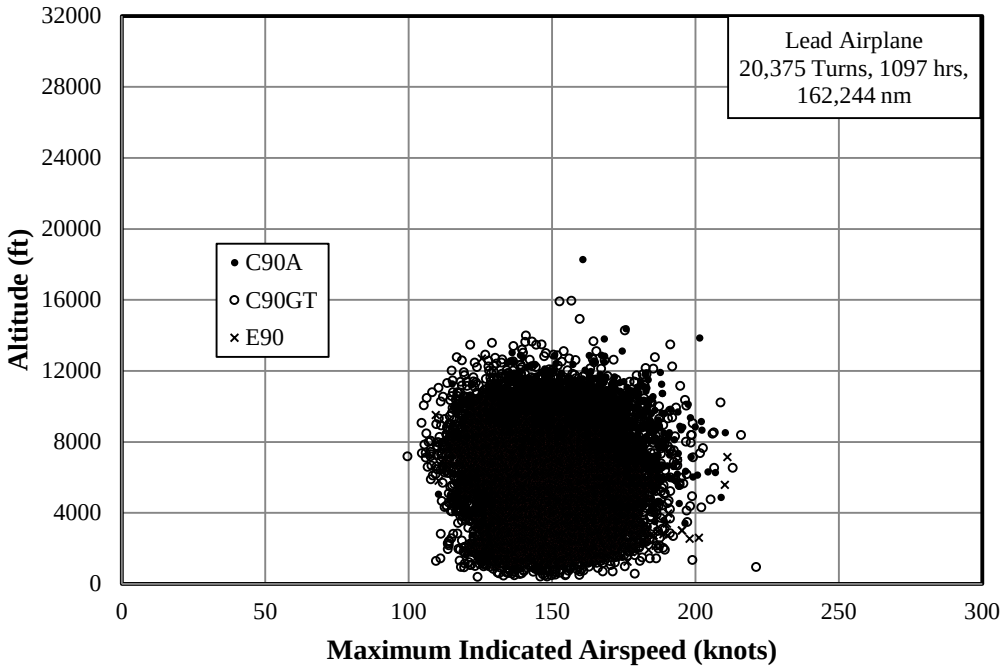

Figure A-86. Maximum indicated airspeed and coincident altitude, turn phase

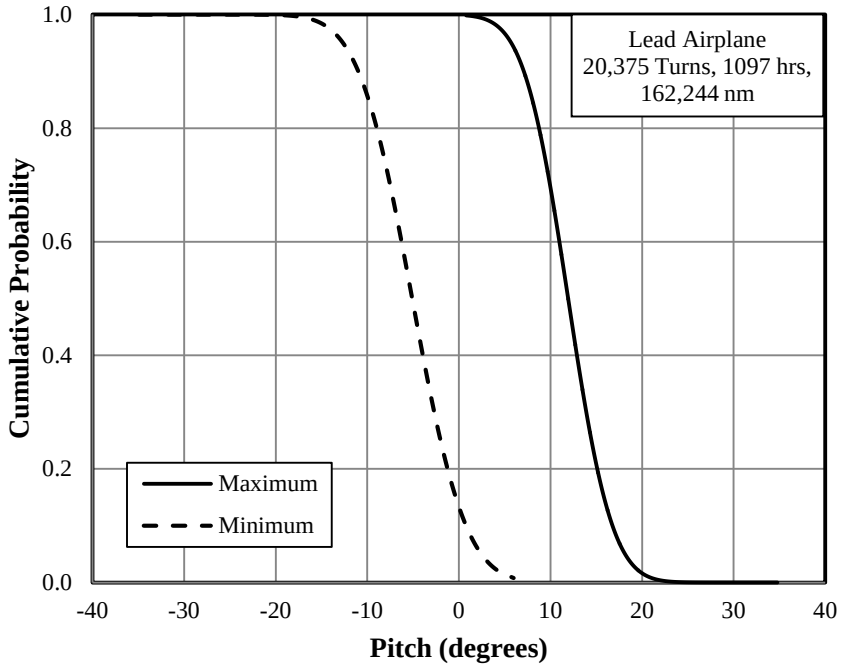

Figure A-87. Cumulative probability of pitch angle, turn phase

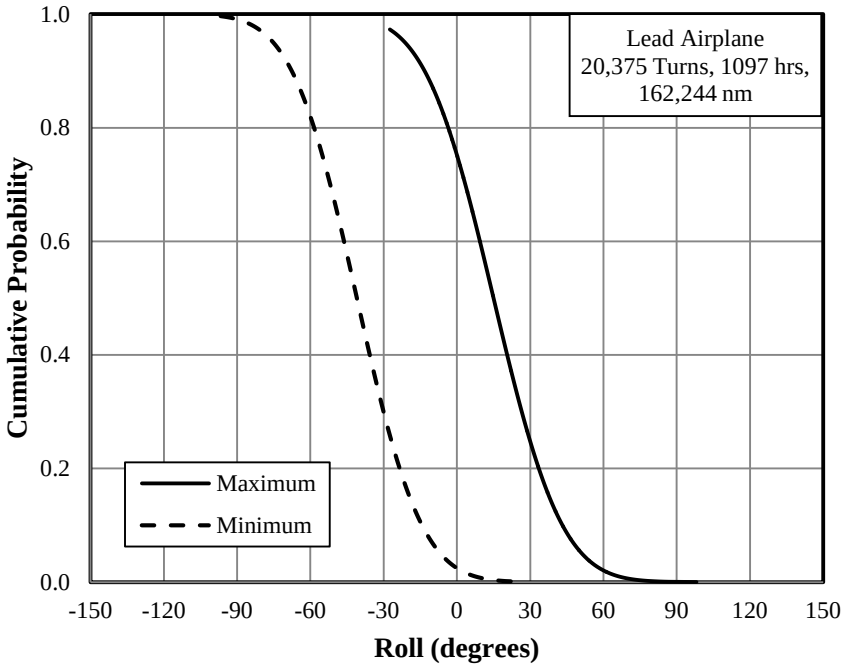

Figure A-88. Cumulative probability of roll angle, turn phase

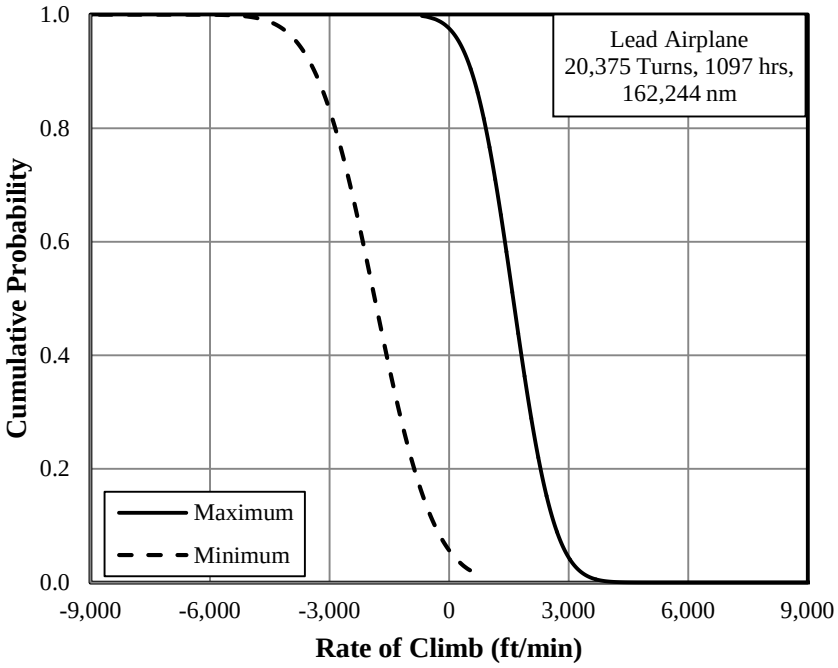

Figure A-89. Cumulative probability of rate of climb, turn phase

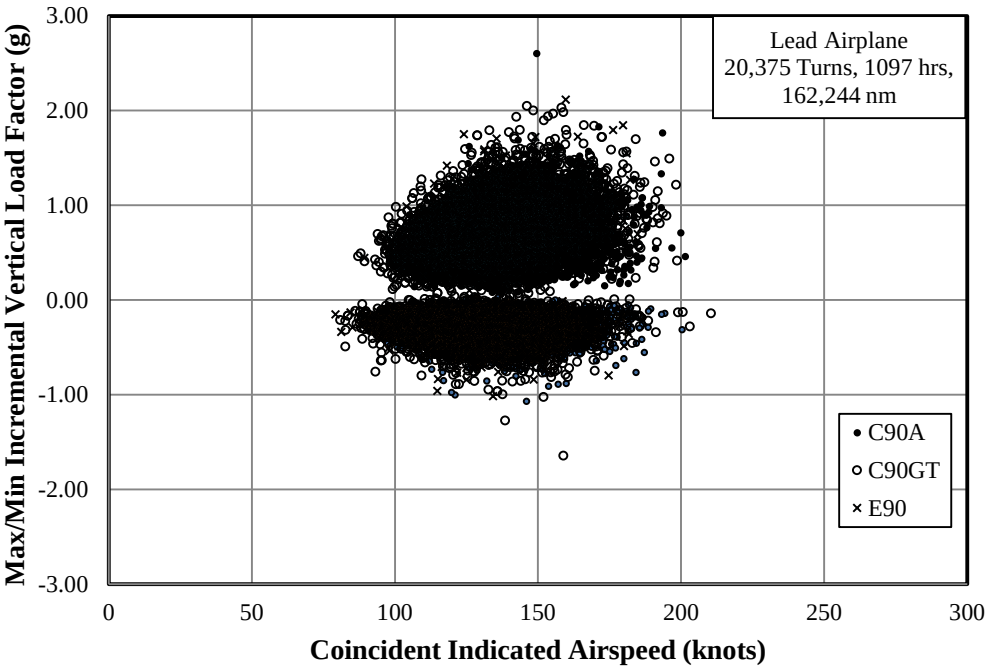

Figure A-90. *V-n* diagram, turn phase

Flap Usage	Ferry	Firefighting
Per 100 GAG cycles	103.6	722.1
Per 100 flight hours	88.9	340.6

Figure A-91. Number of flap deployments per mission type

Percentage of Flights with	Number of Flap Deployments				
	1 to 2	3 to 5	6 to 10	11 to 15	>15
Ferry	99.3	0.7	0.0	0.0	0.0
Firefighting	29.5	21.4	23.1	13.0	13.0

Figure A-92. Flap deployment per flight as a percentage of flights

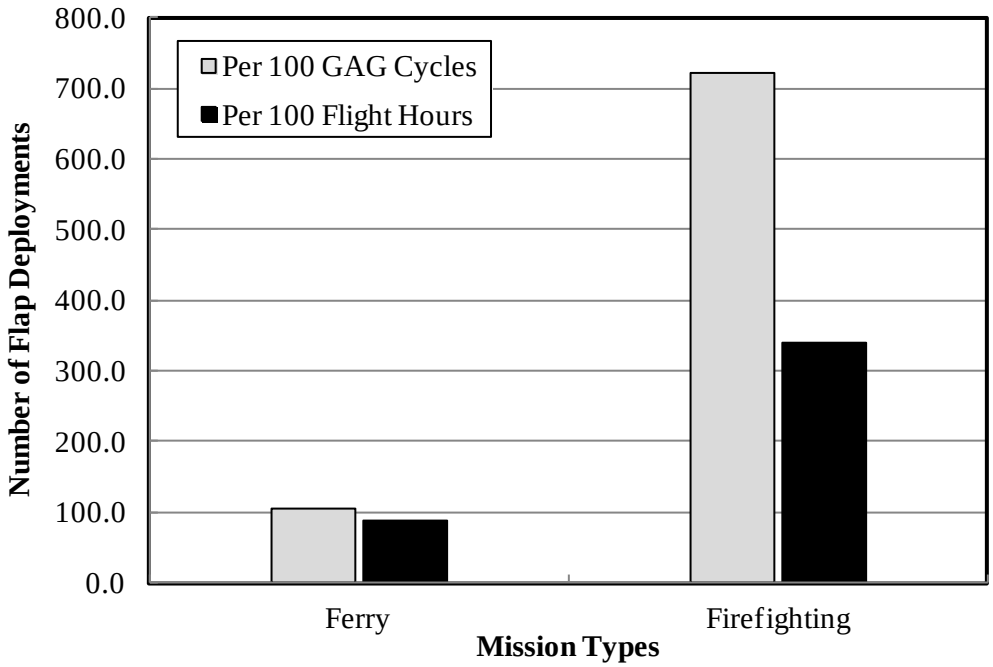

Figure A-93. Number of flap deployments per mission type

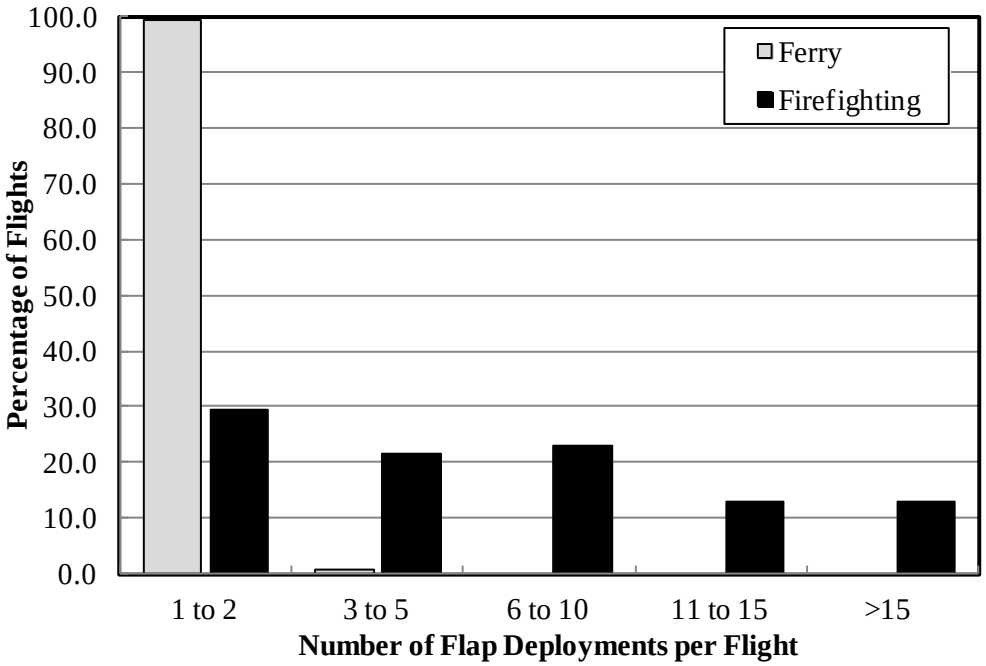

Figure A-94. Flap deployment per flight as a percentage of flights

APPENDIX B—FLIGHT LOADS BY MEAN SEA LEVEL ALTITUDE

Phase	Number of Phases	Duration (hr)	Distance (nm)
Cruise 1	1,858	840.7	166,719.9
Cruise 2	1,858	767.9	141,127.4
Entry	4,763	79.5	11,528.4
Lead	4,763	16.8	2,472.7
Exit	4,763	79.5	11,660.2
Turn	20,375	1,097.3	162,244.6
Overall flight	3,829	7,075.8	1,290,515.2

Figure B-1. Summary of durations and distances for all flight phases

Altitude Band Ceiling (ft)	Duration (hr)	Distance (nm)
500	1.13	136.25
1,500	8.01	1,109.38
4,500	73.84	11,937.94
9,500	353.12	64,788.92
14,500	290.60	61,466.07
19,500	107.52	25,664.53
24,500	4.45	1,104.98
35,000	2.02	511.99
Total	840.7	166,720

Figure B-2. Summary of durations and distances for Cruise 1 phases

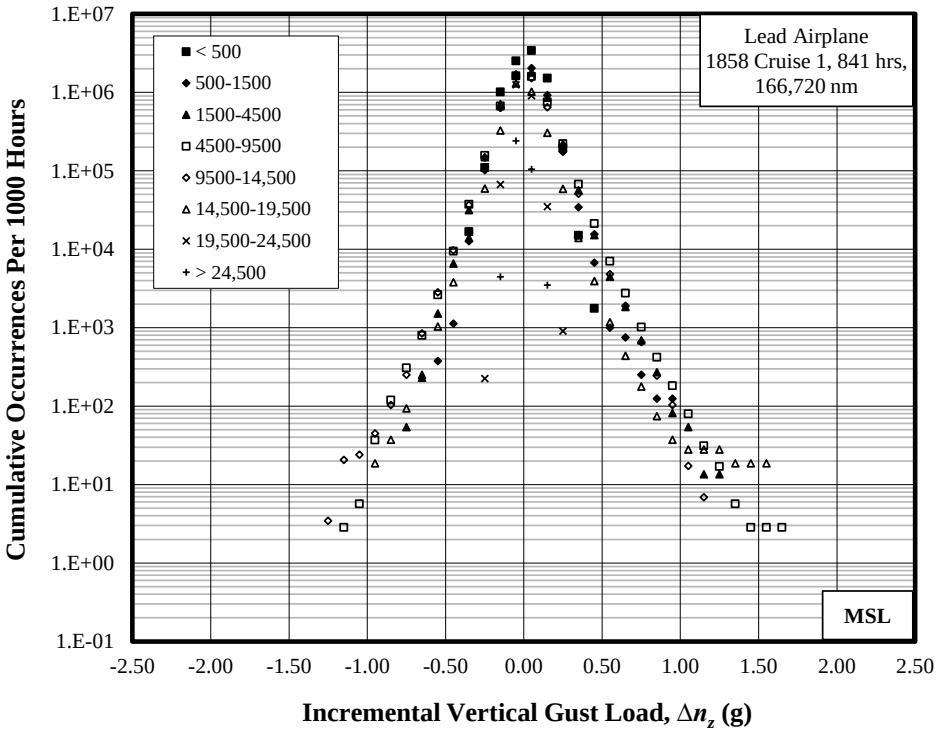

(a) Per 1000 hours

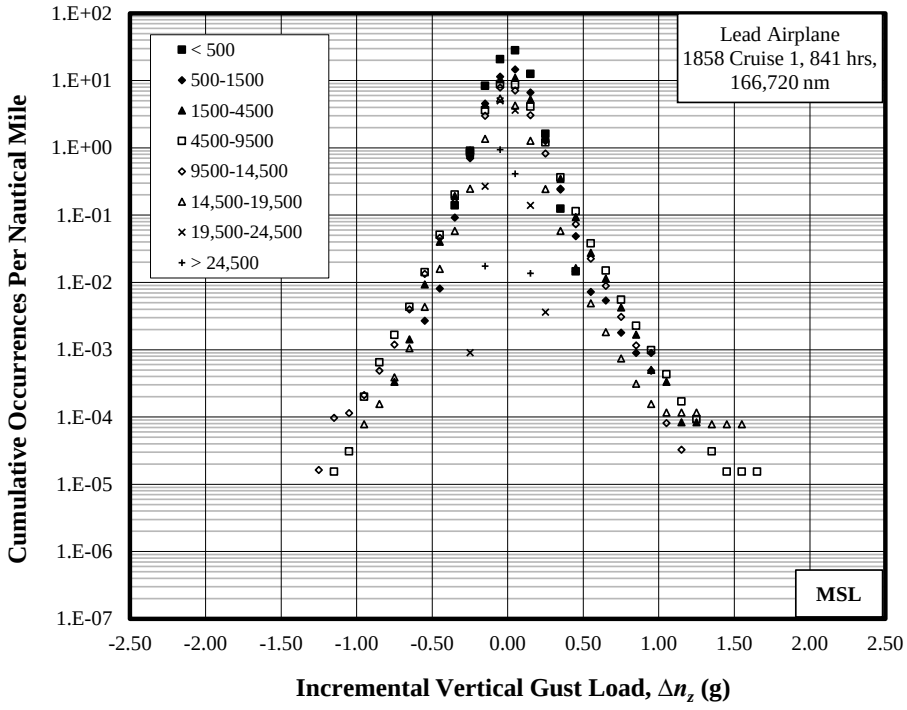

(b) Per nautical mile

Figure B-3. Cumulative occurrences of incremental vertical gust load factor, Cruise 1 phases, (a) per 1000 hours and (b) per nautical mile

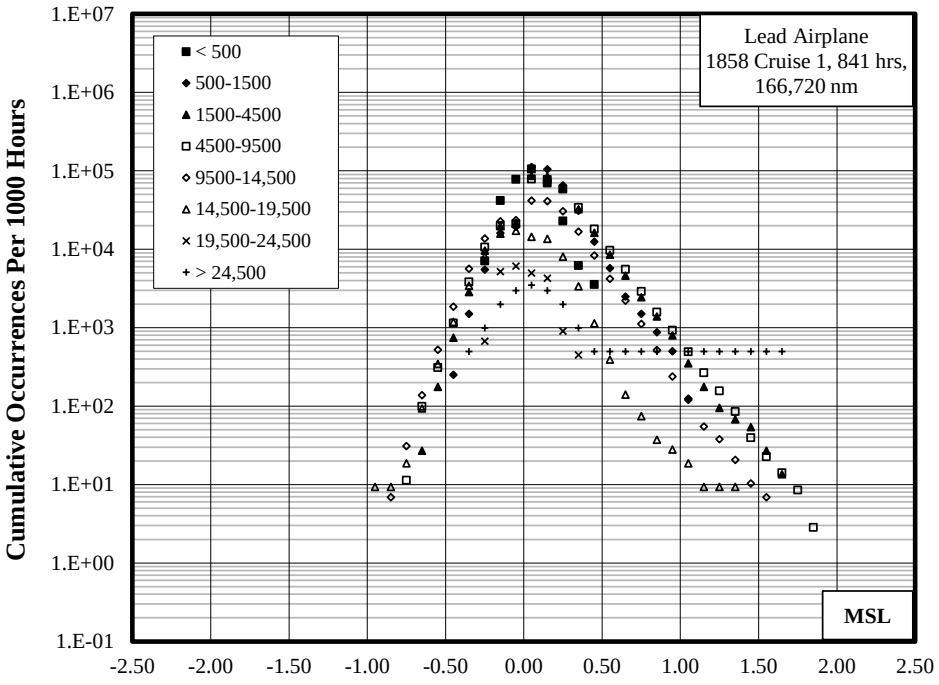

(a) Per 1000 hours

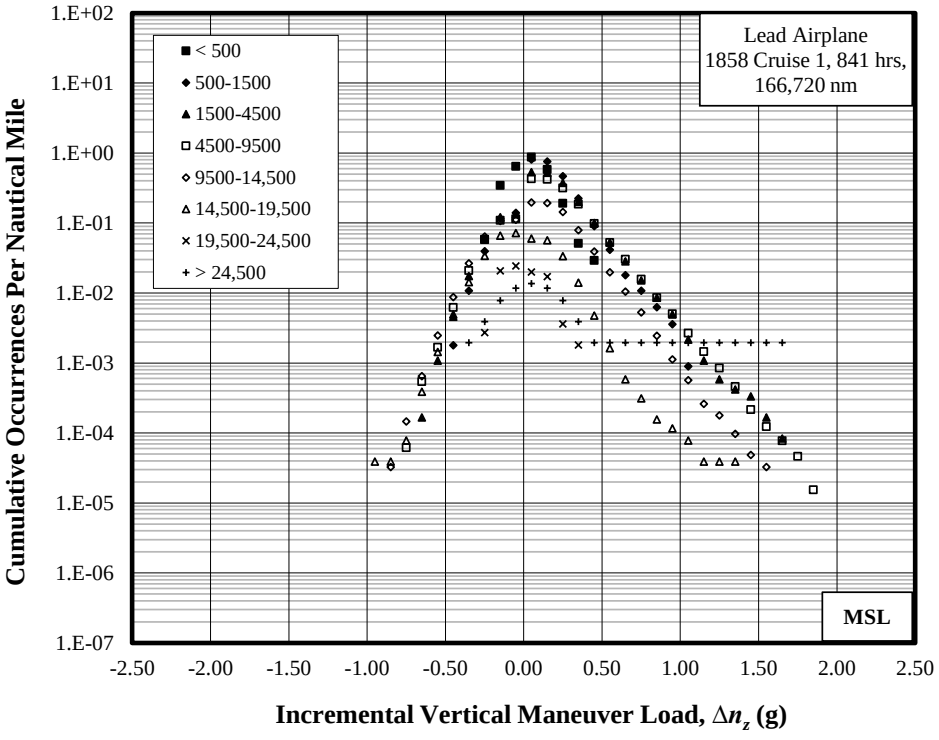

(b) Per nautical mile

Figure B-4. Cumulative occurrences of incremental vertical maneuver load factor, Cruise 1 phases, (a) per 1000 hours and (b) per nautical mile

Altitude Band Ceiling (ft)	Duration (hr)	Distance (nm)
500	1.29	128.62
1,500	12.28	1,497.16
4,500	106.27	16,847.27
9,500	414.20	73,833.28
14,500	191.63	38,756.19
19,500	38.42	9,129.93
24,500	1.53	365.91
35,000	2.26	569.00
Total	767.9	141,127

Figure B-5. Summary of durations and distances for Cruise 2 phases

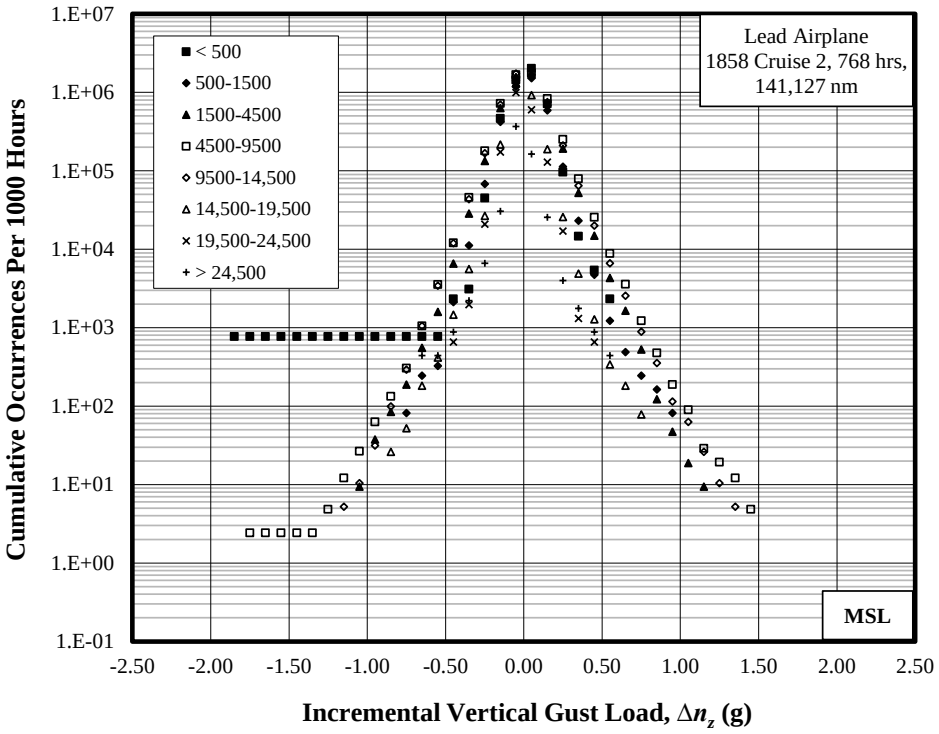

(a) Per 1000 hours

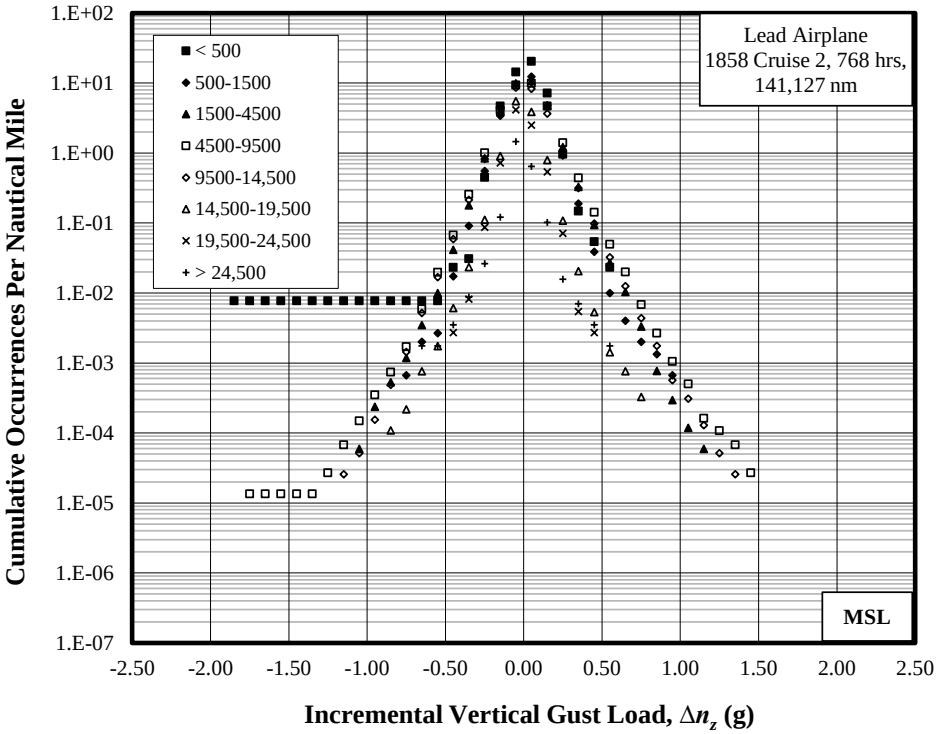

(b) Per nautical mile

Figure B-6. Cumulative occurrences of incremental vertical gust load factor, Cruise 2 phases, (a) per 1000 hours and (b) per nautical mile

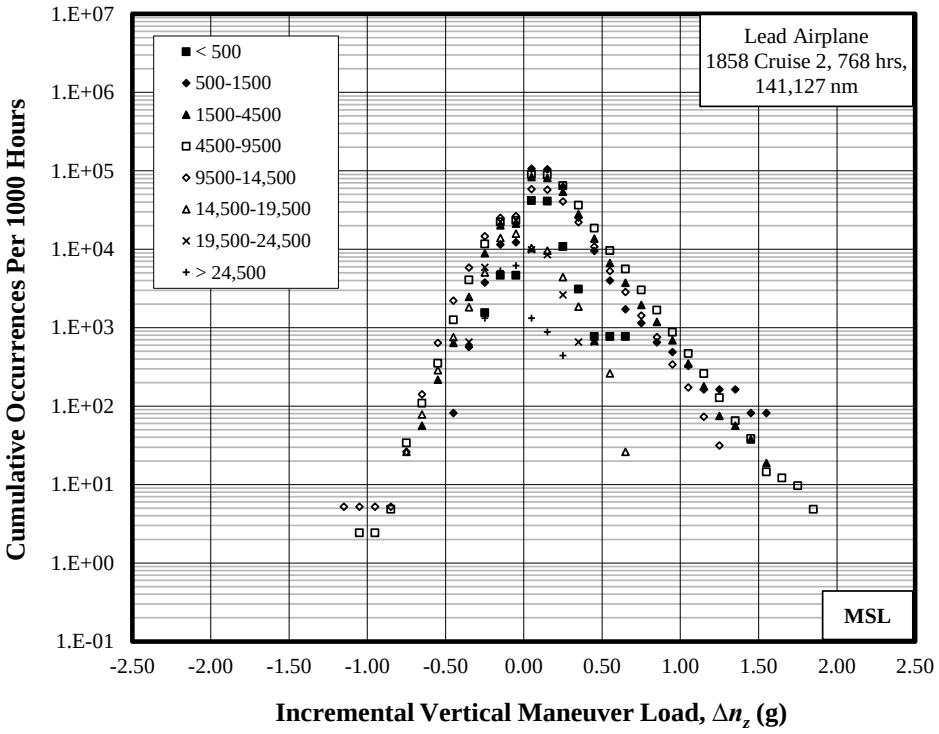

(a) Per 1000 hours

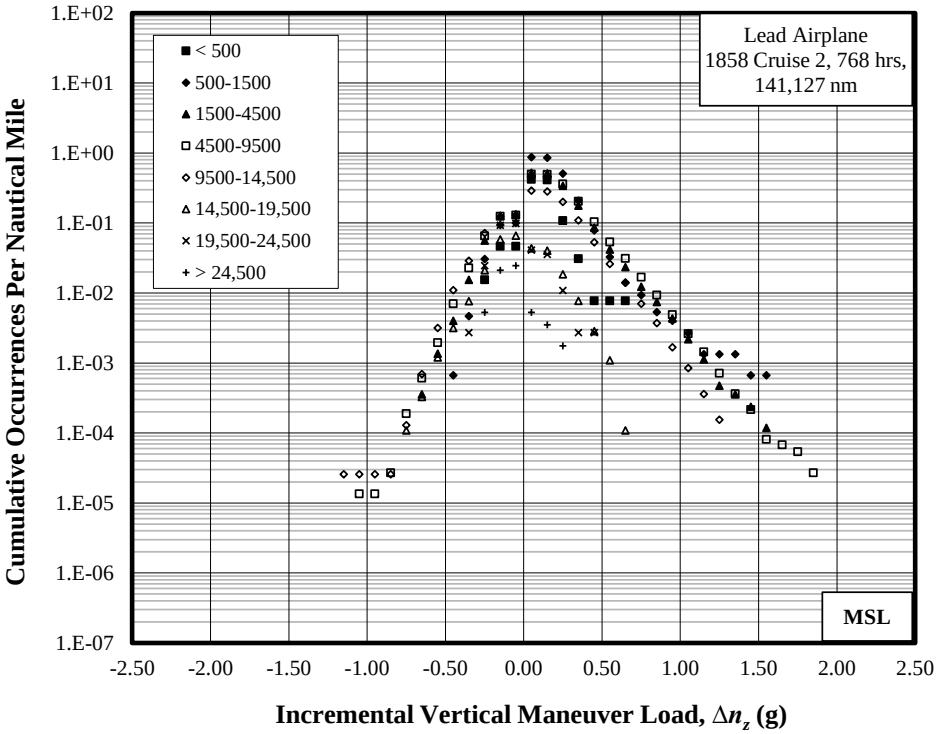

(b) Per nautical mile

Figure B-7. Cumulative occurrences of incremental vertical maneuver load factor, Cruise 2 phases (a) per 1000 miles and (b) per nautical mile

Altitude Band Ceiling (ft)	Duration (hr)	Distance (nm)
500	0.25	32.68
1,500	2.89	385.87
4,500	20.99	2,928.38
9,500	52.35	7,701.72
14,500	3.07	479.75
19,500	0	0
24,500	0	0
35,000	0	0
Total	79.5	11,528

Figure B-8. Summary of durations and distances for entry phases

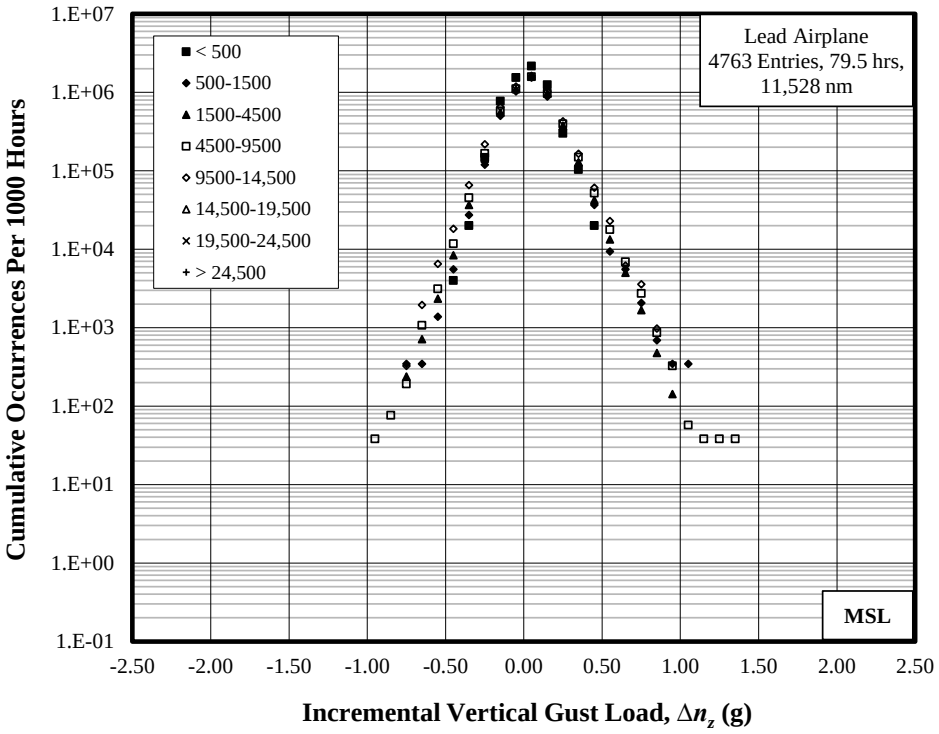

(a) Per 1000 hours

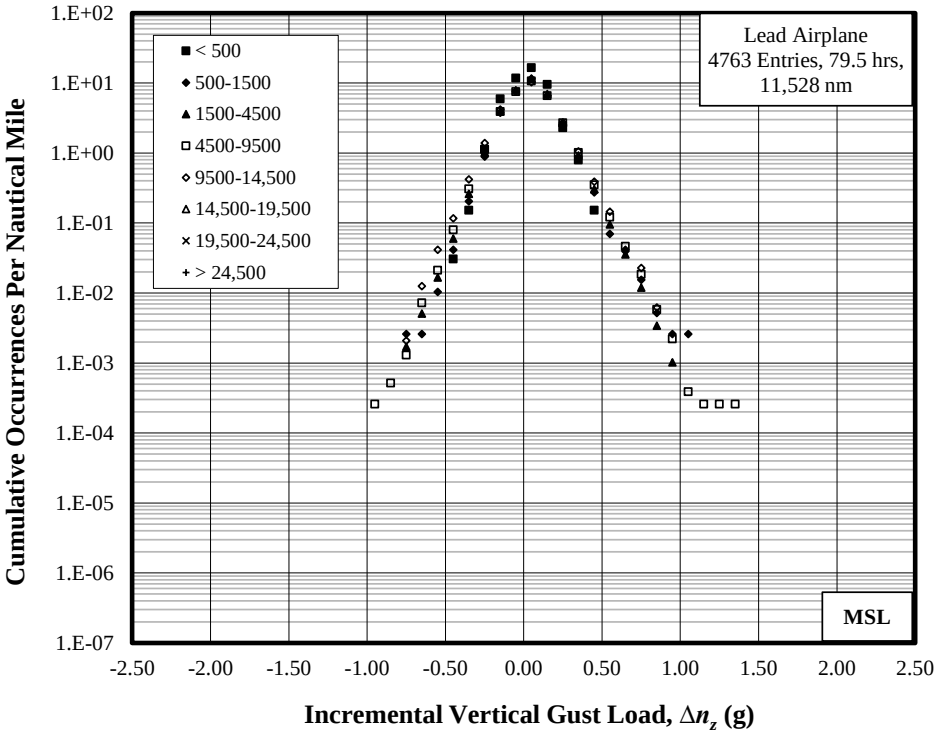

(b) Per nautical mile

Figure B-9. Cumulative occurrences of incremental vertical gust load factor, entry phases (a) per 1000 hours and (b) per nautical mile

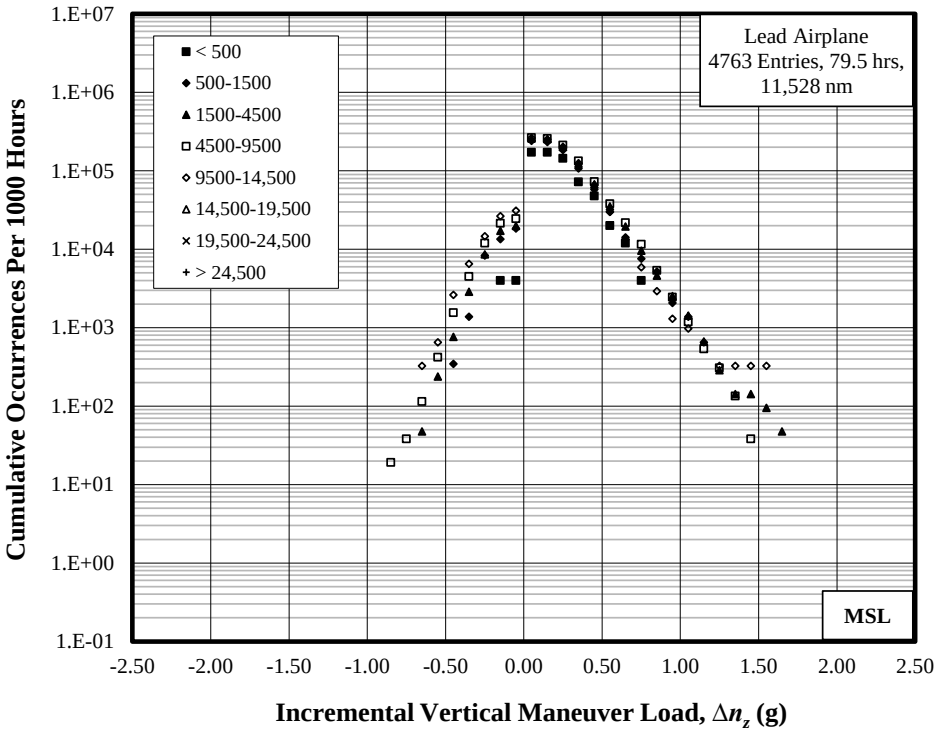

(a) Per 1000 hours

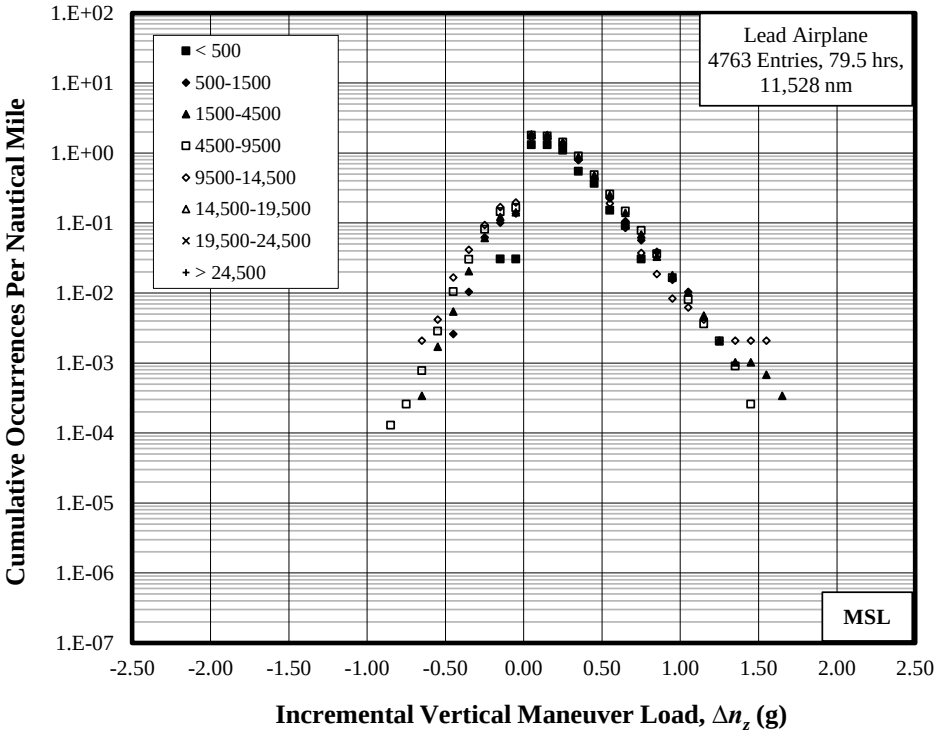

(b) Per nautical mile

Figure B-10. Cumulative occurrences of incremental vertical maneuver load factor, entry phases (a) per 1000 hours and (b) per nautical mile

Altitude Band Ceiling (ft)	Duration (hr)	Distance (nm)
500	0.13	16.78
1,500	0.69	96.36
4,500	4.95	699.91
9,500	10.92	1,634.54
14,500	0.16	25.09
19,500	0	0
24,500	0	0
35,000	0	0
Total	16.8	2,473

Figure B-11. Summary of durations and distances for lead phases

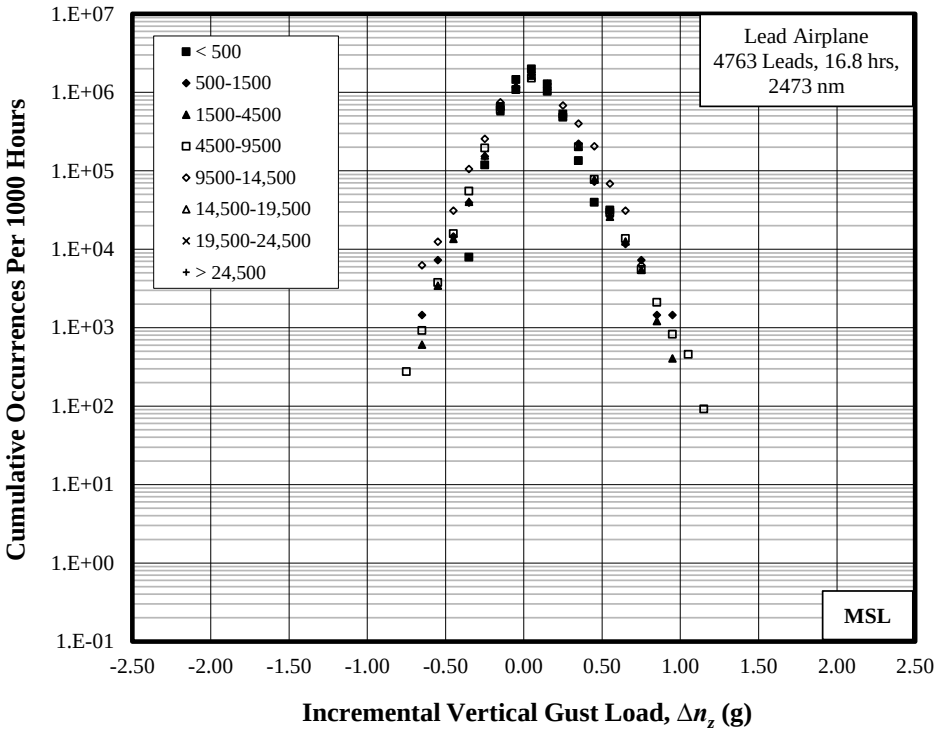

(a) Per 1000 hours

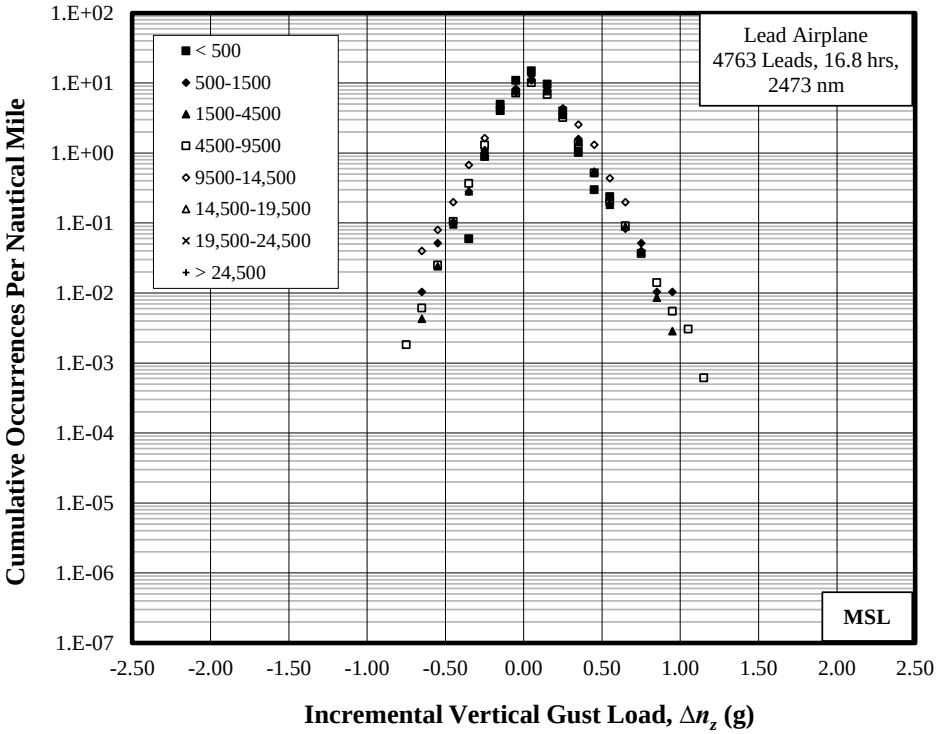

(b) Per nautical mile

Figure B-12. Cumulative occurrences of incremental vertical gust load factor, lead phases (a) per 1000 miles and (b) per nautical mile

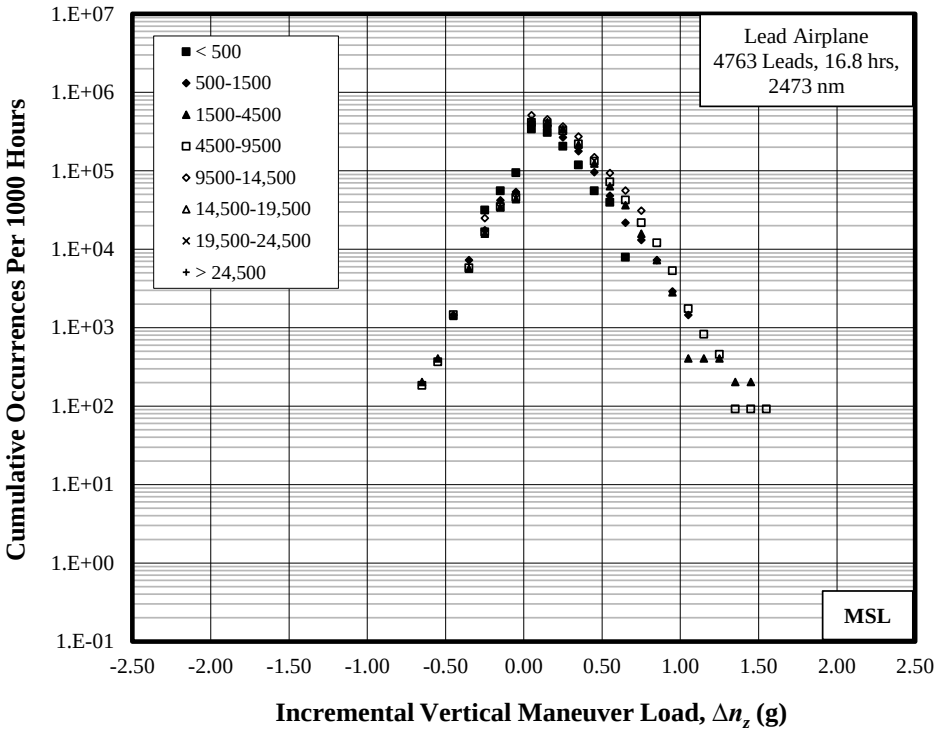

(a) Per 1000 hours

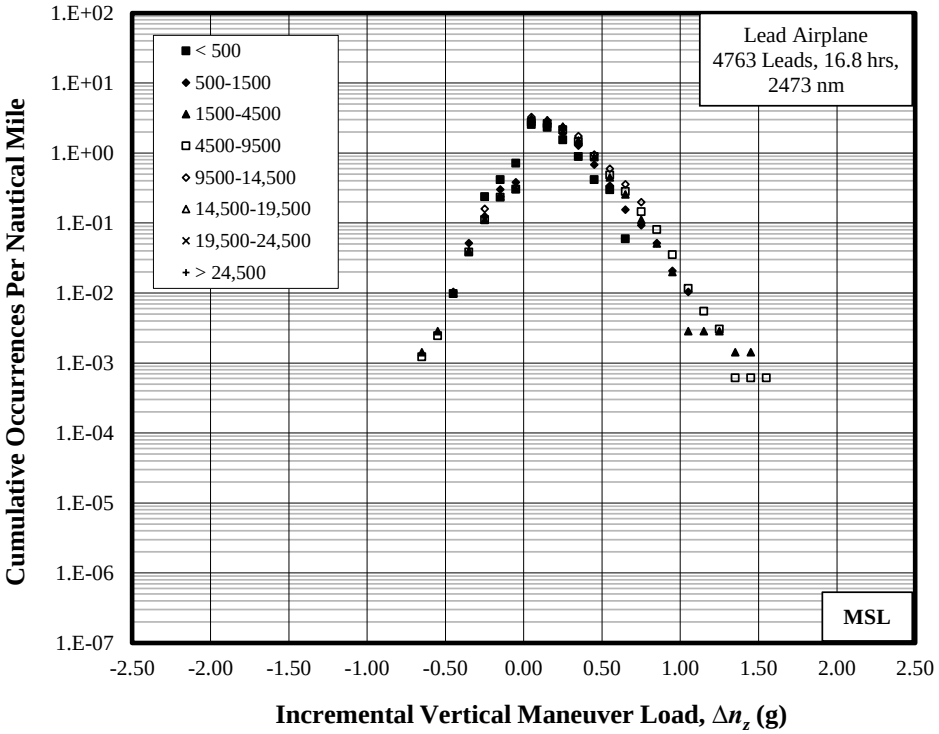

(b) Per nautical mile

Figure B-13. Cumulative occurrences of incremental vertical maneuver load factor, lead phases (a) per 1000 hours and (b) per nautical mile

Altitude Band Ceiling (ft)	Duration (hr)	Distance (nm)
500	0.17	22.54
1,500	2.89	389.05
4,500	21.58	3,047.03
9,500	52.37	7,799.8
14,500	2.54	401.71
19,500	0	0
24,500	0	0
35,000	0	0
Total	79.5	11,660

Figure B-14. Summary of durations and distances for exit phases

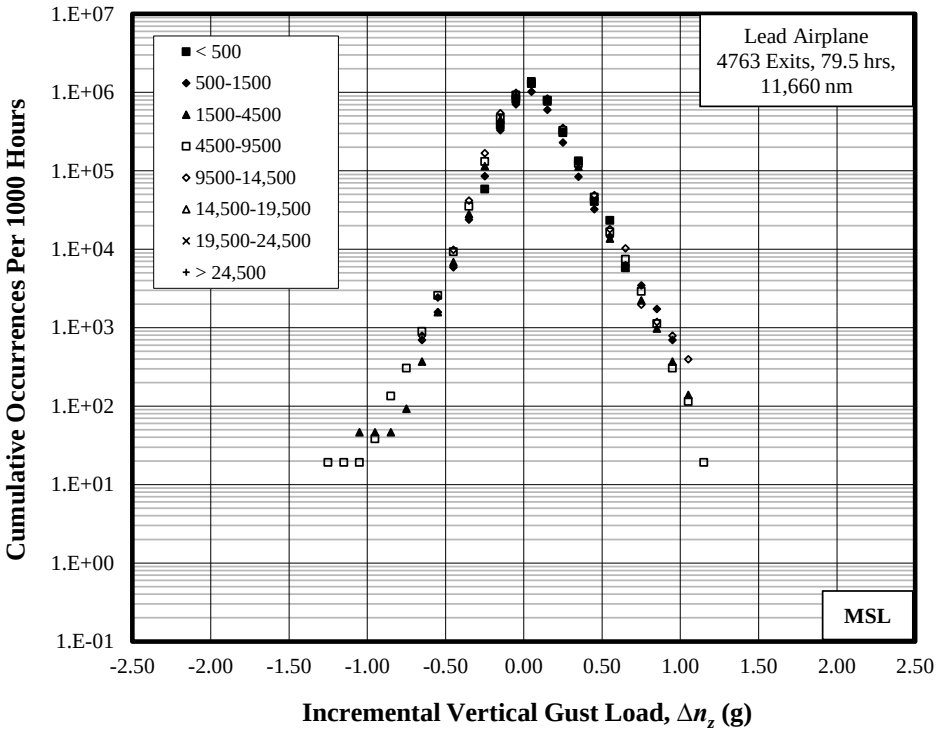

(a) Per 1000 hours

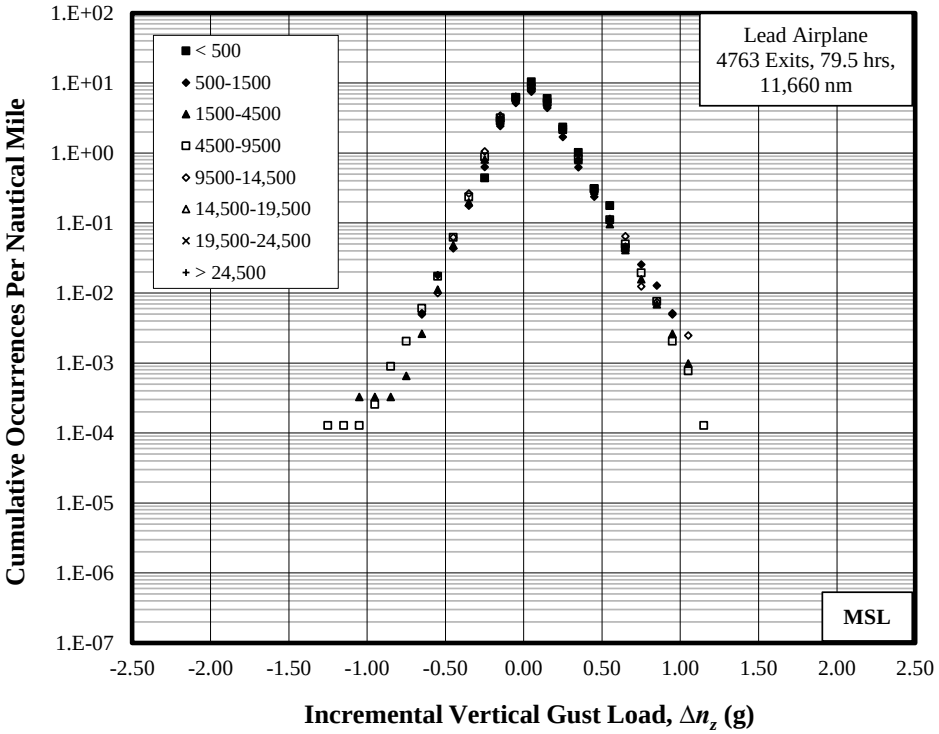

(b) Per nautical mile

Figure B-15. Cumulative occurrences of incremental vertical gust load factor, exit phases (a) per 1000 miles and (b) per nautical mile

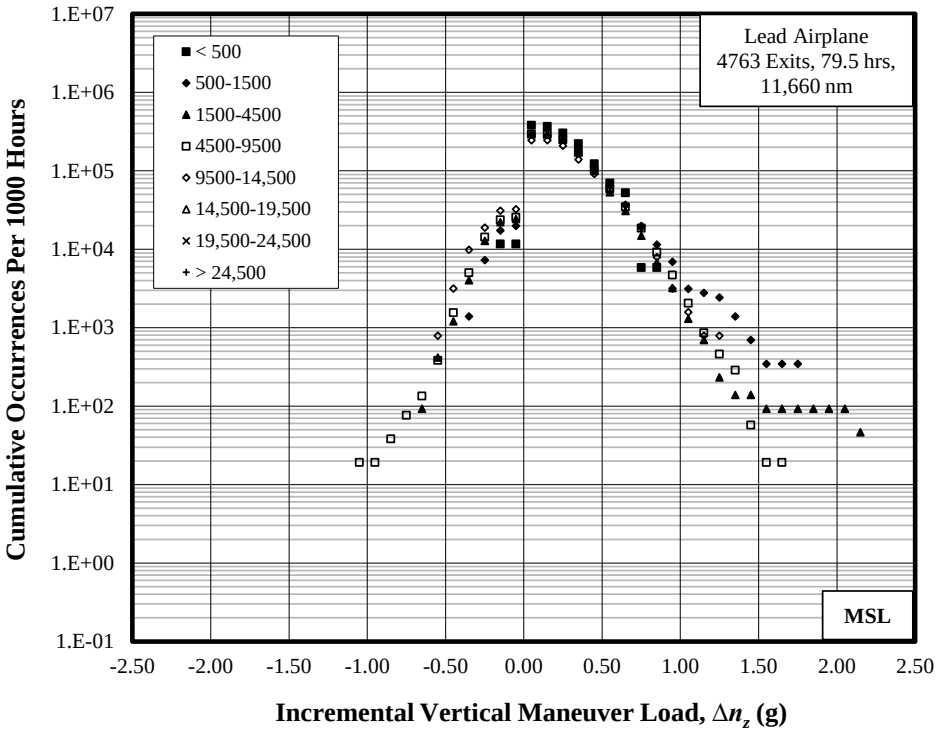

(a) Per 1000 hours

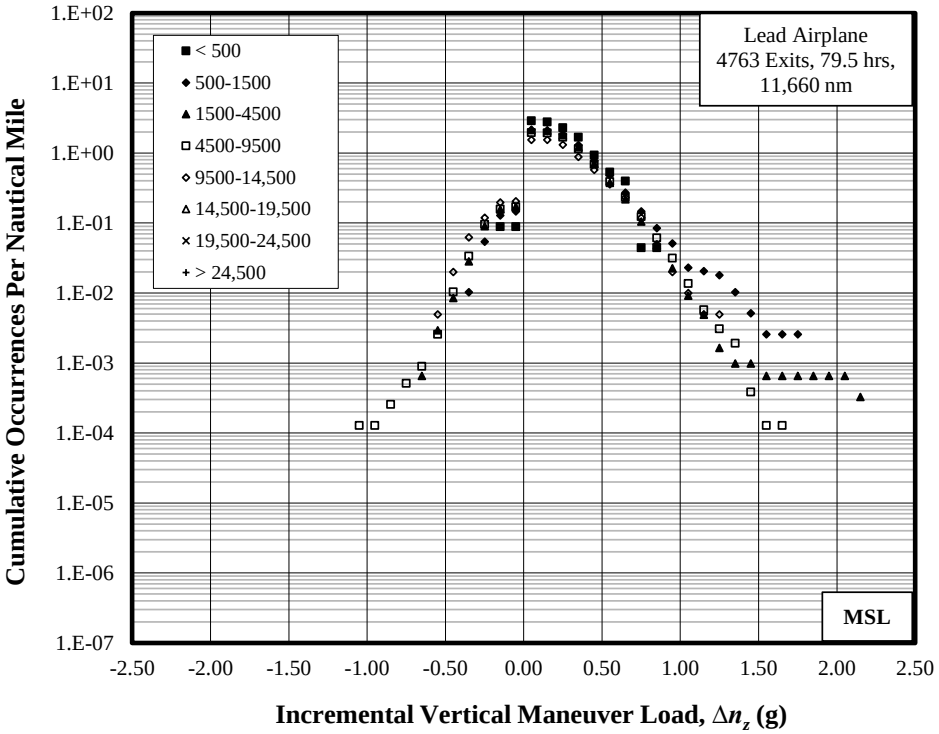

(b) Per nautical mile

Figure B-16. Cumulative occurrences of incremental vertical maneuver load factor, exit phases (a) per 1000 hours and (b) per nautical mile

Altitude Band Ceiling (ft)	Duration (hr)	Distance (nm)
500	0.04	5.63
1,500	12.11	1,589.23
4,500	215.59	30,334.17
9,500	733.46	108,781.83
14,500	135.82	21,470.72
19,500	0.33	62.92
24,500	0	0
35,000	0	0
Total	1,097.3	162,245

Figure B-17. Summary of durations and distances for turn phases

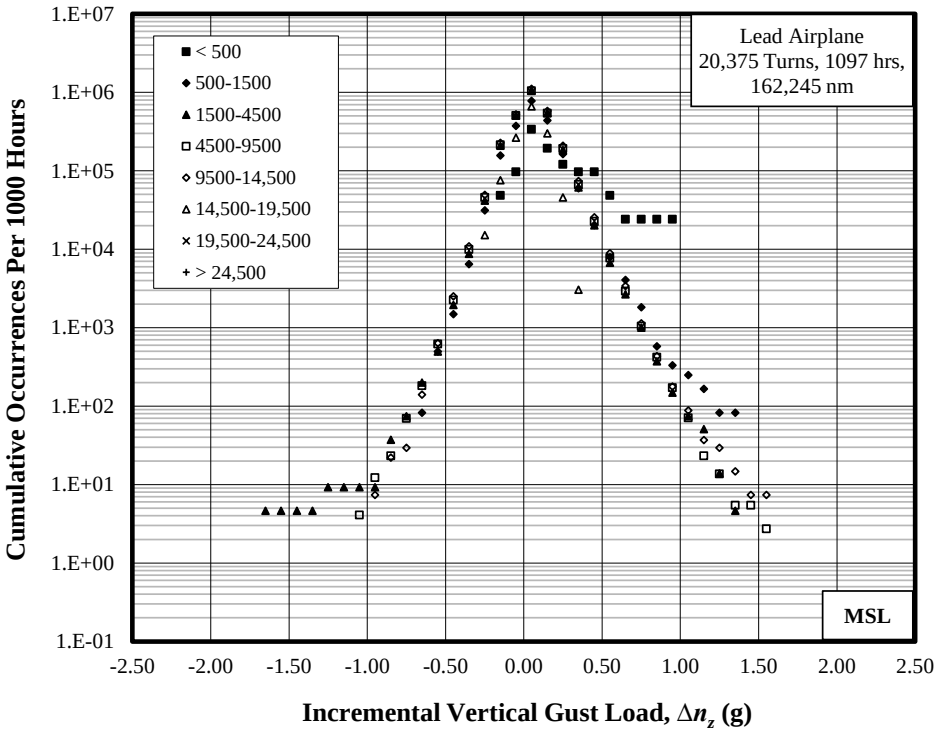

(a) Per 1000 hours

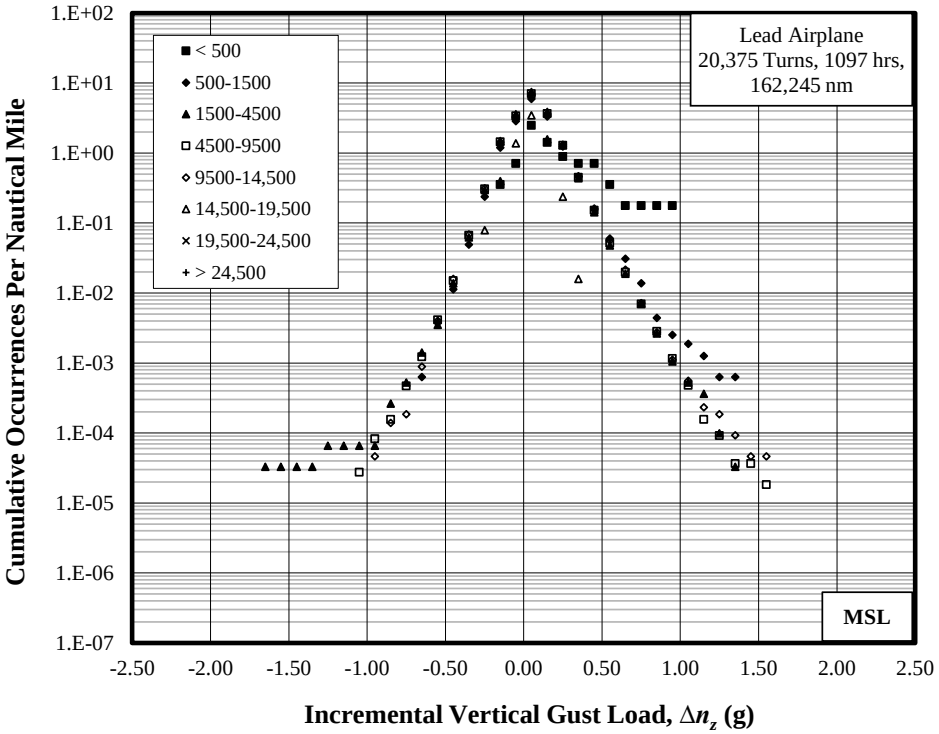

(b) Per nautical mile

Figure B-18. Cumulative occurrences of incremental vertical gust load factor, turn phases (a) per 1000 hours and (b) per nautical mile

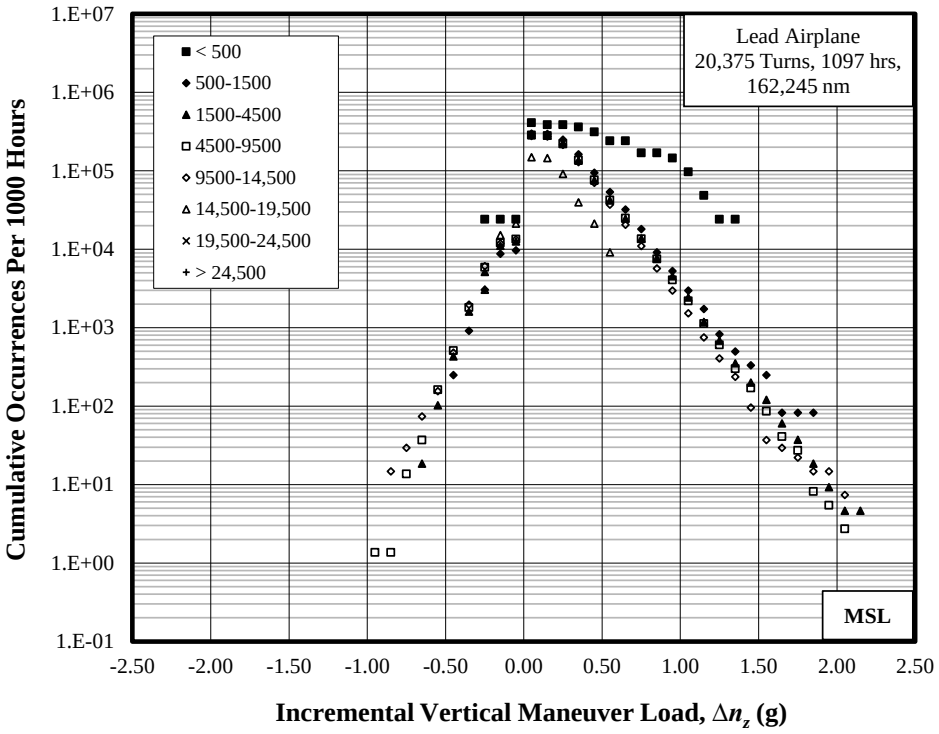

(a) Per 1000 hours

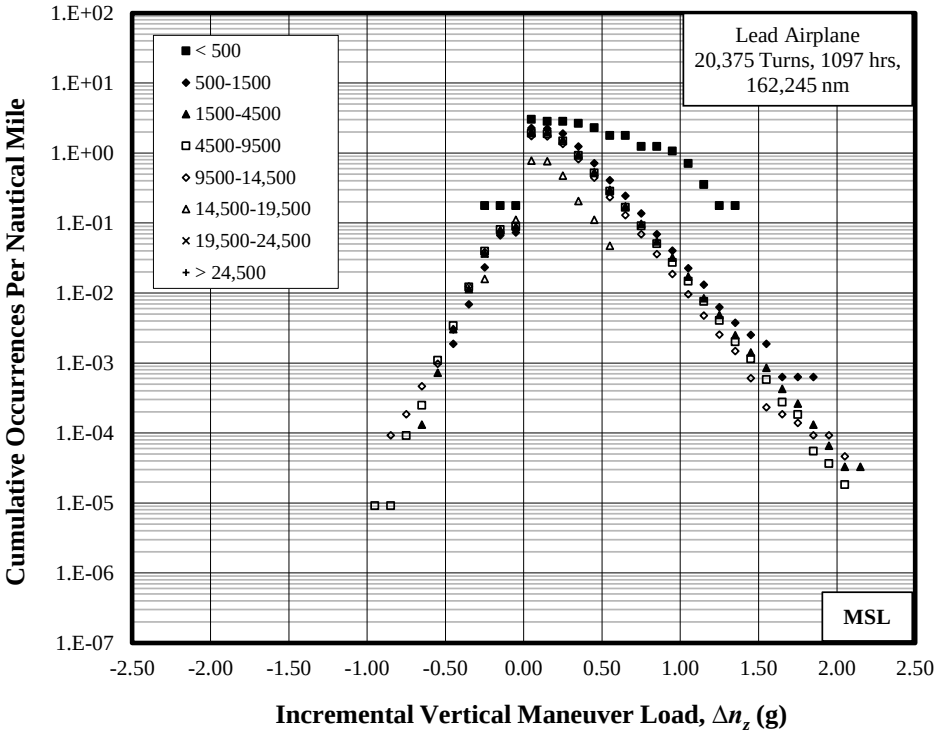

(b) Per nautical mile

Figure B-19. Cumulative occurrences of incremental vertical maneuver load factor, turn phases (a) per 1000 hours and (b) per nautical mile

Altitude Band Ceiling (ft)	Duration (hr)	Distance (nm)
500	7.06	787.63
1500	73.34	9,525.74
4500	880.77	129,819.58
9500	3,343.96	541,673.27
14,500	1,334.79	260,078.44
19,500	555.52	131,628.63
24,500	560.62	138,116.58
35,000	319.70	78,885.80
Total	7,075.8	1,290,516

Figure B-20. Summary of durations and distances for the overall flight

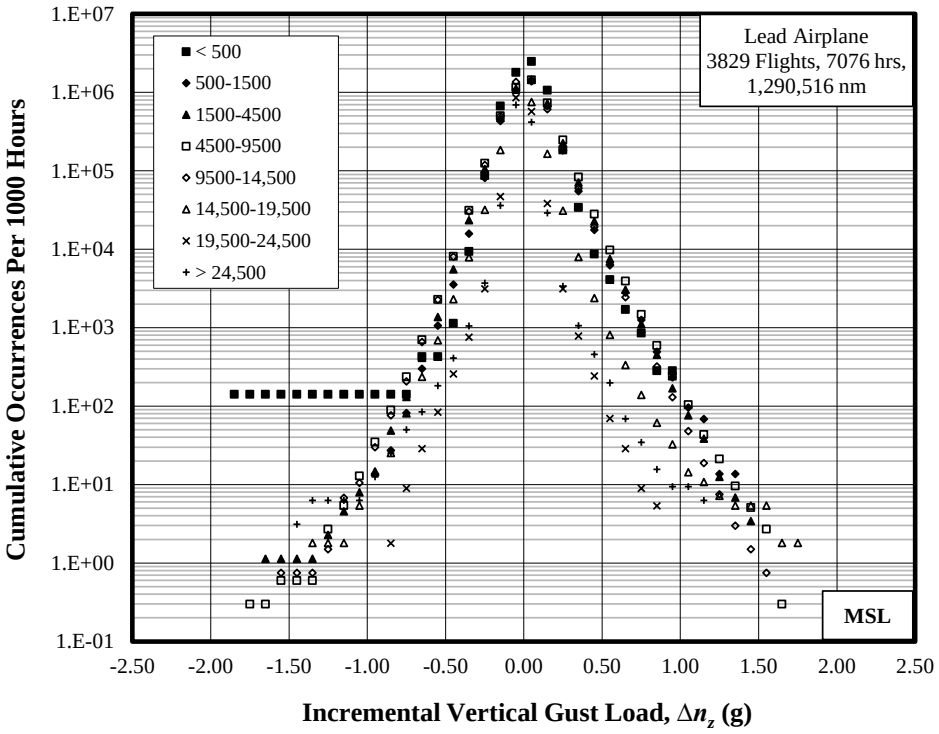

(a) Per 1000 hours

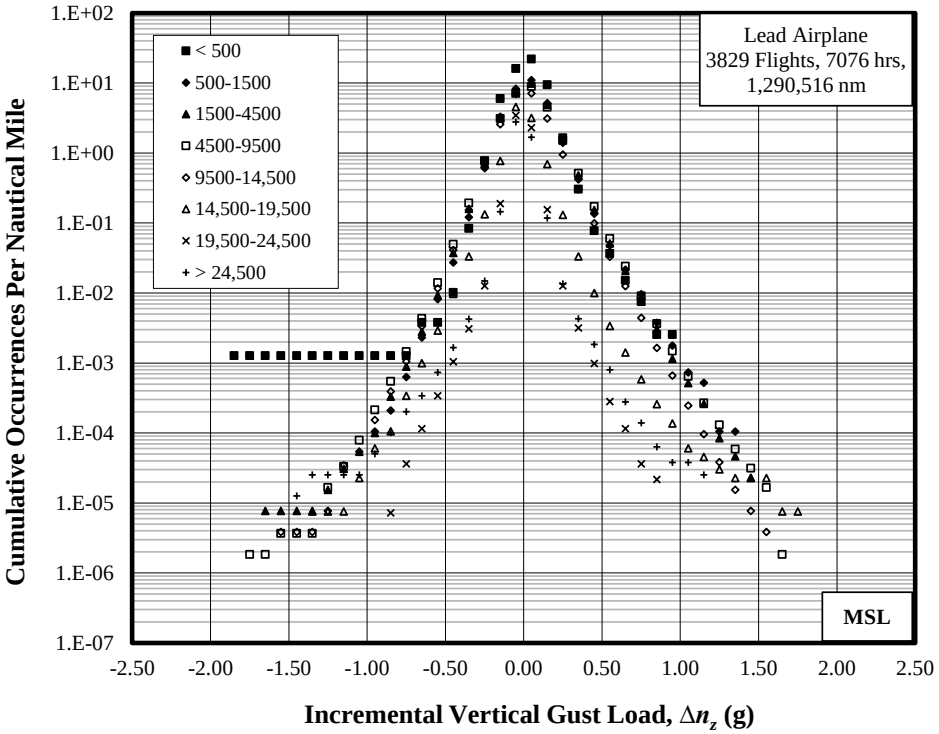

(b) Per nautical mile

Figure B-21. Cumulative occurrences of incremental vertical gust load factor, overall flight (a) per 1000 hours and (b) per nautical mile

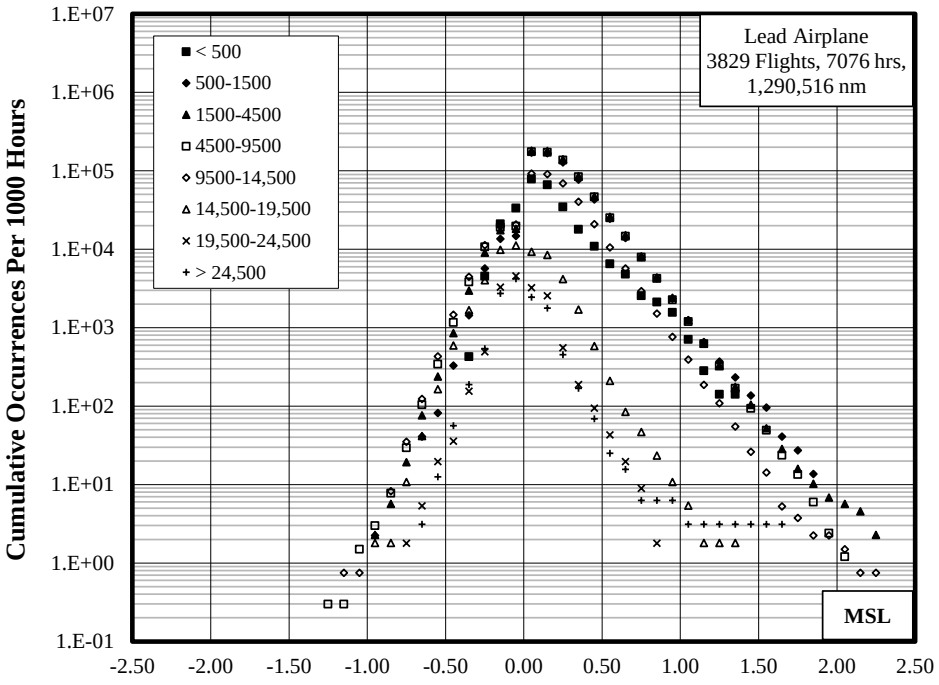

(a) Per 1000 hours

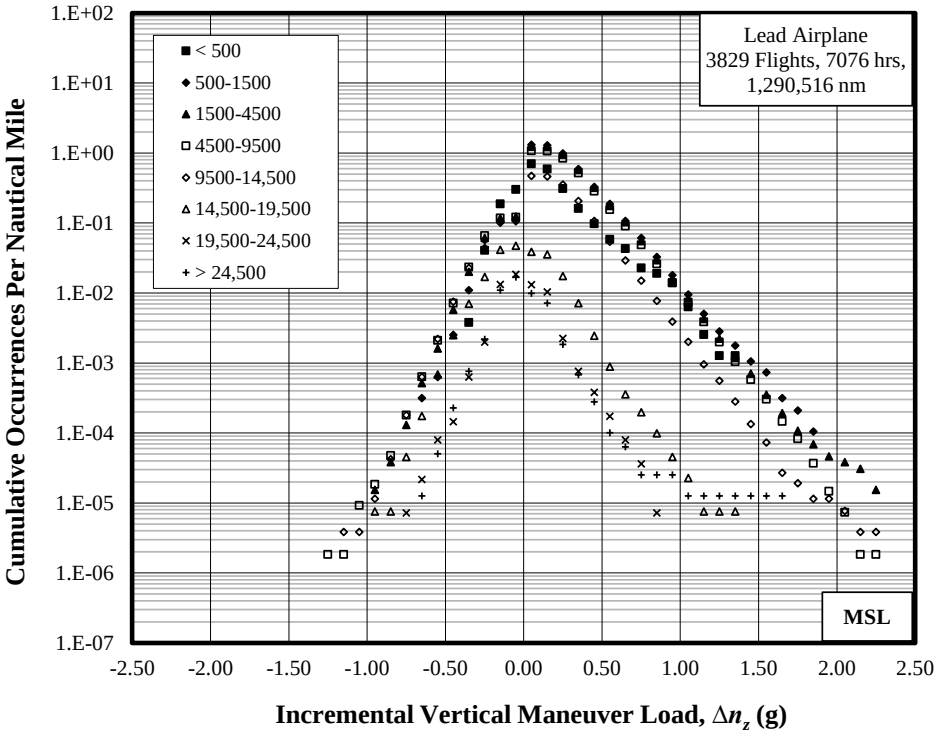

(b) Per nautical mile

Figure B-22. Cumulative occurrences of incremental vertical maneuver load factor, overall flight (a) per 1000 miles and (b) per nautical mile

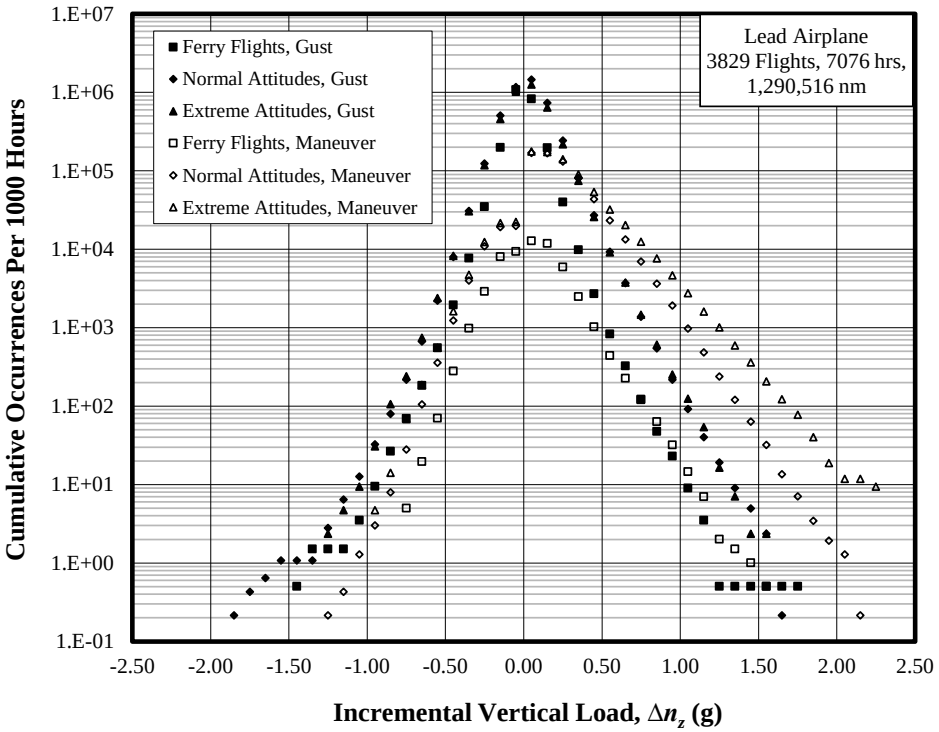

(a) Per 1000 hours

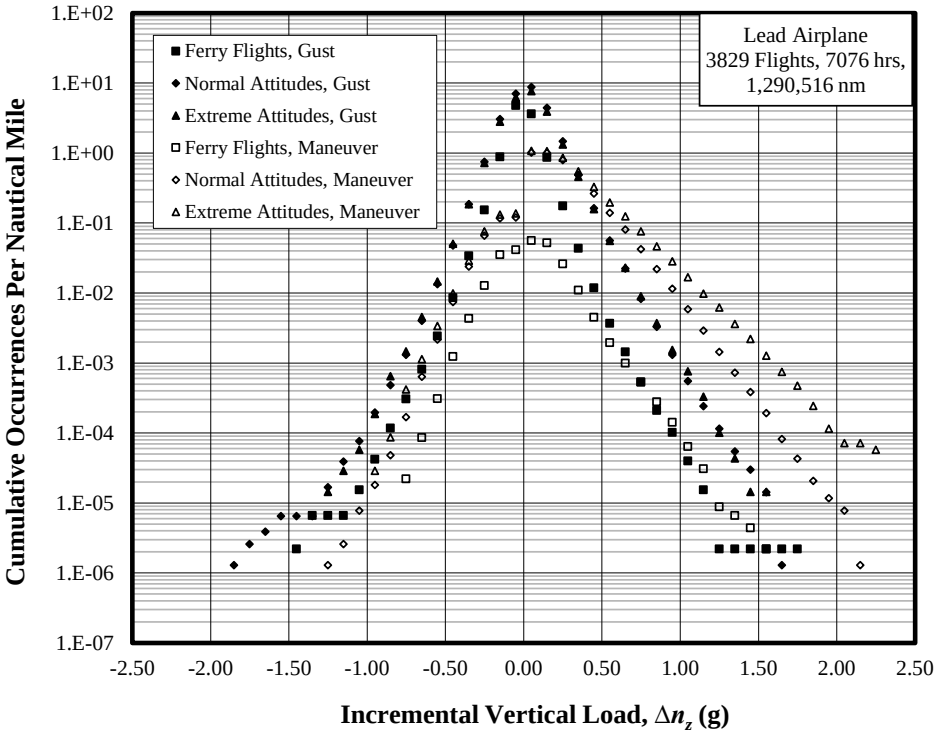

(b) Per nautical mile

Figure B-23. Cumulative occurrences of incremental vertical load factor for different types of flights (a) per 1000 hours and (b) per nautical mile

APPENDIX C—FLIGHT LOADS BY ABOVE GROUND LEVEL ALTITUDE

Phase	Number of Phases	Duration (hr)	Distance (nm)
Cruise 1	1,858	840.7	166,719.9
Cruise 2	1,858	767.9	141,127.4
Entry	4,763	79.5	11,528.4
Lead	4,763	16.8	2,472.7
Exit	4,763	79.5	11,660.2
Turn	20,375	1,097.3	162,244.6
Total		2,881.7	495,753.2

Figure C-1. Summary of durations and distances for all flight phases

Altitude Band Ceiling (ft)	Duration (hr)	Distance (nm)
500	24.85	3,500.74
1,500	95.19	15,583.54
4,500	331.80	61,288.98
9,500	276.38	59,447.54
14,500	85.06	20,148.36
19,500	23.92	5,875.91
24,500	3.49	874.81
35,000	0	0
Total	840.7	166,719.9

Figure C-2. Summary of durations and distances for Cruise 1 phases

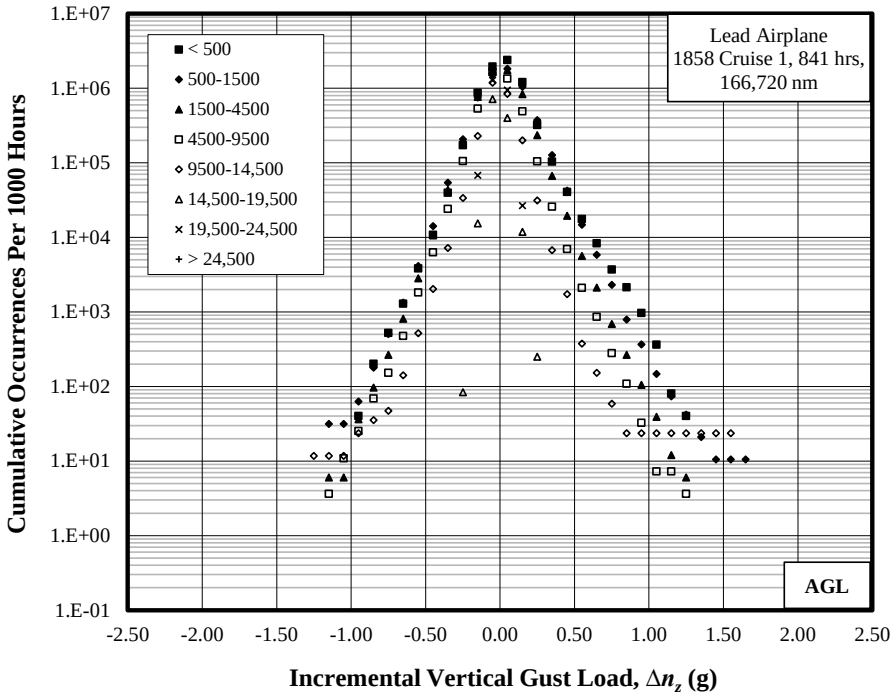

(a) Per 1000 hours

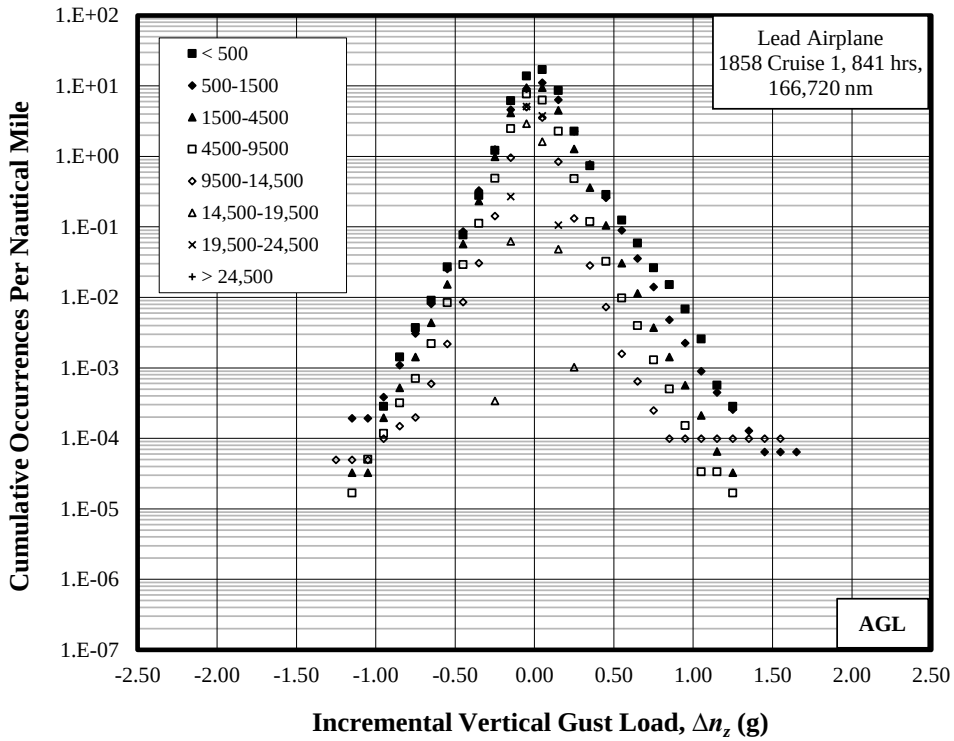

(b) Per nautical mile

Figure C-3. Cumulative occurrences of incremental vertical gust load factor, Cruise 1 phases, (a) per 1000 hours and (b) per nautical mile

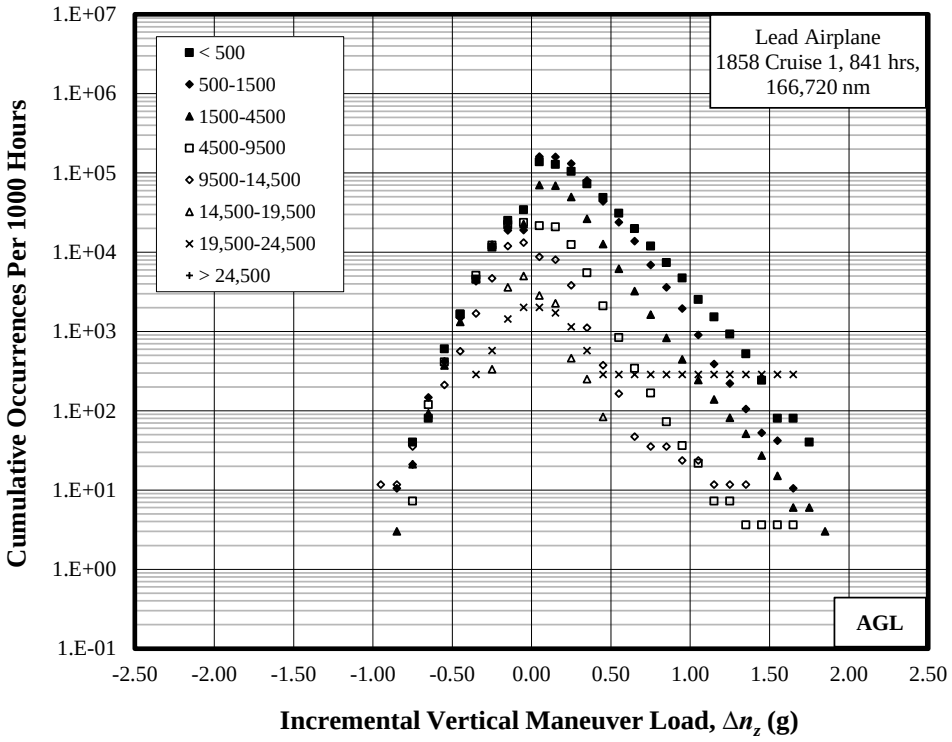

(a) Per 1000 hours

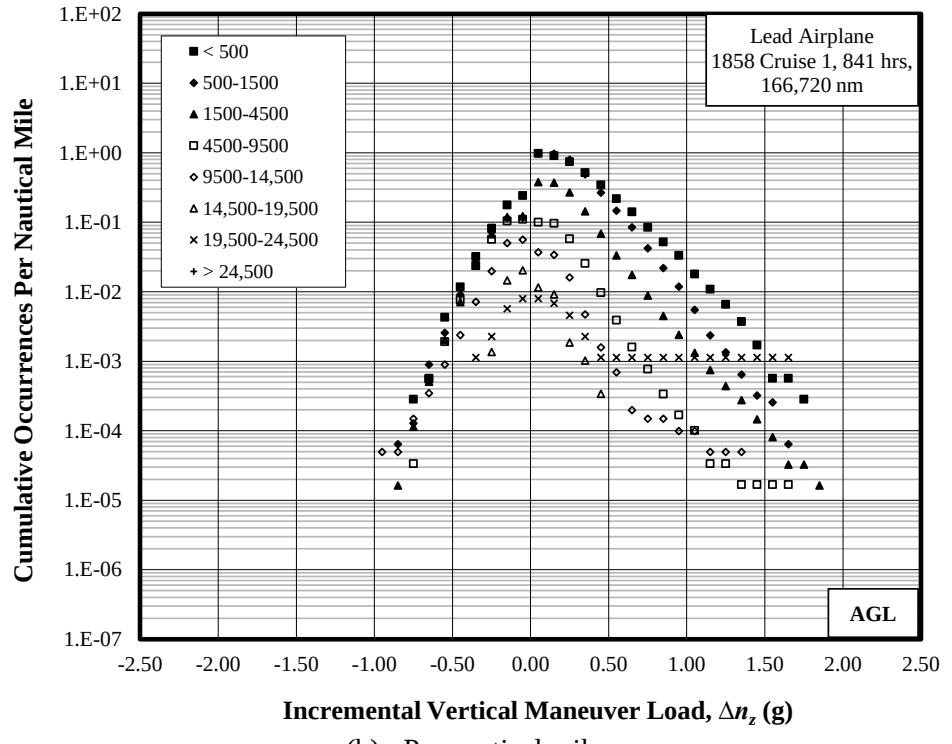

(b) Per nautical mile

Figure C-4. Cumulative occurrences of incremental vertical maneuver load factor, Cruise 1 phases, (a) per 1000 hours and (b) per nautical mile

Altitude Band Ceiling (ft)	Duration (hr)	Distance (nm)
500	35.51	4,556.60
1,500	150.15	23,412.20
4,500	387.97	70,573.55
9,500	149.48	31,921.34
14,500	36.44	8,624.67
19,500	5.34	1,292.73
24,500	2.40	594.17
35,000	0.61	152.12
Total	767.9	141,127.4

Figure C-5. Summary of durations and distances for Cruise 2 phases

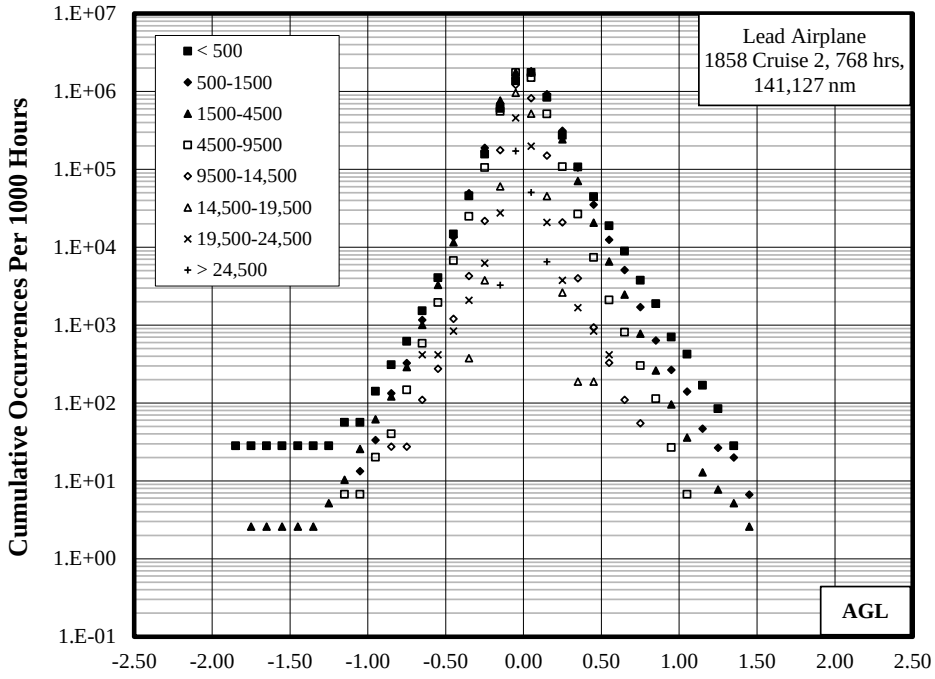

(a) Per 1000 hours

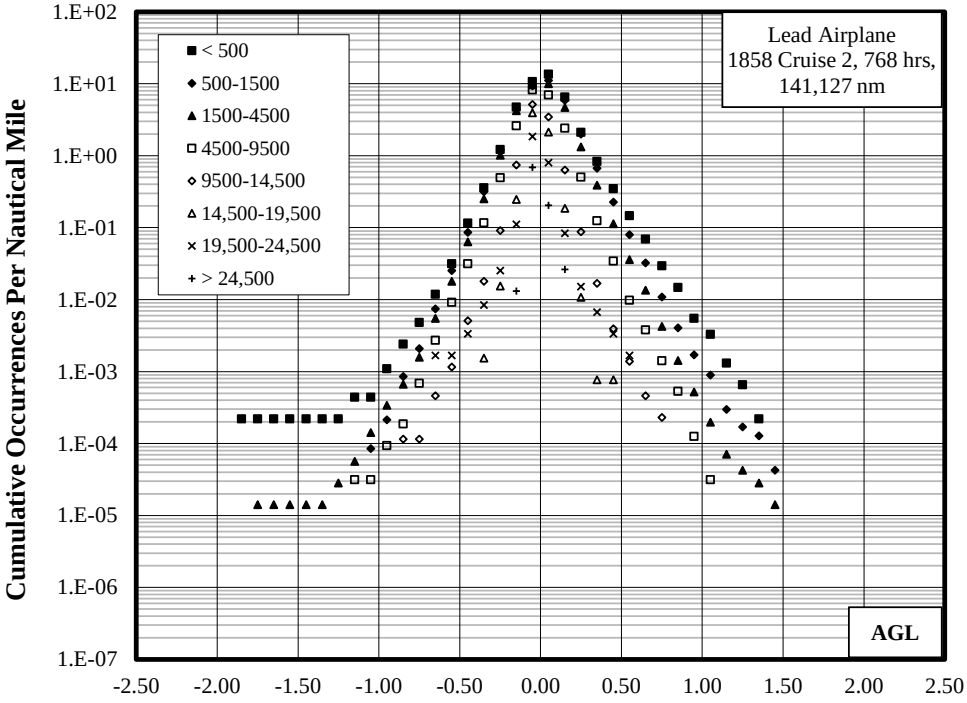

(b) Per nautical mile

Figure C-6. Cumulative occurrences of incremental vertical gust load factor, Cruise 2 phases, (a) per 1000 hours and (b) per nautical mile

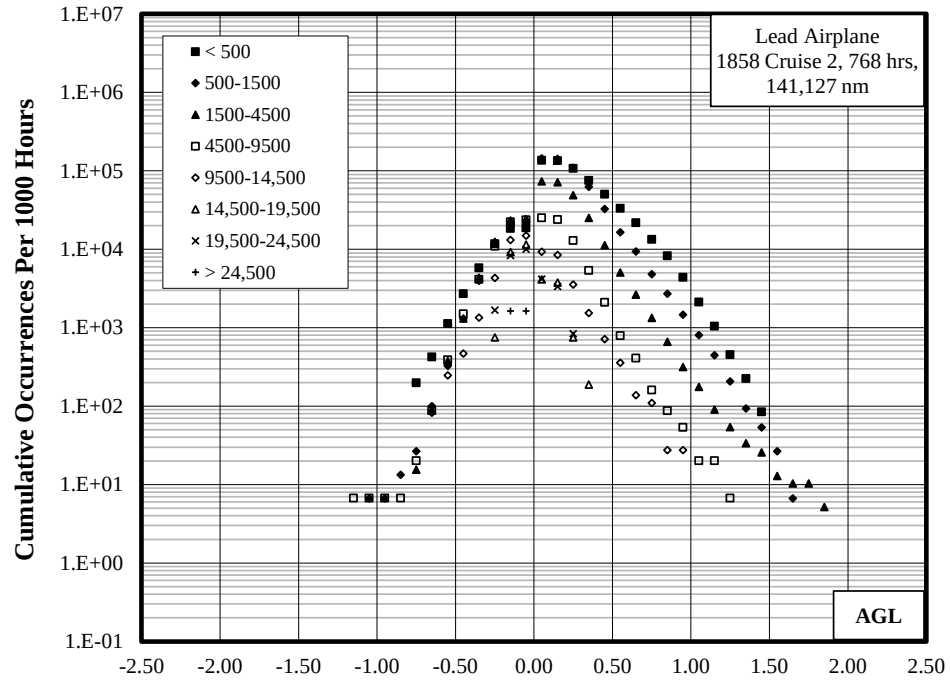

(a) Per 1000 hours

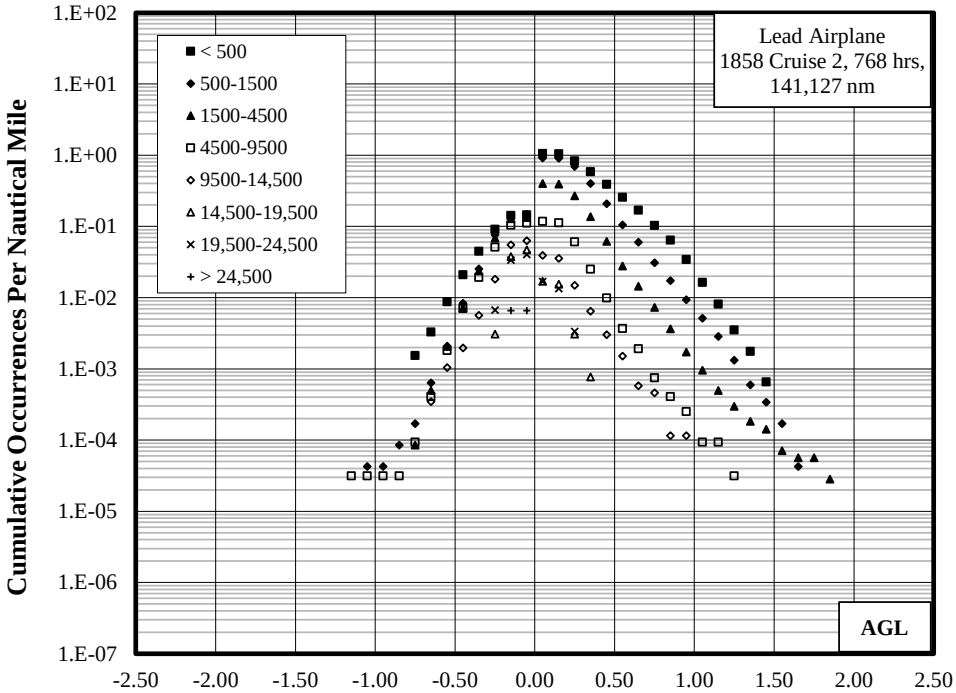

(b) Per nautical mile

Figure C-7. Cumulative occurrences of incremental vertical maneuver load factor, Cruise 2 phases, (a) per 1000 hours and (b) per nautical mile

Altitude Band Ceiling (ft)	Duration (hr)	Distance (nm)
500	30.76	4,455.62
1,500	44.03	6,369.33
4,500	4.75	703.27
9,500	0.0013	0.22
14,500	0	0
19,500	0	0
24,500	0	0
35,000	0	0
Total	79.5	11,528.4

Figure C-8. Summary of durations and distances for entry phases

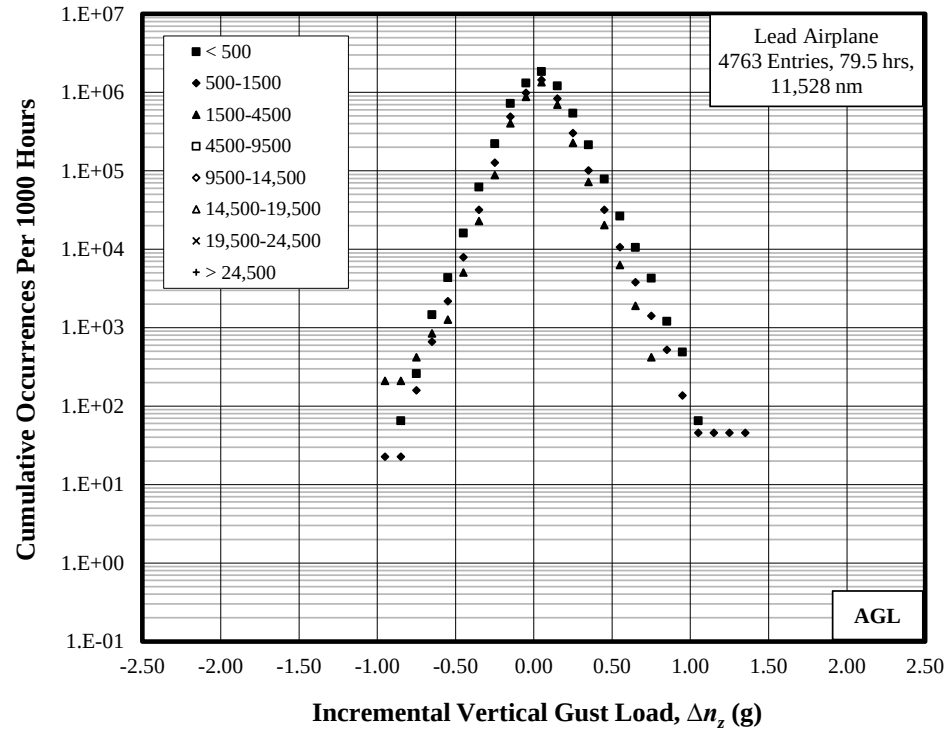

(a) Per 1000 hours

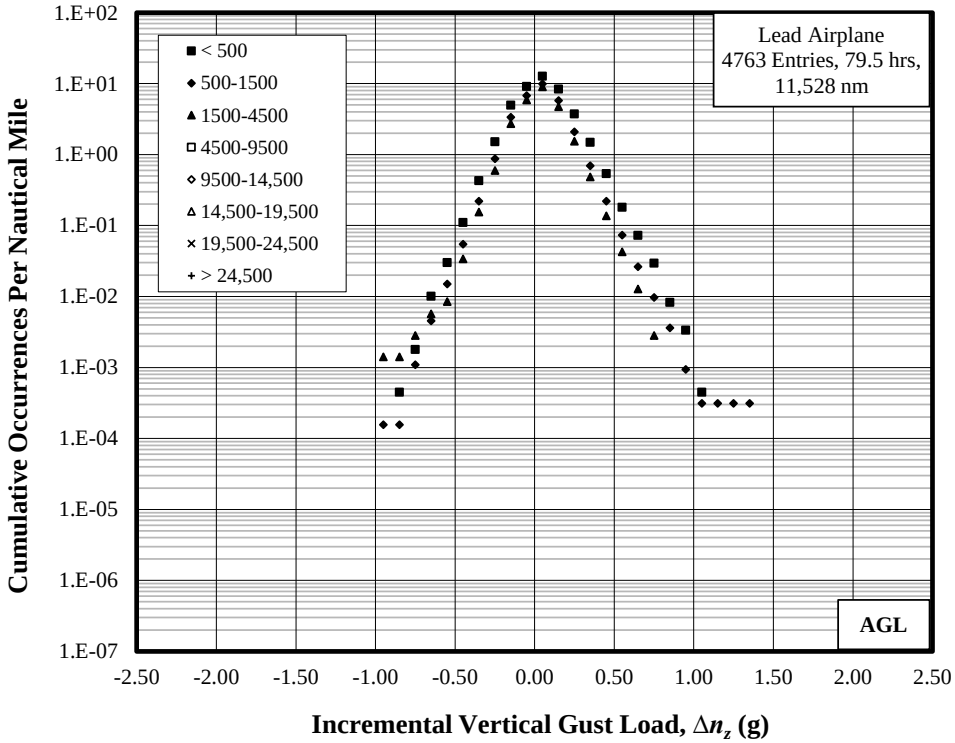

(b) Per nautical mile

Figure C-9. Cumulative occurrences of incremental vertical gust load factor, entry phases, (a) per 1000 hours and (b) per nautical mile

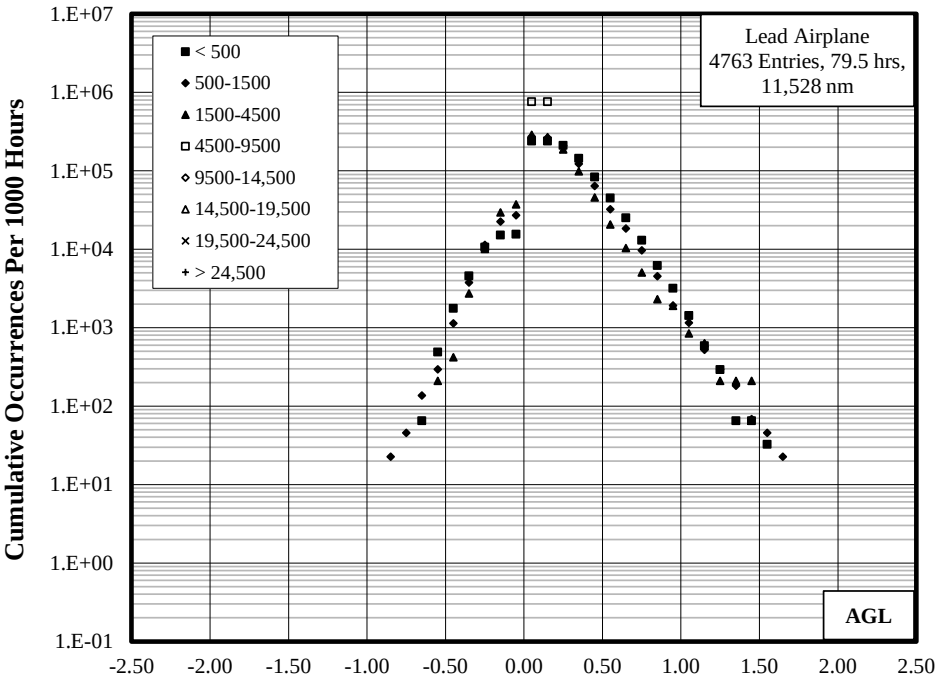

(a) Per 1000 hours

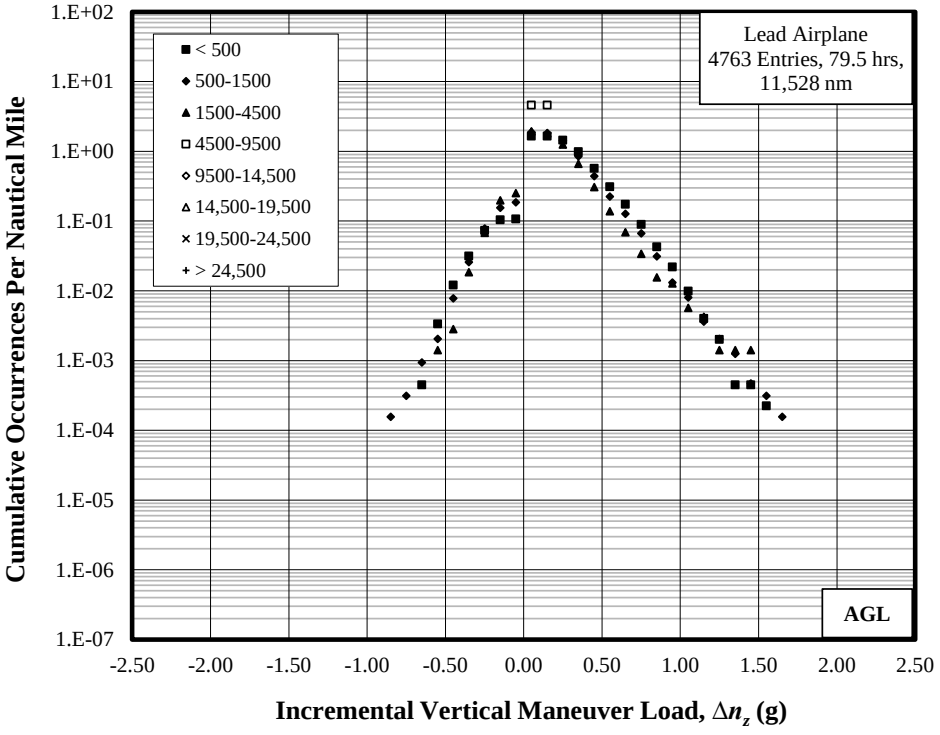

(b) Per nautical mile

Figure C-10. Cumulative occurrences of incremental vertical maneuver load factor, entry phases, (a) per 1000 hours and (b) per nautical mile

Altitude Band Ceiling (ft)	Duration (hr)	Distance (nm)
500	12.64	1860.31
1500	3.99	580.48
4500	0.21	31.87
9500	0	0
14,500	0	0
19,500	0	0
24,500	0	0
35,000	0	0
Total	16.8	2472.7

Figure C-11. Summary of durations and distances for lead phases

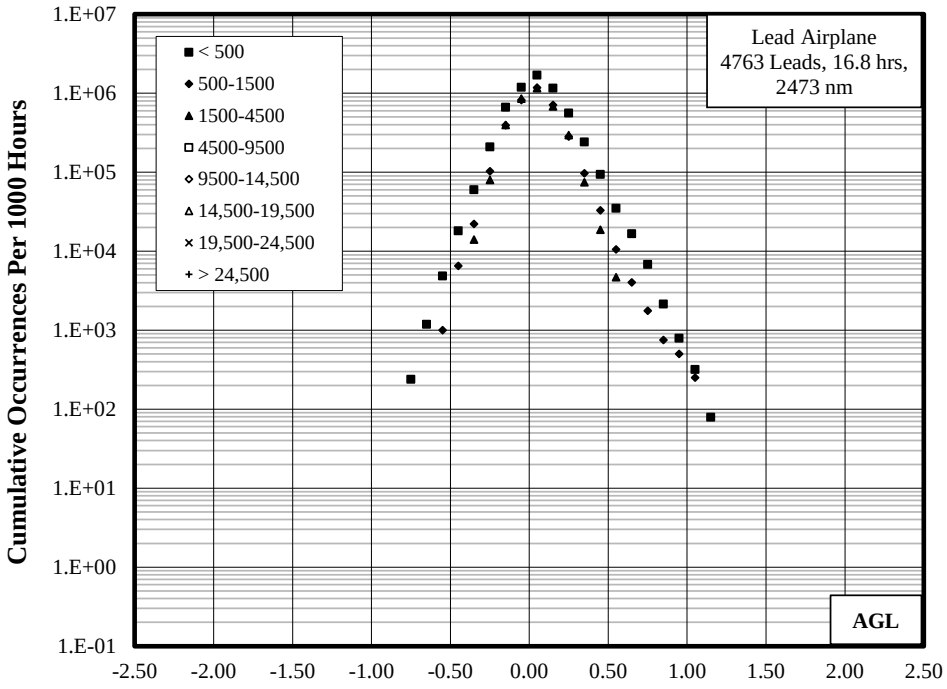

(a) Per 1000 hours

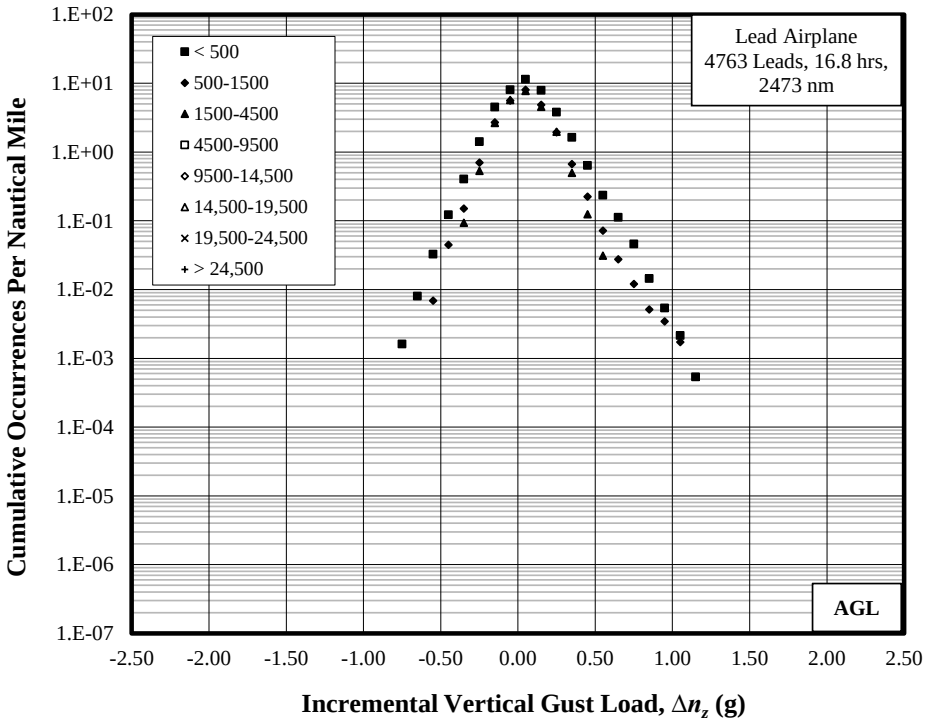

(b) Per nautical mile

Figure C-12. Cumulative occurrences of incremental vertical gust load factor, lead phases, (a) per 1000 hours and (b) per nautical mile

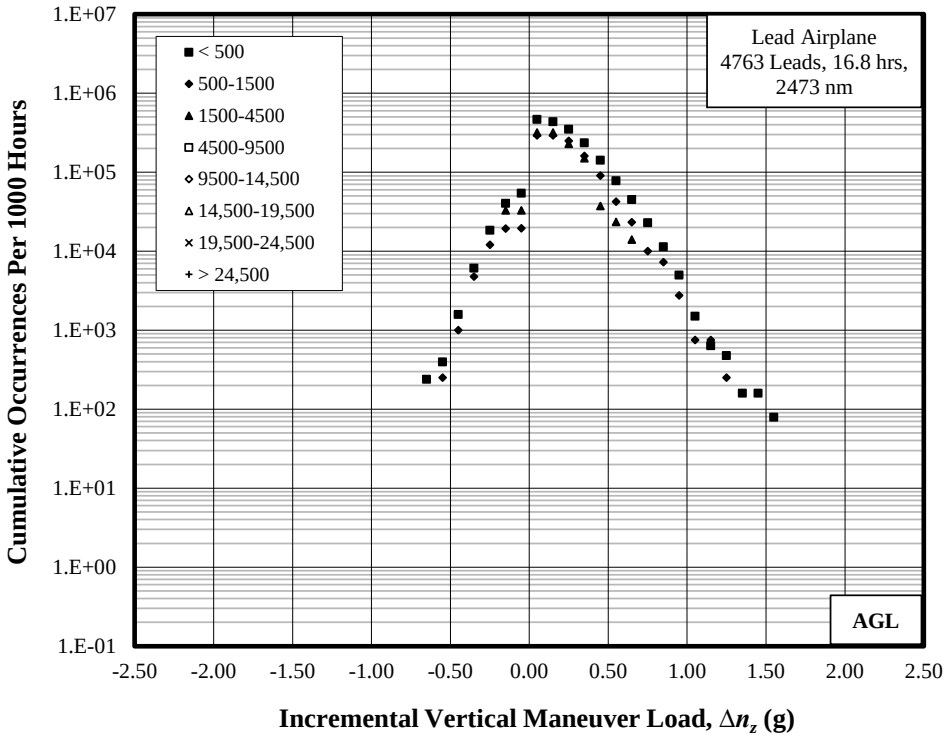

(a) Per 1000 hours

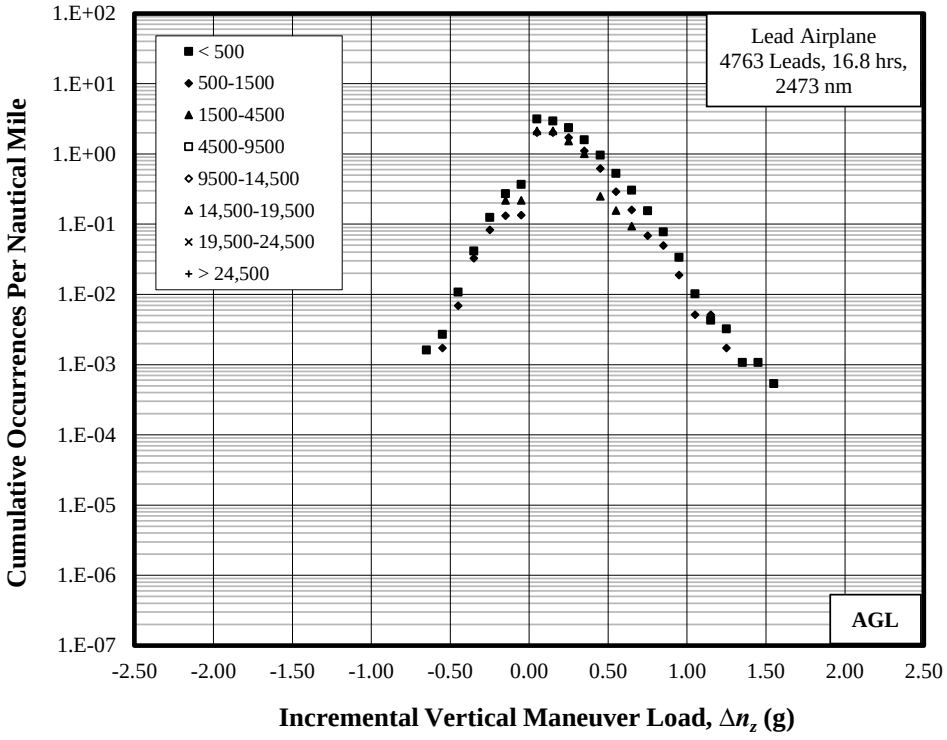

(b) Per nautical mile

Figure C-13. Cumulative occurrences of incremental vertical maneuver load factor, lead phases, (a) per 1000 hours and (b) per nautical mile

Altitude Band Ceiling (ft)	Duration (hr)	Distance (nm)
500	23.33	3,401.30
1,500	49.51	7,254.75
4,500	6.72	1,004.19
9,500	0	0
14,500	0	0
19,500	0	0
24,500	0	0
35,000	0	0
Total	79.5	11,660.2

Figure C-14. Summary of durations and distances for exit phases

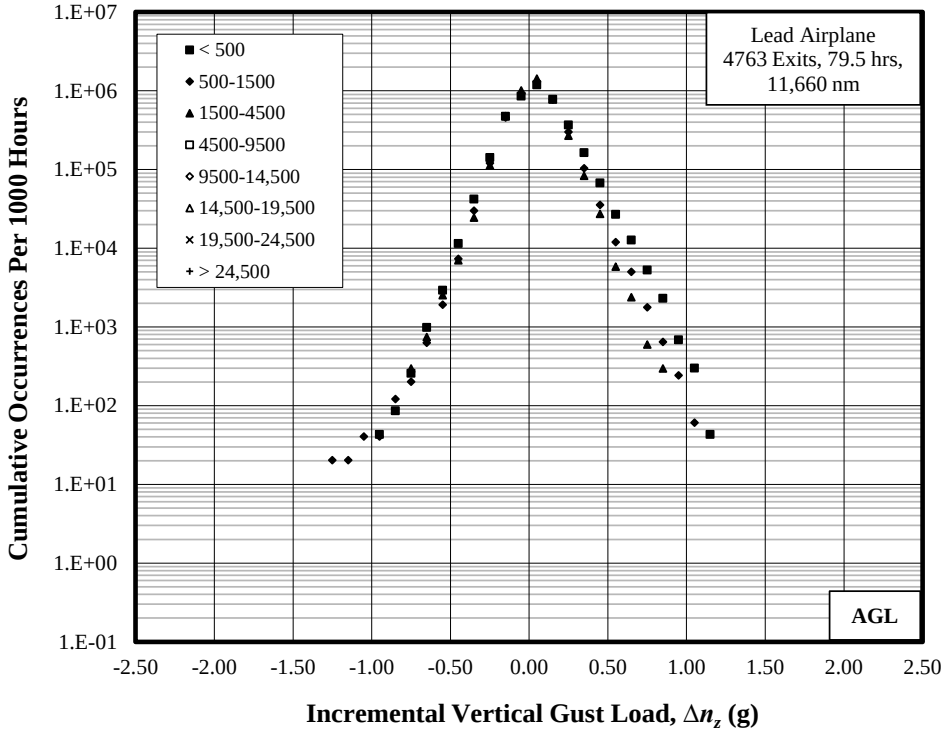

(a) Per 1000 hours

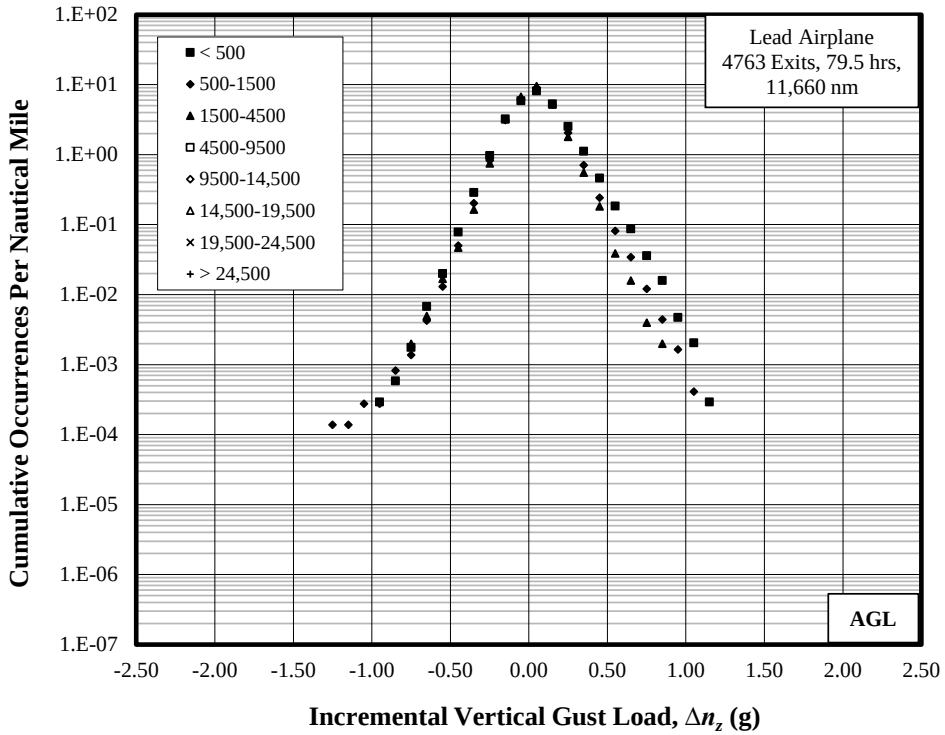

(b) Per nautical mile

Figure C-15. Cumulative occurrences of incremental vertical gust load factor, exit phases, (a) per 1000 hours and (b) per nautical mile

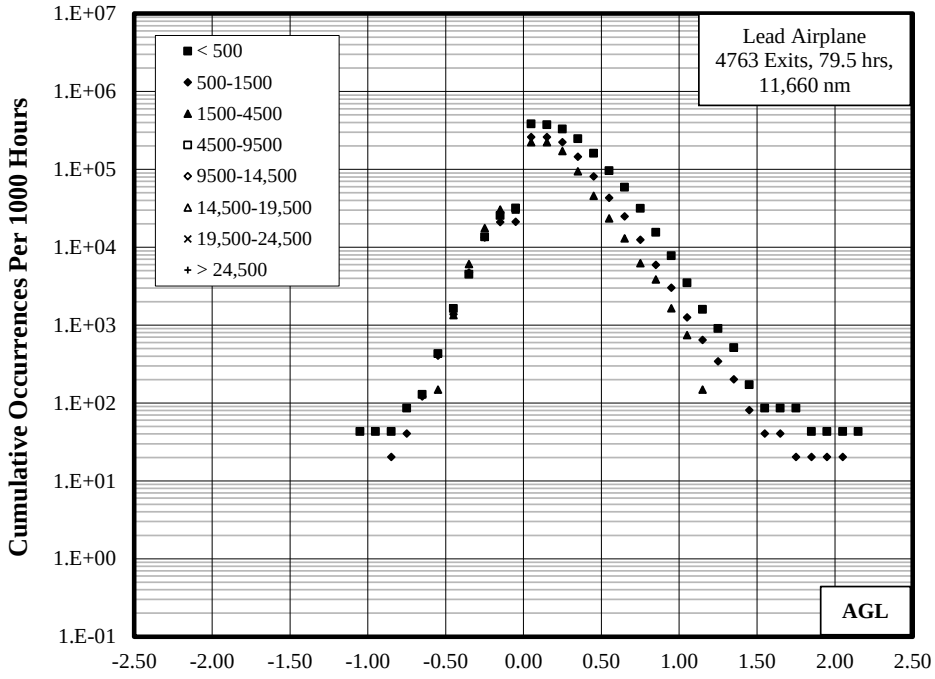

(a) Per 1000 hours

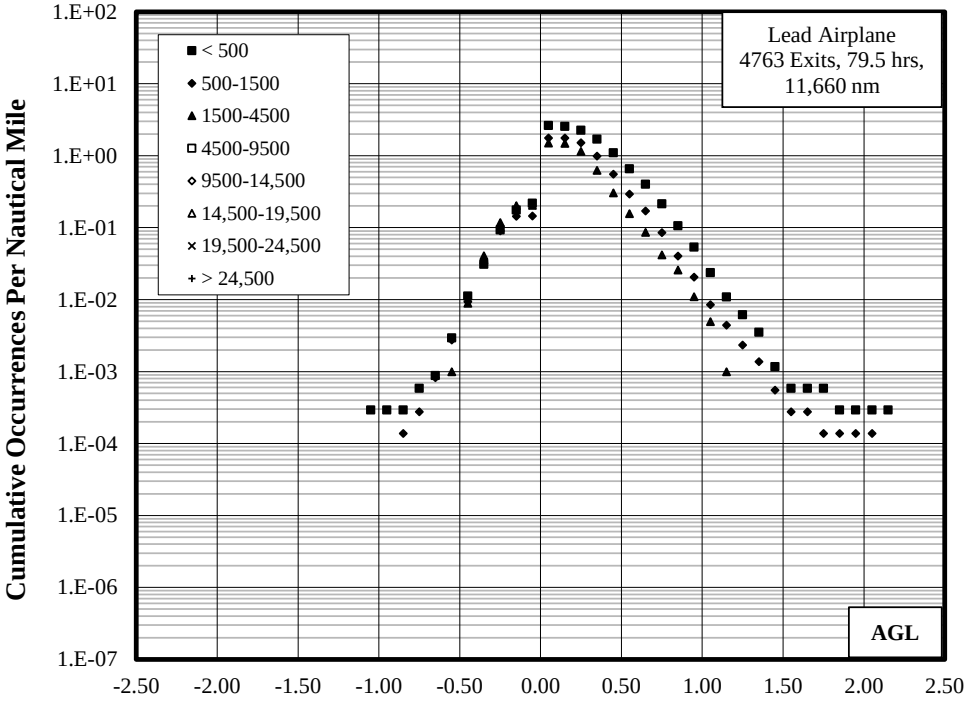

(b) Per nautical mile

Figure C-16. Cumulative occurrences of incremental vertical maneuver load factor, exit phases, (a) per 1000 hours and (b) per nautical mile

Altitude Band Ceiling (ft)	Duration (hr)	Distance (nm)
500	48.42	7,066.84
1500	493.95	71,123.86
4500	537.43	81,194.75
9500	17.28	2,804.74
14,500	0.27	54.45
19,500	0	0
24,500	0	0
35,000	0	0
Total	1,097.3	162,244.6

Figure C-17. Summary of durations and distances for turn phases

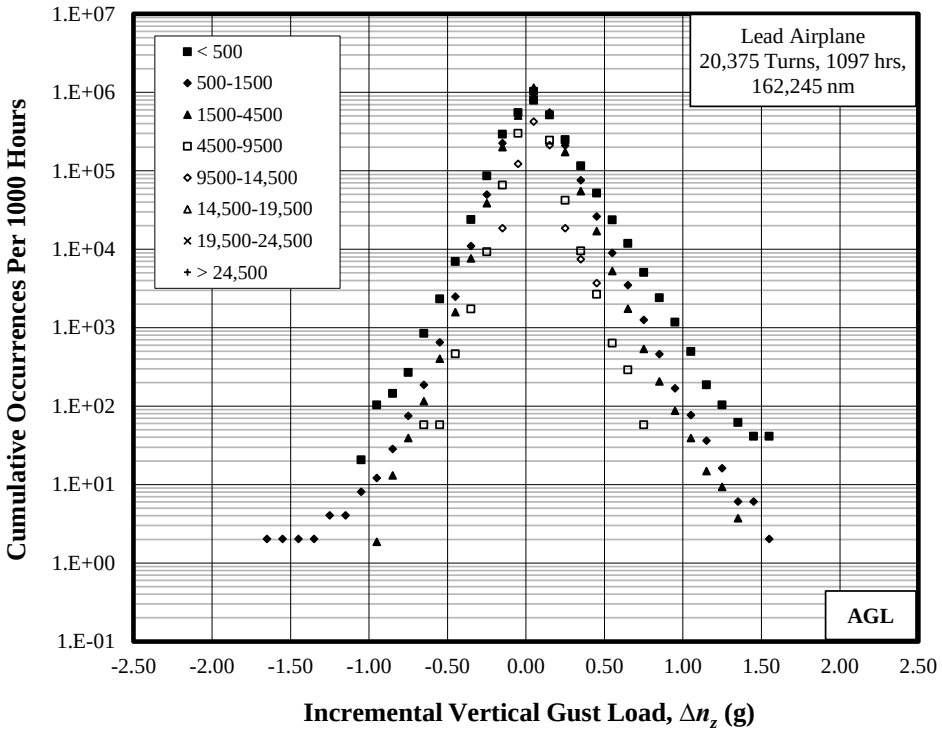

(a) Per 1000 hours

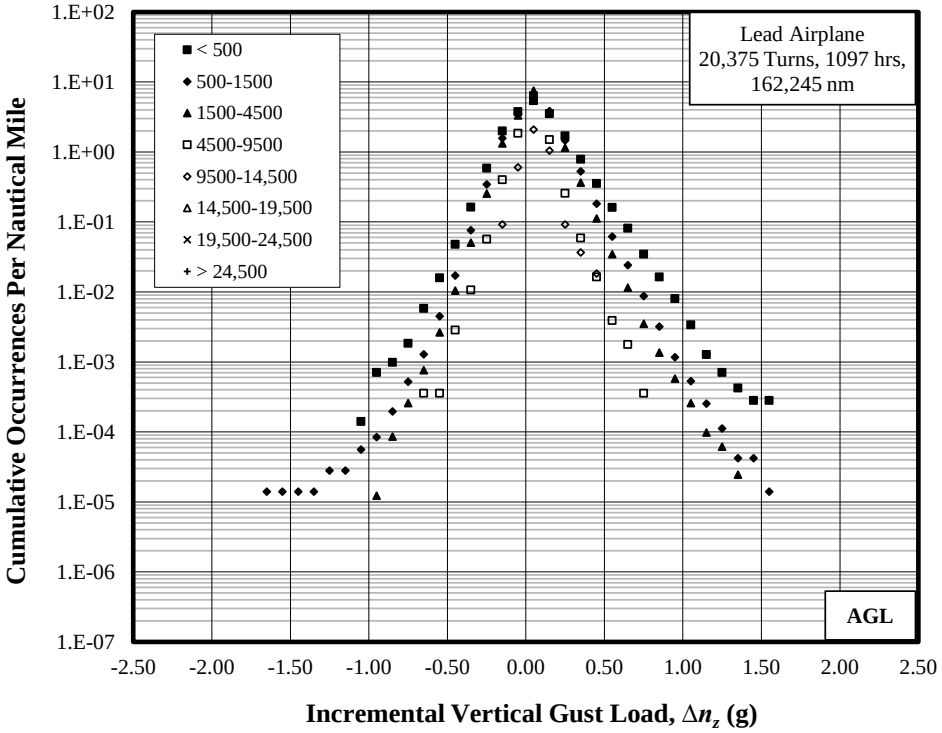

(b) Per nautical mile

Figure C-18. Cumulative occurrences of incremental vertical gust load factor, turn phases, (a) per 1000 hours and (b) per nautical mile

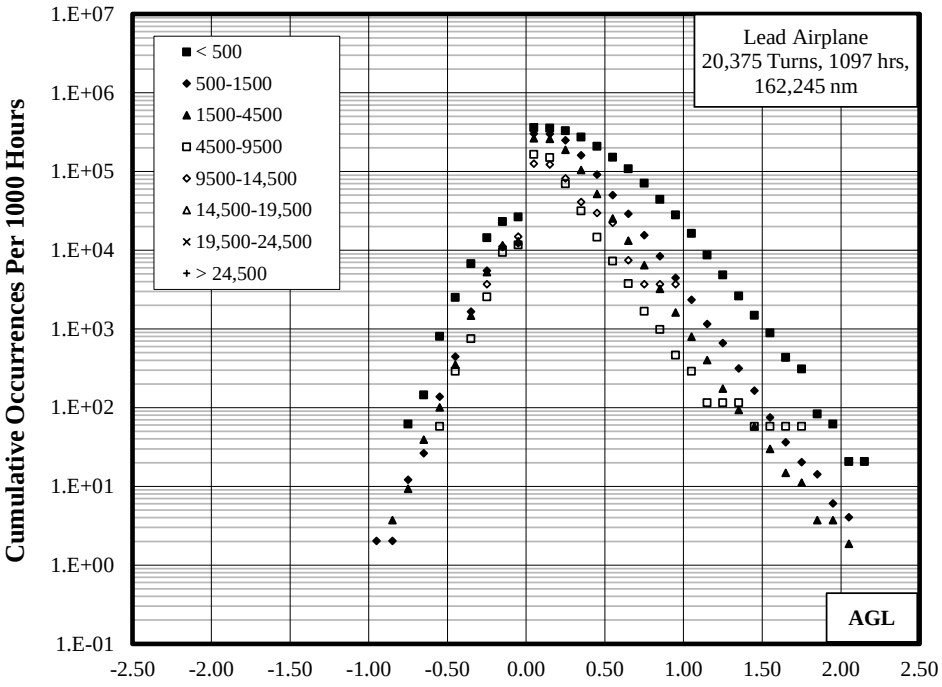

(a) Per 1000 hours

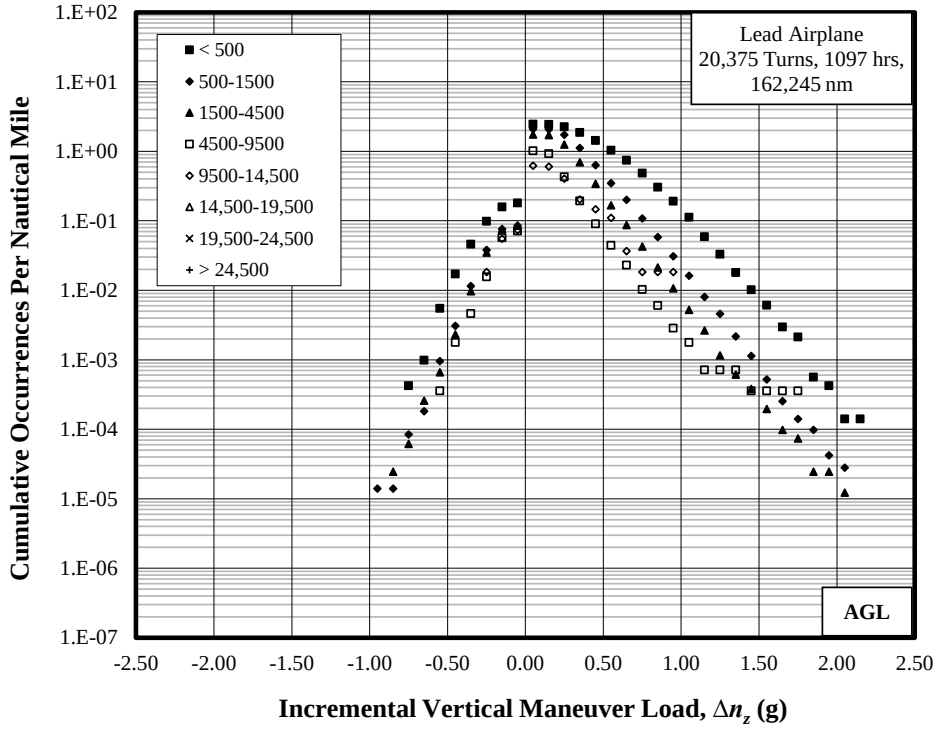

(b) Per nautical mile

Figure C-19. Cumulative occurrences of incremental vertical maneuver load factor, turn phases, (a) per 1000 hours and (b) per nautical mile

Altitude Band Ceiling (ft)	Duration (hr)	Distance (nm)
500	366.94	52,368.25
1,500	1,789.54	267,084.62
4,500	2,502.99	416,324.27
9,500	942.95	198,679.25
14,500	542.94	127,780.60
19,500	593.49	145,650.95
24,500	297.19	72,988.37
35,000	39.72	9,638.94
Total	7,075.8	1,290,515.2

Figure C-20. Summary of durations and distances for the overall flight

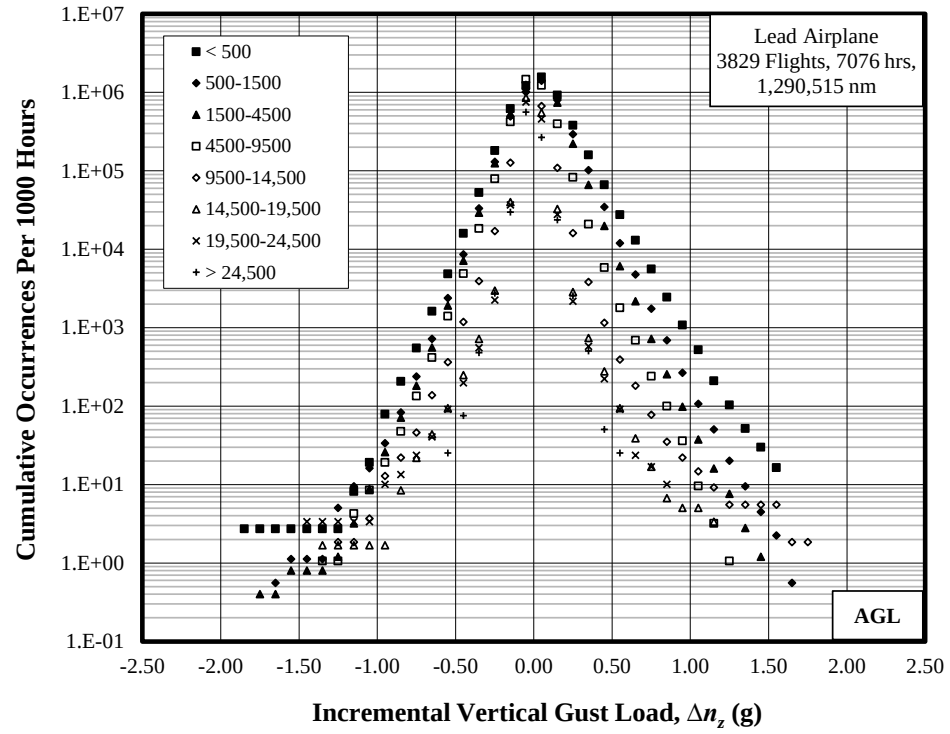

(a) Per 1000 hours

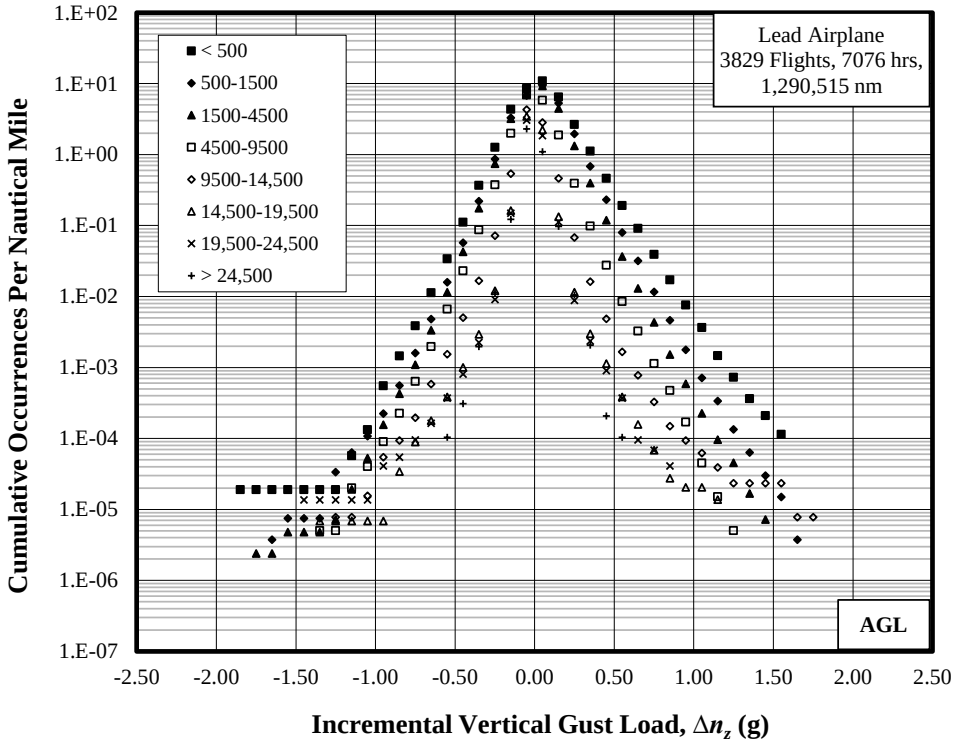

(b) Per nautical mile

Figure C-21. Cumulative occurrences of incremental vertical gust load factor, overall flight, (a) per 1000 hours and (b) per nautical mile

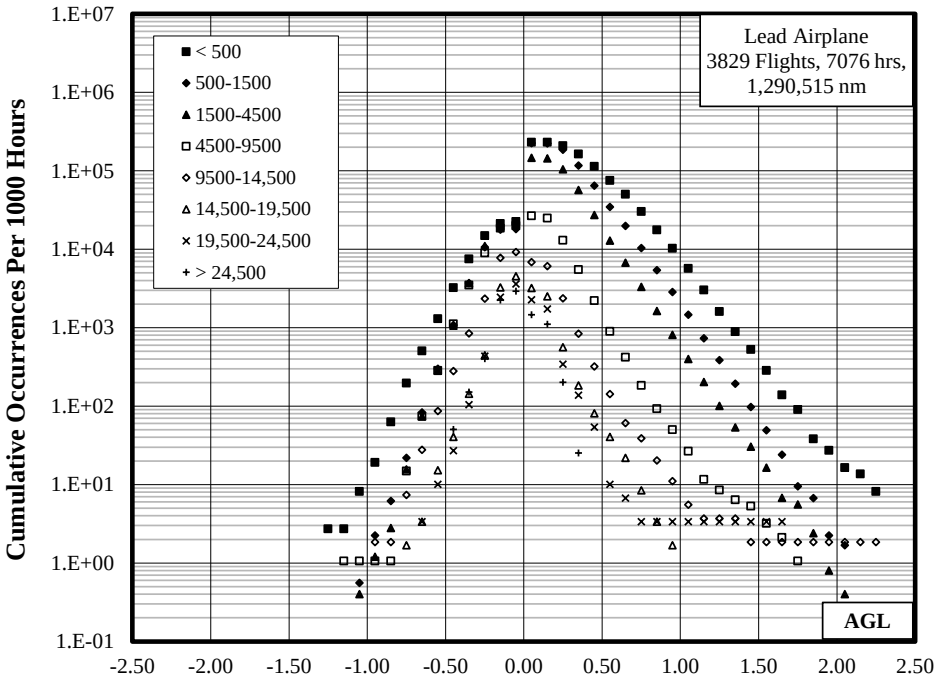

(a) Per 1000 hours

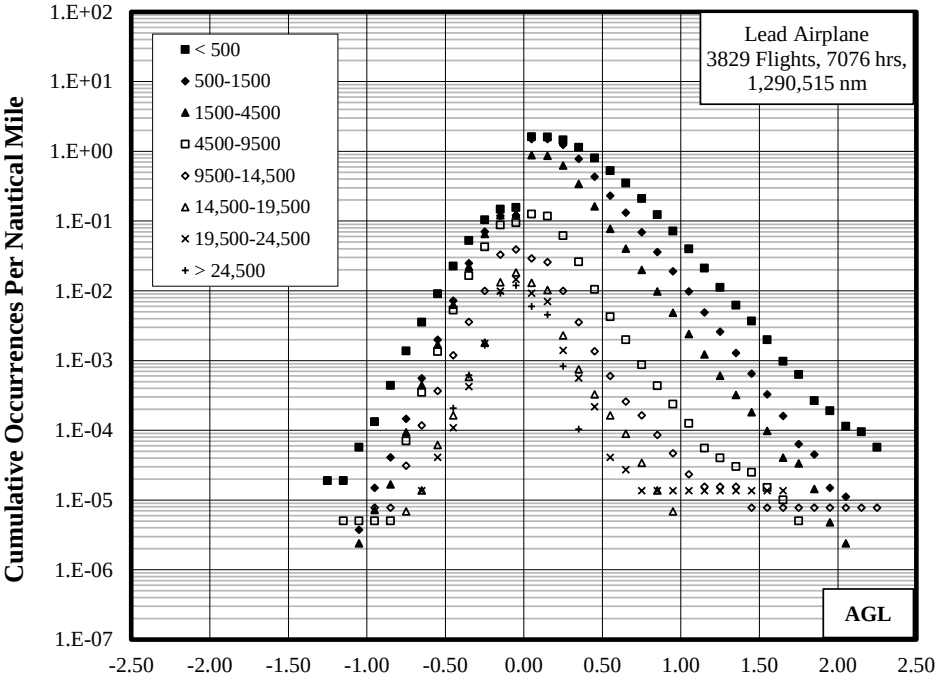

(b) Per nautical mile

Figure C-22. Cumulative occurrences of incremental vertical maneuver load factor, overall flight, (a) per 1000 hours and (b) per nautical mile

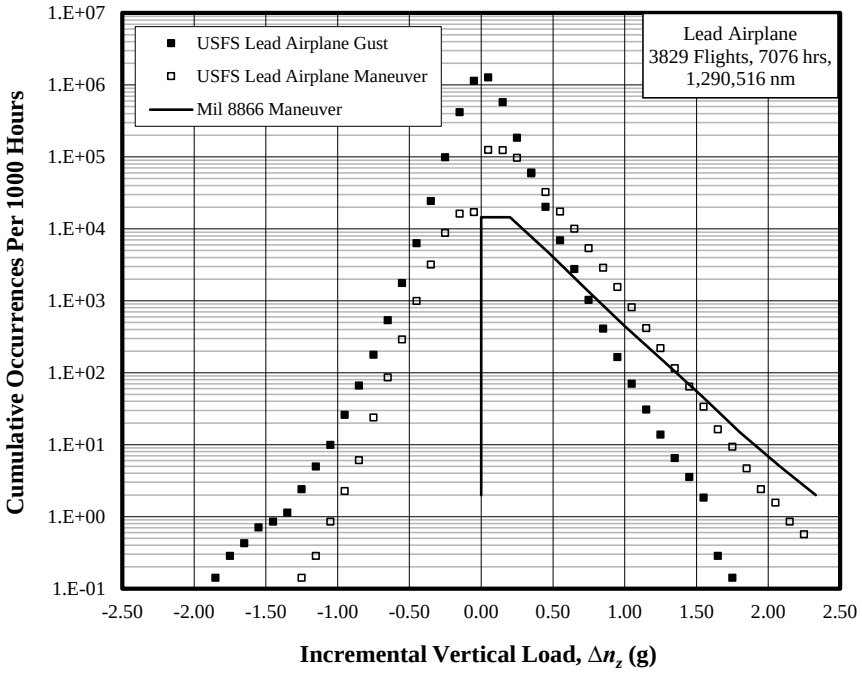

Figure D-1. Cumulative occurrences of incremental vertical load factor compared with MIL 8866 maneuver loads for overall flight

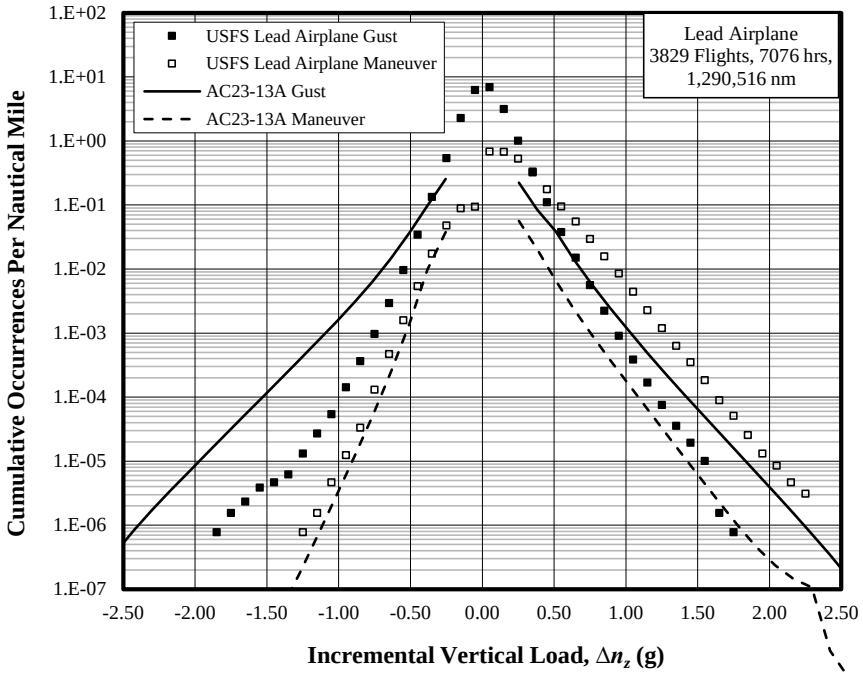

Figure D-2. Cumulative occurrences of incremental vertical load factor compared with AC 23-13A for overall flight

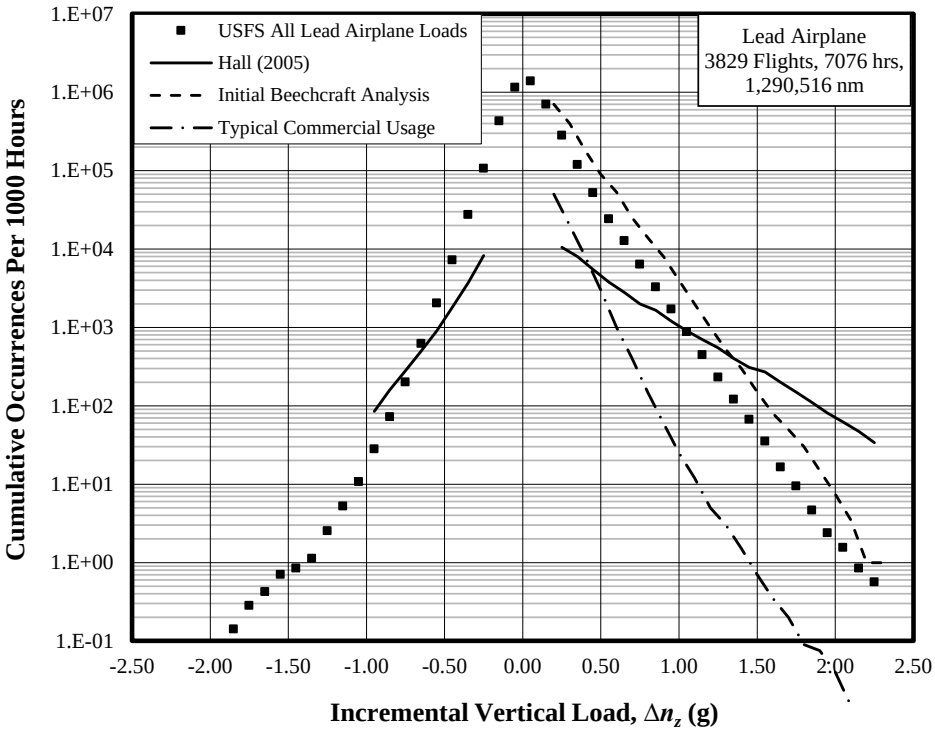

Figure D-3. Cumulative occurrences of incremental vertical load factor per 1000 hours, overall flight

	Number of Flights	Duration		Distance	
		Hours	Percent	Nautical Mile	Percent
Ferry flights	1,557	1,994.8	28%	451,557.5	35%
Normal attitudes	2,125	4,656.1	66%	769,701.1	60%
Unusual attitudes	147	424.9	6%	69,257.0	5%
Total	3,829	7,075.8	-----	1,290,515.7	------

Figure D-4. Summary of durations and distances for different types of flights

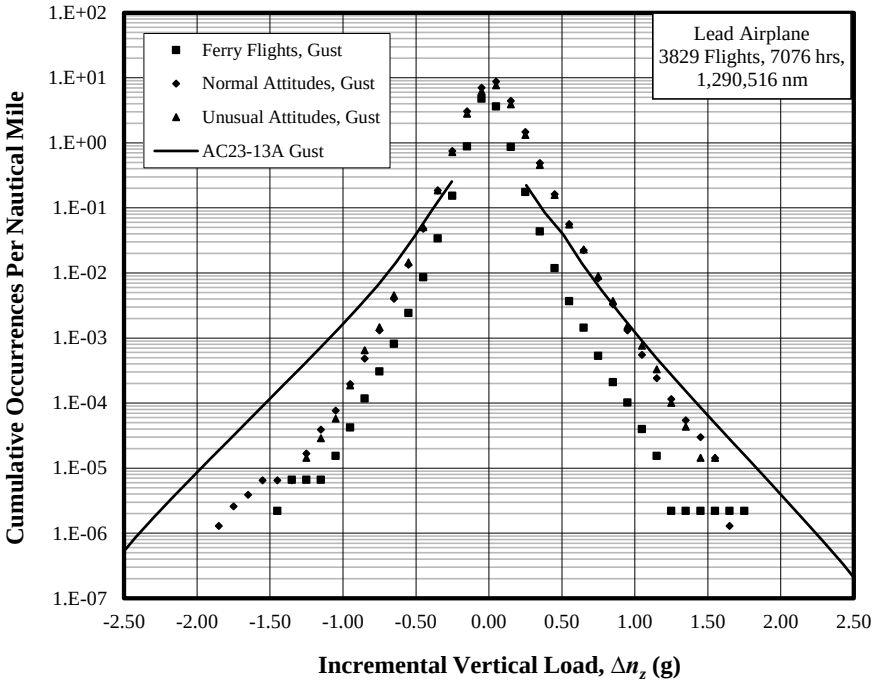

Figure D-5. Cumulative occurrences of incremental vertical gust load factor for different types of flights compared with AC 23-13A

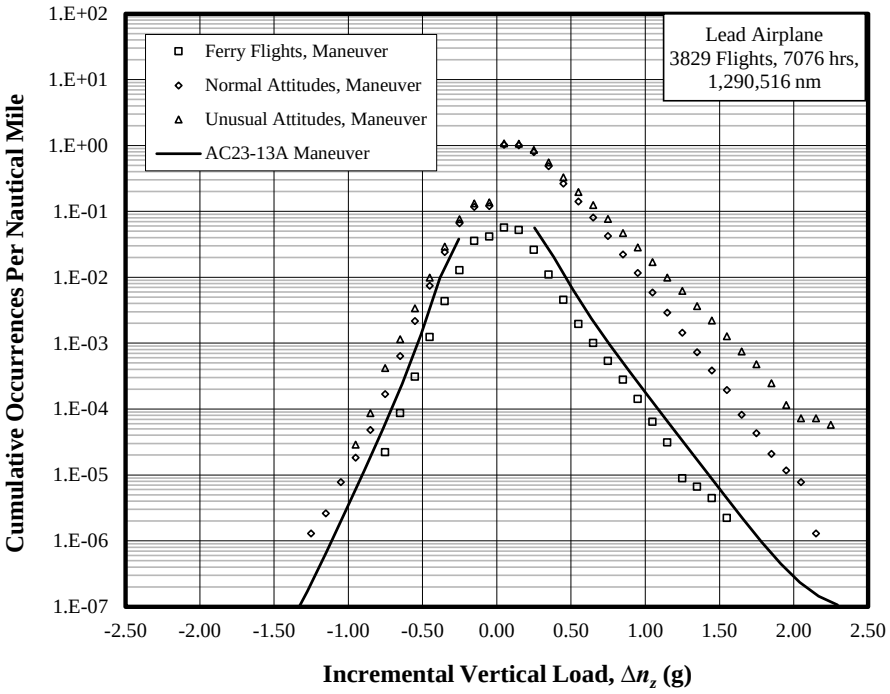

(a) Per nautical mile

Figure D-6. Cumulative occurrences of incremental vertical maneuver load factor for different types of flights compared with AC 23-13A (a) per nautical mile

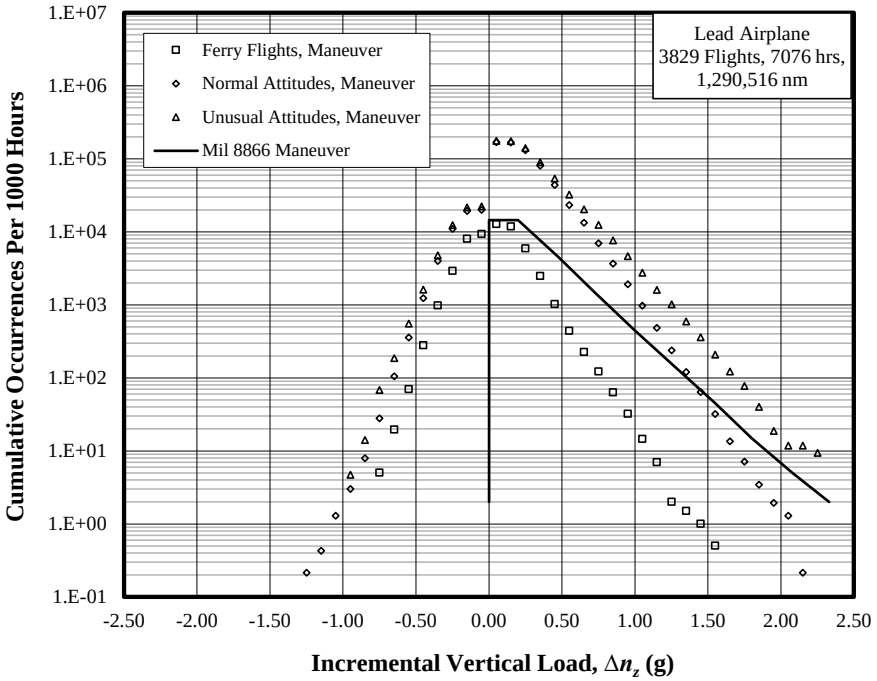

Figure D-7. Cumulative occurrences of incremental vertical maneuver load factor for different types of flights compared with MIL 8866

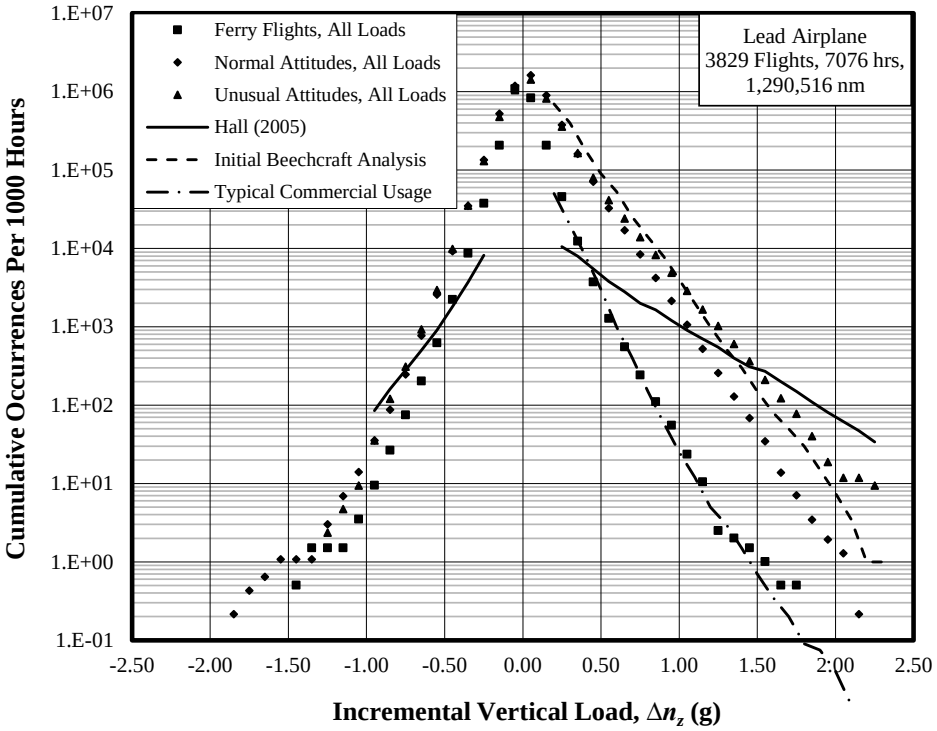

Figure D-8. Cumulative occurrences of incremental vertical load factor for different types of flights

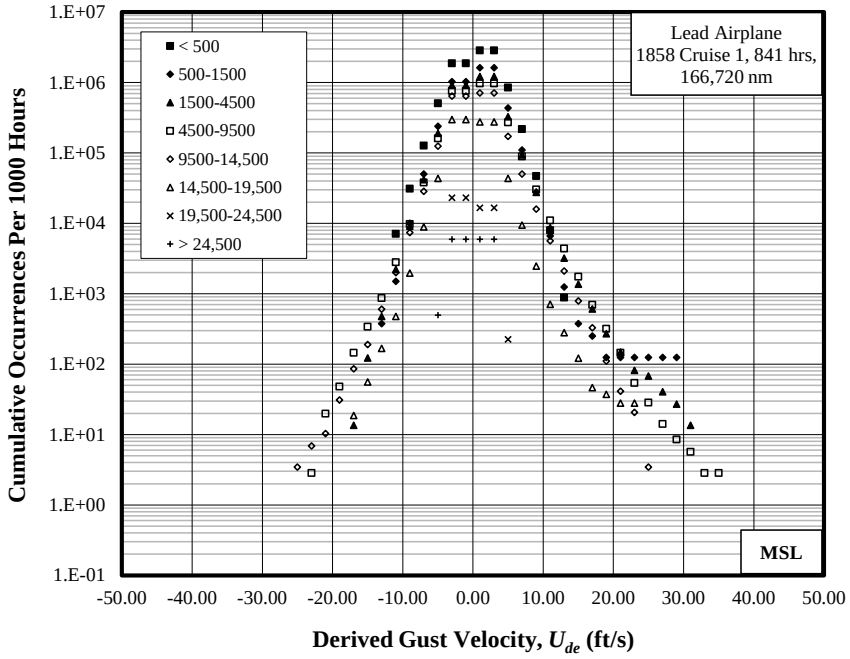

(a) Per 1000 hours

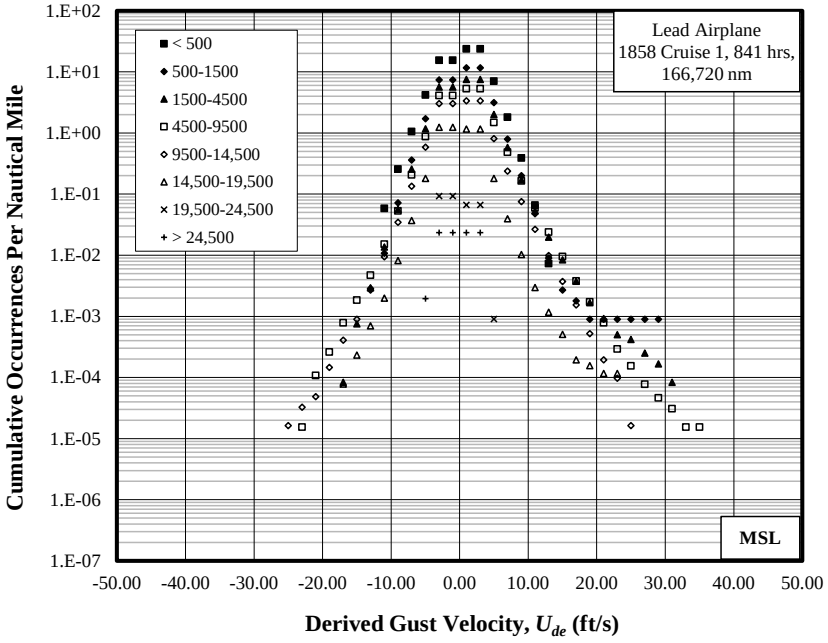

(b) Per nautical mile

Figure E-1. Cumulative occurrences of derived gust velocities, Cruise 1 phase, (a) per 1000 hours and (b) per nautical mile

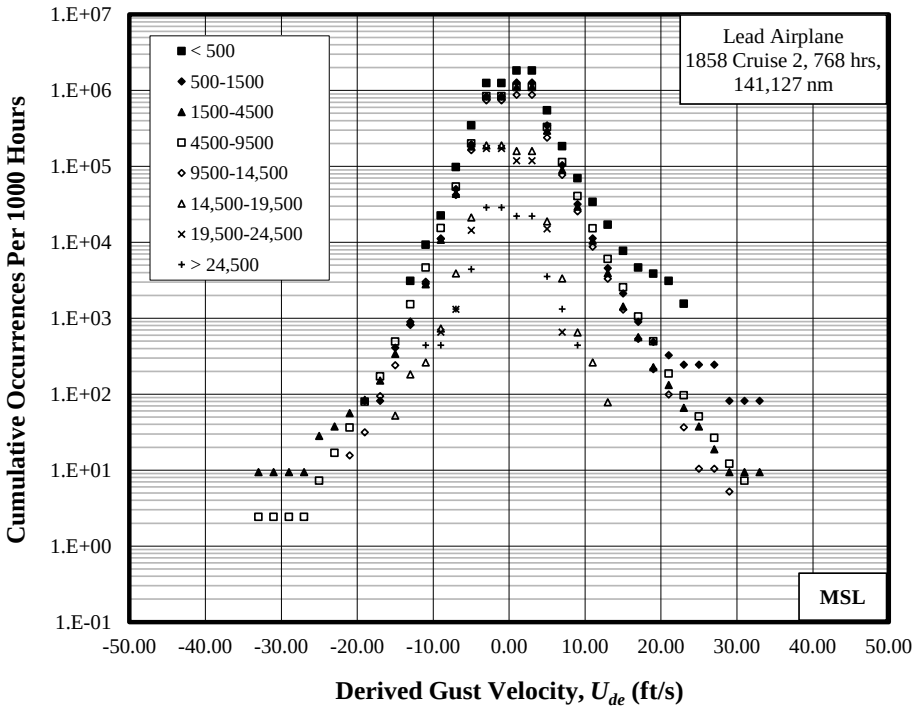

(a) Per 1000 hours

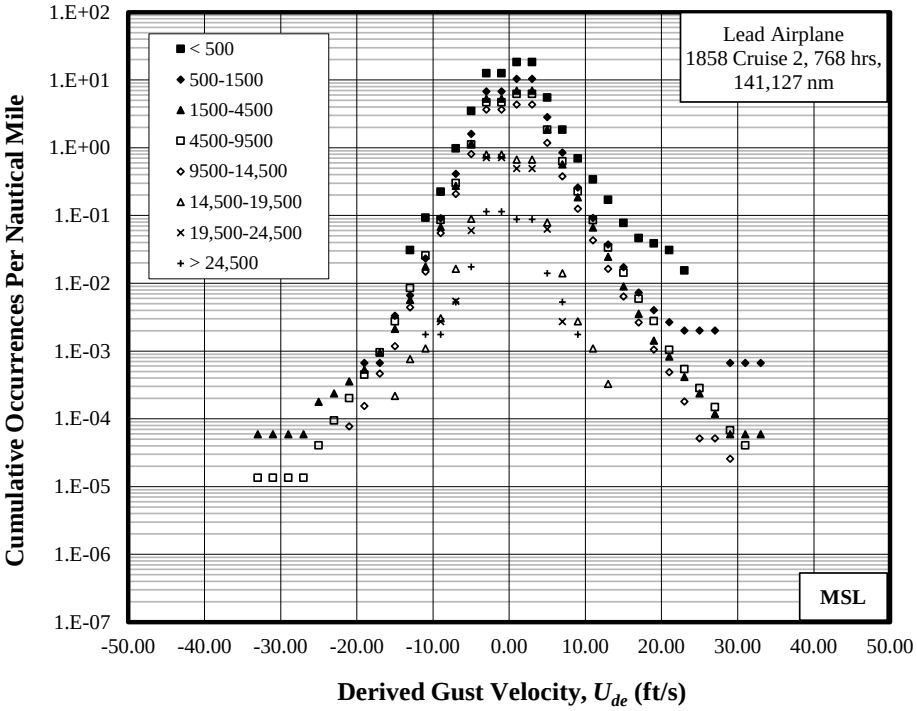

(b) Per nautical mile

Figure E-2. Cumulative occurrences of derived gust velocity, Cruise 2 phase, (a) per 1000 hours and (b) per nautical mile

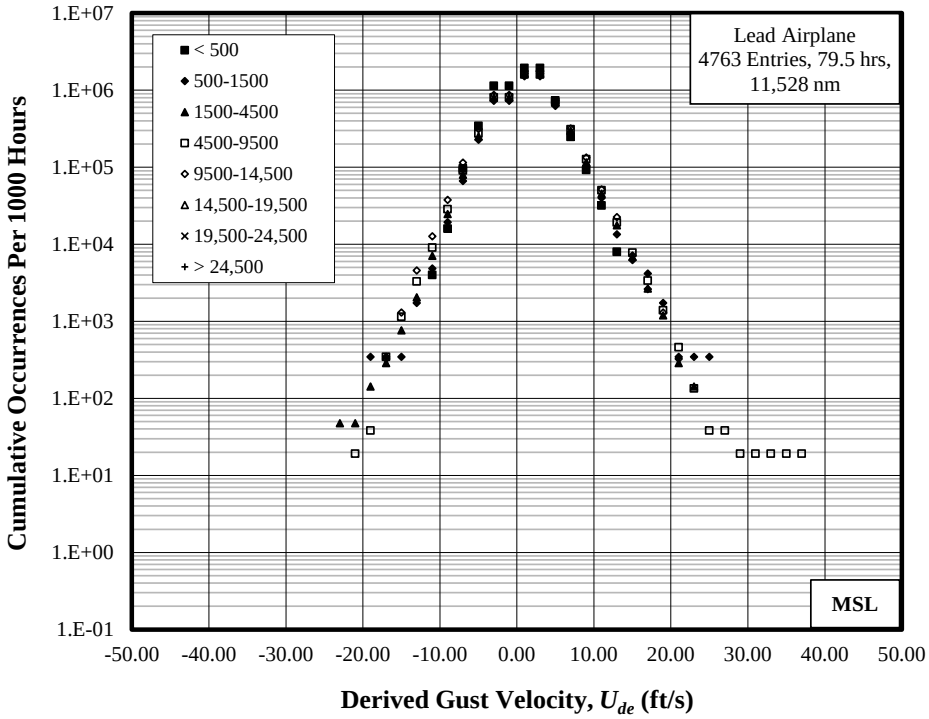

(a) Per 1000 hours

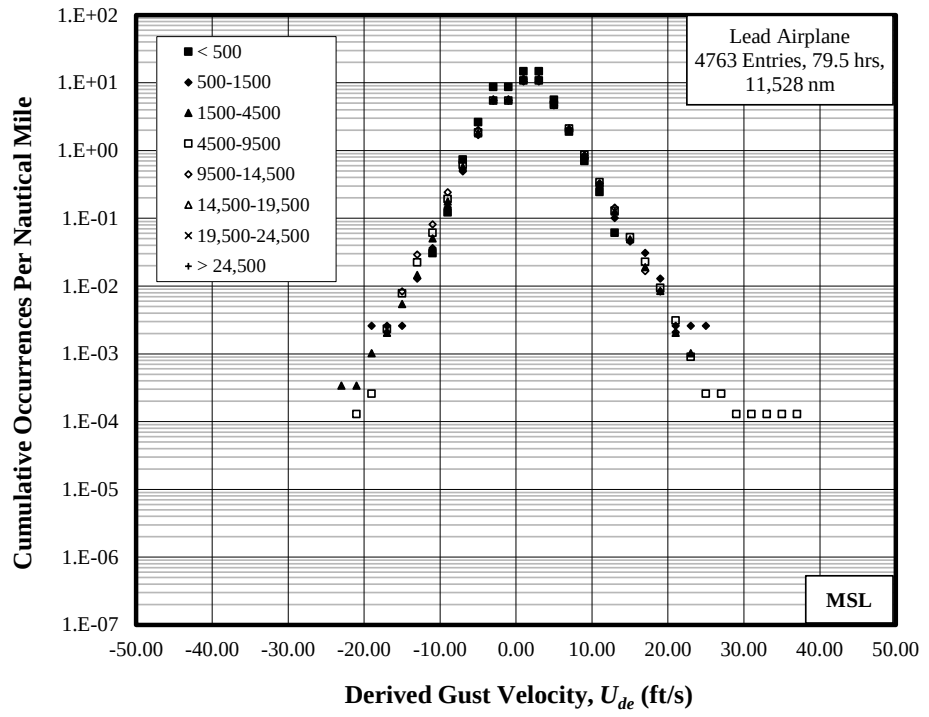

(b) Per nautical mile

Figure E-3. Cumulative occurrences of derived gust velocity, entry phase, (a) per 1000 hours and (b) per nautical mile

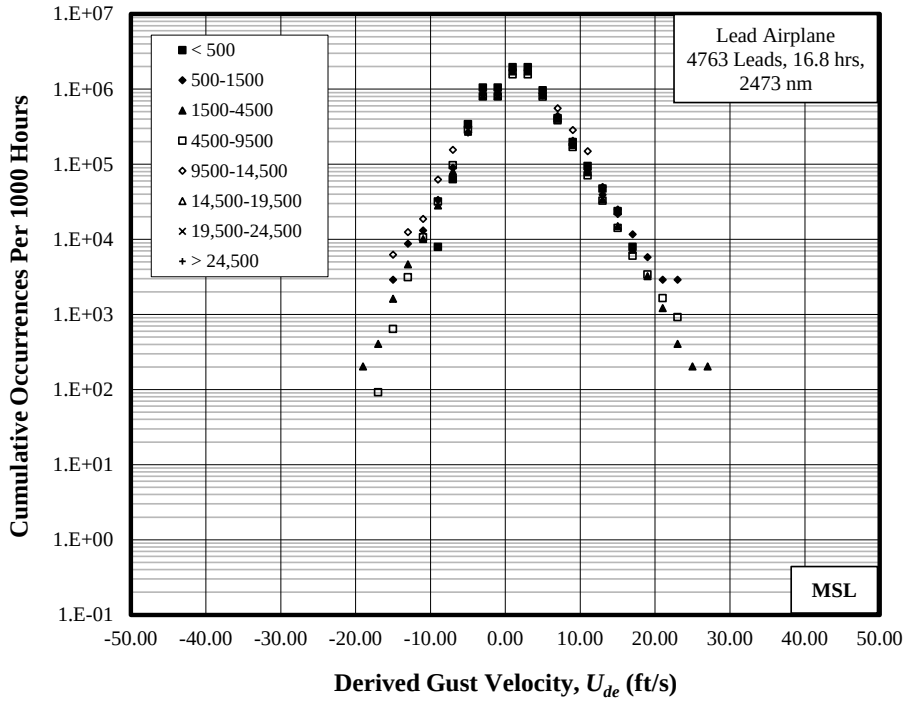

(a) Per 1000 hours

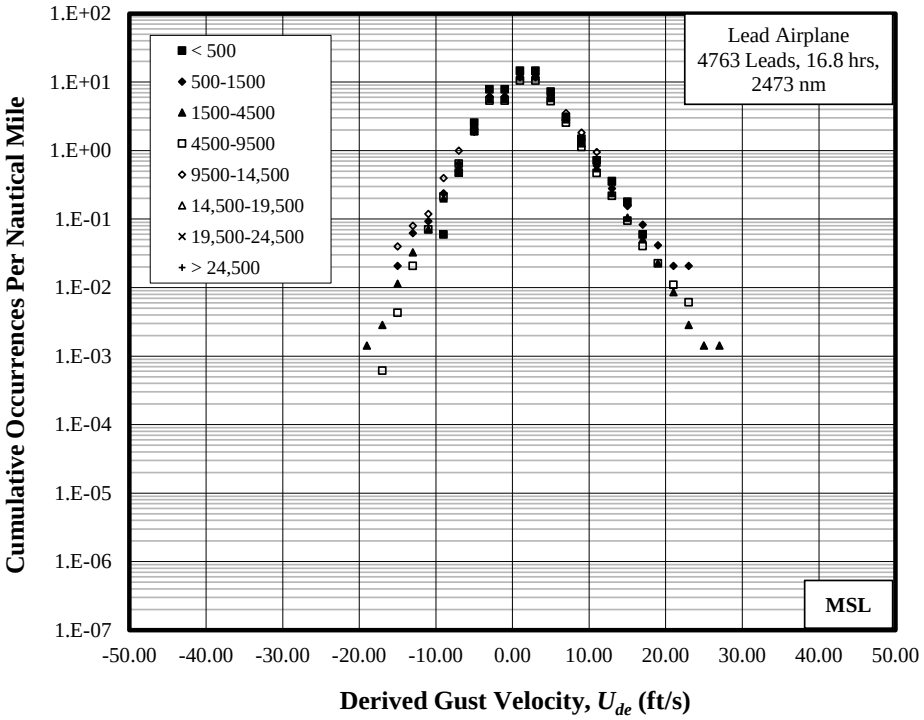

(b) Per nautical mile

Figure E-4. Cumulative occurrences of derived gust velocity, lead phase, (a) per 1000 hours and (b) per nautical mile

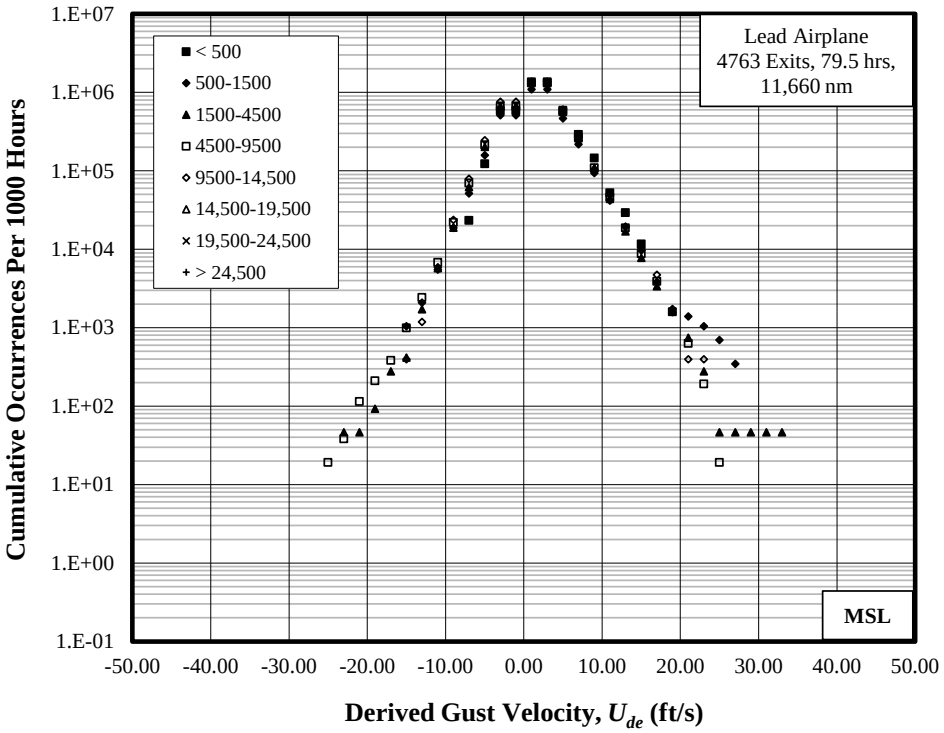

(a) Per 1000 hours

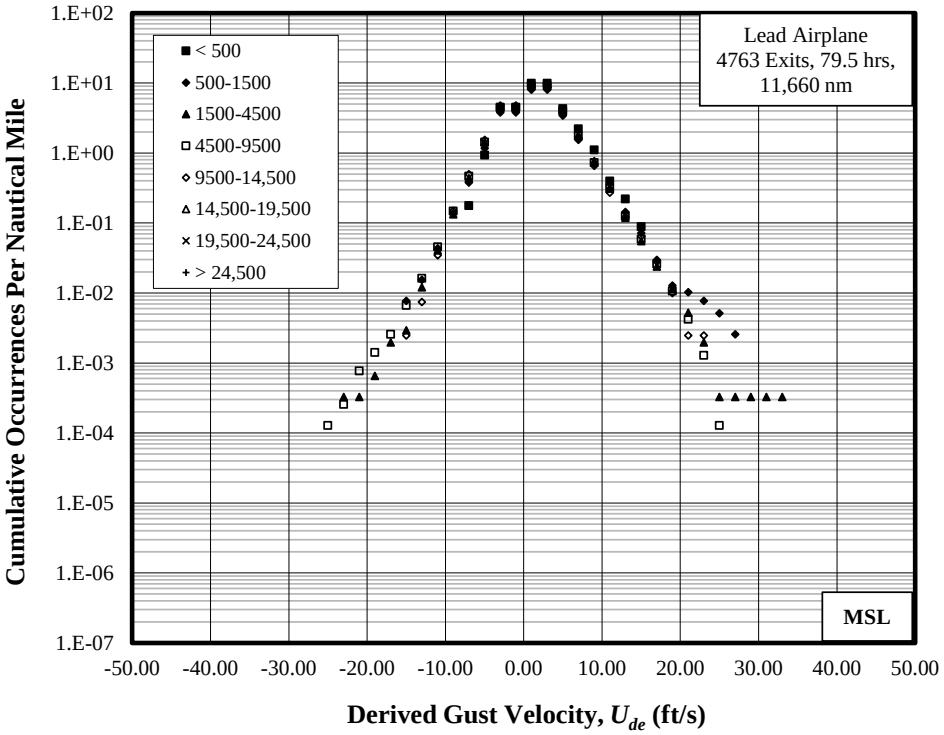

(b) Per nautical mile

Figure E-5. Cumulative occurrences of derived gust velocity, exit phase, (a) per 1000 hours and (b) per nautical mile

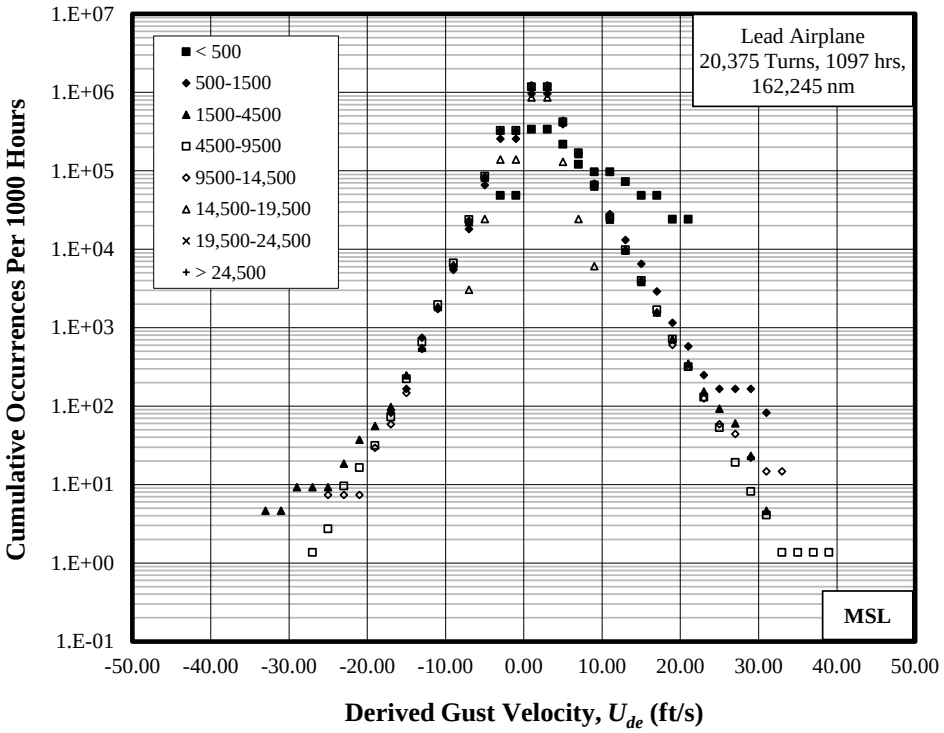

(a) Per 1000 hours

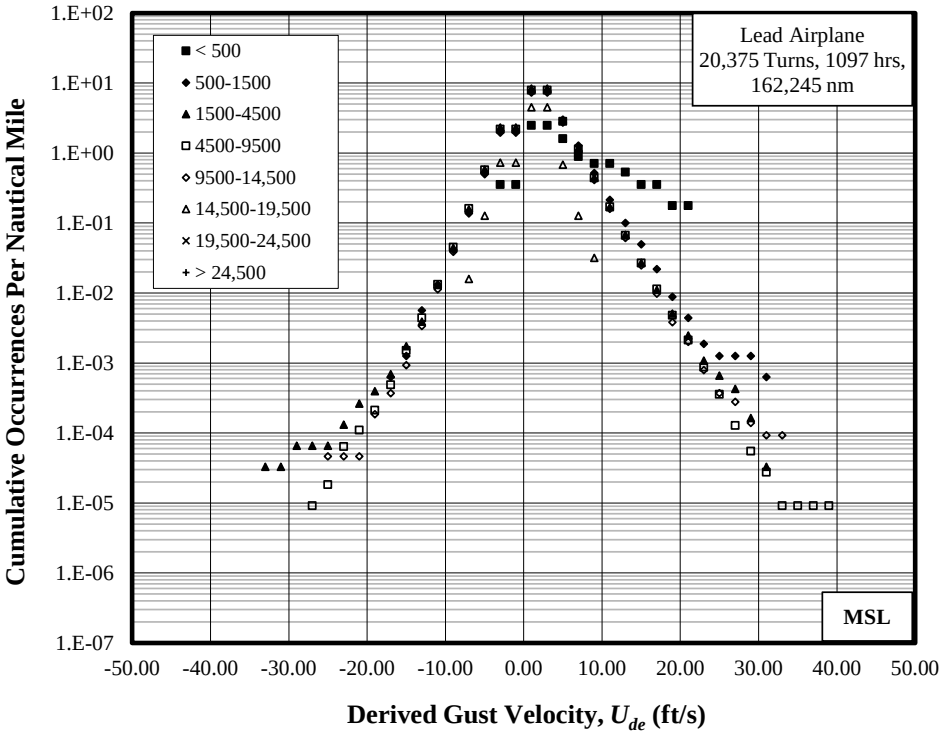

(b) Per nautical mile

Figure E-6. Cumulative occurrences of derived gust velocity, turn phase, (a) per 1000 hours and (b) per nautical mile

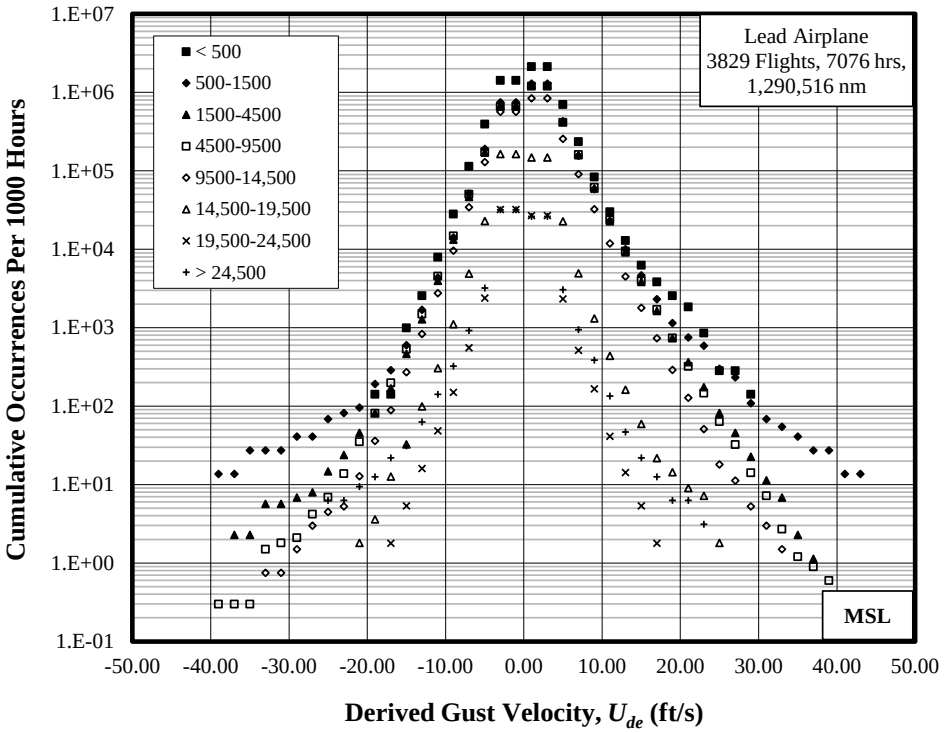

(a) Per 1000 hours

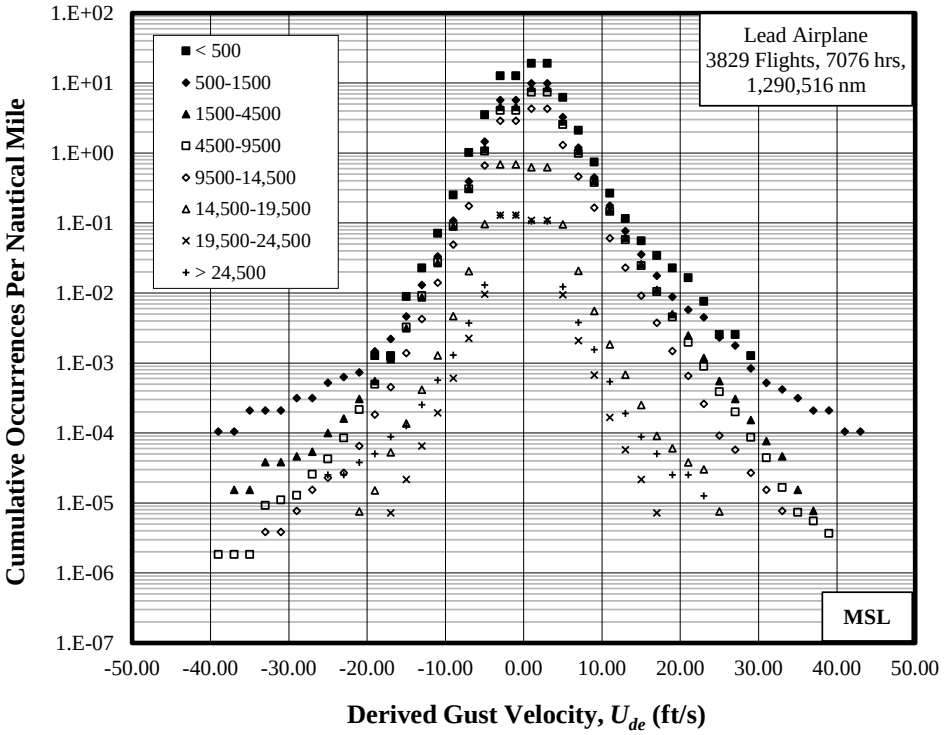

(b) Per nautical mile

Figure E-7. Cumulative occurrences of derived gust velocity, overall flight with all phases, (a) per 1000 hours and (b) per nautical mile

APPENDIX F—DERIVED GUST VELOCITIES BY ABOVE-GROUND-LEVEL ALTITUDE

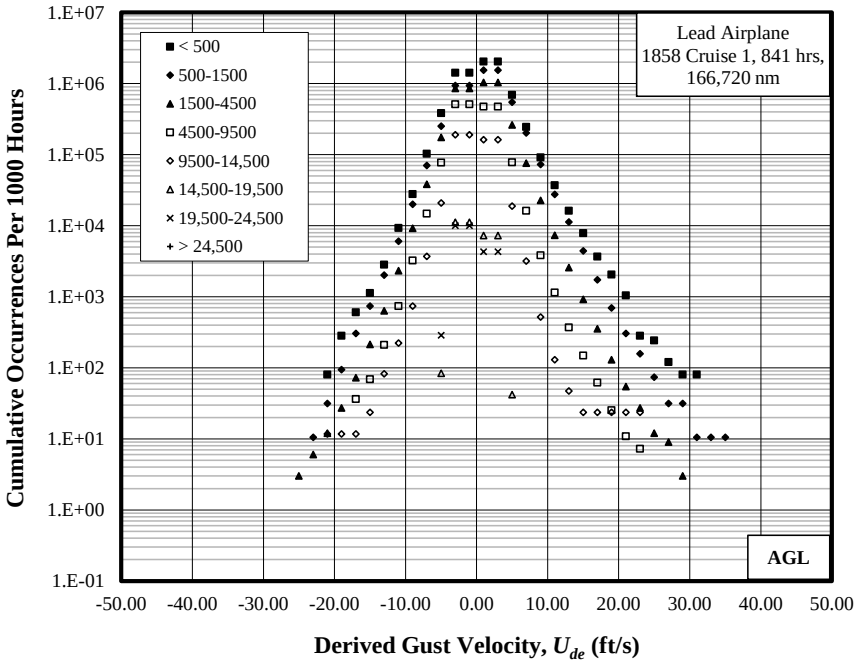

(a) Per 1000 hours

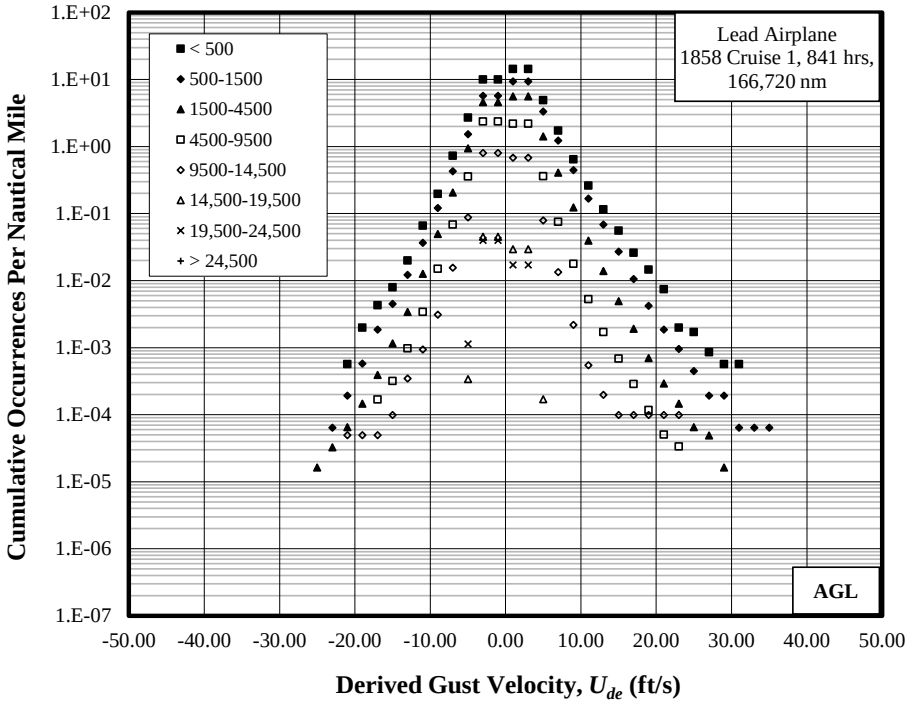

(b) Per nautical mile

Figure F-1. Cumulative occurrences of derived gust velocities, Cruise 1 phase, (a) per 1000 hours and (b) per nautical mile

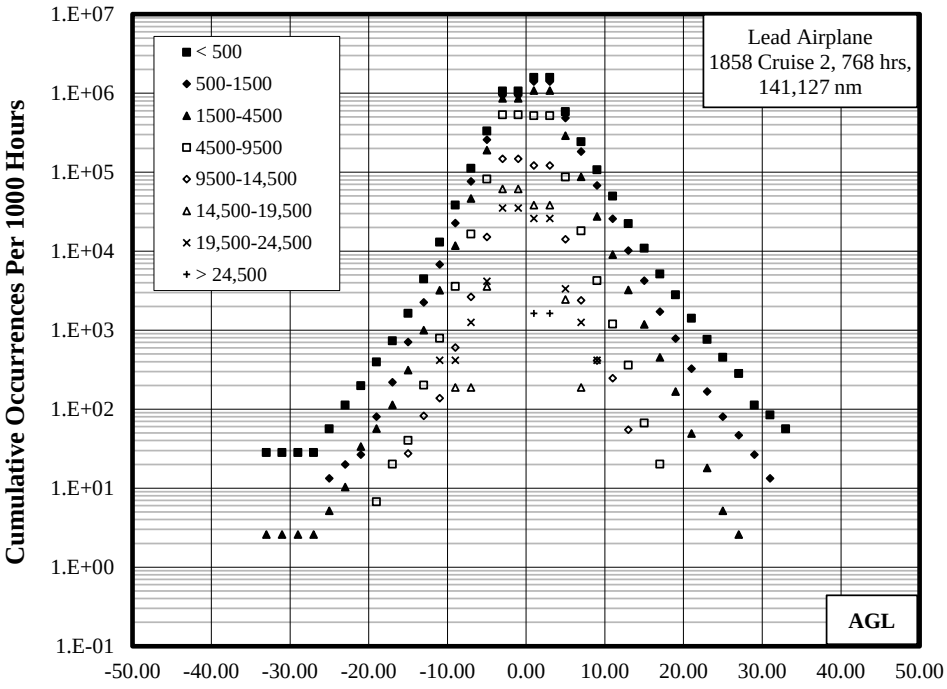

(a) Per 1000 hours

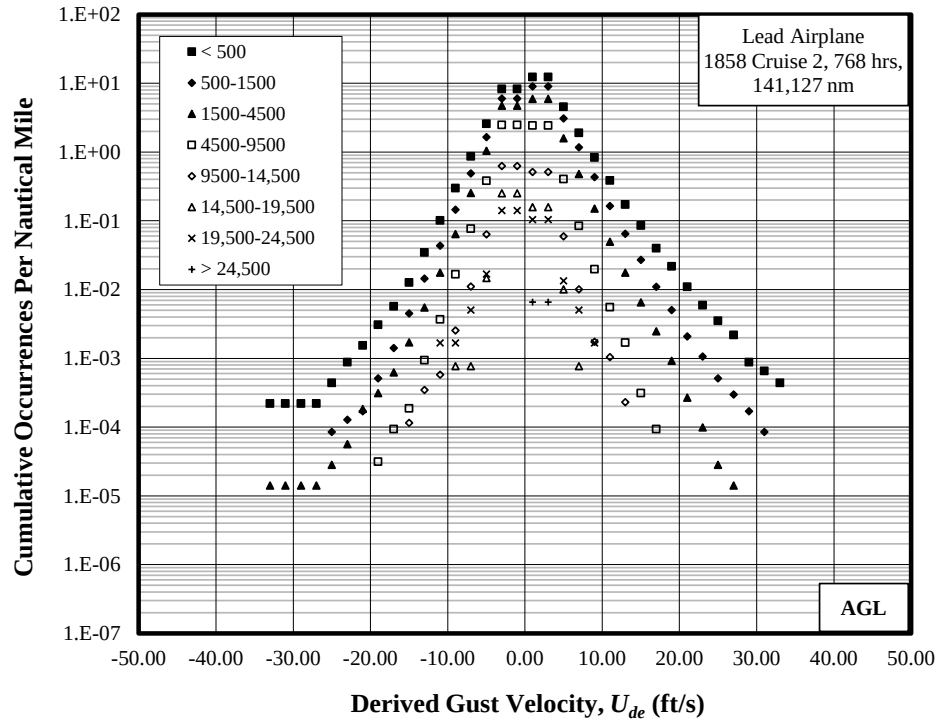

(b) Per nautical mile

Figure F-2. Cumulative occurrences of derived gust velocity, Cruise 2 phase, (a) per 1000 hours and (b) per nautical mile

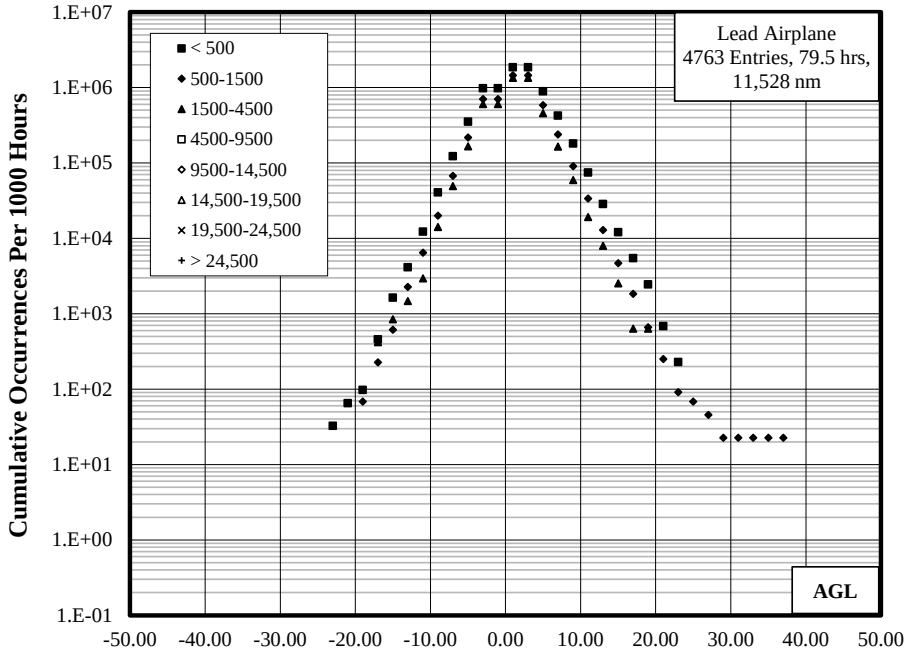

(a) Per 1000 hours

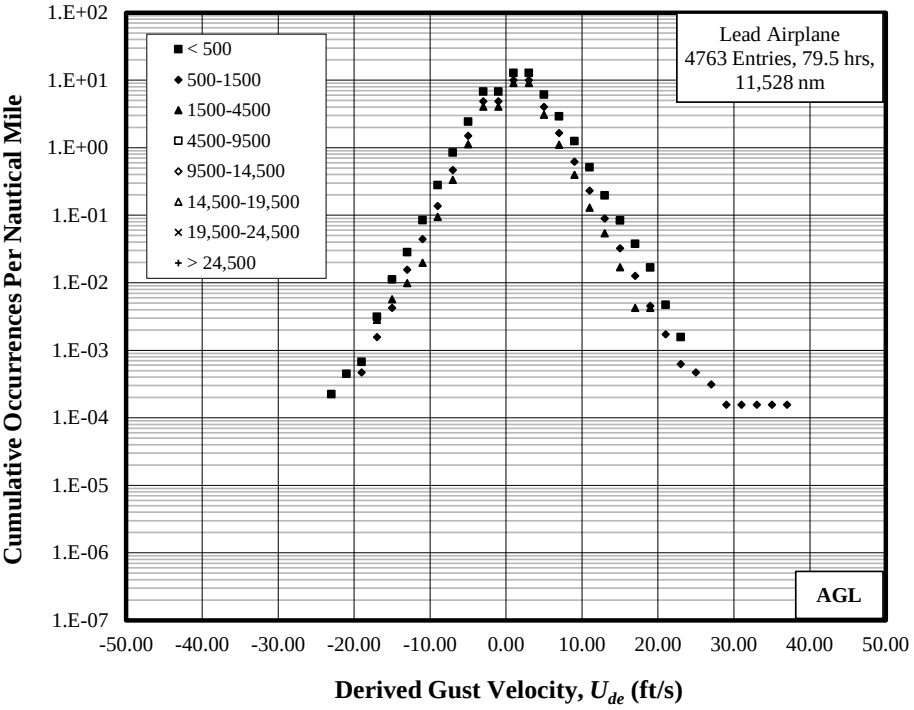

(b) Per nautical mile

Figure F-3. Cumulative occurrences of derived gust velocity, entry phase, (a) per 1000 hours and (b) per nautical mile

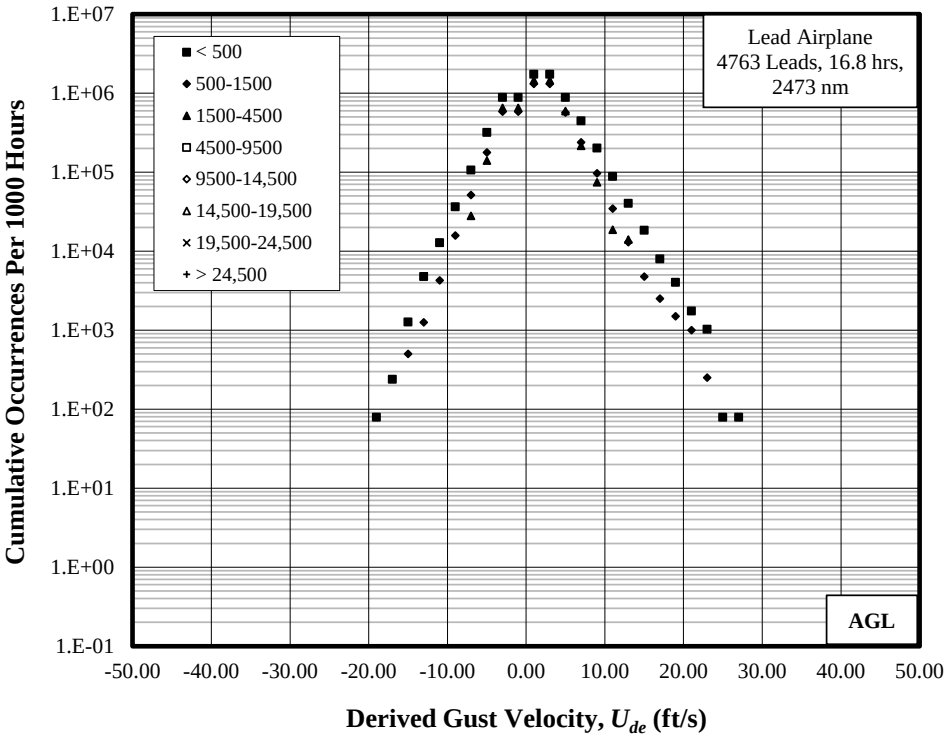

(a) Per 1000 hours

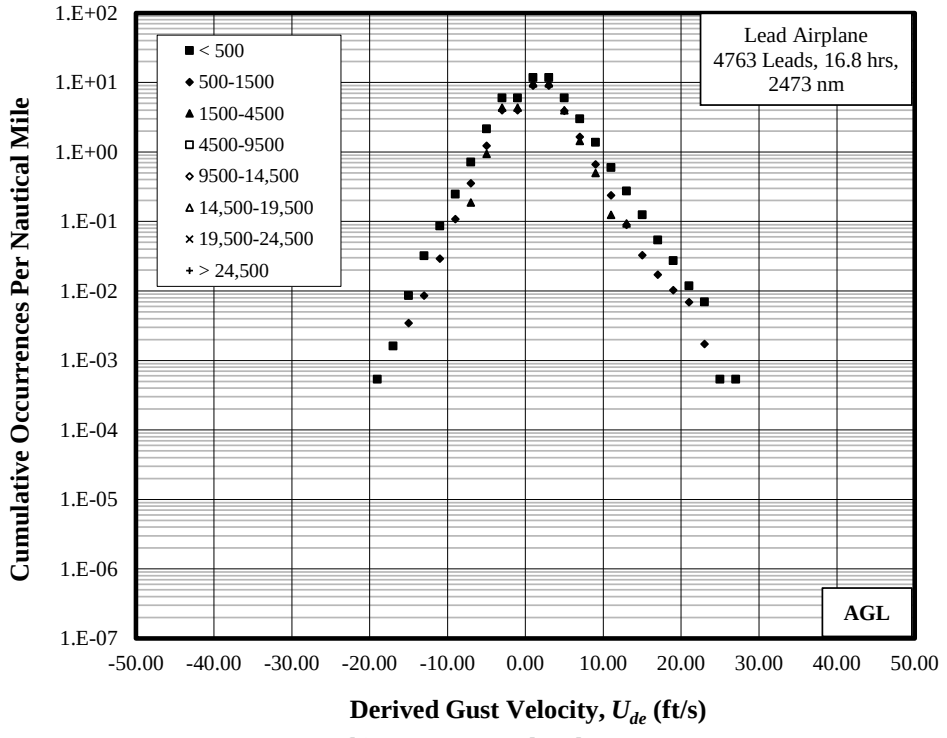

(b) Per nautical mile

Figure F-4. Cumulative occurrences of derived gust velocity, lead phase, (a) per 1000 hours and (b) per nautical mile

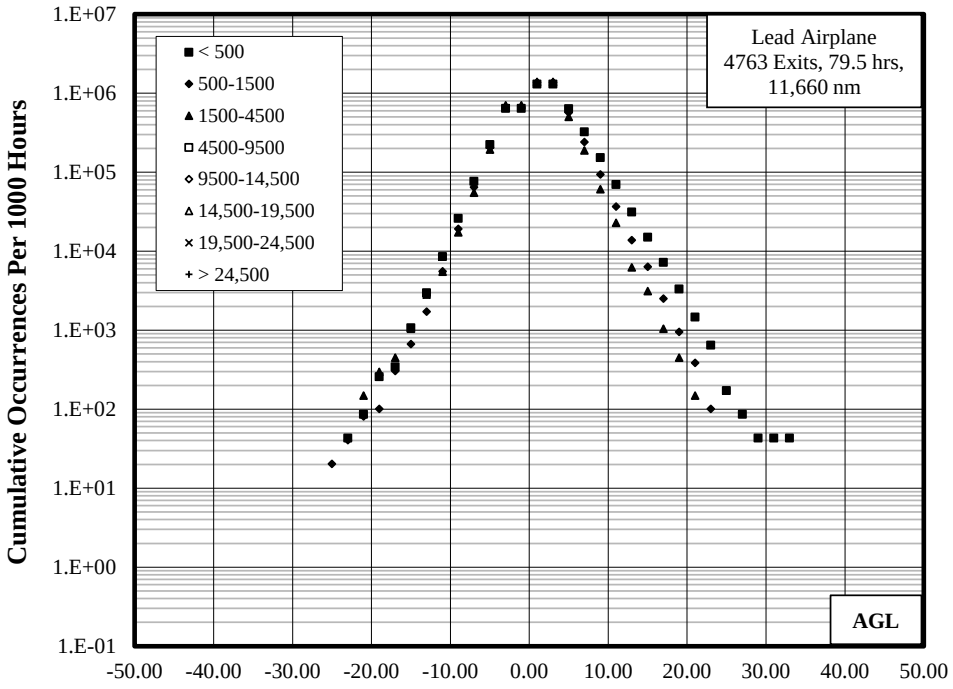

(a) Per 1000 hours

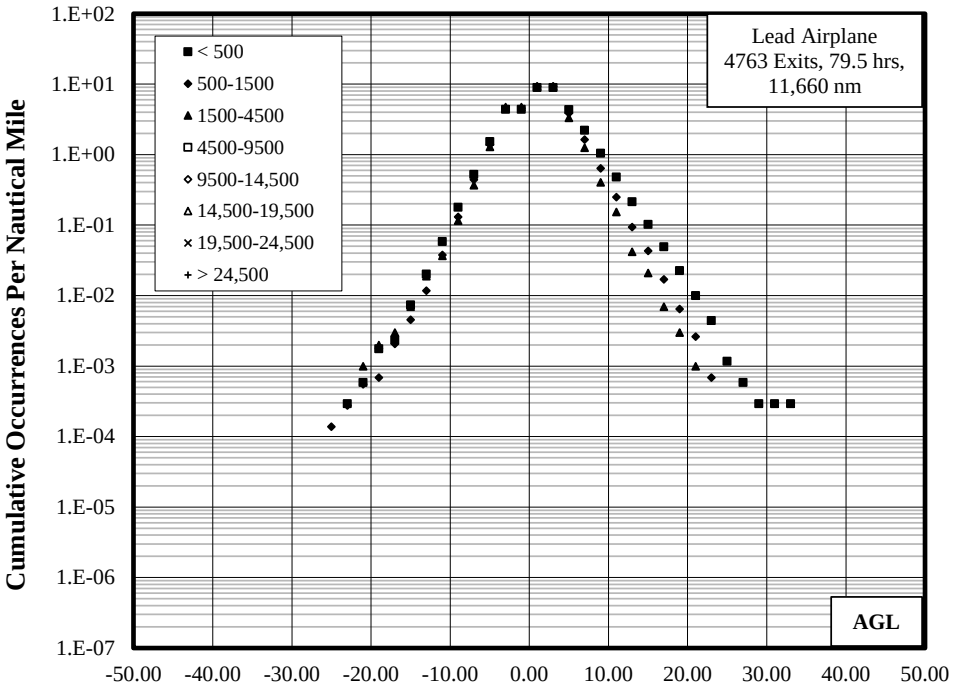

(b) Per nautical mile

Figure F-5. Cumulative occurrences of derived gust velocity, exit phase, (a) per 1000 hours and (b) per nautical mile

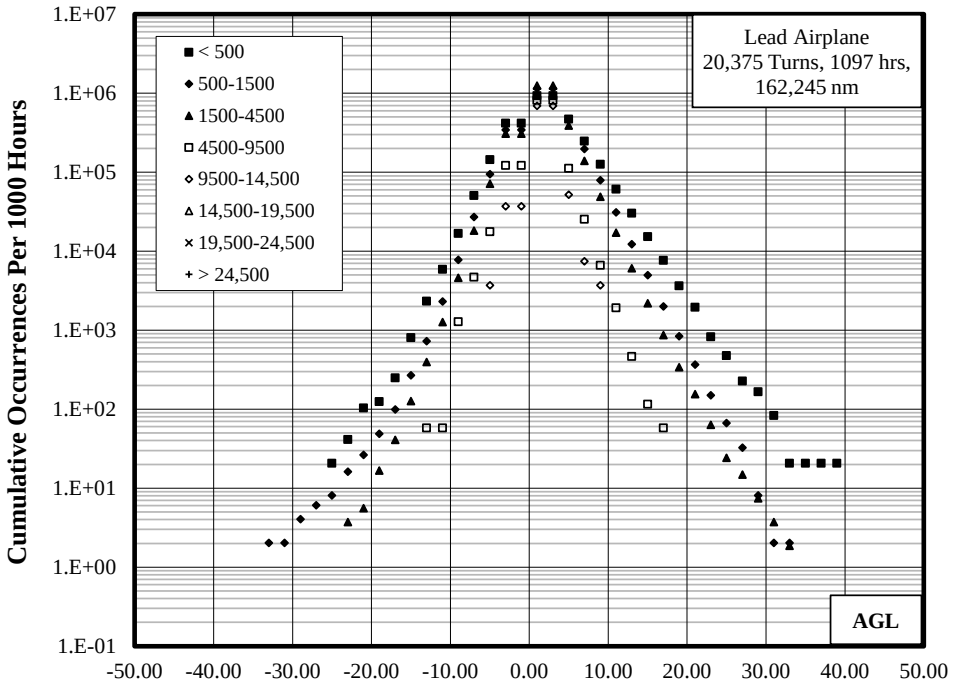

(a) Per 1000 hours

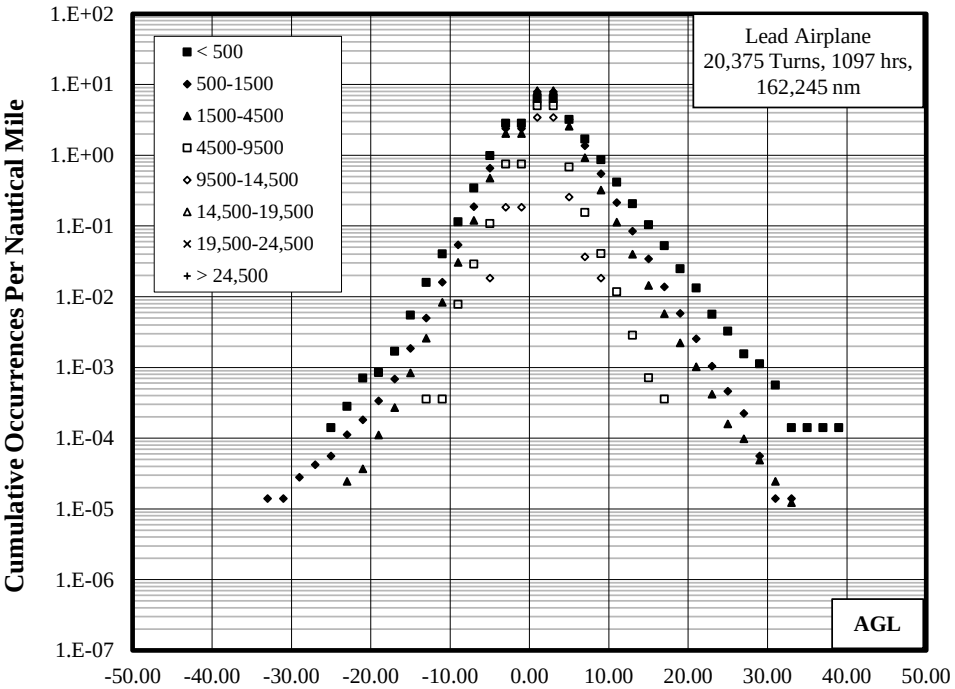

(b) Per nautical mile

Figure F-6. Cumulative occurrences of derived gust velocity, turn phase, (a) per 1000 hours and (b) per nautical mile

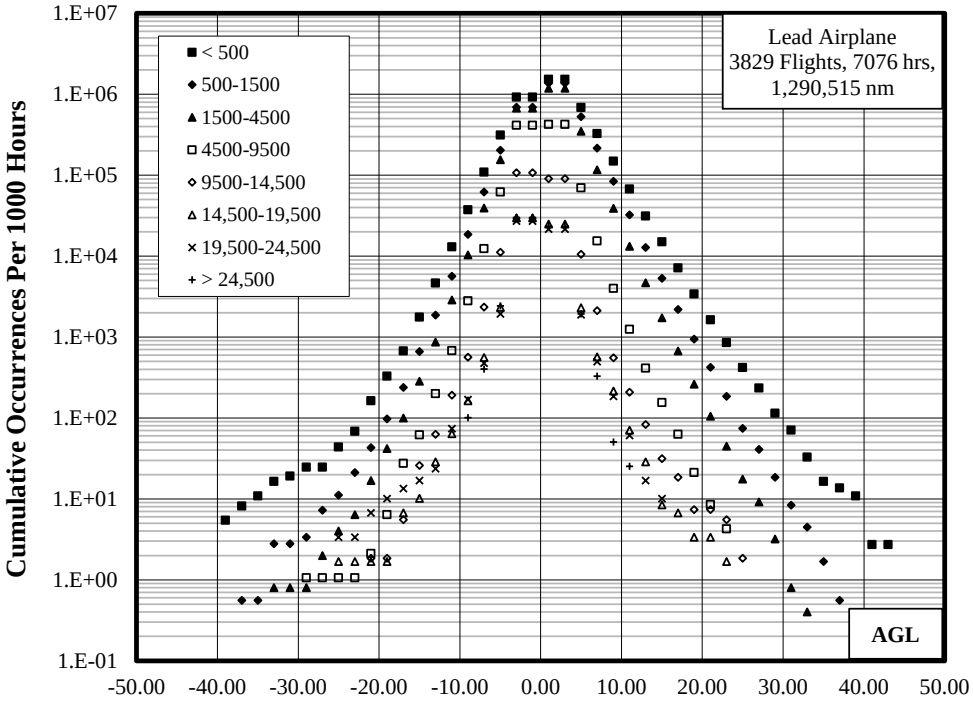

(a) Per 1000 hours

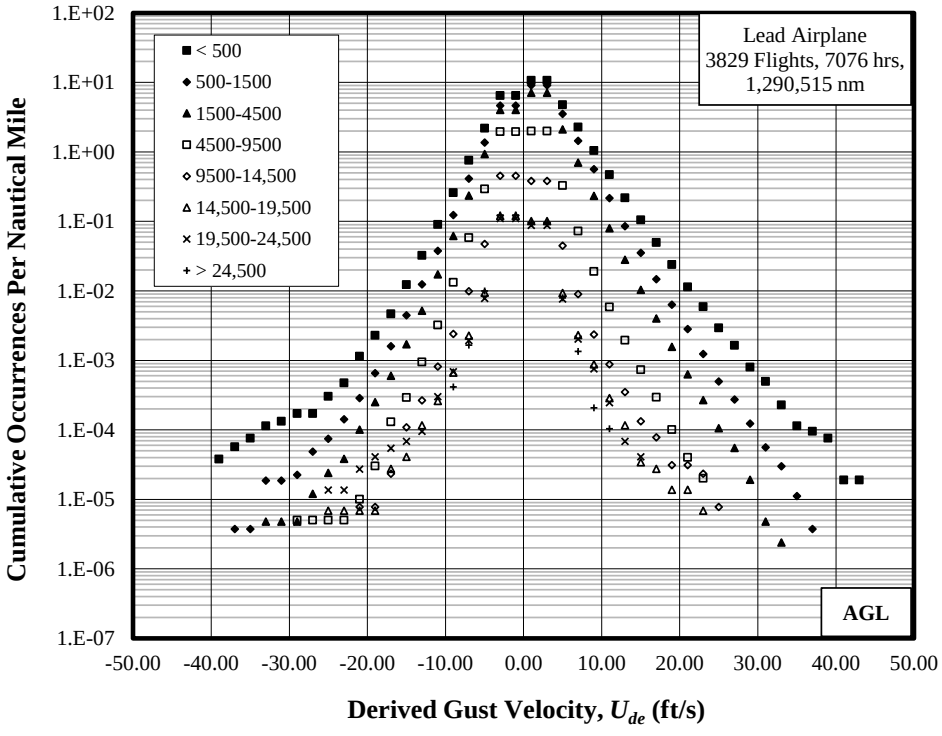

(b) Per nautical mile

Figure F-7. Cumulative occurrences of derived gust velocity, overall flight with all phases, (a) per 1000 hours and (b) per nautical mile